Université de Toulouse

THÈSE

En vue de l'obtention du

DOCTORAT DE L'UNIVERSITÉ DE TOULOUSE

Délivré par :
Institut National des Sciences Appliquées de Toulouse (INSA Toulouse)

Discipline ou spécialité :

Génie Mécanique

Présentée et soutenue par :
Muhammad Rizwan SHAD

le : 17 Mars 2011

Titre :
Modélisation et Analyse du Comportement
Dynamique Non-linéaire des Rotors
Modeling and Analysis of
Nonlinear Dynamic Behavior of Rotors

JURY

Waqar ASRAR	Professeur, Int. Isl. Univ. of Malaysia	Rapporteur
Thouraya BARANGER	MCF-HDR, Université Lyon I	Rapporteur
Alain BERLIOZ	Professeur, Université Toulouse III	Directeur de thèse
Régis DUFOUR	Professeur, INSA Lyon	Président
Guilhem MICHON	Ingénieur-Chercheur, ISAE	Co-directeur de thèse
Pascal SWIDER	Professeur, Université Toulouse III	Examinateur

---

Ecole doctorale :
Mécanique, Energétique, Génie civil et Procédés (MEGeP)

Unité de recherche :
Institut Clément Ader

Directeur(s) de Thèse :

BERLIOZ Alain et MICHON Guilhem

Rapporteurs :

BARANGER Thouraya et ASRAR Waqar

Acknowledgements

There are many people I want to acknowledge from the bottom of my heart who have provided help and/or motivation in any sort during this PhD work. I would like to express my deep and sincere gratitude to my director, **Prof. Alain Berlioz** and co-director, **Dr. Guilhem Michon** for providing whatever advice and resources necessary for me to achieve my goals. Their understanding, encouraging and personal guidance have provided a good basis for the present thesis. A special thanks to **Prof. Alain Berlioz** for introducing me to the wonderful field of nonlinear rotordynamics. His wide knowledge and logical way of thinking have been of great value to me.

I would like to acknowledge HEC, Higher Education Commission of Pakistan, for funding the scholarship and Sfère, Société française d'exportation des ressources éducatives, for regulating the scholarship.

I would also like to thank all the co-workers who have helped in the research and have provided inspiration as friends throughout the period of this PhD. Thank you **Leonardo Sanches**, **Simon Foucaud**, **Joseph Morlier and Miguel Charlotte** for whatever help and company you all have provided.

There are many other friends who are not co-workers but they have been very nice friends through these years. I would like to recognize them for their wonderful company and moral support. Thank you **Majid Shahzad**, **Rashid Hameed**, **Toufeer Mehdi**, **Shahid Zeeshan**, **Muazzam Ghoas**, **Muhammd Kaleem and Dr. M. Ilyas** for your inspiration and friendship over the years.

I would like to thank and admire all my family members specially my **parents** for their well wishes, motivation and support. Specially, I would like to dedicate this PhD thesis to the loving memories of my **father** who passed away last year. He was always there for me in providing whatever resources, motivation and advice for accomplishing my academic and professional goals. Miss You Dad!

Love for all!

[This page intentionally left blank]

Table of Contents

Nomenclature

A	Cross sectional area of shaft	m^2
a_E	Amplitude at the equilibrium position	m
C	Geometric center of the shaft	
c	Coefficient of damping	$N.s.m^{-1}$
d_1	Position of mass unbalance on disk	m
E	Modulus of elasticity	$N\ m^{-2}$
E_f, E_m	Elastic moduli for the fiber and matrix material	$N\ m^{-2}$
E_1, E_2	Elastic moduli in the orthotropic axis	$N\ m^{-2}$
EI	Homogenized flexural inertia	$N\ m^{-2}$
V_f, V_m	Volume fraction for the fiber and matrix material	$N\ m^{-2}$
v_f, v_m	Poisson ratio for the fiber and matrix material	$N\ m^{-2}$
K_f, K_m	Plain strain bulk moduli for the fiber and matrix material	$N\ m^{-2}$
G_{12}, G_{13}, G_{23}	Shear moduli for the matrix material	$N\ m^{-2}$
G_m	Shear modulus for the matrix material	$N\ m^{-2}$
G_E	Equivalent shear modulus	$N\ m^{-2}$
GS	Equivalent shear rigidity	$N\ m^{-2}$
C_r	Viscous damping coefficient	$N\ m^{-2}$
H_r	Hysteretic damping coefficient	$N\ m^{-2}$
e	Wall thickness of the tube shaft	m
G	Shear Modulus	$N\ m^{-2}$
h	Thickness of disk	m
I	Area moment of inertia of shaft	m^4
I_{dx}	Mass moment of inertia of disk in direction x	$kg.m^2$
I_{dy}	Mass moment of inertia of disk in direction y	$kg.m^2$
I_{dz}	Mass moment of inertia of disk in direction z	$kg.m^2$
k	Shear correction factor	

L	Length of shaft	m
l_1	Position of disk on shaft	m
M_d	Mass of disk	kg
m_u	Mass Unbalance	Kg
N_0	Constant static axial force	N
N_A	Dynamic axial force	N
n	Mode number	
R_1	Cross sectional radius of shaft/inner radius of disk	m
R_2	Outer radius of disk	m
R_m	Mean radius of the composite shaft	m
R_p , R_{p-1}	External and internal radius of layer p	m
r	Slenderness Ratio	
T_d	Kinetic energy of the disk	N.m
T_R	Total kinetic energy of rotor	N.m
T_s	Kinetic energy of the shaft	N.m
T_u	Kinetic energy of the mass unbalance	N.m
U	Discretized displacement along axis *x*	m
W	Discretized displacement along axis *z*	m
$\dot{U}, \dot{W}$	Derivatives with respect to time	$m.s^{-1}$
U_R	Total strain (deformation) energy of rotor	N.m
U_s	Strain (deformation) energy of shaft	N.m
V_x	Shear force along x axis	N
V_z	Shear force along z axis	N
$u(y,t)$	Displacement along *x* axis of rotor	m
$w(y,t)$	Displacement along *z* axis of rotor	m
β_x	Shear angle about x axis	rad
β_z	Shear angle about z axis	rad
ν	Poisson ratio	
Ω	Angular Speed of rotor	$rad.sec^{-1}$
ϕ_p	Angle of ply between the shaft and fiber axis	rad

ρ	Density of the material	$Kg.m^{-3}$
ω_1, ω_2	Angular frequencies of rotor	$rad.sec^{-1}$
σ_1	Detuning parameter	$rad.sec^{-1}$
θ_x	Angular displacement around x axis	rad
θ_y	Angular displacement around y axis	rad
θ_z	Angular displacement around z axis	rad
$\alpha_1, \alpha_2, \beta_1, \beta_2$	Functions of geometric and material properties of rotor	

[This page intentionally left blank]

Objective of the Thesis

The objective of the present work is to investigate the nonlinear dynamic behavior of the rotor systems analytically and numerically, taking into account the significant effects, for example, higher order large deformations in bending, geometric nonlinearity and shear effects. The work is divided into two major parts. In the first part, various mathematical models are developed considering different effects, for example, by considering nonlinearity due to higher order large deformations in bending and shear effects. In addition, if the supports of the rotor do not allow the shaft to move in the axial direction, then there will be a dynamic force acting axially on the rotor as it operates. This force will also produce large deformations in bending. Rotor large deformation can be result of overloading, over-speed, resonance, whirling, accident, component failure, surge, stall, off design operation, etc and may lead to stress exceeding the safe limit, failure of machine component, machine explosion and equipment coming apart. Each scenario can cause serious damages and injuries. For reliability and safety assessment of all possible scenarios of rotating machine malfunction, it is necessary to model and analyze the dynamic behavior of rotors under large deformations. Large deflection of rotor entails large strain to sensitive multi-component structure and may impose excessive stress to each component of rotor which could lead to damage or even collapse. Repair processes of rotors are very expensive and time consuming. Also shut down results in loss of plant revenue for repair period. Therefore, operation of machine must be carried out with reasonable prediction and knowledge of deformations in rotor and forces to machine components.

Moreover, there are other secondary effects that should be considered for increasing the accuracy of the predicted results. These include rotary inertia effects, gyroscopic effects and rotor mass unbalance effects. These models consist of 2^{nd} order nonlinear differential equations of motion when shear deformations are not considered. When the shear effects are also taken into account, the developed mathematical models consist of 4^{th} order nonlinear differential equations of motion. In the second part the challenge of solving various nonlinear models developed in the preceding part is addressed. Analytical and numerical methods are applied in order to treat the nonlinear equations of motion.

Hamilton's principle [GR92] is used to formulate the equations of motion. The linear part of the various models developed is analyzed for the first mode to obtain the natural frequencies of vibrations. Then, in order to solve the complete model including nonlinear terms, the Method of Multiple Scales (MMS) [NM95] is applied. This is a well known perturbation method [N93] and has been proven to be very effective for solving nonlinear equations of motion. See, for example, [MMPD08], [MAG06], [JZ98]. Resonant curves are plotted for different possible resonances and the effect of nonlinearity is discussed in comparison to the linear analysis. The forced response of the rotor system due to an unbalanced mass by changing different rotor parameters is also presented and the results are plotted graphically and discussed. When shear deformations are taken into account, the analysis is conducted for various slenderness ratios to highlight shear effects on the dynamics of both rotating shafts and shaft-disk rotor systems.

[This page intentionally left blank]

Thesis Organization

Chapter 1

This chapter illustrates a state of the art for the dynamic analysis of the rotors. The objective and contribution of the thesis is discussed in the light of the bibliographic work. A brief introduction of various important aspects of rotordynamics is discussed. The significance of considering the nonlinearities on the dynamic behavior of rotors is discussed with references to some research work available in the literature to date.

Chapter 2

This chapter is dedicated to the mathematical modelling for analyzing the dynamic behavior of rotors. Various models containing nonlinear differential equations of motion are developed for different rotor configurations. These models consist of 2^{nd} and 4^{th} order nonlinear differential equations of motion. Technical and theoretical aspects of taking into account various effects like higher order large deformations, geometric nonlinearity, shear effects, gyroscopic and rotary inertia effects are visualized and discussed. The models are developed using both the Euler-Bernoulli and Timoshenko beam theories.

Chapter 3

This chapter analyzes some of the mathematical models developed in the preceding chapter. Effects which give rise to nonlinearity like higher order large bending deformations and geometric nonlinearities are combined in a single model. The model thus developed is solved using method of multiple scales (MMS). There are two methods for the application of this method .i.e., direct method and discretized method. The analysis procedure for both of these approaches is discussed. The discretization approach is applied in order to find the nonlinear dynamic response of the equations of motion which were developed for the work of this thesis. The results are obtained both analytically and numerically. Three methods are used for analyzing the results: The method of multiple scales, a step by step method in Matlab and Simulink and a continuation procedure called Matcont. The results obtained by different methods are compared, graphically presented and discussed. Effects of varying different rotor parameters on the nonlinear dynamic response of the rotor system under investigation are also presented and discussed.

Chapter 4

This chapter focuses on the combined effect of nonlinearities and shear effects on the linear and nonlinear dynamic behavior of the rotors. The mathematical model which is treated in this chapter consists of 4^{th} order nonlinear differential equations of motion. The method of multiple scales is applied to the 4^{th} order derivatives with respect to time. The nonlinear response of the system is discussed and graphically presented as resonance curves.The influence of various parameters on the nonlinear behavior is analyzed. The effects of shear are discussed in detail both on the linear as well as nonlinear response of the rotor system under study.

Chapter 5

This chapter discusses the overall conclusions of the thesis. Also, based on the work performed for this thesis, there are future perspectives, which are also mentioned in detail. A description of the work already carried out is given which can be extended in future. The main perspectives include the study of nonlinear dynamic behavior of the rotors under some base movements. i.e. the supports of the rotor are not fixed but can be subjected to different movements like simple translation, a constant acceleration, sinusoidal translatory motion, simple rotation and sinusoidal rotation.

Chapter 1: Identification of the Problem - State of the Art

This chapter illustrates a state of the art for the dynamic analysis of the rotors. The objective and contribution of the thesis is discussed in the light of the bibliographic work. A brief introduction of various important aspects of rotordynamics is discussed. The significance of considering the nonlinearities on the dynamic behavior of rotors is discussed with references to some research work available in the literature to date.

1.1. Introduction

Rotordynamics is a subset of vibration analysis that deals with the dynamic characteristics of rotating machines. Over the years rotordynamics has become an important field in many engineering applications such as jet engines, helicopter rotors, turbines, compressors and the spindles of machine tools, etc. Rotor dynamics has a remarkable history of developments, largely due to the interplay between its theory and its practice. The research in this field has been carried out for many years. Dr. Ales Tondl [T65] discussed some basic problems of rotordynamics.

Rotor dynamics has been driven more by its practice than by its theory. This statement is particularly relevant to the early history of rotor dynamics. Research on rotor dynamics spans at least 14 decades of history. Reliability assessment and risk analysis of rotating machine rotors in various overload and malfunction situations present challenge to engineers and operators. Among the components of machines designed to transmit power, the most important are the shaft or shaft-disk assemblies. The analysis in all the above mentioned works is based on linear equations of motion. The prediction and analysis of the dynamic behavior of rotor systems are crucial because their rotating components possess unlimited amounts of energy that can be transformed into vibrations. However, these vibrations can disturb the performance of the rotor system and even cause its total destruction.

The mechanical system that contains rotating elements is usually referred to as rotor system. A rotor is a body suspended through a set of cylindrical hinges or bearings that allow it to rotate freely about an axis fixed in space. Engineering components concerned with the subject of rotor dynamics are rotors in machines, especially of turbines, generators, motors, compressors, blowers and the like. Rotors of machines have, while in operation, a great deal of rotational energy, and a small amount of vibrational energy. The purpose of rotor dynamics as a subject is to keep the vibrational energy as small as possible. In operation rotors undergo bending, axial and torsional vibrations.

Kinetic energy of these rotating elements forms an internal source of energy. This internal source of energy can be considered infinite because due to the connection of the rotor system with the driving system the kinetic energy accumulated in the rotating elements always exists. It means that, in certain circumstances, unlimited amount of energy can be transferred into vibration of the rotor-system. These vibrations disturb the technological processes the machine is design for, resulting in shorter life-times and very often leading to its destruction. These vibrations can be developed even if there are no external forces acting on the rotor-system. Therefore prediction and attenuation of vibrations of the rotor - system are very important from an engineering point of view on both: the design stage and during maintenance. Prediction of the dynamic behavior of the rotor-system requires analysis of the mathematical model that quantitatively reflects its dynamic properties. Computations of critical speeds and steady-state response at synchronous and subcritical resonances become essential for system design, identification, diagnosis, and control. In the practical design of

rotating machinery, it is necessary to know accurately the natural frequencies, modes and forced responses to unbalances in complex-shaped rotor systems. The most common representative techniques used for this purpose are TMM (Transfer Matrix Method), FEM (Finite Element Method) and Method of Multiple Scales (MMS). TMM is particularly useful for multi-rotor-bearing systems. See [YI01].

1.1.1. Significance of Nonlinearities in Rotordynamics

These days there is a tendency to produce machines which operate at high speed and are lightweight, for example, the gas turbine for propulsion of an aircraft, power-plant turbine, etc. In the present rotating machinery, non-linear vibration phenomena sometimes occur in the shrinkage fit rotor, in the assembly rotor and in the power-plant rotor with coil. Non-linear vibration phenomena also occur in a high polymer rotor, which is used for lightweight construction of an aircraft engine. Vibration analysis of such rotor systems is usually performed by the finite element method (FEM) with linear model. When a large amplitude vibration occurs, however, linearized spring and damping coefficients cannot model the complicated non-linear rotor system. It is important to consider the non-linear characteristics in vibration analysis and design of rotor systems. On the other hand, it is necessary that a high-speed rotor system used for the gas turbine for propulsion of an aircraft, power-plant turbine, etc. promptly pass a critical speed. Accordingly, the casing is often modelled elastically to decrease the critical speed. When such a rotor-bearing-casing system vibrates, the casing is excited and can come in contact with the rotor. Also there is a danger that the bearing will be damaged. Therefore, the investigation of the response of a rotating machine is very important from the viewpoint of stable operation. To construct a real mathematical model in vibration analysis, dynamic characteristics of rotor, bearing and casing should be considered. These conditions may cause non-linear vibrations. In the analysis of a large complex degrees of freedom (d.o.f.) mechanical system, the substructure synthesis method (SSM) has been studied for efficient vibration analysis, Iwatsubo *et al.* [IKM98] proposed an approximate analytical method to analyze the dynamic problems of a non-linear rotor-bearing-casing system using the SSM and a perturbation method. They applied the SSM technique to reduce the overall size of the problem and obtained approximate solutions by applying the perturbation method. Moon *et al.* [MKY99] presented an analytical method to analyze the vibration of a non-linear rotor-bearing-casing system by applying the perturbation method. They considered the non-linearity in the shaft and bearing part and considered the effect of non-linear sensitivity in the subsystem. They derived the formulation of perturbation first order under the condition that the exciting force is near the first critical frequency of the system.

Also the increasing need of optimized performance of machines adds to the importance of considering nonlinear effects on their dynamics. Nonlinearities in rotating machines can arise due to many reasons. For example, clearances in a ball bearing, see, [KWC02], oil film in a journal bearing, clearance in a squeeze-film damper bearing, magnetic force between the rotor and stator in a motor, contact between rotor and stator [Y01].

Chang and Cheng [CC93] analyzed the instability and nonlinear dynamics of a slender rotating shaft with a rigid disk at the midspan.The analysis was conducted using centre manifold theory. Nonlinearities also occur when the deflections become large, for example, a high polymer rotor used for lightweight construction of an aircraft, turbine shaft, a composite helicopter-rotor. Almasi presented a model for large deformations of a rotor based on virtual work theory [A09] When a large amplitude vibration occurs, linearized spring and damping coefficients cannot model the

complicated non-linear rotor system. Therefore, it is important to consider the non-linear characteristics in vibration analysis and design of rotor systems. For small amplitude oscillations the response of a deformable body can be adequately described by linear equations and boundary conditions. However as the amplitude of oscillation increases, nonlinear effects come into play. The source of the nonlinearities may be geometric, inertial, or material in nature. The geometric nonlinearity may be caused by nonlinear stretching or large curvatures. Nonlinear stretching of the midplane of a deformable body accompanies its transverse vibrations if it is supported in such a way as to restrict movement of its ends and/or edges. This stretching leads to a nonlinear relationship between the strain and the displacement. If the large amplitude vibrations are accompanied by large changes in the curvature, it is necessary to employ a nonlinear relationship between the curvature and the displacement. Nonlinear inertial effects are caused by the presence of concentrated or distributed masses. Material nonlinearity occurs whenever the stresses are nonlinear functions of the strains.

The modal analysis technique is one of the most valuable tools for analyzing linear structures and from its results the response of a structure may be found by solving ordinary differential equations with constant coefficients. The modal analysis allowed the development of reduction techniques that are very well developed nowadays. For example, the pseudo-modal method (Lalanne and Ferraris, 1990), the phenomena causing non-linearties lead to non-linear differential equations of motion to express the system dynamics. Various methods are available for analyzing nonlinear structures, such as perturbation methods, harmonic balance methods, normal forms and center manifold methods. The method of the invariant manifold approach is also well-known which brings the concept of modal analysis to nonlinear problems. This technique has been numerically investigated for a nonlinear rotor-bearing system by Villa *et al.* see [VST05].

The approach in predicting dynamic behavior of rotors can be linear or nonlinear. In linear systems the restoring force terms, damping terms, and inertia terms are represented by the first order functions of deflection, velocity and acceleration. However, such equations of motion are approximate expressions since deflections are considered small. But when the deflections become large, phenomenon due to nonlinearity may occur. The importance of considering the nonlinear and/or material constitution effects in the dynamic analysis of rotating equipment has increased in line with current demand for accurate and optimized performance. Thus this field has become more challenging because the analysis of the nonlinear phenomena is far more difficult in comparison to linear analysis. In additions, since a rotor executes a whirling motion due to gyroscopic moment, analytical methods used in the analysis of rectilinear systems cannot be applied directly to rotor systems. In a recent special issue of the Journal of Nonlinear Dynamics on ‘Recent Advances in Nonlinear Rotordynamics’, various topics concerning nonlinear rotordynamics have been addressed [WI09].

Practically many resources may contribute to nonlinearity. For example, higher order large deformations, rotor-base excitations, geometric nonlinearities, oil film in journal bearings, magnetic bearings, clearance in a ball bearing, clearance in a squeeze-film damper bearing, and magnetic force between the rotor and a stator in a motor. One important source of nonlinearity comes from material considerations. For example if the shaft of a rotor system is made up of a composite material, it can produce vibrations of much larger amplitudes than those of metallic shafts, leading the system to become nonlinear. In general, analysis of rotor under large deformations requires: nonlinear complex behavior simulation, changes in stiffness due to the changes in rotor geometry, nonlinear restraint of support and consideration of contact with the other machine components. Due

to their many benefits composite materials are being used in various present day rotors especially in aerospace applications where weight reduction and optimized design is of great interest.

Shabaneh and Zu [SZ03] investigated the dynamic analysis of a single-rotor shaft system with nonlinear elastic bearings at the ends mounted on viscoelastic suspension. Timoshenko shaft model was utilized to incorporate the flexibility of the shaft; the disk was considered to be rigid but located at the mid-span of the shaft.

1.1.2. Contribution of the Present Work

In the present thesis the nonlinear dynamic behavior of the rotors is investigated considering the effects like higher order large deformations in bending, geometric nonlinearity and the effects of shear deformations. Both analytical and numerical approaches are used. Various mathematical models incorporating different effects are developed and the detailed derivation of equations of motion is presented and discussed. New energy expressions for the strain energy of the shaft undergoing large bending deformations and geometric nonlinearity are developed. Rayleigh-Ritz method, Hamilton's principle and Lagrange equations are used to formulate the equations of motion. The equations of motion are nonlinear differential equations. Due to the contribution of higher order large deformations in bending the equations of motion are 2^{nd} order nonlinear differential equations. However when shear deformations are also taken into account, the developed mathematical model consists of 4^{th} order nonlinear differential equations of motion. Also if the supports of the rotor do not allow the shaft to move in the axial direction, then a dynamic force will act on the rotor axially [INIL96]. This force will also produce large deformations in bending. The equations of motion developed considering this dynamic force are also 2^{nd} order nonlinear equations of motion. A case study for the dynamic analysis of the composite rotors is also performed. Vibration analysis of the composite rotors with one disk considering the gyroscopic effect is presented. Campbell diagrams are plotted for determining the critical rotor speeds. The results are compared with those already available in the literature.

Then some of the various mathematical models developed are analyzed both analytically and numerically. The linear part of these models developed is analyzed for the first mode to obtain the natural frequencies of vibrations. Then, in order to solve the complete model including nonlinear terms, MMS is applied. After the resolution of nonlinear equations of motion, resonant curves are plotted for different possible resonances and the effect of nonlinearity is discussed in comparison to the linear analysis. The forced response of the rotor system due to an unbalanced mass by changing different rotor parameters is also presented and the results are plotted graphically and discussed. When shear deformations are taken into account, the analysis is conducted for various slenderness ratios to highlight shear effects on the dynamics of both rotating shafts and shaft-disk rotor systems. The effects of shear were discussed in detail for both the linear as well as nonlinear response of the rotor system. The results of the linear analysis, for a rotating shaft and a shaft-disk rotor system, showed that with the inclusion of shear deformations the critical speeds of the rotor tend to decrease. This difference becomes more visible for higher values of the slenderness ratio r. As compared to a shaft-disk rotor system the shear effects have more notable influence in the case of a solid and tube sections of the shaft.

It is presented and discussed that nonlinearities along with other phenomena like gyroscopic, rotary inertia and mass unbalance effects significantly influence the dynamics of the rotor system. The linear analysis showed that resonance existed only at the second critical speed, but in the nonlinear analysis another resonance appeared at the first critical speed. Furthermore, nonlinearities caused the

resonance curves to be of hard spring type. The combined effect of nonlinearities and shear effects on the linear and nonlinear dynamic behavior of the rotors have also been studied.

1.2. Predictions of the Dynamic Behavior of Rotors

A rotor system consists of the basic elements like the disk, the shaft, the bearing and the seals. When we design rotating machinery, we have to predict the dynamic behavior of the rotor in torsion and in bending. It is necessary to find the natural frequencies. The critical speeds are determined with the natural frequencies. See. [LF98]. The general rotor equations are derived by the means of the following steps:

The kinetic energy of the disk and the shaft, the strain energy of the shaft and the virtual work of the external forces are calculated for the elements of the system.

The Rayleigh-Ritz method is applied for a small number of DOF and Finite Element Method is used for engineering applications.

1.3. Classification of Rotor Systems

A rotor system can consist of disks of various shapes, shafts of various diameters and bearings situated at various positions. In vibration analysis the complex rotor system is simplified and a suitable mathematical model is used. In modeling process we must know which parameters are important for the system. Rotating machines are classified according to their characteristics as follows:

1.3.1. Rigid Rotor:

If the deformation of the rotating shaft is negligible in the operating speed range, it is called a rigid rotor.

1.3.2. Flexible Rotor:

If the shaft deforms appreciably at some rotational speeds in the operating speed range, it is called a flexible rotor.

The deformation of a rotor becomes highest in the vicinity of the critical speeds. Therefore the range of the operating speed relative to the critical speeds determines whether the rotor is rigid or flexible.

1.3.3. Lumped parameter system:

In some systems the disk is considered to be rigid and the distributed mass of an elastic shaft is concentrated at the disk positions. Such a system is called a lumped parameter system.

1.3.4. Continuous Rotor System:

If a flexible rotor with distributed mass and stiffness is considered, this model is called a distributed parameter system or a continuous rotor system.

1.4. Modes and Critical Speeds of Rotating Machinery

Real structures can be viewed as a series of finer and finer lumped mass approximations that approach a continuous mass distribution. The continuous structure has an infinite number of natural frequencies, each with its own characteristic vibration shape (mode).

As an example, consider a simple beam structure supported by pin joints at each end. This structure is simple enough that a closed-form solution to the natural frequencies and mode shapes is possible. The first three mode shapes are shown in Fig 1.

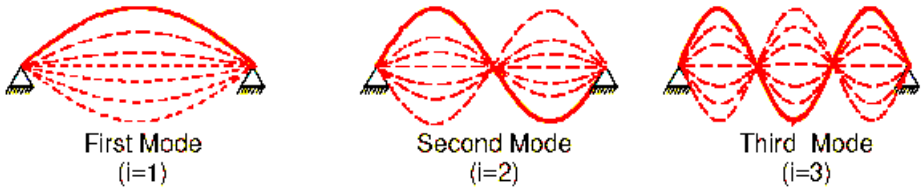

Fig. 1. First three mode shapes of pinned-pinned beam [SPW05]

The rotating machinery equivalent to the single spring-mass damper system is a lumped mass on a mass less, elastic shaft. This model, historically referred to as a '**Jeffcott**' or '**Laval**' model, is a single degree of freedom system that is generally used to introduce rotor dynamic characteristics. Swanson and Powel [SPW05] have used a slightly more complex multi-degree of freedom model corresponding to a physical rotor as shown in Fig 2.

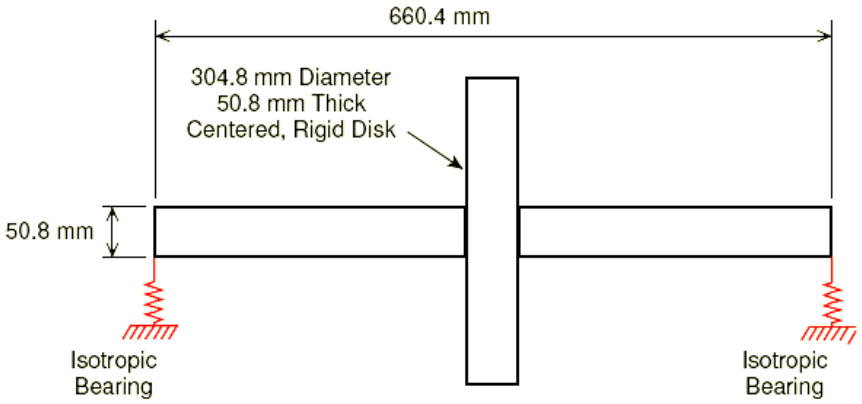

Fig. 2. Basic Machine Model cross section [SPW05]

If it is supposed that the machine is not spinning and that there are three versions of this machine with soft, intermediate and stiff bearings. Then by performing a model test we can find a set of natural frequencies and modes. Fig. 3 shows the first three mode shapes and frequencies for the three bearing stiffnesses.

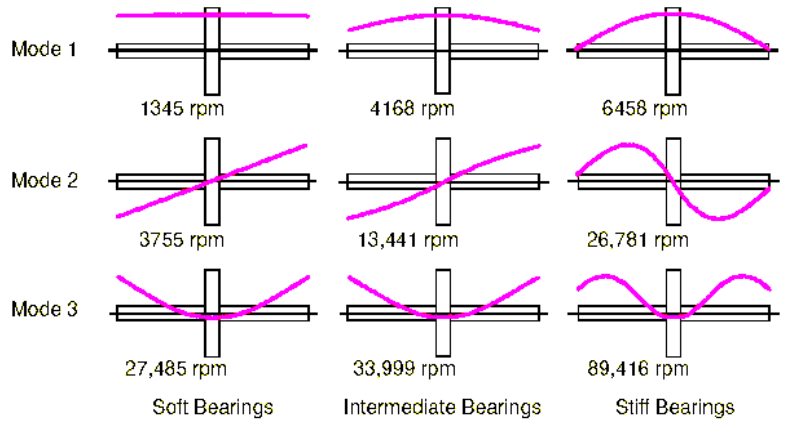

Fig. 3. Mode shapes versus bearing stiffness [SPW05]

Ratio of the bearing stiffness to the shaft stiffness has a significant impact on the mode shapes. For the soft and intermediate bearings the shaft does not bend much in the lower two modes. These are generally called ***'Rigid Rotor' modes***.

If we consider the rotating motion of the rotor now, mode shapes will look very much like as in non-rotating case. But now they involve circular motions instead of planner motions. See Figures (4) and (5).

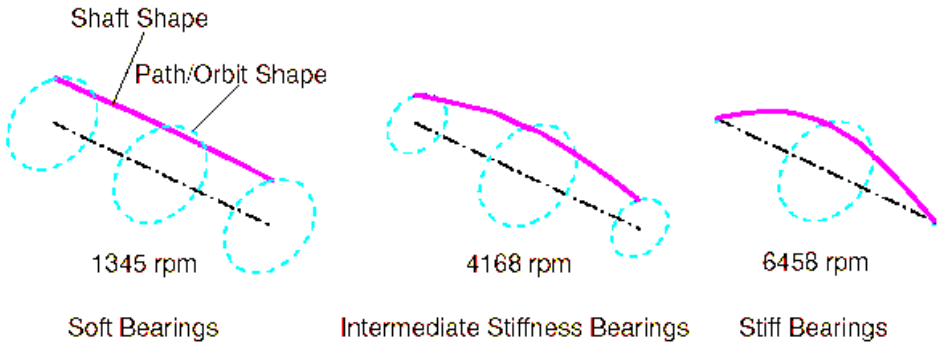

Fig. 4. 1st mode shapes and frequencies in rpm of rotating shaft [SPW05]

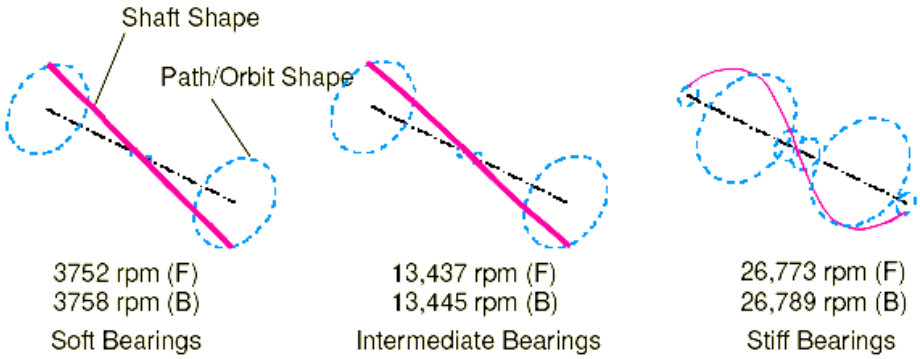

Fig. 5. 2nd mode shapes and frequencies in rpm of rotating shaft [SPW05]

As depicted in Fig. 5, the rotation of the shaft traces outline of a bulging cylinder. This mode, therefore, is called '***Cylindrical mode'.***

As depicted in Fig. 6, the rotation of the shaft traces outline of bulging cones. This mode, therefore, is called ***'Conical mode'.***

1.4.1. Forward and Backward whirls:

The whirling motion of the rotor can be in the same direction as the shaft rotation, 'Forward Whirl', or in the opposite direction of the shaft rotation 'Backward Whirl'. Fig. 6 shows rotor cross sections over the course of time for both synchronous forward and synchronous backward whirl. Note that for forward whirl, a point on the surface of the rotor moves in the same direction as the whirl. So that a point at the outside of the rotor remains to the outside of the whirl orbit. Simultaneous forward and backward whirling at different points of a Jeffcott rotor supported on identical journal bearings, has been examined by Rao, Bhat and Xistris. See [RBX95].

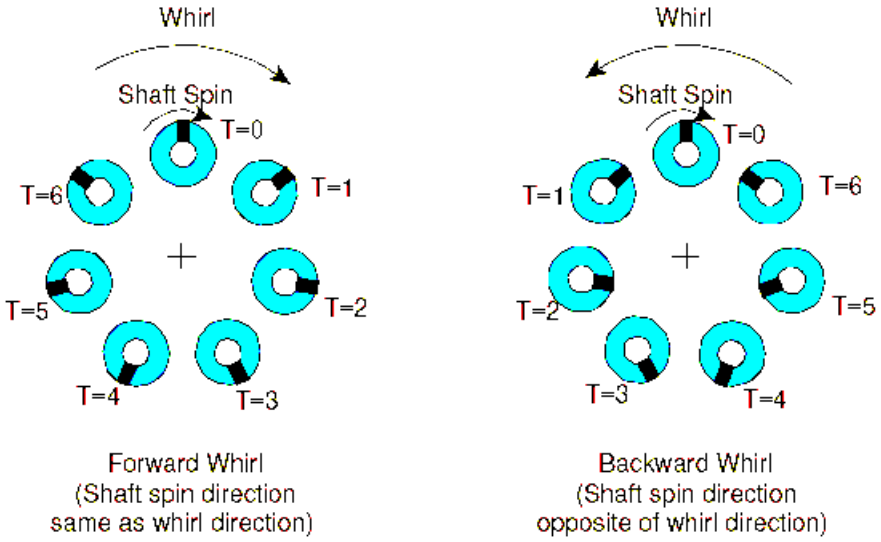

Fig. 6. Forward and Backward Whirl [SPW05]

The modal test can be performed to see the effects of changing shaft speeds, from non-spinning to a high spin speed and follow the two frequencies associated with the conical mode. Fig. 7 plots the forward and backward natural frequencies over a wide speed range. From this figure, we can see that the frequencies of the conical modes do change over the speed range. The backward mode drops in frequency, while the forward mode increases. The explanation for this surprising behavior is a ***'gyroscopic effect'*** that occurs whenever the mode shape has an angular (conical/rocking) component. First consider forward whirl. As shaft speed increases, the gyroscopic effects essentially act like an increasingly stiff spring on the central disk for the rocking motion. Increasing stiffness acts to increase the natural frequency. For backward whirl, the effect is reversed. Increasing rotor spin speed acts to reduce the effective stiffness, thus reducing the natural frequency. The gyroscopic terms are generally written as a skew-symmetric matrix added to the damping matrix.

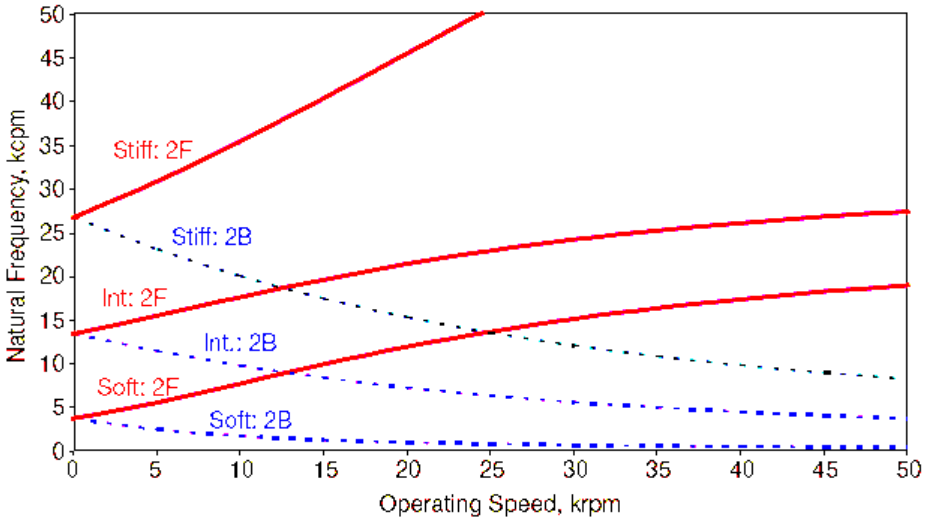

Fig. 7. Effect of operating speed on 2nd natural frequencies [SPW05]

1.4.2. Critical Speeds:

The American Petroleum Institute (API), in API publication 684 (First Edition, 1996), defines critical speeds and resonances as follows:

A shaft rotational speed that corresponds to the peak of a noncritically damped (amplification factor > 2.5) rotor system resonance frequency. The frequency location of the critical speed is defined as the frequency of the peak vibration response as defined by a Bodé plot (for unbalanced excitation). Whenever the rotor speed passes through a speed where a rotor with the appropriate unbalanced distribution excites a corresponding damped natural frequency, and the output of a properly placed sensor displays a distinct peak in response versus speed, the machine has passed through a critical speed. Critical speeds could also be referred to as “peak response” speeds. As with the structural case, one can also consider a speed (i.e., unbalance excitation frequency) that coincides with a damped natural frequency (i.e., a resonance), generally termed “damped critical speeds.” Numerically, these are distinct from critical speeds as defined by the API specification. For very light damping, they are fairly close. For increasing levels of damping, they become noticeably different.

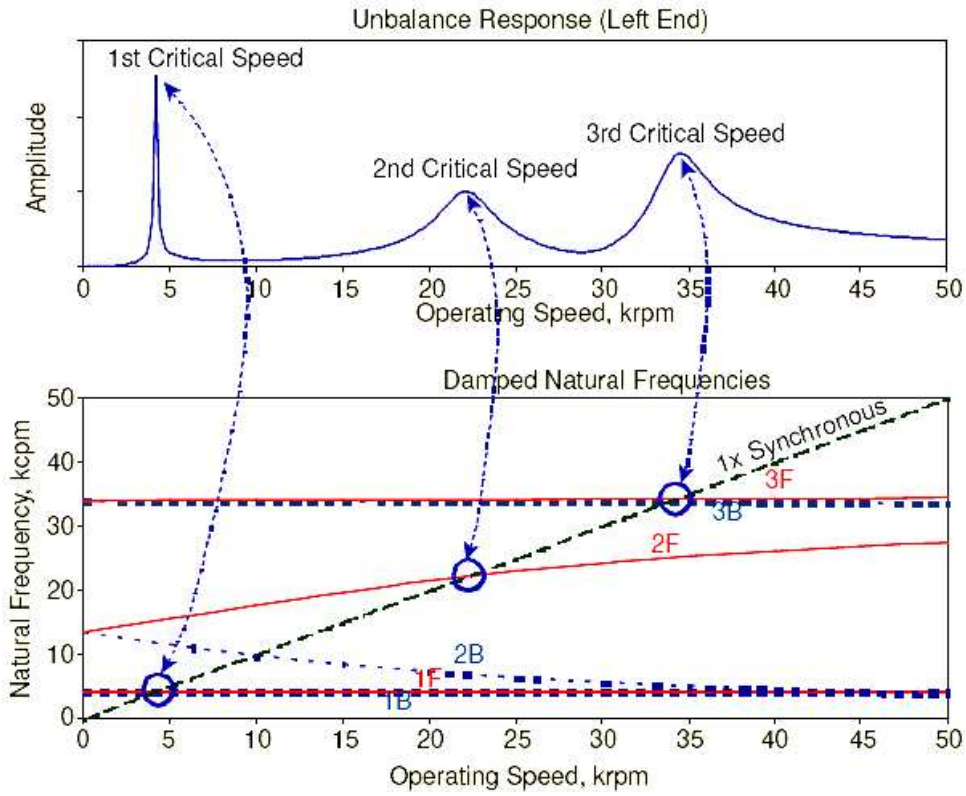

Fig. 8. Natural frequency versus Critical speeds [SPW05]

If a medium stiffness centre disk model is used and an unbalance distribution that excited the first three modes is added, the resulting vertical displacement response as a function of speed is shown in Fig. 8. The damped natural frequency versus speed plot is called 'Campbell Diagram' is also shown above in Fig. 8.

1.5. The Method of Multiple Scales

Another technique is the method of multiple scales in which solution is obtained by introducing multiple time scales and a dimensionless parameter, say ε. In the analysis of nonlinear systems, there are a lot of analyzed research works using the method of multiple scales for the single d.o.f. and multi d.o.f of non-linear vibration system. See [N73], [M78], [HM87], [N93] and [NM95]. However, the study, which applied the method of multiple scales to the non-linear vibration analysis of rotor system, was not reported until Moon and Kang analyzed the harmonically excited non-linear system using this method. See [MK03]. Their method was based on the substructure synthesis formulation and a multiple scales procedure, which was applied to the analysis of non-linear responses. A rotor bearing system was used. The Fig 10 shows the rotor-bearing casing system. The rotor is supported by bearings that are fixed on the casing. The casing and the foundation are elastically connected. The rotor has the material non-linearity. The whole system is divided into three components. The rotor has non-linear restoring force so that it is regarded as a non-linear component, while the casing is considered to be a linear component and the bearing is modeled as a linear assembling component.

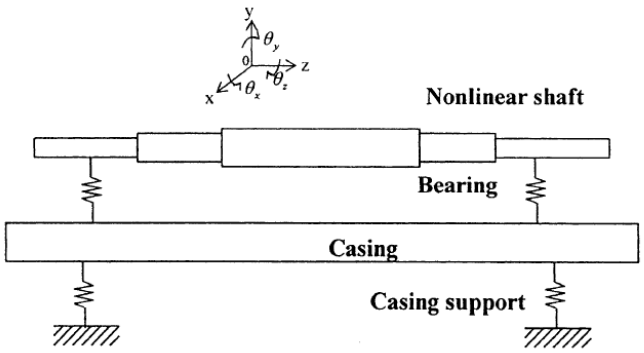

Fig. 9. Rotor-bearing-casing system [MK03]

An analytical technique was presented based on the method of multiple scales theory and the mode superposition principle for the dynamic analysis of non-linear mechanical systems. It was shown that by applying the method of multiple scales, the governing equations of the complex nonlinear system attained a compact form and could be solved.

Ji and Zu. [JZ98] applied method of multiple scales for vibration analysis of rotor–shaft systems with non-linear bearing pedestal model. This method was adopted for free vibration analysis and forced vibration analysis of shaft rotor systems with a non-linear bearing pedestal model. The shaft was modeled based on the Timoshenko beam theory. A typical roller bearing model was assumed which had cubic non-linear spring and linear damping characteristics. Non-linear natural frequency response and steady state response were obtained using the third order perturbation expansion. A typical non-linear rotor bearing system was simulated to show the effectiveness of the analysis method and to illustrate the non-linear effect on the free and forced vibrations of the system.

Das *et al.* [DRP05] investigated large amplitude free vibration of a rotating beam with non-linear spring and mass system as shown in Fig. 10.

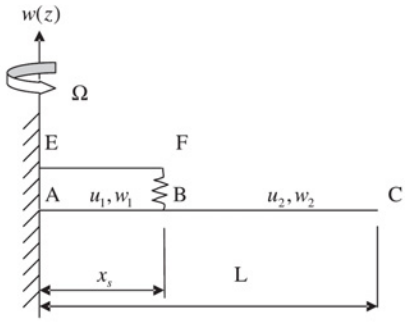

Fig. 10. Rotating Beam with Spring-Mass System [DRP05]

The equation of motion of a rotating beam with a non-linear constraint starting from transverse/axial coupling through axial strain was formulated. The non-linear constraint appears in the boundary condition and its mass was considered during the analysis. A non-linear solution was determined by applying methods of multiple time-scales directly to the partial differential equations and the boundary conditions. The influence of the location of the non-linear constraint on non-linear frequencies was also studied.

1.6. On the Study of Dynamic Analysis of Composite Rotors

In present days composite materials are being incorporated in rotors especially in aerospace (helicopter) industry [B94] and automotive applications. Studies on composite shafts started in 1970's, with two viable materials, boron/epoxy and carbon/epoxy. The two U.S. patents by Worgan and Smith [1978] and Yates and Rezin [1979] indicate that the preliminary hurdles to a composite driveshaft design were overcome. Hetherington *et al.* [HKD90] demonstrated the feasibility of a supercritical composite helicopter power transmission shaft. Singh and Gupta [SG95] estimated the critical speeds and unbalance response by a layerwise theory. They have shown that a layerwise theory gives more realistic stress field in tubular composite shaft. Detailed theoretical dynamic analysis and rotordynamic experiments on composite shafts have been carried out by Singh [S92]. In the early developments, composite shafts were designed to operate in the sub-critical range. Therefore, initial studies were directed towards design requirements and in overcoming the problems in practical application. Subsequently, in order to derive greater advantage in terms of reduction of weight, the possibility of super-critical operations of composite shafts was explored.

There are few analytical and experimental studies on rotordynamic aspects of composite shaft behavior. Table1. Summarizes the various configurations used for composite shaft rotordynamic studies. It may be noticed, from the table that the shaft geometric parameters Length/radius and thickness/radius ratios) vary over a wide range, which might explain some of the differing experiences of various authors.

Table. 1. Configurations used for tubular composite shaft rotordynamic analysis [SG96a]

Author	Shaft Dimensions	Operation (Max. Speed)	Material [Fiber Lay-up]
Zinberg and Symmonds [1970]	R = 12.7cm L/R = 20.6 t/R = 0.103	Sub-critical (< 5500 RPM)	boron/epoxy [90°, 45°, −45°, 0_6°, 90°]
Bauchau [1981]	R = 4.48cm L/R = 32.3 t/R = .07–.14 (Tapered Shafts)	Sub-critical	graphite/epoxy [$0°_2$, 45°, $0°_2$, −45°, $0°_2$, 45°, −45°]
Zorzi and Giordano [1985]	R = 1.59cm L/R = 68.6 t/R = 0.19	Super-Critical 9500 RPM (with disks)	Hybrid of glass/epoxy and graphite/epoxy [±45° (HS), ±10° (HM), 90° (E-glass)]
Kraus [1988]	R = 1.2cm L/R = 203 t/R = 0.074	Super-Critical 3800 RPM	graphite/epoxy [± 40°, ± 5°]
Singh and Gupta [1996a]	R = 5.2cm L/R = 21.7 t/R = 0.096	Super-Critical 4000 RPM	graphite/epoxy [±45° (I, S45M) ±60° (II, S60M)]

R = Mean Radius; L = Length; t = Wall Thickness.

A boron/ epoxy composite tail rotor driveshaft for a helicopter was described by Zinberg and Symmonds [ZS70]. The critical speeds were determined using equivalent modulus beam theory, assuming the shaft to be a thin walled circular tube simply supported at the ends. The shaft critical speed was determined by extrapolation of the unbalance response curve which was obtained in the sub-critical region.

Rotordynamic experiments on an aluminium shaft as well as on a composite shaft were conducted by Zorzi and Giordano [ZG85].They reported excellent matching between theoretical and experimental results. The composite shafts consisted of three different layers of graphite/epoxy and

glass/epoxy and were filament wound. Experimental testing was carried out on all three shafts, with and without lumped mass disks. Some important observations were made during the experimental studies. The super-synchronous component corresponding to first critical speed became significant when the shaft speed reached 1/2 or 1/3 of the first critical speed. It was shown that, although the shafts were not of optimized design, a substantial payoff in terms of critical speed was achievable. The shafts were shown to have increased sensitivity to unbalance near the critical speed. This was determined from the large values of influence coefficients near the critical speeds and a very small value of the final correction masses.

The critical speeds of a composite shaft including the effects of bending-twisting coupling were obtained by Kim and Bert [KB93] .The shaft was modeled as a Bresse-Timoshenko beam. The shaft gyroscopic effects were also included. The results compare well with Zinberg's rotor [ZS70].

A series of studies on composite shafts were carried out by Lim and Darlow [LD86] and Hetherington *et al.* [HKD90].They have shown the possibility of reduction of 60% in the total system weight of the tail drive rotor. The optimized shafts were tested for rotordynamic performance. The shafts were tested under no load condition. In order to balance the shaft up to the second critical speed a unified balancing approach was used. An aluminium shaft was tested for comparison purposes. A beat motion with constituent frequencies as synchronous speed and shaft natural frequency was observed just above the first critical speed.

EL-Mahdy and Gadelrab [EG00] analyzed the free vibration of a unidirectional fiber reinforcement composite rotor and compared it with traditional material rotors. It was observed that the composite rotor system may give higher natural frequencies than those made of conventional materials due to higher stiffness to mass ratio. Four composite materials were considered, graphite-epoxy, carbon-epoxy, boron-epoxy and E-glass-epoxy, for the fabrication of the rotor system. Typical design data of different composite materials for the 1st three natural frequencies were presented. Experimental work has been carried out on a composite rotor made of E-glass/epoxy with fiber volume fraction ($V_f = 0.43$) having one steel disk at the mid-span. The structure equation of motion was obtained as,

$$[M]\ddot{X} + [K][X] = [0] \tag{1.1}$$

The results for the Young's modulus and the densities of the composite material (E_{11} and ρ_{11} respectively) were written as,

$$\rho_{11} = \rho_f V_f + \rho_m V_m \tag{1.2}$$

$$E_{11} = \left(E_f V_f + E_m V_m\right) + \left[\frac{4V_f V_m \left(\nu_f - \nu_m\right)^2}{\left(V_m / K_f + V_f / K_m + 1/G_m\right)}\right] \tag{1.3}$$

Where,

$$K_f = \frac{E_f}{3\left(1-2\nu_f\right)}$$
$$K_m = \frac{E_m}{3\left(1-2\nu_m\right)} \tag{1.4}$$

Also,

E_f, V_f, v_f, K_f are the elastic modulus, volume fraction, the Poisson ratio and plane strain bulk modulus for the fiber material, respectively.

E_m, V_m, v_m, K_m are the elastic modulus, volume fraction, the Poisson ratio and plane strain bulk modulus for the matrix material, respectively.

G_m is the shear modulus for the matrix.

Fig. 11 below, shows the experimental frequency response function for rotor.

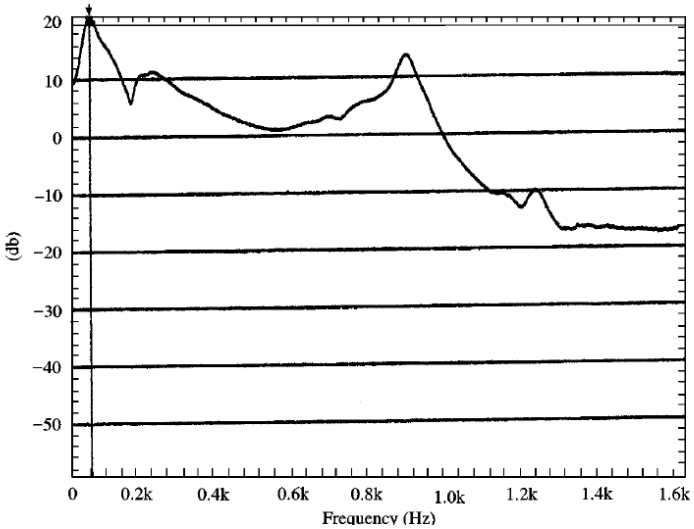

Fig. 11. Frequency Response Function (Steel) [EG99]

The natural frequencies of the rotor (shaft and disk having different materials) are given in Table 2 as a reference. It was concluded that the E-glass/Epoxy gives the lowest values of the natural frequencies because E_{11} for the material was lower than that of the other composite materials.

Table. 2. The natural frequencies of rotor (Hz) with different materials

Disk	Shaft	Symbol	f_1	f_2	f_3
E-glass/epoxy	Boron/epoxy	Eg/Bor	61·7	401·7	840
Graphite/epoxy	Boron/epoxy	Gr/Bor	63·3	408·3	845
Boron/epoxy	Carbon/epoxy	Bor/Cr	65·5	440	936·7
E-glass/epoxy	Carbon/epoxy	Eg/Cr	66·3	443·3	938·3
Graphite/epoxy	Carbon/epoxy	Gr/Cr	69	450	943·3
E-glass/epoxy	Graphite/epoxy	Eg/Cr	70	468	995
Boron/epoxy	E-glass/epoxy	Bor/Eg	18·3	121·5	256·7
Boron/epoxy	Graphite/epoxy	Bor/Gr	68·7	465	933·3
Carbon/epoxy	Boron/epoxy	Cr/Bor	63·3	406·7	845
Carbon/epoxy	E-glass/epoxy	Cr/Eg	19·2	123·7	258·3
Carbon/epoxy	Graphite/epoxy	Cr/Gr	71·1	473.3	998.3
Graphite/epoxy	E-glass/epoxy	Gr/Eg	19·3	124·3	260

Singh and Gupta [SG96] studied the effect of shear-normal coupling on rotor natural frequencies and modal damping. They analysed the results of the Equivalent Modulus Beam Theory **(EMBT)**

and the Layerwise Beam Theory **(LBT)** derived from a shell theory in order to understand their limitations and relative advantages. Formulation was outlined based on Ritz method for unbalance response and stability analysis of a multimass composite rotor (with tubular shaft) mounted on general eight coefficient bearings. Case studies of rotors mounted on rolling element and fluid film bearings were presented in order to bring out the salient features of the analysis. The moduli was expressed in terms of the tube parameters and the invariants of the material as,

$$E = \frac{\left\{4\left(U_1 - U_5\right)\left(U_5 + U_3\gamma_c\right) - \beta_c{}^2 U_2^2\right\}}{U_1 - \beta_c U_2 + U_3\gamma_c} \tag{1.5}$$

Where

$$\gamma_c = \sum_{i=1}^{n} \frac{t_i}{t}\cos 4\alpha_i$$
$$\beta_c = \sum_{i=1}^{n} \frac{t_i}{t}\cos 2\alpha_i \tag{1.6}$$

U_1, U_2, U_3, U_4, U_5 are laminate invariants. Invariants are combinations of stress or strain components that remain constant under coordinate transformation. They are important for assessing the relative performance of composite laminates. If invariants, such as the maximum normal strain of a laminate, are not used, the composite design may depend on the choice of the coordinate system.

Equivalent shear modulus is $G_E = U_5 - U_3\gamma_c$

Equivalent moduli were determined, and the conventional Timoshenko beam theory was extended in two dimensions and the additional rotor effects were included. The non-symmetric cross-coupled effects arise from bearing stiffness, bearing damping, gyroscopic effects and hysteretic material damping. Material damping was assumed in the form of discrete damping coefficients (viscous Cr and hysteretic Hr) at the mass locations. The dissipation function was calculated on the basis of effective displacements $W^e(X_r)$ and $V^e(X_r)$ which represent the total rotor deflection minus the deflection due to the rigid body motion. A composite rotor as per EMBT is shown in Fig. 12.

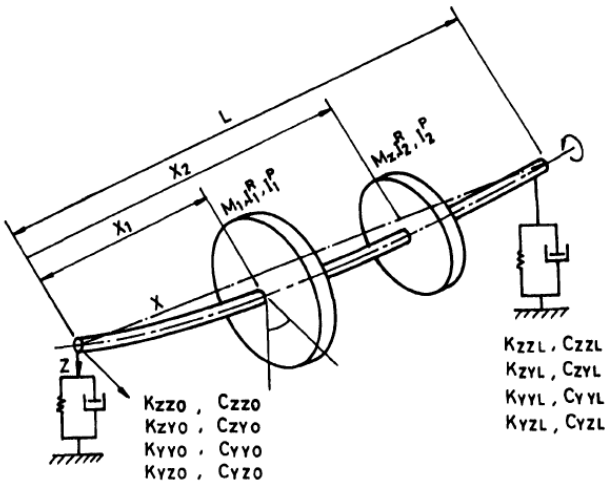

Fig. 12. A composite rotor as used by Singh and Gupta [SG96]

Layerwise Beam Theory can produce more accurate results. This theory can be obtained by reduction from a Layerwise shell theory by imposing the condition of zero cross sectional distortion. See [SG95].

A relationship between circumferential displacement v and radial displacement w was used. The resulting displacement in shell theory as used by Singh and Gupta [SG96], is

$$\begin{aligned} \bar{u}_{zi} &= u_i(x)\cos\theta \\ \bar{v}_{zi} &= -w(x)\sin\theta \\ \bar{w} &= w(x)\cos\theta \end{aligned} \tag{1.7}$$

Fig. 13 shows the displacement field in Layerwise beam theory. These conditions can be used in shell theory expressions and the strain and kinetic energies can be expressed in terms of u_i (x) and w(x) which becomes the displacement field for LBT.

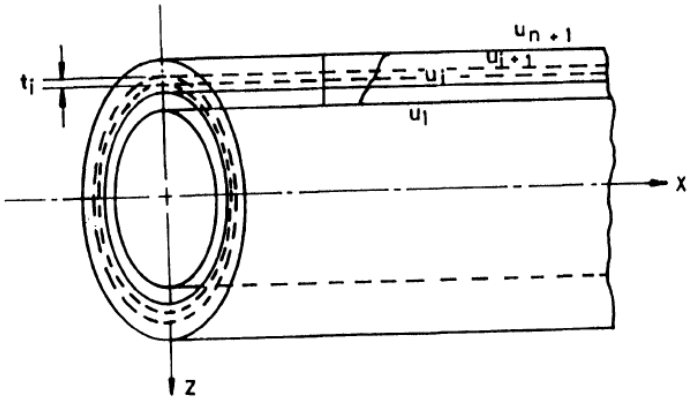

Fig. 13. Displacement Field in LBT [SG96]

The displacement field was extended in two perpendicular directions and additional rotor effects were incorporated. Rotordynamics were studied for both rolling element bearing as well as fluid film bearing.

Stacking sequence was varied to view the difference in results. See Table.3

Table. 3. Flexural Frequencies for different stacking sequences using LBT [SG96a]

Stacking Scheme (From inner radius)	1st Flexural (Hz)	2nd Flexural (Hz)	3rd Flexural (Hz)
0,45,45,45	305	1134	2313
45,0,45,45	310	1152	2349
45,45,0,45	315	1170	2386
45,45,45,0	321	1180	2422
EMBT value	314	1166	2376

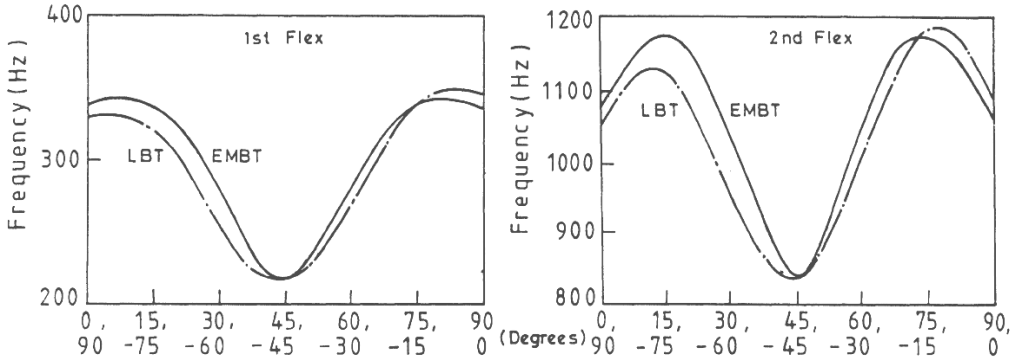

Fig. 14. Flexural frequency for two layered shaft [SG96a]

The first four modal frequencies and damping ratios at different speeds of rotation, for the test rotor supported on fluid film bearings were given for ply angles 30°,45°and 60°.Cambell plot for 30° ply angle is given in Fig.16 as a reference.

They also carried out the experimental rotordynamics studies on two filament wound carbon/epoxy shafts with constant winding angles (±45 and ± 60). See [SG96a] .It was observed that the presence of super synchronous components was more pronounced in the shaft having 60 fiber angle (compared to 45 fiber angle) and was suppressed when the balance condition of the rotor improved. The most likely cause appears to be material non-linearity derived from the matrix.

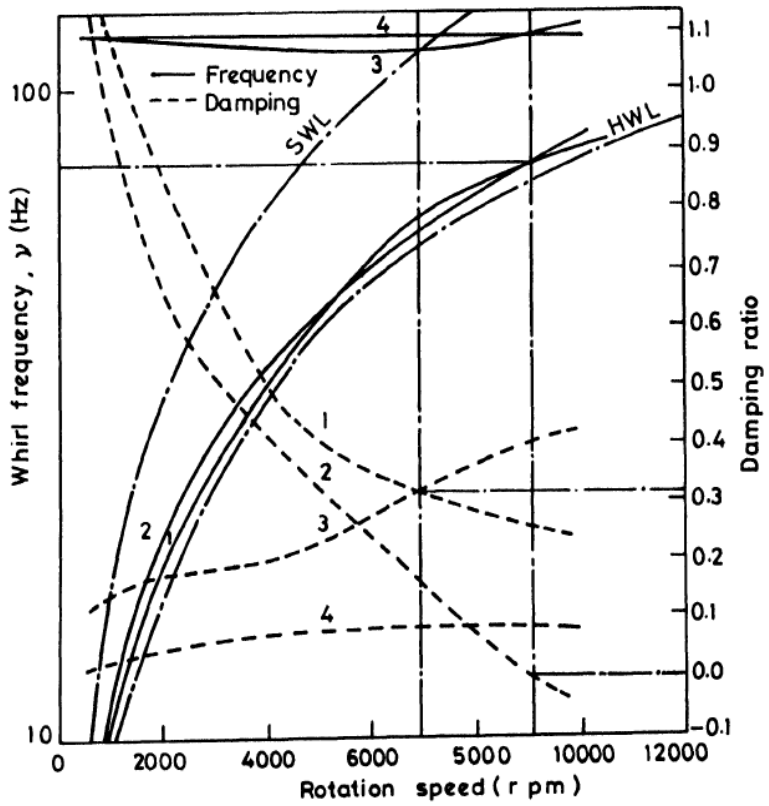

Fig. 15. Campbell diagram for 30° composite rotor on FF bearing [CLR02]

Chatelet *et al.* [CLR02] argued that analytical or numerical approaches based on beam theories can be limited by the assumptions involved. They showed that a direct finite element discretization can

overcome these limitations. They presented a numerical technique based on a three dimensional finite element discretization of the assembly for the calculation of natural frequencies and mode shapes of composite rotors. A model reduction based on the mode shapes at rest was used to calculate the behavior of the rotating structure and the disk-shaft assembly was assumed to be cylindrically symmetric. Their results showed the effects of possible couplings between shaft and disk deformations.

1.7. Conclusions

This chapter presented a state of the art for the dynamic analysis of the rotors. The objective and contribution of the thesis was discussed in the light of the bibliographic work. A brief introduction of various important aspects of rotordynamics was given. The significance of considering the nonlinearities on the dynamic behavior of rotors was discussed with references to some research work available in the literature to date. It is concluded that the study of the dynamic behavior of rotors has been a subject of practical importance for many years. A lot of work has been carried out in predicting the dynamics of metallic as well as composite rotors. But this is still an ongoing research especially when nonlinear effects are included to be investigated. In the present PhD thesis the main emphasis will be to incorporate and further expand the effect of nonlinearities on the dynamic behavior of rotors.

Chapter 2: Mechanical Modeling

This chapter is dedicated to the mathematical modelling for analyzing the dynamic behavior of rotors. Various models containing nonlinear differential equations of motion are developed for different rotor configurations. These models consist of 2^{nd} and 4^{th} order nonlinear differential equations of motion. Technical and theoretical aspects of taking into account various effects like higher order large deformations, geometric nonlinearity, shear effects, gyroscopic and rotary inertia effects are visualized and discussed. The models are developed using both the Euler-Bernoulli and Timoshenko beam theories.

2.1. Characterization of Rotor Elements - Classical Linear Approach

This section concerns with the theoretical approach for the characterization of different rotor elements which include the disk, the shaft, the bearings and the mass unbalance. The geometry of the rotor system considered for this work is shown in Fig. 16. The shaft, considered to be a beam of circular cross section of length L and radius R_1, is modeled by its kinetic and strain energies. The disk of external radius R_2 and internal radius R_1 positioned at a distance $y=L/3$, is considered to be rigid and hence only requires kinetic energy for its characterization. The mass unbalance denoted by m_u is located at a distance d_1 from the geometric center of the shaft.

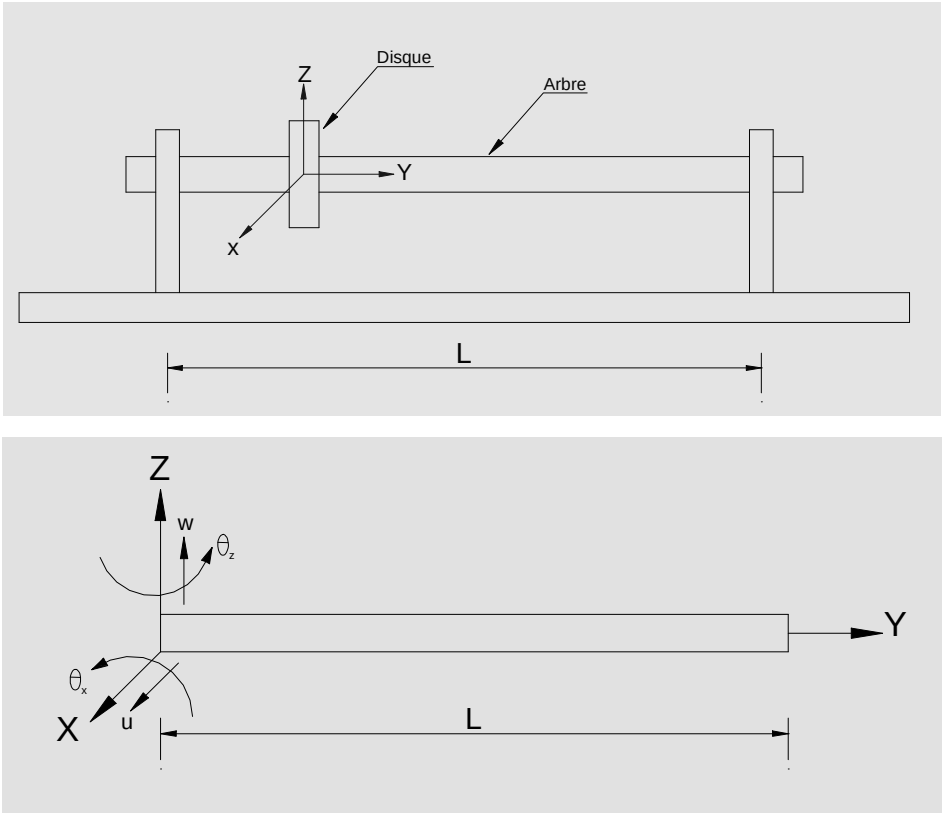

Fig. 16. Rotor System with shaft and disk

The basic characteristics of these elements are presented as below.

2.1.1. Kinetic Energy of the Disk

The disk is characterized by its kinetic energy as it is assumed to be rigid. In Fig. 2.1 the frames of reference for a disk mounted on a rotating shaft are shown. $R_0(XYZ)$ is an inertial frame and $R(x,y,z)$ is fixed to the disk. The reference frame fixed to the disk is related to the inertial frame of reference through a set of three angles θ_x, θ_y and θ_z. In order to find the orientation of the disk, it is rotated around the Z axis by an amount θ_z, then by an amount θ_x around the new axis which is x_1. Finally it is rotated by an amount θ_y around the new y axis.

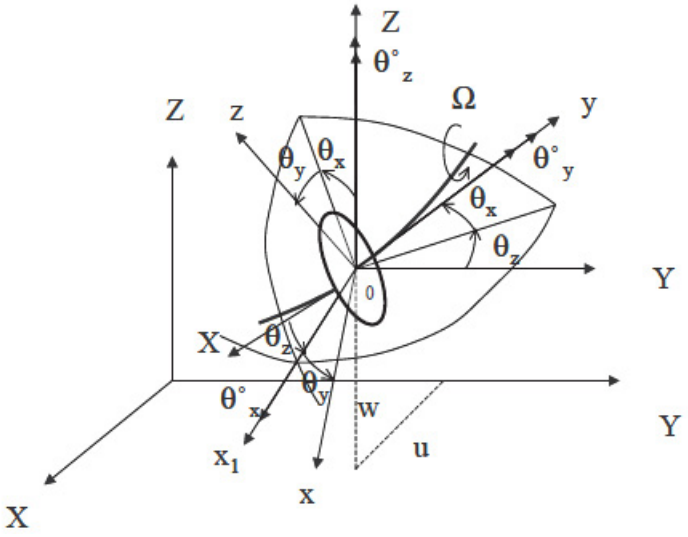

Fig. 17. Rotating frames of a disk on a rotating flexible shaft

The instantaneous angular velocity vector of the frame xyz is given by,

$$\vec{\omega}_{R/R_0} = \dot{\theta}_z \vec{Z} + \dot{\theta}_x \vec{x}_1 + \dot{\theta}_y \vec{y} \tag{2.1.1}$$

Where,

Z, x_1 and y are the unit vectors along the respective axis.

$\dot{\theta}_x, \dot{\theta}_y, \dot{\theta}_z$ are derivates with respect to time of angular displacements along x, y and z axis respetively.

The kinetic energy of the disk is derived in the reference from R. Therefore the angular velocity vector becomes,

$$\vec{\omega}_{R/R_0} = \begin{bmatrix} \omega_x \\ \omega_y \\ \omega_z \end{bmatrix}_R = \begin{bmatrix} -\dot{\theta}_z \cos\theta_x \sin\theta_y + \dot{\theta}_x \cos\theta_y \\ \dot{\theta}_y + \dot{\theta}_z \sin\theta_x \\ -\dot{\theta}_z \cos\theta_x \cos\theta_y + \dot{\theta}_x \sin\theta_y \end{bmatrix}_R \tag{2.1.2}$$

Let u and w denote the coordinates of O in R_0, the coordinate along Y being constant. In addition, the mass of the disk is M_D and its tensor of inertia in O as xyz are principal directions of inertia is,

$$I/O = \begin{bmatrix} I_{dx} & 0 & 0 \\ 0 & I_{dy} & 0 \\ 0 & 0 & I_{dz} \end{bmatrix}_R \tag{2.1.3}$$

The kinetic energy of the disk can be written as,

$$T_d = \frac{1}{2} m_d \left(\dot{u}^2 + \dot{w}^2 \right) + \frac{1}{2} \left(I_{dx} \omega_x^2 + I_{dy} \omega_y^2 + I_{dz} \omega_z^2 \right) \tag{2.1.4}$$

If the disk is symmetric i.e. $I_{dx} = I_{dz}$, the angles θ_x and θ_z are small, and the angular velocity is constant i.e. $\dot{\theta}_y = \Omega$, the Eq. (2.1.4) can be written as follows,

$$T_d = \frac{M_d}{2} \left(\dot{u}^2 + \dot{w}^2 \right) + \frac{I_{dx}}{2} \left(\dot{\theta}_x^{\,2} + \dot{\theta}_z^{\,2} \right) + I_{dy} \Omega \dot{\theta}_z \theta_x \tag{2.1.5}$$

Where, the last term represents the gyroscopic (Coriolis) effect.

2.1.2. Kinetic Energy of the Shaft

If the kinetic energy of the disk given by Eq. (2.1.5) is extended for an element of length L, the following expression for the kinetic energy of the disk is obtained.

$$T_s = \int_0^L \frac{\rho A}{2} \left(\dot{u}^2 + \dot{w}^2 \right) dy + \int_0^L \frac{\rho I}{2} \left(\dot{\theta}_x^{\,2} + \dot{\theta}_z^{\,2} \right) dy + \int_0^L 2 \rho I \Omega \dot{\theta}_z \theta_x \, dy \tag{2.1.6}$$

Where, the first integral is the general expression for the kinetic energy of the beam in bending, the second integral represents the secondary effect of rotatory inertia and the last integral is due to the gyroscopic effect.

2.1.3. Strain Energy of the Shaft

The shaft is modeled as a beam of circular cross section in bending (Fig.18). The displacements in the *x, y* and *z* directions of the beam are given below,

$$u_x = u \ , \ u_y = -z\theta_x + x\theta_z \ , \ u_z = w \tag{2.1.7}$$

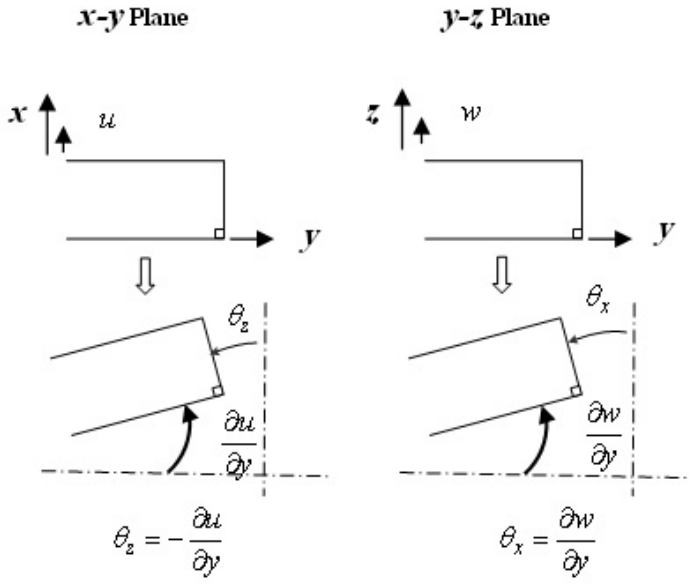

Fig. 18. Transverse vibrations (beam in bending)

The longitudinal strain (deformation) in the *y* direction can be shown to be,

$$\varepsilon_{yy} = \underbrace{-z\frac{\partial\theta_x}{\partial y} + x\frac{\partial\theta_z}{\partial y}}_{\varepsilon_l} + \underbrace{\frac{1}{2}\theta_x^{\,2} + \frac{1}{2}\theta_z^{\,2}}_{\varepsilon_{nl}\,(\text{higher order deformations})} \tag{2.1.8}$$

The strain energy can be given as,

$$U_{s1} = \frac{1}{2}\int_0^L\iint_A \left(\sigma_{yy}\varepsilon_{yy}\right) dA dy \tag{2.1.9}$$

By using the relation $\sigma_{yy} = E\varepsilon_{yy}$, the strain energy can be written as:

$$U_{s1} = \frac{E}{2}\int_0^L\iint_A \varepsilon_{yy}^{\,2}\, dA dy \tag{2.1.10}$$

By using Eq. 2.1.8,

$$U_{s1} = \frac{E}{2}\int_0^L\iint_A \left[-z\frac{\partial\theta_x}{\partial y} + x\frac{\partial\theta_z}{\partial y} + \frac{1}{2}\theta_x^{\,2} + \frac{1}{2}\theta_z^{\,2}\right]^2 dA dy \tag{2.1.11}$$

By expanding the above equation and neglecting the higher order terms, the strain energy of the shaft can be written as,

$$U_{s1} = \frac{E}{2}\int_0^L\iint_A \left[z^2\left(\frac{\partial\theta_x}{\partial y}\right)^2 + x^2\left(\frac{\partial\theta_z}{\partial y}\right)^2 - 2xz\left(\frac{\partial\theta_x}{\partial y}\right)\left(\frac{\partial\theta_z}{\partial y}\right)\right] dA dy \tag{2.1.12}$$

The 3rd term in the above equation can be neglected due to the symmetry of the cross-section. Also, $I_x = \int_A z^2 dA$, $I_z = \int_A x^2 dA$, $I = I_x = I_z$ (due to symmetry) and $\int_S ds = A$ is the area of the cross section.

Therefore, Eq. (2.1.12) becomes,

$$U_{s1} = \frac{EI}{2} \int_0^L \left[\left(\frac{\partial \theta_x}{\partial y} \right)^2 + \left(\frac{\partial \theta_z}{\partial y} \right)^2 \right] dy \tag{2.1.13}$$

2.1.4. Kinetic Energy of the Mass Unbalance

The main cause of vibrations in a rotor is the excitation due to inevitable mass unbalance. Residual unbalances occur due to many reasons for example, manufacturing error, thermal deformation and material inhomogeneity.

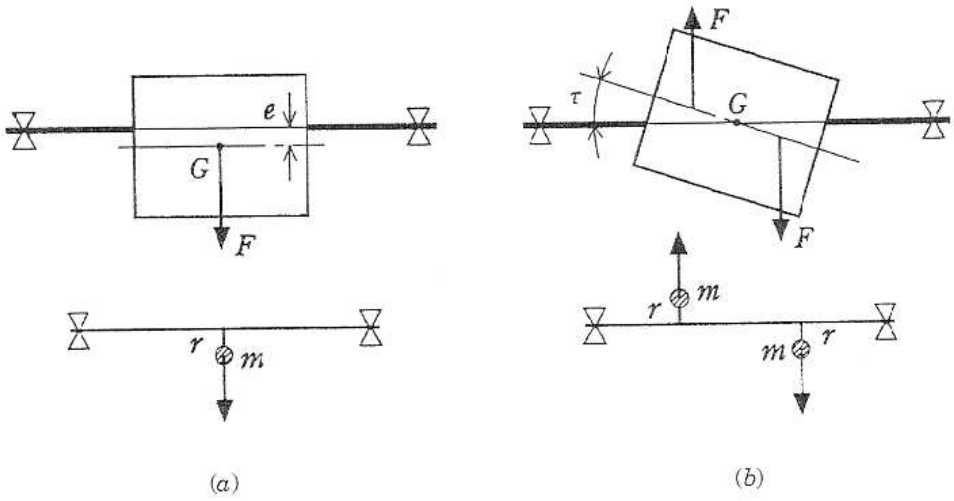

Fig. 19. Types of Mass Unbalances (a) Static (b) Dynamic

As shown in the Fig. 19 two types of unbalance exist in a rotor system consisting of a rigid rotor and a flexible shaft. One is static unbalance, which is state represented by a geometric eccentricity of the center of gravity of a rotor from the centerline of the shaft. This unbalance produces a centrifugal force proportional to the square of the rotational speed. The static unbalance can be detected without operating the rotor because the unbalance is always directed downwards if the shaft is supported horizontally by bearings with little friction. The other is dynamic unbalance , which is the state represented by the angular misalignment of principal axis of moment of inertia of the rotor with respect to the centerline of the shaft. The magnitude of the dynamic unbalance is determined by the angle τ as shown in the Fig. 19 (b) this type of unbalance cannot be detected without rotating the shaft. As shown in the Fig. 19 (b) these unbalances are represented by models with one and two concentrated masses, respectively.

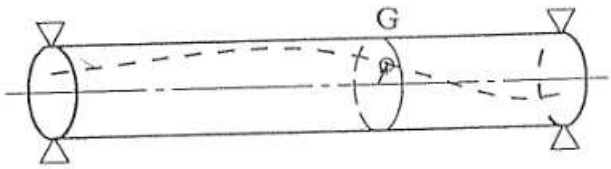

Fig. 20. Unbalances in a continuous rotor

For the present work the unbalance is defined by a mass m_u which is located at a distance d_1 from the geometric center of the shaft. The kinetic energy of this mass T_u is calculated as follows.

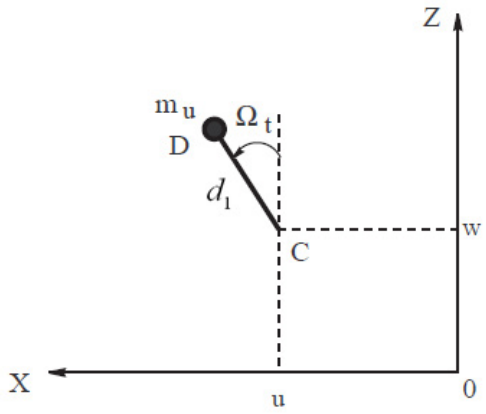

Fig. 21. Position of the Mass Unbalance on the Rotor

The mass remains in a plane perpendicular to the y-axis and its coordinate along this axis is a constant (Fig. 21). The coordinates of the mass in the frame of reference R_0 are,

$$OD = \begin{vmatrix} u + d_1 \sin \Omega t \\ \text{constant} \\ w + d_1 \cos \Omega t \end{vmatrix} \tag{2.1.14}$$

Therefore,

$$V = \frac{dOD}{dt} = \begin{vmatrix} \dot{u} + d_1 \Omega \cos \Omega t \\ 0 \\ \dot{w} + d_1 \Omega \sin \Omega t \end{vmatrix} \tag{2.1.15}$$

The kinetic energy of the mass unbalance can therefore be written as,

$$T_u = \frac{m_u}{2}\left(\dot{u}^2 + \dot{w}^2 + \Omega^2 d_1^2 + 2\Omega d_1 \dot{u} \cos \Omega t - 2\Omega \dot{w} d_1 \sin \Omega t\right) \tag{2.1.16}$$

The third term in the above equation is a constant and has no influence on the equations. The mass unbalance is much smaller as compared to the mass of the rotor. This leads to the following equation for the kinetic energy of the mass unbalance.

$$T_u = m_u \Omega d_1 \left(\dot{u} \cos \Omega t - \dot{w} \sin \Omega t\right) \tag{2.1.17}$$

By adding Eqs. (2.1.5), (2.1.6) and (2.1.17) the total kinetic energy of the rotor system become $T_R = T_d + T_s + T_u$ and can be written as,

$$T_R = \frac{M_d}{2}\left(\dot{u}^2 + \dot{w}^2\right) + \frac{I_{dx}}{2}\left(\dot{\theta}_x^2 + \dot{\theta}_z^2\right) + I_{dy}\Omega\dot{\theta}_z\theta_x + \int_0^L \frac{\rho A}{2}\left(\dot{u}^2 + \dot{w}^2\right) dy$$
$$+ \int_0^L \frac{\rho I}{2}\left(\dot{\theta}_x^2 + \dot{\theta}_z^2\right) dy + \int_0^L 2\rho I\Omega\dot{\theta}_z\theta_x \, dy + m_u\Omega d_1\left(\dot{u}\cos\Omega t - \dot{w}\sin\Omega t\right) \tag{2.1.18}$$

Since the strain energy of the rotor is contributed by only the shaft which is flexible, the total strain energy of the rotor system can now be written as $U_R = U_{s_1}$ which gives,

$$\mathrm{U_R} = \frac{EI}{2}\int_0^L \left[\left(\frac{\partial\theta_x}{\partial y}\right)^2 + \left(\frac{\partial\theta_z}{\partial y}\right)^2\right] dy \tag{2.1.19}$$

2.2. Characterization of Shaft Elements – Nonlinear Approach

In section 2.1.3, the nonlinear terms in Eq. (2.1.8) were neglected while passing from Eq. (2.1.11) to Eq. (2.1.12). But if nonlinear terms are also retained then the following equation for the strain energy is obtained.

$$U_{s1} = \frac{E}{2}\int_0^L \iint_A \left[z^2\left(\frac{\partial\theta_x}{\partial y}\right)^2 + x^2\left(\frac{\partial\theta_z}{\partial y}\right)^2 - 2xz\left(\frac{\partial\theta_x}{\partial y}\right)\left(\frac{\partial\theta_z}{\partial y}\right) + \frac{1}{4}\theta_x^4 + \frac{1}{4}\theta_z^4 + \frac{1}{2}\theta_x^2\theta_z^2 \right.$$
$$\left. - 2\left[z\frac{\partial\theta_x}{\partial y} + x\frac{\partial\theta_z}{\partial y}\right]\left[\frac{1}{2}\theta_x^2 + \frac{1}{2}\theta_z^2\right]\right] dA\,dy \tag{2.2.1}$$

The 3rd and 7th terms in the above equation disappear due to the symmetry of the cross-section. Therefore, this equation is now reduced to give the following equation.

$$U_{s1} = \frac{E}{2}\int_0^L \iint_A \left[z^2\left(\frac{\partial\theta_x}{\partial y}\right)^2 + x^2\left(\frac{\partial\theta_z}{\partial y}\right)^2 + \frac{1}{4}\theta_x^4 + \frac{1}{4}\theta_z^4 + \frac{1}{2}\theta_x^2\theta_z^2\right] dA\,dy \tag{2.2.2}$$

Also, $I_x = \int_A z^2 dA$, $I_z = \int_A x^2 dA$, $I = I_x = I_z$ (due to symmetry) and $\int_S ds = A$ is the area of the cross section.

Therefore, Eq. (2.2.2) becomes,

$$\mathbf{U_{s1}} = \frac{\boldsymbol{EI}}{\mathbf{2}}\int_0^L \left[\left(\frac{\partial\boldsymbol{\theta}_x}{\partial y}\right)^2 + \left(\frac{\partial\boldsymbol{\theta}_z}{\partial y}\right)^2\right] dy + \frac{\boldsymbol{EA}}{\mathbf{2}}\int_0^L \left[\frac{\mathbf{1}}{\mathbf{4}}\boldsymbol{\theta}_x^4 + \frac{\mathbf{1}}{\mathbf{4}}\boldsymbol{\theta}_z^4 + \frac{\mathbf{1}}{\mathbf{2}}\boldsymbol{\theta}_x^2\boldsymbol{\theta}_z^2\right] dy \tag{2.2.3}$$

2.3. Application of the Rayleigh-Ritz Method

Rayleigh's method approximates a continuous system by an equivalent single degree of freedom system (SDOF) via assuming a single deformation shape. A continuous system is reduced to a discrete multi degree of freedom system (MDOF). The number of DOF is equal to the number of Ritz modes chosen. This method is applied in the present work as follows. The displacements in the x and z directions can be expressed as,

$$u(y,t) = f(y)U(t)$$
$$w(y,t) = f(y)W(t) \tag{2.3.1}$$

The angular displacements can be approximated as,

$$\theta_x = \partial w/\partial y = f'(y)W(t) = g(y)W(t)$$
$$\theta_z = -\partial u/\partial y = -f'(y)U(t) = -g(y)U(t) \tag{2.3.2}$$

$$\partial\theta_x/\partial y = f''(y)W(t) = h(y)W(t)$$
$$\partial\theta_z/\partial y = -f''(y)U(t) = -h(y)U(t) \tag{2.3.3}$$

Where the prime denotes the derivative with respect to *y*. Using the above expressions, the kinetic energy of the rotor system T_R in Eq. (2.1.18) can now be written in a compact form as below,

$$T_R = \frac{1}{2}b_1\left(\dot{U}^2 + \dot{W}^2\right) - \Omega b_2\dot{U}W(t) + m_u\Omega d_1 f(l_1)\left(\dot{U}\cos\Omega t - \dot{W}\sin\Omega t\right) \tag{2.3.4}$$

Where,

$$b_1 = M_D f^2(l_1) + I_{Dx}g^2(l_1) + \rho A\int_0^L f^2(y)dy + \rho I\int_0^L g^2(y)dy \tag{2.3.5}$$

$$b_2 = I_{Dy}g^2(l_1) + 2\rho I\int_0^L g^2(y)dy \tag{2.3.6}$$

The strain energy of the rotor in Eq. (2.1.19) can be written in a compact form as,

$$U_R = \frac{k_1}{2}\left(U^2(t) + W^2(t)\right) \tag{2.3.7}$$

Where,

$$k_1 = EI\int_0^L h^2(y)dy \tag{2.3.8}$$

2.4. Derivation of Equations of Motion for Different Rotor Configurations

Various rotor configurations have been studied and investigated. Different effects have been considered. In the following sections, some mathematical models for different rotor configurations and effects are presented.

From now on, in order to avoid the complications of the mathematical expressions, the discretized displacements $U(t)$ and $W(t)$ will be written as U and W respectively.

2.4.1. Linear Model

Using the Hamilton principle as $\int_{t_1}^{t_2}\delta\left(T_R - U_R\right)dt = 0$, we can write

$$\int_{t_1}^{t_2}\delta\left(T_R - U_R\right)dt = \int_{t_1}^{t_2}\delta T_R\,dt - \int_{t_1}^{t_2}\delta U_R\,dt = 0 \tag{2.4.1}$$

The two terms in the above equation are treated one by one. The first term gives

$$\int_{t_1}^{t_2} \delta T_R dt = \int_{t_1}^{t_2} \left(\frac{\partial T_R}{\partial W} \delta W + \frac{\partial T_R}{\partial \dot{U}} \delta \dot{U} + \frac{\partial T_R}{\partial \dot{W}} \delta \dot{W} \right) dt \tag{2.4.2}$$

Different terms in the above equation can be treated as follows,

$$\int_{t_1}^{t_2} \frac{\partial T_R}{\partial W} \delta W dt = -\int_{t_1}^{t_2} \Omega b_2 \dot{U} \delta W dt \tag{2.4.3}$$

$$\begin{aligned} \int_{t_1}^{t_2} \frac{\partial T_R}{\partial \dot{W}} \delta \dot{W} dt &= \left(\frac{\partial T_R}{\partial \dot{W}} \delta W \right)_{t_1}^{t_2} - \int_{t_1}^{t_2} \frac{\partial}{\partial t} \left(\frac{\partial T_R}{\partial \dot{W}} \right) \delta W dt \\ &= \left(\frac{\partial T_R}{\partial \dot{W}} \delta W \right)_{t_1}^{t_2} - \int_{t_1}^{t_2} \frac{\partial}{\partial t} \left(b_1 \dot{W} - m_u \Omega d_1 f(l_1) \sin \Omega t \right) \delta W dt \end{aligned} \tag{2.4.4}$$

Similarly, the second term in the Eq. (2.4.1) gives,

$$\int_{t_1}^{t_2} \delta U_R dt = \int_{t_1}^{t_2} \left(\frac{\partial U_R}{\partial U} \delta U + \frac{\partial U_R}{\partial W} \delta W \right) dt \tag{2.4.5}$$

The two terms in the above equation can be written as,

$$\int_{t_1}^{t_2} \frac{\partial U_R}{\partial U} \delta U dt = \int_{t_1}^{t_2} \left(k_1 U \right) \delta U dt \tag{2.4.6}$$

$$\int_{t_1}^{t_2} \frac{\partial U_R}{\partial W} \delta W dt = \int_{t_1}^{t_2} \left(k_1 W \right) \delta W dt \tag{2.4.7}$$

Finally, the equations of motion for the linear undamped system can be written by collecting the terms of the type $\delta U dt$ *and* $\delta W dt$ in Eqs. (2.4.3) , (2.4.4) , (2.4.5) , (2.4.6) and (2.4.7).

Collection all the terms of the type $\delta U dt$, the following equations is obtained,

$$-\int_{t_1}^{t_2} \left(\frac{\partial}{\partial t} \left(b_1 \dot{U} - \Omega b_2 W + m_u \Omega d_1 f(l_1) \cos \Omega t \right) - k_1 U \right) \delta U dt = 0 \tag{2.4.8}$$

By simplifying and re-arranging, the differential equation describing the discretized displacement in the x-direction is obtained as,

$$b_1 \ddot{U} - \Omega b_2 \dot{W} + k_1 U = m_u \Omega^2 d_1 f(l_1) \sin \Omega t \tag{2.4.9}$$

In the same manner collecting all the terms of the type $\delta U dt$, the following equation is obtained,

$$-\int_{t_1}^{t_2} \left(\frac{\partial}{\partial t} \left(b_1 \dot{W} - m_u \Omega d_1 f(l_1) \sin \Omega t \right) - \Omega b_2 \dot{U} - k_1 W \right) \delta W dt = 0 \tag{2.4.10}$$

By simplifying and re-arranging, the following equation for the discretized displacement in the z-direction is obtained as,

$$b_1 \ddot{W} + \Omega\, b_2 \dot{U} + k_1 W = m_u \Omega^2 d_1 f(l_1)\cos\Omega t \tag{2.4.11}$$

2.4.2. Nonlinear Model considering the Effect of Higher Order large Deformations and a Static Axial Force (N_0)

The following expression for the strain energy of the shaft taking into account higher order large deformations is derived in Appendix A.

$$U_{s1} = \int_0^L \frac{EI}{2}\left[\left(\frac{\partial \theta_x}{\partial y}\right)^2 + \left(\frac{\partial \theta_z}{\partial y}\right)^2\right] dy + \int_0^L \frac{EA}{2}\left[\frac{1}{4}\theta_x^4 + \frac{1}{4}\theta_z^4 + \frac{1}{2}\theta_x^2\theta_z^2\right] dy \tag{2.4.12}$$

If there exists a constant force N_0, there is another contribution to the strain energy above [LF98],

$$U_{N_0} = \frac{N_0}{2}\int_0^L \left(\theta_x^2 + \theta_z^2\right) dy \tag{2.4.13}$$

Total strain energy of the rotor U_R now becomes,

$$U_R = U_{s1} + U_{N_0} \tag{2.4.14}$$

$$U_R = \int_0^L \frac{EI}{2}\left[\left(\frac{\partial \theta_x}{\partial y}\right)^2 + \left(\frac{\partial \theta_z}{\partial y}\right)^2\right] dy + \int_0^L \frac{EA}{2}\left[\frac{1}{4}\theta_x^4 + \frac{1}{4}\theta_z^4 + \frac{1}{2}\theta_x^2\theta_z^2\right] dy + \frac{N_0}{2}\int_0^L \left(\theta_x^2 + \theta_z^2\right) dy \tag{2.4.15}$$

After application of Rayleigh Ritz method the strain energy of the rotor given by Eq. (2.4.15) can be written in a compact form as follows,

$$U_R = \frac{k_1}{2}\left(U^2 + W^2\right) + \frac{k_2}{8}\left(U^4 + W^4 + 2U^2W^2\right) + \frac{N_0}{2}k_{N_0}(U^2 + W^2) \tag{2.4.16}$$

Where,

$$k_1 = EI\int_0^L h^2(y)dy \;\;;\;\; k_2 = EA\int_0^L g^4(y)dy \;\;;\;\; k_{N_0} = \int_0^L g^2(y)dy \tag{2.4.17}$$

Hamilton principle is then applied on the kinetic and strain energies of the rotor given by Eqs. (2.3.4) and (2.4.17) in the form $\int_{t_1}^{t_2} \delta\left(T_R - U_R\right) dt = 0$

Therefore,

$$\int_{t_1}^{t_2} \delta\left(T_R - U_R\right) dt = \int_{t_1}^{t_2} \delta T_R\, dt - \int_{t_1}^{t_2} \delta U_R\, dt = 0 \tag{2.4.18}$$

The two terms in the above equation are treated separately, the first term gives,

$$\int_{t_1}^{t_2} \delta T_R dt = \int_{t_1}^{t_2} \left(\frac{\partial T_R}{\partial W} \delta W + \frac{\partial T_R}{\partial \dot{U}} \delta \dot{U} + \frac{\partial T_R}{\partial \dot{W}} \delta \dot{W} \right) dt \tag{2.4.19}$$

Different terms in the above equations can be given as,

$$\int_{t_1}^{t_2} \frac{\partial T_R}{\partial W} \delta W dt = -\int_{t_1}^{t_2} \Omega b_2 \dot{U} \delta W dt \tag{2.4.20}$$

$$\begin{aligned} \int_{t_1}^{t_2} \frac{\partial T_R}{\partial \dot{U}} \delta \dot{U} dt &= \left(\frac{\partial T_R}{\partial \dot{U}} \delta U \right)_{t_1}^{t_2} - \int_{t_1}^{t_2} \frac{\partial}{\partial t} \left(\frac{\partial T_R}{\partial \dot{U}} \right) \delta U dt \\ &= \left(\frac{\partial T_R}{\partial \dot{U}} \delta U \right)_{t_1}^{t_2} - \int_{t_1}^{t_2} \frac{\partial}{\partial t} \left(b_1 \dot{U} - \Omega b_2 W + m_u \Omega d_1 f(l_1) \cos \Omega t \right) \delta U dt \end{aligned} \tag{2.4.21}$$

$$\begin{aligned} \int_{t_1}^{t_2} \frac{\partial T_R}{\partial \dot{W}} \delta \dot{W} dt &= \left(\frac{\partial T_R}{\partial \dot{W}} \delta W \right)_{t_1}^{t_2} - \int_{t_1}^{t_2} \frac{\partial}{\partial t} \left(\frac{\partial T_R}{\partial \dot{W}} \right) \delta W dt \\ &= \left(\frac{\partial T_R}{\partial \dot{W}} \delta W \right)_{t_1}^{t_2} - \int_{t_1}^{t_2} \frac{\partial}{\partial t} \left(b_1 \dot{W} - m_u \Omega d_1 f(l_1) \sin \Omega t \right) \delta W dt \end{aligned} \tag{2.4.22}$$

The 2nd term in Eq. (2.4.18) can be expanded as follows,

$$\int_{t_1}^{t_2} \delta U_R dt = \int_{t_1}^{t_2} \left(\frac{\partial U_R}{\partial U} \delta U + \frac{\partial U_R}{\partial W} \delta W \right) dt \tag{2.4.23}$$

The two terms in the above equation give,

$$\int_{t_1}^{t_2} \frac{\partial U_R}{\partial U} \delta U dt = \int_{t_1}^{t_2} \left(k_1 U + \frac{1}{2} k_2 \left(U^3 + U W^2 \right) + N_0 k_{N_0} U \right) \delta U dt \tag{2.4.24}$$

And

$$\int_{t_1}^{t_2} \frac{\partial U_R}{\partial W} \delta W dt = \int_{t_1}^{t_2} \left(k_1 W + \frac{1}{2} k_2 \left(W^3 + U^2 W \right) + N_0 k_{N_0} W \right) \delta W dt \tag{2.4.25}$$

By collecting the terms of type $\delta U dt$ in Eqs. (2.4.20), (2.4.21), (2.4.22), (2.4.24) and (2.4.25), following equation is obtained.

$$-\int_{t_1}^{t_2} \left(\begin{array}{l} \frac{\partial}{\partial t} \left(b_1 \dot{U} - \Omega b_2 W + m_u \Omega d_1 f(l_1) \cos \Omega t \right) - k_1 U \\ \quad - \frac{1}{2} k_2 \left(U^3 + U W^2 \right) - N_0 k_{N_0} U \end{array} \right) \delta U dt = 0 \tag{2.4.26}$$

By simplifying and re-arranging the above equation,

$$b_1\ddot{U} - \Omega b_2\dot{W} + k_1 U + \frac{1}{2}k_2\left(U^3 + UW^2\right) + N_0 k_{N_0} U = m_u \Omega^2 d_1 f(l_1)\sin\Omega t \tag{2.4.27}$$

Similarly, by collecting the terms of the type $\delta W dt$ in Eqs. (2.4.20), (2.4.21), (2.4.22), (2.4.24) and (2.4.25), the following equation is obtained,

$$-\int_{t_1}^{t_2} \begin{bmatrix} \frac{\partial}{\partial t}\left(b_1\dot{W} - m_u \Omega d_1 f(l_1)\sin\Omega t\right) - \Omega b_2 \dot{U} - k_1 W \\ -\frac{1}{2}k_2\left(W^3 + U^2 W\right) - N_0 k_{N_0} W \end{bmatrix} \delta W dt = 0 \tag{2.4.28}$$

By simplifying and re-arranging the above equation,

$$b_1\ddot{W} + \Omega b_2\dot{U} + k_1 W + \frac{1}{2}k_2\left(W^3 + U^2 W\right) + N_0 k_{N_0} W = m_u \Omega^2 d_1 f(l_1)\cos\Omega t \tag{2.4.29}$$

Equations (2.4.55) and (2.4.57) can be further written as,

$$\ddot{U} - \Omega\alpha_1\dot{W} + \alpha_2 U + \frac{1}{2}\beta_1\left(U^3 + UW^2\right) + N_0 k_{N_0} U + c\dot{U} = m_1\Omega^2 d_1 f(l_1)\sin\Omega t \tag{2.4.30}$$

$$\ddot{W} + \Omega\alpha_1\dot{U} + \alpha_2 W + \frac{1}{2}\beta_1\left(W^3 + WU^2\right) + N_0 k_{N_0} W + c\dot{W} = m_1\Omega^2 d_1 f(l_1)\cos\Omega t \tag{2.4.31}$$

The above two equations are 2nd order nonlinear differential equations of motion, where,

$$\alpha_1 = b_2/b_1\ ,\ \alpha_2 = k_1/b_1\ ,\ \beta_1 = k_2/b_1\ ,\ m_1 = m_u/b_1 \tag{2.4.32}$$

And c is a damping term. In the above equation, different constants are the functions of the properties of the material and the geometry of the rotor.

2.4.3. Nonlinear Model considering the Effect of a Dynamic Axial Force

Two types of continuous rotor models are shown in Fig. 22. If the supports are such that they allow the shaft to shift in the axial direction as in Fig. 22 (a), the restoring force of the shaft has linear spring characteristics. On the other hand if the supports are fixed as shown in 2.5Fig. 22 (b), the shaft elongates as it deflects and acquires nonlinear spring characteristics of a hard spring type. This type of nonlinearity is called geometric nonlinearity. This nonlinearity becomes more effective when the shaft deflection becomes large.

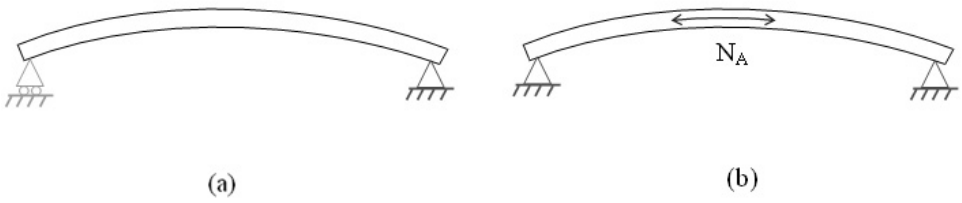

Fig. 22. Continuous rotor models (a) No axial force (b) Dynamic Axial force

An axial force N_A will act dynamically on the shaft. This force leads to another contribution to the strain energy of the shaft given by,

$$U_{s2} = \int_0^L \frac{N_A}{2}\left(\theta_x^{\,2} + \theta_z^{\,2}\right) dy \tag{2.4.33}$$

Where N_A can be derived as follows. In the Fig. 23 , a sliced element of the shaft is shown. The length of the element is **dy** and it is assumed that it deflects during the whirling motion of the rotor. The geometric center M shifts from the position (0, 0, y) to (x, y, z).

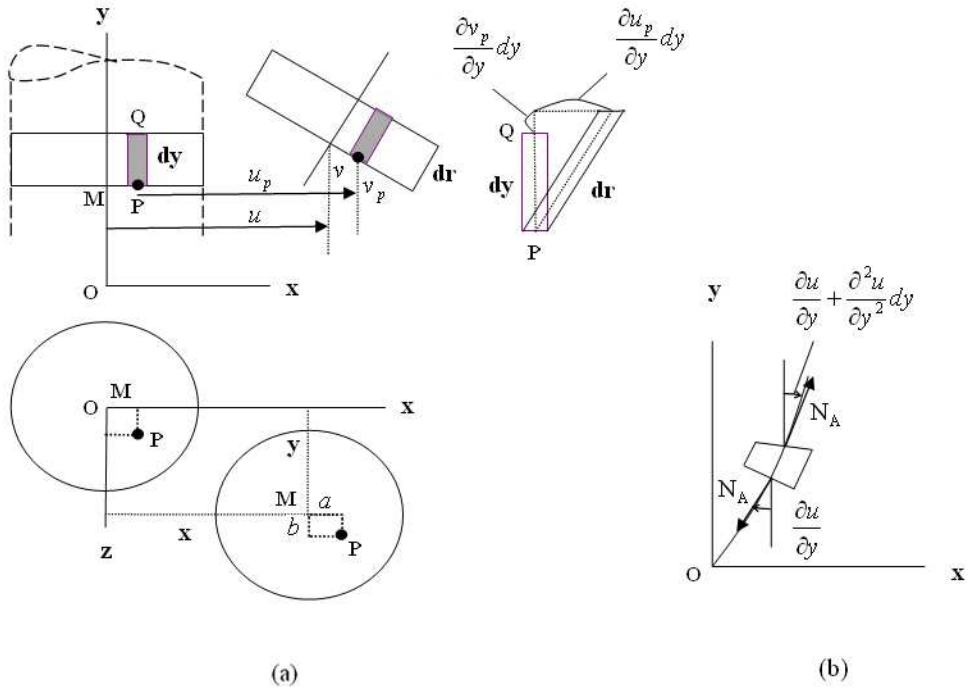

Fig. 23. Dynamic Axial Force (a) Sliced Element (b) Deflection Curve

The deflections along the coordinate axes are represented by u, v and w respectively. The point P shifts from position (a, b, y) to (x_p, y_p, z_p). This deflection is represented by u_p, v_p and w_p respectively.

From Fig. 23 we have,

$$u_p = u \ , \ w_p = w \ , \ v_p = v - a\frac{\partial u}{\partial y} - b\frac{\partial w}{\partial y} \tag{2.4.34}$$

Also point $Q(a, y_0 + dy, b)$, separated from point P by dy, shifts by u_Q, v_Q and w_Q which are given approximately by,

$$u_Q = u_P + \frac{\partial u_P}{\partial y}dy,\ v_Q = v_P + \frac{\partial v_P}{\partial y}dy,\ w_Q = w_P + \frac{\partial w_P}{\partial y}dy \tag{2.4.35}$$

Therefore after deformation, the length **dr** of the sliced element at point **P** can be written as,

$$dr = \sqrt{\left(dy + \frac{\partial v_P}{\partial y}dy\right)^2 + \left(\frac{\partial u_P}{\partial y}dy\right)^2 + \left(\frac{\partial w_P}{\partial y}dy\right)^2}$$
$$\cong dy\left(1 + \frac{\partial v_P}{\partial y} + \frac{1}{2}\left(\frac{\partial u_P}{\partial y}dy\right)^2 + \frac{1}{2}\left(\frac{\partial w_P}{\partial y}dy\right)^2\right) \tag{2.4.36}$$

Where the condition $\frac{\partial v_P}{\partial y} << \frac{\partial u_P}{\partial y} = \frac{\partial w_P}{\partial y}$ and the approximation $\sqrt{1+\Delta} \cong 1 + \Delta/2$ (for $\Delta << 1$) are used.

Using Eqs. (2.4.34) and (2.4.36) the strain $\in (a,b)$ in the y-direction is expressed as,

$$\in = \frac{dr - dy}{dy} = \frac{\partial v}{\partial y} - a\frac{\partial^2 u}{\partial y} - b\frac{\partial^2 w}{\partial y} + \frac{1}{2}\left(\left(\frac{\partial u}{\partial y}\right)^2 + \left(\frac{\partial w}{\partial y}\right)^2\right) \tag{2.4.37}$$

Using Hooke's law the stress at point P is $\sigma = \in E$. Integrating it over the entire cross section with area A, the expression for the axial dynamic force can be written as,

$$N_A = \int_A \sigma dA = EA\frac{\partial v}{\partial y} + \frac{1}{2}EA\left(\left(\frac{\partial u}{\partial y}\right)^2 + \left(\frac{\partial w}{\partial y}\right)^2\right) \tag{2.4.38}$$

Integrating the above expression over the direction y considering that the axial force N_A is constant in this direction, the following expression is obtained.

$$v(y) = \frac{1}{EA}N_A - \frac{1}{2}\int_0^y \left(\left(\frac{\partial u}{\partial y}\right)^2 + \left(\frac{\partial w}{\partial y}\right)^2\right)dy + C \tag{2.4.39}$$

Applying the condition that the deflection is zero at $y = 0$, namely $v(0) = 0$, the constant $C = 0$. The condition that $v(L) = 0$, the expression for the axial force is,

$$N_A = \int_0^y \frac{EA}{2L}\left(\left(\frac{\partial u}{\partial y}\right)^2 + \left(\frac{\partial w}{\partial y}\right)^2\right)dy \tag{2.4.40}$$

Which can be further written as,

$$N_A = \int_0^L \frac{EA}{2L}\left(\theta_x^{\,2} + \theta_z^{\,2}\right)dy \tag{2.4.41}$$

Substituting the above equation in Eq. (2.4.33),

$$U_{s2} = \int_0^L\int_0^L \frac{EA}{4L}\left(\theta_x^{\,2} + \theta_z^{\,2}\right)dy\left(\theta_x^{\,2} + \theta_z^{\,2}\right)dy \tag{2.4.42}$$

Therefore, the strain energy of the rotor given by Eq. (2.4.33) now becomes $U_R = U_{s1} + U_{s2}$ and is given by,

$$U_R = \int_0^L \left[\frac{EI}{2} \left(\frac{\partial \theta_x}{\partial y} \right)^2 + \left(\frac{\partial \theta_z}{\partial y} \right)^2 \right] dy + \int_0^L \int_0^L \frac{EA}{4L} \left(\theta_x^2 + \theta_z^2 \right) dy \left(\theta_x^2 + \theta_z^2 \right) dy \tag{2.4.43}$$

After the application of Rayleigh-Ritz method as in section 2.3 the strain energy of the rotor given by Eq. (2.4.43) can be written in the compact form as follows,

$$U_R = \frac{k_1}{2} \left(U^2 + W^2 \right) + \frac{k_3}{4} \left(U^4 + W^4 + 2U^2 W^2 \right) \tag{2.4.44}$$

Where,

$$k_1 = EI \int_0^L h^2(y) dy \quad ; \quad k_3 = \frac{EA}{L} \int_0^L \int_0^L h^4(y) dy dy \tag{2.4.45}$$

The kinetic energy of the rotor in the compact form is the same as given by Eq. (2.3.4).

Hamilton's principle is then applied on the kinetic and strain energies of the rotor given by Eqs. (2.3.4) and (2.4.44), in the form $\int_{t_1}^{t_2} \delta \left(T_R - U_R \right) dt = 0$

Therefore,

$$\int_{t_1}^{t_2} \delta \left(T_R - U_R \right) dt = \int_{t_1}^{t_2} \delta T_R \, dt - \int_{t_1}^{t_2} \delta U_R \, dt = 0 \tag{2.4.46}$$

The two terms in the above equation are treated separately, the first term gives,

$$\int_{t_1}^{t_2} \delta T_R dt = \int_{t_1}^{t_2} \left[\frac{\partial T_R}{\partial W} \delta W + \frac{\partial T_R}{\partial \dot{U}} \delta \dot{U} + \frac{\partial T_R}{\partial \dot{W}} \delta \dot{W} \right] dt \tag{2.4.47}$$

Different terms in the above equations can be given as,

$$\int_{t_1}^{t_2} \frac{\partial T_R}{\partial W} \delta W dt = -\int_{t_1}^{t_2} \Omega b_2 \dot{U} \delta W dt \tag{2.4.48}$$

$$\begin{aligned} \int_{t_1}^{t_2} \frac{\partial T_R}{\partial \dot{U}} \delta \dot{U} dt &= \left[\frac{\partial T_R}{\partial \dot{U}} \delta U \right]_{t_1}^{t_2} - \int_{t_1}^{t_2} \frac{\partial}{\partial t} \left[\frac{\partial T_R}{\partial \dot{U}} \right] \delta U dt \\ &= \left[\frac{\partial T_R}{\partial \dot{U}} \delta U \right]_{t_1}^{t_2} - \int_{t_1}^{t_2} \frac{\partial}{\partial t} \left(b_1 \dot{U} - \Omega b_2 W + m_u \Omega d_1 f(l_1) \cos \Omega t \right) \delta U dt \end{aligned} \tag{2.4.49}$$

$$\begin{aligned} \int_{t_1}^{t_2} \frac{\partial T_R}{\partial \dot{W}} \delta \dot{W} dt &= \left[\frac{\partial T_R}{\partial \dot{W}} \delta W \right]_{t_1}^{t_2} - \int_{t_1}^{t_2} \frac{\partial}{\partial t} \left[\frac{\partial T_R}{\partial \dot{W}} \right] \delta W dt \\ &= \left[\frac{\partial T_R}{\partial \dot{W}} \delta W \right]_{t_1}^{t_2} - \int_{t_1}^{t_2} \frac{\partial}{\partial t} \left(b_1 \dot{W} - m_u \Omega d_1 f(l_1) \sin \Omega t \right) \delta W dt \end{aligned} \tag{2.4.50}$$

The 2nd term in Eq. (2.4.46) can be expanded as follows,

$$\int_{t_1}^{t_2} \delta U_R dt = \int_{t_1}^{t_2} \left(\frac{\partial U_R}{\partial U} \delta U + \frac{\partial U_R}{\partial W} \delta W \right) dt \tag{2.4.51}$$

The two terms in the above equation give,

$$\int_{t_1}^{t_2} \frac{\partial U_R}{\partial U} \delta U dt = \int_{t_1}^{t_2} \left(k_1 U + k_3 \left(U^3 + U W^2 \right) \right) \delta U dt \tag{2.4.52}$$

$$\int_{t_1}^{t_2} \frac{\partial U_R}{\partial W} \delta W dt = \int_{t_1}^{t_2} \left(k_1 W + k_3 \left(W^3 + U^2 W \right) \right) \delta W dt \tag{2.4.53}$$

By collecting the terms of type $\delta U dt$ in Eqs. (2.4.48) , (2.4.49) , (2.4.50) , (2.4.52) and (2.4.53) ,

$$-\int_{t_1}^{t_2} \left(\frac{\partial}{\partial t} \left(b_1 \dot{U} - \Omega b_2 W + m_u \Omega d_1 f(l_1) \cos \Omega t \right) - k_1 U - k_3 \left(U^3 + U W^2 \right) \right) \delta U dt = 0 \tag{2.4.54}$$

By simplifying and re-arranging the above equation,

$$b_1 \ddot{U} - \Omega b_2 \dot{W} + k_1 U + k_3 \left(U^3 + U W^2 \right) = m_u \Omega^2 d_1 f(l_1) \sin \Omega t \tag{2.4.55}$$

Similarly, by collecting the terms of the type $\delta W dt$ in Eqs. (2.4.48) , (2.4.49) , (2.4.50) , (2.4.52) and (2.4.53) , the following equation is obtained,

$$-\int_{t_1}^{t_2} \left(\frac{\partial}{\partial t} \left(b_1 \dot{W} - m_u \Omega d_1 f(l_1) \sin \Omega t \right) - \Omega b_2 \dot{U} - k_1 W - k_3 \left(W^3 + U^2 W \right) \right) \delta W dt = 0 \tag{2.4.56}$$

By simplifying and re-arranging the above equation,

$$b_1 \ddot{W} + \Omega b_2 \dot{U} + k_1 W + k_3 \left(W^3 + U^2 W \right) = m_u \Omega^2 d_1 f(l_1) \cos \Omega t \tag{2.4.57}$$

Equations (2.4.55) and (2.4.57) can be further written as,

$$\ddot{U} - \Omega \alpha_1 \dot{W} + \alpha_2 U + \beta_2 \left(U^3 + U W^2 \right) + c \dot{U} = m_1 \Omega^2 d_1 f(l_1) \sin \Omega t \tag{2.4.58}$$

$$\ddot{W} + \Omega \alpha_1 \dot{U} + \alpha_2 W + \beta_2 \left(W^3 + W U^2 \right) + c \dot{W} = m_1 \Omega^2 d_1 f(l_1) \cos \Omega t \tag{2.4.59}$$

The above two equations are 2nd order nonlinear differential equations of motion for the analysis of the rotor system considering the effect of a dynamic axial force.

where,

$$\alpha_1 = b_2 / b_1 \ , \ \alpha_2 = k_1 / b_1 \ , \ \beta_2 = k_3 / b_1 \ , \ m_1 = m_u / b_1 \tag{2.4.60}$$

And c is a damping term

2.5. Derivation of Equations of Motion Taking into Account the Shear Effects.

Classical beam theories neglect shear contribution to deformations. Timoshenko Beam theory takes into account this contribution. Since Timoshenko's work on bending of beams and Reissner and Mindlin's works in shear deformation of plates, shear deformability has been a well succeeded research area. Timoshenko proposed a shear correction factor, k. This factor is a compatibility criterion between real shear stress and distortion of beams.

Timoshenko introduces this factor in beam theory, in order to account for warping and distortion of transverse (or as referred in classical literature: cross) section. Cowper [C66] studied the influence of shear coefficient, obtained by means of three dimensional elasticity equations. Levinson and Cook, [LC83I], [LC83II], proposed new formulations to shear coefficient, considering that plane sections, normal to beam longitudinal axis, in the non deformed configuration, becomes curved and deformed, after bending.

If the shear modulus of the beam material approaches infinity - and thus the beam becomes rigid in shear - and if rotational inertia effects are neglected, Timoshenko beam theory converges towards ordinary beam theory.

The Timoshenko beam theory includes the effects of shear deformation and rotary inertia on the vibrations of slender beams. The theory contains a shear coefficient which has been the subject of much previous research.

In the present work, the problem of including the shear effects is addressed by two ways. The first one is to develop the energy equations of different rotor components and then the Hamilton's Principle is applied directly without first discretizing the displacements and rotations. The equations of motion thus obtained can be used to apply the direct method of multiple scales explained in Chapter 3.

In the 2nd method the energy equations are first discretized using Rayleigh Ritz method and then Lagrange equations are applied. The equations of motion thus obtained are treated using the discretization method of multiple scales presented in Chapter 3.

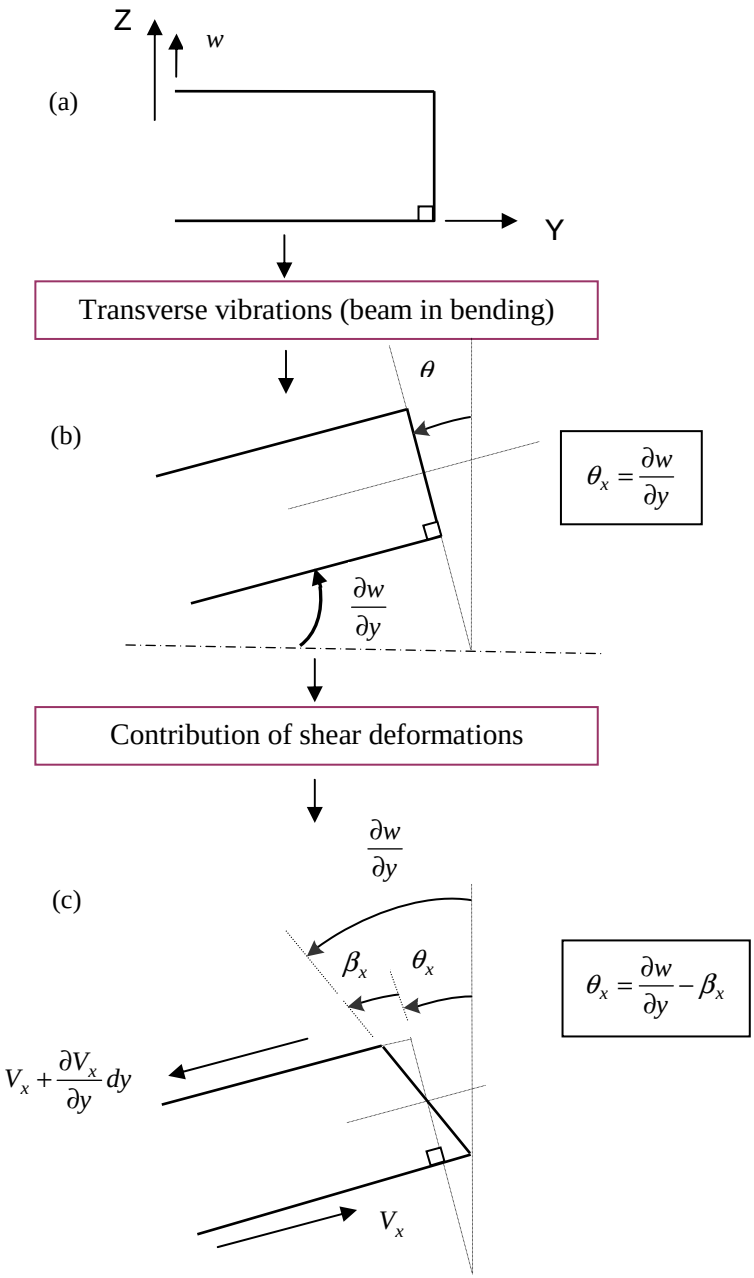

Fig. 24. Description of shear angle and shear force

2.5.1. Nonlinear Model with Shear Effects and Higher Order Deformations (Direct Method)

In order to take into account the effect of shear deformations, the shaft of the rotor is modeled as a Timoshenko beam of circular cross section. The deformation energy of the rotor U_{Rs} is derived as follows.

Referring to Fig. 25 , C is the geometric centre of the beam , B(x , z) is an arbitrary point on the cross section of the beam , E is the Young's modulus of the material, ε and σ are strains and stresses , and u and w are displacements of C w.r.t x and z axis. The axis along the rotor centre line is y.

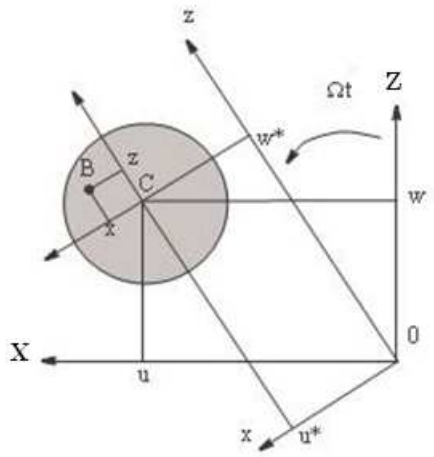

Fig. 25. Coordinates of the geometric centre C and an arbitrary point B on the circular beam.

Displacements:

$$\begin{aligned} u_x &= u \\ u_y &= -z\theta_x + x\theta_z \\ u_z &= w \end{aligned} \tag{2.5.1}$$

Deformations:

$$\varepsilon_{yy} = \underbrace{-z\frac{\partial \theta_x}{\partial y} + x\frac{\partial \theta_z}{\partial y}}_{\downarrow\ \varepsilon_l} \quad + \quad \underbrace{\frac{1}{2}\theta_x^{\,2} + \frac{1}{2}\theta_z^{\,2}}_{\downarrow\ \varepsilon_{nl}\,(higher\,order\ deformations)} \tag{2.5.2}$$

The shear deformations along y-z and y-x planes are given as,

$$\begin{aligned} \gamma_{yz} &= -\theta_x + \frac{\partial w}{\partial y} \\ \gamma_{yx} &= \theta_z + \frac{\partial u}{\partial y} \end{aligned} \tag{2.5.3}$$

The strain energy can be given as:

$$U_1 = \frac{1}{2}\int_0^L \iint_A \left(\sigma_{yy}\varepsilon_{yy} + \tau_{yz}\gamma_{yz} + \tau_{yx}\gamma_{yx}\right) dA dy \tag{2.5.4}$$

Using the relations $\sigma_{yy} = E\varepsilon_{yy}$, $\int \tau_{yz} ds = kAG\gamma_{yz}$, $\int \tau_{yx} ds = kAG\gamma_{yx}$

Where, G is the shear modulus and k is the shear correction factor.

Thus strain energy can be written as:

$$U_1 = \frac{1}{2}\int_0^L\iint_A E\varepsilon_{yy}\varepsilon_{yy}\,dA\,dy + \int_0^L \left(kAG\gamma_{yz}\gamma_{yz} + kAG\gamma_{yx}\gamma_{yx}\right)dy \tag{2.5.5}$$

$$U_1 = \frac{E}{2}\int_0^L\iint_A \varepsilon_{yy}{}^2\,dA\,dy + kAG\int_0^L \left(\gamma_{yz}{}^2 + \gamma_{yx}{}^2\right)dy \tag{2.5.6}$$

$$\begin{aligned} U_1 = \frac{E}{2}\int_0^L\iint_A \left(-z\frac{\partial\theta_x}{\partial y} + x\frac{\partial\theta_z}{\partial y} + \frac{1}{2}\theta_x{}^2 + \frac{1}{2}\theta_z{}^2\right)^2 dA\,dy \\ + \frac{kAG}{2}\int_0^L \left(-\theta_x + \frac{\partial w}{\partial y}\right)^2 + \left(\theta_z + \frac{\partial u}{\partial y}\right)^2 dy \end{aligned} \tag{2.5.7}$$

$$\begin{aligned} U_1 = \frac{E}{2}\int_0^L\iint_A \Big(z^2\left(\frac{\partial\theta_x}{\partial y}\right)^2 + x^2\left(\frac{\partial\theta_z}{\partial y}\right)^2 - 2xz\left(\frac{\partial\theta_x}{\partial y}\right)\left(\frac{\partial\theta_z}{\partial y}\right) + \frac{1}{4}\theta_x{}^4 + \frac{1}{4}\theta_z{}^4 + \frac{1}{2}\theta_x{}^2\theta_z{}^2 \\ -2\left(-z\frac{\partial\theta_x}{\partial y} + x\frac{\partial\theta_z}{\partial y}\right)\left(\frac{1}{2}\theta_x{}^2 + \frac{1}{2}\theta_z{}^2\right)\Big)\,dA\,dy \\ + \frac{kAG}{2}\int_0^L \left(-\theta_x + \frac{\partial w}{\partial y}\right)^2 + \left(\theta_z + \frac{\partial u}{\partial y}\right)^2 dy \end{aligned} \tag{2.5.8}$$

The 3rd and 7th term in the above equation can be erased due to symmetry of the cross-section.

Also $I_x = \int_A z^2\,dA$, $I_z = \int_A x^2\,dA$, $I = I_x = I_z$ (due to symmetry) and $\int_S ds = A$ =area of the cross section.

Thus the above equation becomes,

$$\begin{aligned} U_1 = \frac{EI}{2}\int_0^L \left(\frac{\partial\theta_x}{\partial y}\right)^2 + \left(\frac{\partial\theta_z}{\partial y}\right)^2 dy + \frac{EA}{2}\int_0^L \left(\frac{1}{4}\theta_x{}^4 + \frac{1}{4}\theta_z{}^4 + \frac{1}{2}\theta_x{}^2\theta_z{}^2\right)dy \\ + \frac{kAG}{2}\int_0^L \left(-\theta_x + \frac{\partial w}{\partial y}\right)^2 + \left(\theta_z + \frac{\partial u}{\partial y}\right)^2 dy \end{aligned} \tag{2.5.9}$$

If there exists a constant force N_0, there is another contribution to the strain energy above [LF98].

$$U_2 = \int_0^L N_0\left(\varepsilon_l + \varepsilon_{nl}\right)dy \tag{2.5.10}$$

The total strain energy of the rotor considering shear effects and higher order deformations, thus becomes,

$$\begin{aligned} U_{Rs} &= U_1 + U_2 \\ U_{Rs} &= \int_0^L \frac{EI}{2}\left(\left(\frac{\partial\theta_x}{\partial y}\right)^2 + \left(\frac{\partial\theta z}{\partial y}\right)^2\right)dy + \int_0^L \frac{EA}{2}\left(\frac{1}{4}\theta_x{}^4 + \frac{1}{4}\theta_z{}^4 + \frac{1}{2}\theta_x{}^2\theta_z{}^2\right)dy \\ &\quad + \int_0^L \frac{kAG}{2}\left(-\theta_x + \frac{\partial w}{\partial y}\right)^2 + \left(\theta_z + \frac{\partial u}{\partial y}\right)^2 dy + \int_0^L \frac{N_0}{2}\left(\theta_x{}^2 + \theta_z{}^2\right)dy \end{aligned} \tag{2.5.11}$$

The kinetic energy of the rotor is given as,

$$T_R = T_d + T_s + T_u \tag{2.5.12}$$

Where, T_d, T_s and T_u are given by Eqs. (2.1.5), (2.1.6) and (2.1.17) respectively.

The Hamilton's principle is applied as, $\int_{t_1}^{t_2} \delta\left(T_R - U_{Rs}\right) dt = 0$. Therefore it can be written as,

$$\int_{t_1}^{t_2} \delta\left(T_R - U_{Rs}\right) dt = \int_{t_1}^{t_2} \delta T_d dt + \int_{t_1}^{t_2} \delta T_s dt + \int_{t_1}^{t_2} \delta T_u dt - \int_{t_1}^{t_2} \delta U_{Rs} dt = 0 \tag{2.5.13}$$

The 4 different terms in the above equation are treated one by one. The 1st term gives,

$$\int_{t_1}^{t_2} \delta T_d dt = \int_{t_1}^{t_2} \left(\frac{\partial T_d}{\partial \dot{u}} \delta \dot{u} + \frac{\partial T_d}{\partial \dot{w}} \delta \dot{w} + \frac{\partial T_d}{\partial \dot{\theta}_x} \delta \dot{\theta}_x + \frac{\partial T_d}{\partial \dot{\theta}_z} \delta \dot{\theta}_z + \frac{\partial T_d}{\partial \theta_x} \delta \theta_x \right) dt \tag{2.5.14}$$

Various terms in Eq. (2.5.14) can be expanded as follows,

$$\int_{t_1}^{t_2} \frac{\partial T_d}{\partial \dot{u}} \delta \dot{u}\, dt = \left[\frac{\partial T_d}{\partial \dot{u}} \delta u \right]_{t_1}^{t_2} - \int_{t_1}^{t_2} \frac{d}{dt} \left(\frac{\partial T_d}{\partial \dot{u}} \right) \delta u dt$$

$$= -\int_{t_1}^{t_2} M_d \ddot{u} \delta u dt$$

$$\int_{t_1}^{t_2} \frac{\partial T_d}{\partial \dot{w}} \delta \dot{w}\, dt = \left[\frac{\partial T_d}{\partial \dot{w}} \delta w \right]_{t_1}^{t_2} - \int_{t_1}^{t_2} \frac{d}{dt} \left(\frac{\partial T_d}{\partial \dot{w}} \right) \delta w dt$$

$$= -\int_{t_1}^{t_2} M_d \ddot{w} \delta w dt$$

$$\int_{t_1}^{t_2} \frac{\partial T_d}{\partial \dot{\theta}_x} \delta \dot{\theta}_x\, dt = \left[\frac{\partial T_d}{\partial \dot{\theta}_x} \delta \theta_x \right]_{t_1}^{t_2} - \int_{t_1}^{t_2} \frac{d}{dt} \left(\frac{\partial T_d}{\partial \dot{\theta}_x} \right) \delta \theta_x dt$$

$$= -\int_{t_1}^{t_2} I_{dx} \ddot{\theta}_x \delta \theta_x dt$$

$$\int_{t_1}^{t_2} \frac{\partial T_d}{\partial \dot{\theta}_z} \delta\dot{\theta}_z \, dt = \left[\frac{\partial T_d}{\partial \dot{\theta}_z} \delta\theta_z \right]_{t_1}^{t_2} - \int_{t_1}^{t_2} \frac{d}{dt} \left(\frac{\partial T_d}{\partial \dot{\theta}_z} \right) \delta\theta_z \, dt$$

$$= -\int_{t_1}^{t_2} \left(I_{dx} \ddot{\theta}_z + I_{dy} \Omega \dot{\theta}_x \right) \delta\theta_z \, dt \tag{2.5.15}$$

$$\int_{t_1}^{t_2} \frac{\partial T_d}{\partial \theta_x} \delta\theta_x \, dt = \int_{t_1}^{t_2} I_{dy} \Omega \dot{\theta}_z \delta\theta_x \, dt$$

The 2nd term in Eq. (2.5.13) gives,

$$\int_{t_1}^{t_2} \delta T_s \, dt = \int_{t_1}^{t_2} \left[\frac{\partial T_s}{\partial u} \delta u + \frac{\partial T_s}{\partial w} \delta w + \frac{\partial T_s}{\partial \theta_x} \delta\theta_x + \frac{\partial T_s}{\partial \theta_z} \delta\theta_z + \frac{\partial T_s}{\partial \theta_x} \delta\theta_x \right] dt \tag{2.5.16}$$

Various terms in the above equation can be expanded as follows,

$$\int_{t_1}^{t_2} \frac{\partial T_s}{\partial \dot{u}} \delta\dot{u} \, dt = \left[\frac{\partial T_s}{\partial \dot{u}} \delta u \right]_{t_1}^{t_2} - \int_{t_1}^{t_2} \frac{d}{dt} \left(\frac{\partial T_s}{\partial \dot{u}} \right) \delta u dt$$

$$= \left[\int_0^L \frac{\partial T_s}{\partial \dot{u}} \delta u \right]_{t_1}^{t_2} - \int_{t_1}^{t_2} \int_0^L \rho A \ddot{u} \delta u dy dt$$

$$\int_{t_1}^{t_2} \frac{\partial T_s}{\partial \dot{w}} \delta\dot{w} \, dt = \left[\frac{\partial T_s}{\partial \dot{w}} \delta w \right]_{t_1}^{t_2} - \int_{t_1}^{t_2} \frac{d}{dt} \left(\frac{\partial T_s}{\partial \dot{w}} \right) \delta w dt$$

$$= \left[\int_0^L \frac{\partial T_s}{\partial \dot{w}} \delta w \right]_{t_1}^{t_2} - \int_{t_1}^{t_2} \int_0^L \rho A \ddot{w} \delta w dy dt$$

$$\int_{t_1}^{t_2} \frac{\partial T_s}{\partial \dot{\theta}_x} \delta\dot{\theta}_x \, dt = \left[\frac{\partial T_s}{\partial \dot{\theta}_x} \delta\theta_x \right]_{t_1}^{t_2} - \int_{t_1}^{t_2} \frac{d}{dt} \left(\frac{\partial T_s}{\partial \dot{\theta}_x} \right) \delta\theta_x dt$$

$$= \left[\int_0^L \frac{\partial T_s}{\partial \dot{\theta}_x} \delta\theta_x \right]_{t_1}^{t_2} - \int_{t_1}^{t_2} \int_0^L \rho I \ddot{\theta}_x \delta\theta_x dy dt$$

$$\int_{t_1}^{t_2} \frac{\partial T_s}{\partial \dot{\theta}_z} \delta\dot{\theta}_z \, dt = \left[\frac{\partial T_s}{\partial \dot{\theta}_z} \delta\theta_z \right]_{t_1}^{t_2} - \int_{t_1}^{t_2} \frac{d}{dt} \left(\frac{\partial T_s}{\partial \dot{\theta}_z} \right) \delta\theta_z dt$$

$$= \left[\int_0^L \frac{\partial T_s}{\partial \dot{\theta}_z} \delta\theta_z \right]_{t_1}^{t_2} - \int_{t_1}^{t_2} \int_0^L \left(\rho I \ddot{\theta}_z + 2\rho I \Omega \dot{\theta}_x \right) \delta\theta_z dy dt$$

$$\int_{t_1}^{t_2} \frac{\partial T_s}{\partial \theta_x} \delta\theta_x \, dt = \int_{t_1}^{t_2} \int_0^L 2\rho I \Omega \dot{\theta}_z \delta\theta_x dy dt$$

(2.5.17)

Similarly the 3rd term in Eq. (2.5.13) gives,

$$\int_{t_1}^{t_2} \delta T_u \, dt = \int_{t_1}^{t_2} \left(\frac{\partial T_u}{\partial \dot{u}} \delta \dot{u} + \frac{\partial T_u}{\partial \dot{w}} \delta \dot{w} \right) dt \tag{2.5.18}$$

The 2 terms in the above equation can be treated as below,

$$\begin{aligned} \int_{t_1}^{t_2} \frac{\partial T_u}{\partial \dot{u}} \delta \dot{u} \, dt &= \left(\frac{\partial T_u}{\partial \dot{u}} \delta u \right)_{t_1}^{t_2} - \int_{t_1}^{t_2} \frac{d}{dt} \left(\frac{\partial T_u}{\partial \dot{u}} \right) \delta u dt = \int_{t_1}^{t_2} m_u \Omega^2 d \sin \Omega t \delta u dt \\ \int_{t_1}^{t_2} \frac{\partial T_u}{\partial \dot{w}} \delta \dot{w} \, dt &= \left(\frac{\partial T_u}{\partial \dot{w}} \delta w \right)_{t_1}^{t_2} - \int_{t_1}^{t_2} \frac{d}{dt} \left(\frac{\partial T_u}{\partial \dot{w}} \right) \delta w dt = \int_{t_1}^{t_2} m_u \Omega^2 d \cos \Omega t \delta w dt \end{aligned} \tag{2.5.19}$$

Similarly the 4th term in Eq. (2.5.13) gives,

$$\int_{t_1}^{t_2} \delta U_s \, dt = \int_{t_1}^{t_2} \left(\frac{\partial U_s}{\partial u} \delta u + \frac{\partial U_s}{\partial w} \delta w + \frac{\partial U_s}{\partial \theta_x} \delta \theta_x + \frac{\partial U_s}{\partial \theta_z} \delta \theta_z \right) dt \tag{2.5.20}$$

The various terms in the above equation can be written as below,

$$\int_{t_1}^{t_2} \frac{\partial U_s}{\partial u} \delta u dt = \int_{t_1}^{t_2} \int_0^L \frac{\partial}{\partial y} \left(kAG \left(\theta_z + \frac{\partial u}{\partial y} \right) \right) \delta u dy dt$$

$$\int_{t_1}^{t_2} \frac{\partial U_s}{\partial w} \delta w dt = \int_{t_1}^{t_2} \int_0^L \frac{\partial}{\partial y} \left(kAG \left(-\theta_x + \frac{\partial w}{\partial y} \right) \right) \delta w dy dt$$

$$\int_{t_1}^{t_2} \frac{\partial U_s}{\partial \theta_x} \delta \theta_x dt = \int_{t_1}^{t_2} \int_0^L \left(\begin{array}{l} EI \dfrac{\partial^2}{\partial y^2} \theta_x + \dfrac{EA}{2} \theta_x^3 + \dfrac{EA}{2} \theta_x \theta_z^2 \\ -kAG \left(-\theta_x + \dfrac{\partial w}{\partial y} \right) + N_0 \theta_x \end{array} \right) \delta \theta_x dy dt$$

$$\int_{t_1}^{t_2} \frac{\partial U_s}{\partial \theta_z} \delta \theta_z dt = \int_{t_1}^{t_2} \int_0^L \left(EI \frac{\partial^2}{\partial y^2} \theta_z + \frac{EA}{2} \theta_z^3 + \frac{EA}{2} \theta_z \theta_x^2 + kAG \left(\theta_z + \frac{\partial u}{\partial y} \right) + N_0 \theta_z \right) \delta \theta_z dy dt \tag{2.5.21}$$

The equations of motion can be written by collecting the terms of the type δu , δw , $\delta \theta_x$, $\delta \theta_z$ in the above system of equations.

The terms of the type δu give,

$$-\int_{t_1}^{t_2} M_d \ddot{u} \delta u dt - \int_{t_1}^{t_2} \int_0^L \rho A \ddot{u} \delta u dy dt + \int_{t_1}^{t_2} m_u \Omega^2 d \sin \Omega t \delta u dt - \int_{t_1}^{t_2} \int_0^L \frac{\partial}{\partial y} \left(kAG \left(\theta_z + \frac{\partial u}{\partial y} \right) \right) \delta u dy dt = 0$$

$$\int_{t_1}^{t_2} \left(-M_d \ddot{u} - \int_0^L \rho A \ddot{u} dy + m_u \Omega^2 d \sin \Omega t - \int_0^L \frac{\partial}{\partial y} \left(kAG \left(\theta_z + \frac{\partial u}{\partial y} \right) dy \right) \right) \delta u dt = 0$$

$$\boxed{M_d\ddot{u} + \rho A\int_0^L \ddot{u}dy + kAG\int_0^L \left(\frac{\partial}{\partial y}\theta_z + \frac{\partial^2 u}{\partial y^2}\right)dy = m_u\Omega^2 d\sin\Omega t} \tag{2.5.22}$$

The terms of the type δw give,

$$-\int_{t_1}^{t_2} M_d\ddot{w}\delta w dt - \int_{t_1}^{t_2}\int_0^L \rho A\ddot{w}\delta w dy dt + \int_{t_1}^{t_2} m_u\Omega^2 d\cos\Omega t\delta w dt - \int_{t_1}^{t_2}\int_0^L \frac{\partial}{\partial y}\left(kAG\left(-\theta_x + \frac{\partial w}{\partial y}\right)\right)\delta w dy dt = 0$$

$$\int_{t_1}^{t_2}\left(-M_d\ddot{w} - \int_0^L \rho A\ddot{w}dy + m_u\Omega^2 d\cos\Omega t - \int_0^L \frac{\partial}{\partial y}\left(kAG\left(-\theta_x + \frac{\partial w}{\partial y}\right)\right)dy\right)\delta w dt = 0$$

$$\boxed{M_d\ddot{w} + \rho A\int_0^L \ddot{w}dy + kAG\int_0^L \left(-\frac{\partial}{\partial y}\theta_x + \frac{\partial^2 w}{\partial y^2}\right)dy = m_u\Omega^2 d\cos\Omega t} \tag{2.5.23}$$

The terms of the type $\delta\theta_x$ give,

$$-\int_{t_1}^{t_2} I_{dx}\ddot{\theta}_x\delta\theta_x dt + \int_{t_1}^{t_2} I_{dy}\Omega\dot{\theta}_z\delta\theta_x dt - \int_{t_1}^{t_2}\int_0^L \rho I\ddot{\theta}_x\delta\theta_x dy dt + \int_{t_1}^{t_2}\int_0^L 2\rho I\Omega\dot{\theta}_z\delta\theta_x dy dt -$$

$$\int_{t_1}^{t_2}\int_0^L \left(-EI\frac{\partial^2}{\partial y^2}\theta_x + \frac{EA}{2}\theta_x^3 + \frac{EA}{2}\theta_x\theta_z^2 - kAG\left(-\theta_x + \frac{\partial w}{\partial y}\right) + N_0\theta_x\right)\delta\theta_x dy dt = 0$$

$$\boxed{\begin{aligned} &-I_{dx}\ddot{\theta}_x + I_{dy}\Omega\dot{\theta}_z - \int_0^L \rho I\ddot{\theta}_x dy + \int_0^L 2\rho I\Omega\dot{\theta}_z dy \\ &-\int_0^L \left(-EI\frac{\partial^2}{\partial y^2}\theta_x + \frac{EA}{2}\theta_x^3 + \frac{EA}{2}\theta_x\theta_z^2 - kAG\left(-\theta_x + \frac{\partial w}{\partial y}\right) + N_0\theta_x\right)dy = 0 \end{aligned}} \tag{2.5.24}$$

The terms of the type $\delta\theta_z$ give,

$$-\int_{t_1}^{t_2}\left(I_{dx}\ddot{\theta}_z + I_{dy}\Omega\dot{\theta}_x\right)\delta\theta_z dt - \int_{t_1}^{t_2}\int_0^L \left(\rho I\ddot{\theta}_z + 2\rho I\Omega\dot{\theta}_x\right)\delta\theta_z dy dt -$$

$$\int_{t_1}^{t_2}\int_0^L \left(-EI\frac{\partial^2}{\partial y^2}\theta_z + \frac{EA}{2}\theta_z^3 + \frac{EA}{2}\theta_z\theta_x^2 + kAG\left(\theta_z + \frac{\partial u}{\partial y}\right) + N_0\theta_z\right)\delta\theta_z dy dt = 0$$

$$\boxed{\begin{aligned} &-I_{dx}\ddot{\theta}_z - I_{dy}\Omega\dot{\theta}_x - \int_0^L \rho I\ddot{\theta}_z dy - \int_0^L 2\rho I\Omega\dot{\theta}_x dy \\ &-\int_0^L \left(-EI\frac{\partial^2}{\partial y^2}\theta_z + \frac{EA}{2}\theta_z^3 + \frac{EA}{2}\theta_z\theta_x^2 + kAG\left(\theta_z + \frac{\partial u}{\partial y}\right) + N_0\theta_z\right)dy = 0 \end{aligned}} \tag{2.5.25}$$

Eqs. (2.5.22),(2.5.23), (2.5.24) and (2.5.25) are the equations of motion for the rotor system, considering shear effects and higher order deformations.

2.5.2. Nonlinear Model with Shear Effects and Higher Order Deformations (Discretized Method)

The strain energy given by Eq. (2.4.12) is referred.When shear deformation is not taken into account the angular displacement θ_x and θ_z are equal to $\frac{\partial w}{\partial y}$ and $\frac{\partial u}{\partial y}$ respectively. See Fig. 24 (b), but when shear deformation is also considered (Timoshenko beam) the angular displacements change due to the contribution of the shear angle β_x Fig. 24(c). Shear angle and shear forces are explained in Y-Z plane in Fig. 24.

The angular displacements can be expressed in the form of linear displacement using the following relations,

$$\theta_x = \frac{\partial w}{\partial y} - \beta_x \quad , \quad \theta_z = -\frac{\partial u}{\partial y} + \beta_z \tag{2.5.26}$$

Application of the Newton's 2nd law to Fig. 24 gives,

$$\begin{aligned} \rho A dy \frac{\partial^2 u}{\partial t^2} &= -V_z + \left(V_z + \frac{\partial V_z}{\partial y} dy \right) \\ \rho A dy \frac{\partial^2 w}{\partial t^2} &= -V_x + \left(V_x + \frac{\partial V_x}{\partial y} dy \right) \end{aligned} \tag{2.5.27}$$

This is solved for V_x and V_z to give,

$$\begin{aligned} V_z &= \rho A \int \frac{\partial^2 u}{\partial t^2} dy \\ V_x &= \rho A \int \frac{\partial^2 w}{\partial t^2} dy \end{aligned} \tag{2.5.28}$$

The relation between shear force and shear angle is

$$V_x = \beta_x kAG \ , V_z = \beta_z kAG \tag{2.5.29}$$

Where, k is shear correction factor.

Therefore the angular displacements, using Eqs. (2.5.26) and (2.5.29) can be given as,

$$\begin{aligned} \theta_x &= \frac{\partial w}{\partial y} - \frac{\rho \int \frac{\partial^2 w}{\partial t^2} dy}{kG} \\ \theta_z &= -\frac{\partial u}{\partial y} + \frac{\rho \int \frac{\partial^2 u}{\partial t^2} dy}{kG} \end{aligned} \tag{2.5.30}$$

The displacements $u(y,t)$ and $w(y,t)$ are discretized as follows,

$$u(y,t) = U(t)\sin\frac{n\pi y}{L}$$
$$w(y,t) = W(t)\sin\frac{n\pi y}{L} \tag{2.5.31}$$

Where *U* and *W* are generalized independent coordinates and n represents the number of the mode studied. In the present work n = 1.

Equation (2.5.30) is substituted in Eqs. (2.1.18) and (2.4.12) and Eq. (2.5.31) is used in the resulting equations.

Lagrange equations are applied in the following form,

$$\frac{d}{dt}\left(\frac{\partial T_R}{\partial \dot{U}(t)}\right) - \frac{\partial T_R}{\partial U(t)} + \frac{\partial U_{s1}}{\partial U(t)} = 0 \tag{2.5.32}$$

$$\frac{d}{dt}\left(\frac{\partial T_R}{\partial \dot{W}(t)}\right) - \frac{\partial T_R}{\partial W(t)} + \frac{\partial U_{s1}}{\partial W(t)} = 0 \tag{2.5.33}$$

Finally, the equations of motion obtained are given as below,

$$\begin{aligned}&\ddot{U} - \Omega\alpha_{21}\ddot{W} + \alpha_{31}U - \Omega\alpha_{41}\dot{W} + \alpha_{51}U + c\dot{W} = (-3/2)\beta_{11}(W^2\ddot{U} + 2UW\ddot{W} \\ &+3U^2\ddot{U}) - (3/2)\beta_{21}(U\dot{W}^2 + 2W\dot{U}\dot{W} + 3U\dot{U}^2) - (3/4)\beta_{31}(U^3 + UW^2) \\ &-(3/16)\beta_{41}(\dot{U}^3 + \dot{U}\dot{W}^2) + m_1\Omega^2\sin\Omega t\end{aligned} \tag{2.5.34}$$

$$\begin{aligned}&\ddot{W} + \Omega\alpha_{21}\dot{U} + \alpha_{31}W + \Omega\alpha_{41}\dot{U} + \alpha_{51}W + c\dot{U} = (-3/2)\beta_{11}(U^2\ddot{W} + 2WU\ddot{U} \\ &+3W^2\ddot{W}) - (3/2)\beta_{21}(W\dot{U}^2 + 2U\dot{U}\dot{W} + 3W\dot{W}^2) - (3/4)\beta_{31}(W^3 + WU^2) \\ &-(3/16)\beta_{41}(\dot{W}^3 + \dot{W}\dot{U}^2) + m_1\Omega^2\cos\Omega t\end{aligned} \tag{2.5.35}$$

Eqs. (2.5.34) and (2.5.35) are the 4th order nonlinear differential equations of motion obtained by considering the shear effects and higher order deformations.

Where,

$$\begin{aligned}&\alpha_{21} = \alpha_2/\alpha_1\ ,\ \alpha_{31} = \alpha_3/\alpha_1\ ,\ \alpha_{41} = \alpha_4/\alpha_1\ ,\ \alpha_{51} = \alpha_5/\alpha_1\ , \\ &\beta_{11} = \beta_1/\alpha_1\ ,\ \beta_{21} = \beta_2/\alpha_1\ ,\ \beta_{31} = \beta_3/\alpha_1\ ,\ \beta_{41} = \beta_4/\alpha_1\ , \\ &m_1 = \sqrt{3}m_u d_1/2\alpha_1\end{aligned} \tag{2.5.36}$$

Where $\alpha_1..\alpha_5$ and $\beta_1..\beta_4$ are functions of geometric and material properties of the rotor, given as

$$\begin{aligned}&\alpha_1 = \rho(2\rho IL + I_{dx})/4kG\ ,\ \alpha_2 = \rho(4\rho IL + I_{dy})/4kG\ , \\ &\alpha_3 = \rho EI\pi^2/2kGL + (I_{dx}\pi^2 + 2\rho AL^3 + 3M_d L^2 + 2\rho I\pi^2 L)/4L, \\ &\alpha_4 = \pi^2(4\rho IL + I_{dy})/4L^2\ ,\ \alpha_5 = EI\pi^4/2L^3\ ,\ \beta_1 = \rho AE\pi^2/8LkG, \\ &\beta_2 = \rho^2 EAL/8k^2G^2\ ,\ \beta_3 = EA\pi^4/4L^3\ ,\ \beta_4 = \rho^3 EAL^3/k^3G^3\pi^2\end{aligned} \tag{2.5.37}$$

The linear free dynamic behavior of the rotor system can be investigated by taking into account only the linear portion of these equations given below,

$$\ddot{U} - \Omega\alpha_{21}\dot{W} + \alpha_{31}\dot{U} - \Omega\alpha_{41}W + \alpha_{51}U = 0 \tag{2.5.38}$$

$$\ddot{W} + \Omega\alpha_{21}\dot{U} + \alpha_{31}\dot{W} + \Omega\alpha_{41}U + \alpha_{51}W = 0 \tag{2.5.39}$$

The above two equations can be compared with the equations of motion of a continuous rotor derived by Eshleman and Eubanks [EE69] also reproduced in the book of Yamamoto and Ishida [YI01].

2.5.3. Nonlinear Model with Shear Effects and a Dynamic Axial Force

In the following a nonlinear mathematical model is developed taking into account the combined effects of shear deformations and a dynamic axial force.

The deformation energy of the rotor is given by,

$$U_{Rs} = \int_0^L \frac{EI}{2}\left[\left(\frac{\partial\theta_x}{\partial y}\right)^2 + \left(\frac{\partial\theta z}{\partial y}\right)^2\right]dy + \int_0^L \frac{kAG}{2}\left[\left(-\theta_x + \frac{\partial w}{\partial y}\right)^2 + \left(\theta_z + \frac{\partial u}{\partial y}\right)^2\right]dy + \int_0^L \frac{N_A}{2}\left(\theta_x^{\,2} + \theta_z^{\,2}\right)dy \tag{2.5.40}$$

Where N_A is an axial force given by $\int_0^L \frac{EA}{2L}\left(\theta_x^{\,2} + \theta_z^{\,2}\right)dy$

Therefore, Eq. (2.5.40) now becomes,

$$U_{Rs} = \int_0^L \frac{EI}{2}\left[\left(\frac{\partial\theta_x}{\partial y}\right)^2 + \left(\frac{\partial\theta z}{\partial y}\right)^2\right]dy + \int_0^L \frac{kAG}{2}\left[\left(-\theta_x + \frac{\partial w}{\partial y}\right)^2 + \left(\theta_z + \frac{\partial u}{\partial y}\right)^2\right]dy + \frac{EA}{2L}\int_0^L\left[\int_0^L\left(\theta_x^{\,2} + \theta_z^{\,2}\right)dy\left(\theta_x^{\,2} + \theta_z^{\,2}\right)dy\right]dy$$

The above equation can be further written as,

$$U_{Rs} = \int_0^L \frac{EI}{2}\left[\left(\frac{\partial\theta_x}{\partial y}\right)^2 + \left(\frac{\partial\theta z}{\partial y}\right)^2\right]dy + \int_0^L \frac{kAG}{2}\left[\left(-\theta_x + \frac{\partial w}{\partial y}\right)^2 + \left(\theta_z + \frac{\partial u}{\partial y}\right)^2\right]dy + \frac{EA}{2L}\int_0^L\left[\theta_x^{\,2}\int_0^L\left(\theta_x^{\,2} + \theta_z^{\,2}\right)dy + \theta_z^{\,2}\int_0^L\left(\theta_x^{\,2} + \theta_z^{\,2}\right)dy\right]dy \tag{2.5.41}$$

The kinetic energy of the rotor is given as,

$$T_R = T_d + T_s + T_u \tag{2.5.42}$$

Where, T_d, T_s and T_u are given by Eqs. (2.1.5), (2.1.6) and (2.1.17) respectively.

The Hamilton's principle is applied as, $\int_{t_1}^{t_2}\delta\left(T_R - U_{Rs}\right)dt = 0$. Therefore it can be written as,

$$\int_{t_1}^{t_2} \delta\left(T_R - U_{Rs}\right) dt = \int_{t_1}^{t_2} \delta T_d dt + \int_{t_1}^{t_2} \delta T_s dt + \int_{t_1}^{t_2} \delta T_u dt - \int_{t_1}^{t_2} \delta U_{Rs} dt = 0 \tag{2.5.43}$$

The 4 different terms in the above equation are treated one by one. The 1st term gives,

$$\int_{t_1}^{t_2} \delta T_d dt = \int_{t_1}^{t_2} \left(\frac{\partial T_d}{\partial \dot{u}} \delta \dot{u} + \frac{\partial T_d}{\partial \dot{w}} \delta \dot{w} + \frac{\partial T_d}{\partial \dot{\theta}_x} \delta \dot{\theta}_x + \frac{\partial T_d}{\partial \dot{\theta}_z} \delta \dot{\theta}_z + \frac{\partial T_d}{\partial \theta_x} \delta \theta_x \right) dt \tag{2.5.44}$$

Various terms in Eq. (2.5.44) can be calculated as follows,

$$\int_{t_1}^{t_2} \frac{\partial T_d}{\partial \dot{u}} \delta \dot{u}\, dt = \left[\frac{\partial T_d}{\partial \dot{u}} \delta u \right]_{t_1}^{t_2} - \int_{t_1}^{t_2} \frac{d}{dt} \left(\frac{\partial T_d}{\partial \dot{u}} \right) \delta u dt$$

$$= -\int_{t_1}^{t_2} M_d \ddot{u} \delta u dt$$

$$\int_{t_1}^{t_2} \frac{\partial T_d}{\partial \dot{w}} \delta \dot{w}\, dt = \left[\frac{\partial T_d}{\partial \dot{w}} \delta w \right]_{t_1}^{t_2} - \int_{t_1}^{t_2} \frac{d}{dt} \left(\frac{\partial T_d}{\partial \dot{w}} \right) \delta w dt$$

$$= -\int_{t_1}^{t_2} M_d \ddot{w} \delta w dt$$

$$\int_{t_1}^{t_2} \frac{\partial T_d}{\partial \dot{\theta}_x} \delta \dot{\theta}_x\, dt = \left[\frac{\partial T_d}{\partial \dot{\theta}_x} \delta \theta_x \right]_{t_1}^{t_2} - \int_{t_1}^{t_2} \frac{d}{dt} \left(\frac{\partial T_d}{\partial \dot{\theta}_x} \right) \delta \theta_x dt$$

$$= -\int_{t_1}^{t_2} I_{dx} \ddot{\theta}_x \delta \theta_x dt$$

$$\int_{t_1}^{t_2} \frac{\partial T_d}{\partial \dot{\theta}_z} \delta \dot{\theta}_z\, dt = \left[\frac{\partial T_d}{\partial \dot{\theta}_z} \delta \theta_z \right]_{t_1}^{t_2} - \int_{t_1}^{t_2} \frac{d}{dt} \left(\frac{\partial T_d}{\partial \dot{\theta}_z} \right) \delta \theta_z dt$$

$$= -\int_{t_1}^{t_2} \left(I_{dx} \ddot{\theta}_z + I_{dy} \Omega \dot{\theta}_x \right) \delta \theta_z dt \tag{2.5.45}$$

$$\int_{t_1}^{t_2} \frac{\partial T_d}{\partial \theta_x} \delta \theta_x\, dt = \int_{t_1}^{t_2} I_{dy} \Omega \dot{\theta}_z \delta \theta_x dt$$

The 2nd term in Eq. (2.5.43) gives,

$$\int_{t_1}^{t_2} \delta T_s dt = \int_{t_1}^{t_2} \left(\frac{\partial T_s}{\partial \dot{u}} \delta \dot{u} + \frac{\partial T_s}{\partial \dot{w}} \delta \dot{w} + \frac{\partial T_s}{\partial \dot{\theta}_x} \delta \dot{\theta}_x + \frac{\partial T_s}{\partial \dot{\theta}_z} \delta \dot{\theta}_z + \frac{\partial T_s}{\partial \theta_x} \delta \theta_x \right) dt \tag{2.5.46}$$

Various terms in the above equation can be calculated as follows,

$$\int_{t_1}^{t_2} \frac{\partial T_s}{\partial \dot{u}} \delta\dot{u}\, dt = \left[\frac{\partial T_s}{\partial \dot{u}} \delta u\right]_{t_1}^{t_2} - \int_{t_1}^{t_2} \frac{d}{dt}\left(\frac{\partial T_s}{\partial \dot{u}}\right) \delta u dt$$

$$= \left[\int_0^L \frac{\partial T_s}{\partial \dot{u}} \delta u\, dy\right]_{t_1}^{t_2} - \int_{t_1}^{t_2}\int_0^L \rho A \ddot{u} \delta u dy dt$$

$$\int_{t_1}^{t_2} \frac{\partial T_s}{\partial \dot{w}} \delta\dot{w}\, dt = \left[\frac{\partial T_s}{\partial \dot{w}} \delta w\right]_{t_1}^{t_2} - \int_{t_1}^{t_2} \frac{d}{dt}\left(\frac{\partial T_s}{\partial \dot{w}}\right) \delta w dt$$

$$= \left[\int_0^L \frac{\partial T_s}{\partial \dot{w}} \delta w\, dy\right]_{t_1}^{t_2} - \int_{t_1}^{t_2}\int_0^L \rho A \ddot{w} \delta w dy dt$$

$$\int_{t_1}^{t_2} \frac{\partial T_s}{\partial \dot{\theta}_x} \delta\dot{\theta}_x\, dt = \left[\frac{\partial T_s}{\partial \dot{\theta}_x} \delta\theta_x\right]_{t_1}^{t_2} - \int_{t_1}^{t_2} \frac{d}{dt}\left(\frac{\partial T_s}{\partial \dot{\theta}_x}\right) \delta\theta_x dt$$

$$= \left[\int_0^L \frac{\partial T_s}{\partial \dot{\theta}_x} \delta\theta_x\, dy\right]_{t_1}^{t_2} - \int_{t_1}^{t_2}\int_0^L \rho I \ddot{\theta}_x \delta\theta_x dy dt$$

$$\int_{t_1}^{t_2} \frac{\partial T_s}{\partial \dot{\theta}_z} \delta\dot{\theta}_z\, dt = \left[\frac{\partial T_s}{\partial \dot{\theta}_z} \delta\theta_z\right]_{t_1}^{t_2} - \int_{t_1}^{t_2} \frac{d}{dt}\left(\frac{\partial T_s}{\partial \dot{\theta}_z}\right) \delta\theta_z dt$$

$$= \left[\int_0^L \frac{\partial T_s}{\partial \dot{\theta}_z} \delta\theta_z\, dy\right]_{t_1}^{t_2} - \int_{t_1}^{t_2}\int_0^L \left(\rho I \ddot{\theta}_z + 2\rho I \Omega \dot{\theta}_x\right) \delta\theta_z dy dt \tag{2.5.47}$$

$$\int_{t_1}^{t_2} \frac{\partial T_s}{\partial \theta_x} \delta\theta_x\, dt = \int_{t_1}^{t_2}\int_0^L 2\rho I \Omega \dot{\theta}_z \delta\theta_x dy dt$$

Similarly the 3rd term in Eq. (2.5.43) gives,

$$\int_{t_1}^{t_2} \delta T_u dt = \int_{t_1}^{t_2} \left(\frac{\partial T_u}{\partial \dot{u}} \delta\dot{u} + \frac{\partial T_u}{\partial \dot{w}} \delta\dot{w}\right) dt \tag{2.5.48}$$

The 2 terms in the above equation can be treated as below,

$$\int_{t_1}^{t_2} \frac{\partial T_u}{\partial \dot{u}} \delta\dot{u}\, dt = \left[\frac{\partial T_u}{\partial \dot{u}} \delta u\right]_{t_1}^{t_2} - \int_{t_1}^{t_2} \frac{d}{dt}\left(\frac{\partial T_u}{\partial \dot{u}}\right) \delta u dt = \int_{t_1}^{t_2} m_u \Omega^2 d \sin\Omega t \delta u dt$$

$$\int_{t_1}^{t_2} \frac{\partial T_u}{\partial \dot{w}} \delta\dot{w}\, dt = \left[\frac{\partial T_u}{\partial \dot{w}} \delta w\right]_{t_1}^{t_2} - \int_{t_1}^{t_2} \frac{d}{dt}\left(\frac{\partial T_u}{\partial \dot{w}}\right) \delta w dt = \int_{t_1}^{t_2} m_u \Omega^2 d \cos\Omega t \delta w dt \tag{2.5.49}$$

Similarly the 4th term in Eq. (2.5.43) gives,

$$\int_{t_1}^{t_2} \delta U_{Rs}\, dt = \int_{t_1}^{t_2} \left(\frac{\partial U_{Rs}}{\partial u}\delta u + \frac{\partial U_{Rs}}{\partial w}\delta w + \frac{\partial U_{Rs}}{\partial \theta_x}\delta\theta_x + \frac{\partial U_{Rs}}{\partial \theta_z}\delta\theta_z \right) dt \tag{2.5.50}$$

The various terms in the above equation can be written as below,

$$\int_{t_1}^{t_2} \frac{\partial U_{Rs}}{\partial u}\delta u\, dt = \int_{t_1}^{t_2}\int_0^L \frac{\partial}{\partial y}\left(kAG\left(-\theta_z + \frac{\partial u}{\partial y} \right) \right)\delta u\, dy\, dt$$

$$\int_{t_1}^{t_2} \frac{\partial U_{Rs}}{\partial w}\delta w\, dt = \int_{t_1}^{t_2}\int_0^L \frac{\partial}{\partial y}\left(kAG\left(-\theta_x + \frac{\partial w}{\partial y} \right) \right)\delta w\, dy\, dt$$

$$\int_{t_1}^{t_2} \frac{\partial U_{Rs}}{\partial \theta_x}\delta\theta_x\, dt = \int_{t_1}^{t_2}\int_0^L \left(\begin{array}{l} -EI\dfrac{\partial^2}{\partial y^2}\theta_x - kAG\left(-\theta_x + \dfrac{\partial w}{\partial y} \right) \\ + \dfrac{EA}{L}\theta_x \displaystyle\int_0^L \left(\theta_x^{\,2} + \theta_z^{\,2} \right) dy + \left(\theta_x^{\,2} + \theta_z^{\,2} \right) \int_0^L \theta_x\, dy \end{array} \right) \delta\theta_x\, dy\, dt \tag{2.5.51}$$

$$\int_{t_1}^{t_2} \frac{\partial U_{Rs}}{\partial \theta_z}\delta\theta_z\, dt = \int_{t_1}^{t_2}\int_0^L \left(\begin{array}{l} -EI\dfrac{\partial^2}{\partial y^2}\theta_z + kAG\left(-\theta_z + \dfrac{\partial u}{\partial y} \right) \\ + \dfrac{EA}{L}\theta_z \displaystyle\int_0^L \left(\theta_x^{\,2} + \theta_z^{\,2} \right) dy + \left(\theta_x^{\,2} + \theta_z^{\,2} \right) \int_0^L \theta_z\, dy \end{array} \right) \delta\theta_z\, dy\, dt$$

Collecting the terms of the type δu in Eqs. (2.5.45), (2.5.47), (2.5.49) and (2.5.51),

$$-\int_{t_1}^{t_2} M_d \ddot{u}\delta u\, dt - \int_{t_1}^{t_2}\int_0^L \rho A\ddot{u}\delta u\, dy\, dt + \int_{t_1}^{t_2} m_u \Omega^2 d \sin\Omega t\, \delta u\, dt - \int_{t_1}^{t_2}\int_0^L \frac{\partial}{\partial y}\left(kAG\left(-\theta_z + \frac{\partial u}{\partial y} \right) \right)\delta u\, dy\, dt = 0$$

$$\int_{t_1}^{t_2} \left(-M_d \ddot{u} - \int_0^L \rho A\ddot{u}\, dy + m_u \Omega^2 d \sin\Omega t - \int_0^L \frac{\partial}{\partial y}\left(kAG\left(-\theta_z + \frac{\partial u}{\partial y} \right) \right) dy \right) \delta u\, dt = 0$$

$$\boxed{M_d \ddot{u} + \rho A \int_0^L \ddot{u}\, dy + kAG \int_0^L \left(-\frac{\partial}{\partial y}\theta_z + \frac{\partial^2 u}{\partial y^2} \right) dy = m_u \Omega^2 d \sin\Omega t} \tag{2.5.52}$$

Collecting the terms of the type δw in Eqs. (2.5.45), (2.5.47), (2.5.49) and (2.5.51),

$$-\int_{t_1}^{t_2} M_d \ddot{w}\delta w\, dt - \int_{t_1}^{t_2}\int_0^L \rho A\ddot{w}\delta w\, dy\, dt + \int_{t_1}^{t_2} m_u \Omega^2 d \cos\Omega t\, \delta w\, dt - \int_{t_1}^{t_2}\int_0^L \frac{\partial}{\partial y}\left(kAG\left(-\theta_x + \frac{\partial w}{\partial y} \right) \right)\delta w\, dy\, dt = 0$$

$$\int_{t_1}^{t_2} \left(-M_d \ddot{w} - \int_0^L \rho A\ddot{w}\, dy + m_u \Omega^2 d \cos\Omega t - \int_0^L \frac{\partial}{\partial y}\left(kAG\left(-\theta_x + \frac{\partial w}{\partial y} \right) \right) dy \right) \delta w\, dt = 0$$

$$\boxed{M_d \ddot{w} + \rho A \int_0^L \ddot{w}\, dy + kAG \int_0^L \left(-\frac{\partial}{\partial y}\theta_x + \frac{\partial^2 w}{\partial y^2} \right) dy = m_u \Omega^2 d \cos\Omega t} \tag{2.5.53}$$

Collecting the terms of the type $\delta\theta_x$ in Eqs. (2.5.45), (2.5.47), (2.5.49) and (2.5.51),

$$-\int_{t_1}^{t_2} I_{dx}\ddot{\theta}_x \delta\theta_x dt + \int_{t_1}^{t_2} I_{dy}\Omega\dot{\theta}_z \delta\theta_x dt - \int_{t_1}^{t_2}\int_0^L \rho I\ddot{\theta}_x \delta\theta_x dy dt + \int_{t_1}^{t_2}\int_0^L 2\rho I\Omega\dot{\theta}_z \delta\theta_x dy dt -$$

$$\int_{t_1}^{t_2}\int_0^L \left[EI\frac{\partial^2}{\partial y^2}\theta_x - kAG\left(\theta_x + \frac{\partial w}{\partial y}\right) + \frac{EA}{L}\theta_x \int_0^L \left(\theta_x^2 + \theta_z^2\right) dy + \left(\theta_x^2 + \theta_z^2\right)\int_0^L \theta_x dy\right] \delta\theta_x dy dt = 0$$

$$\begin{aligned} &-I_{dx}\ddot{\theta}_x + I_{dy}\Omega\dot{\theta}_z - \int_0^L \rho I\ddot{\theta}_x dy + \int_0^L 2\rho I\Omega\dot{\theta}_z dy \\ &-\int_0^L \left[EI\frac{\partial^2}{\partial y^2}\theta_x - kAG\left(\theta_x + \frac{\partial w}{\partial y}\right) + \frac{EA}{L}\theta_x \int_0^L \left(\theta_x^2 + \theta_z^2\right) dy + \left(\theta_x^2 + \theta_z^2\right)\int_0^L \theta_x dy\right] dy = 0 \end{aligned} \tag{2.5.54}$$

Collecting the terms of the type $\delta\theta_z$ in Eqs. (2.5.45), (2.5.47), (2.5.49) and (2.5.51),

$$-\int_{t_1}^{t_2} \left(I_{dx}\ddot{\theta}_z + I_{dy}\Omega\dot{\theta}_x\right)\delta\theta_z dt - \int_{t_1}^{t_2}\int_0^L \left(\rho I\ddot{\theta}_z + 2\rho I\Omega\dot{\theta}_x\right)\delta\theta_z dy dt$$

$$-\int_{t_1}^{t_2}\int_0^L \left[EI\frac{\partial^2}{\partial y^2}\theta_z + kAG\left(\theta_z + \frac{\partial u}{\partial y}\right) + \frac{EA}{L}\theta_z \int_0^L \left(\theta_x^2 + \theta_z^2\right) dy + \left(\theta_x^2 + \theta_z^2\right)\int_0^L \theta_z dy\right] \delta\theta_z dy dt = 0$$

$$\begin{aligned} &-I_{dx}\ddot{\theta}_z - I_{dy}\Omega\dot{\theta}_x - \int_0^L \rho I\ddot{\theta}_z dy - \int_0^L 2\rho I\Omega\dot{\theta}_x dy \\ &-\int_0^L \left[EI\frac{\partial^2}{\partial y^2}\theta_z + kAG\left(\theta_z + \frac{\partial u}{\partial y}\right) + \frac{EA}{L}\theta_z \int_0^L \left(\theta_x^2 + \theta_z^2\right) dy + \left(\theta_x^2 + \theta_z^2\right)\int_0^L \theta_z dy\right] dy = 0 \end{aligned} \tag{2.5.55}$$

Eqs. (2.5.52), (2.5.53), (2.5.54) and (2.5.55) are the equations of motion of the rotor system considering the combined effects of shear deformations and a dynamic axial force.

2.6. A Case Study for the Dynamic Analysis of Composite Rotors

Composite materials have become very attractive for rotating systems due to their high strength to weight ratio. Behavior of the rotating system can be predetermined in terms of critical speeds by changing arrangements of different composite layers. Some studies on the dynamic behaviour of composite rotors have been performed by different authors, most of them being recent. In the following paragraphs we briefly discuss some aspects of dynamic analysis of a composite rotor that we have studied.

The shaft shown consists of different plies of composite material. Each ply has a orthotropic mechanical behavior.

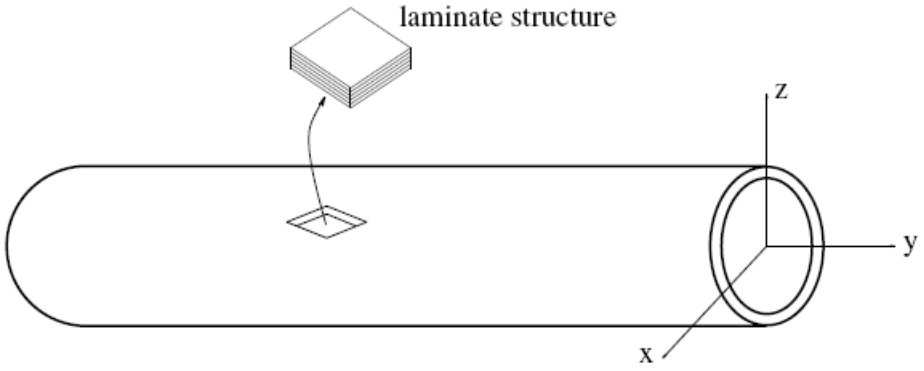

Fig. 26. Shaft of a composite rotor

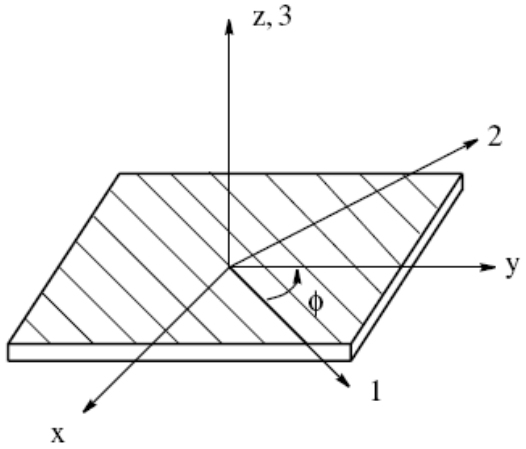

Fig. 27. Plan of Pli

2.6.1. Finite Element Analysis of the composite shaft

The generalized Hook's Law gives the following relation between stress strain fields.

$$\begin{bmatrix} \varepsilon_1 \\ \varepsilon_2 \\ \gamma_{12} \\ \gamma_{23} \\ \gamma_{13} \end{bmatrix} = \begin{bmatrix} 1/E_1 & -\nu_{21}/E_2 & 0 & 0 & 0 \\ -\nu_{21}/E_1 & 1/E_2 & 0 & 0 & 0 \\ 0 & 0 & 1/G_{12} & 0 & 0 \\ 0 & 0 & 0 & 1/G_{23} & 0 \\ 0 & 0 & 0 & 0 & 1/G_{13} \end{bmatrix} \begin{bmatrix} \sigma_1 \\ \sigma_2 \\ \tau_{12} \\ \tau_{23} \\ \tau_{13} \end{bmatrix} \tag{2.6.1}$$

Where E_1 and E_2 are Young's moduli in the orthotropic axis. G_{23} , G_{13} and G_{12} are transversal shear moduli and ν_{12} , ν_{21} are Poisson's ratios.Each ply has a plane stress state $\sigma_{33} = 0$.

First we develop the elastic and damping properties of the orthotropic ply. Each ply 'p' is at an angle ϕ_p between the shaft and fibre axis. By using a transfer matrix [T] the equations of the ply can be written in global frame (x, y, and z).

$$[T] = \begin{bmatrix} c^2 & s^2 & -2cs \\ s^2 & c^2 & 2cs \\ sc & -sc & (c^2 - s^2) \end{bmatrix} \tag{2.6.2}$$

Where, $c = \cos(\phi_p)$, $s = \sin(\phi_p)$

The compliance matrix including the coupling terms can be expressed as follows.

$$\begin{bmatrix} \varepsilon_x \\ \varepsilon_y \\ \gamma_{yx} \\ \gamma_{xz} \\ \gamma_{yz} \end{bmatrix} = \begin{bmatrix} 1/E_x & -\upsilon_{yx}/E_y & \eta_{xy}/G_{xy} & & \\ -\upsilon_{xy}/E_x & 1/E_y & \mu_{xy}/G_{xy} & & \\ \eta_x/E_x & \mu_y/E_y & 1/G_{xy} & & \\ & & & 1/G_{xz} & 0 \\ & & & 0 & 1/G_{yz} \end{bmatrix} \begin{bmatrix} \tau_x \\ \tau_y \\ \tau_{yx} \\ \tau_{xz} \\ \tau_{yz} \end{bmatrix} \tag{2.6.3}$$

2.6.2. Energy Equations for the composite shaft

If the stacking sequence of the shaft is symmetric, it can be modelled using classical beam theory with a constant circular cross section. We use SHBT (Simplified Homogenized Beam Theory) as used by Sino *et al.* [SCB08].

The continuous displacement field across the rotor cross section can be written as,

$$\{u(x,y,z)\} = \begin{bmatrix} u_x(x,y,z) = u(y) \\ u_y(x,y,z) = -z\theta_x(y) + x\theta_z(y) \\ u_z(x,y,z) = w(y) \end{bmatrix} \tag{2.6.4}$$

The elastic energy of the rotor and the wirtual work can be written as,

$$U = \frac{1}{2}\int_0^L \iint_S \left(\sigma_{yy}^p \varepsilon_{yy} + \tau_{yz}^p \gamma_{yz} + \tau_{yx}^p \gamma_{yx}\right) dSdy \tag{2.6.5}$$

$$\delta W = \frac{1}{2}\int_0^L \iint_S \left(\sigma_{yy}^{*p} \delta\varepsilon_{yy} + \tau_{yz}^{*p} \gamma_{yz} + \tau_{yx}^{*p} \gamma_{yx}\right) dSdy \tag{2.6.6}$$

Where,

S is the cross section of the shaft.

σ_{yy}^p, τ_{yz}^p are normal cross-section stresses and transverse shear stresses while σ_{yy}^{*p} and τ_{yz}^{*p} are associated normal and shear stresses linked to damping.

The elastic energy can be written as a function of the displacement field components.

$$U = \frac{1}{2}\int_0^L \iint_S E_y^p \left[z^2 \left(\frac{\partial \theta_x}{\partial y} \right)^2 + x^2 \left(\frac{\partial \theta_z}{\partial y} \right)^2 \right] dSdy + \frac{1}{2}\int_0^L \iint_S \left[G_{yz}^p \left(-\theta_x + \frac{\partial w}{\partial y} \right)^2 + G_{yx}^p \left(\theta_z + \frac{\partial u}{\partial y} \right)^2 \right] dSdy \tag{2.6.7}$$

The virtual work can be written as a function of the stress field components,

$$\delta W = \int_0^L \iint_S E_y^{*p} \left[-z \frac{\partial \hat{\theta}_x}{\partial y} + x \frac{\partial \hat{\theta}_z}{\partial y} \right] \left[-z \frac{\partial \delta\theta_x}{\partial y} + x \frac{\partial \delta\theta_z}{\partial y} \right] dSdy + \int_0^L \iint_S \left[G_{yz}^{*p} \left(-\hat{\theta}_x + \frac{\partial \hat{w}}{\partial y} \right) \left(-\delta\theta_x + \frac{\partial \delta w}{\partial y} \right) \right] dSdy + \int_0^L \iint_S \left[G_{yx}^{*p} \left(-\hat{\theta}_z + \frac{\partial \hat{u}}{\partial y} \right) \delta\theta_z + \frac{\partial \delta u}{\partial y} \right] dSdy \tag{2.6.8}$$

By evaluating the integrals over the cross section the above two eqns can be written as,

$$U = \frac{1}{2}\int_0^L \left[EI_x \left(\frac{\partial \theta_x}{\partial y} \right)^2 + EI_z \left(\frac{\partial \theta_z}{\partial y} \right)^2 \right] dy + \frac{1}{2}\int_0^L \left[GS_{yz} \left(-\theta_x + \frac{\partial w}{\partial y} \right)^2 + GS_{yx} \left(\theta_z + \frac{\partial u}{\partial y} \right)^2 \right] dSdy \tag{2.6.9}$$

$$\delta W = \int_0^L \left[EI_x^* \frac{\partial \hat{\theta}_x}{\partial y} \frac{\partial \delta\theta_x}{\partial y} + EI_z^* \frac{\partial \hat{\theta}_z}{\partial y} \frac{\partial \delta\theta_z}{\partial y} \right] dy + \int_0^L \left[GS_{yz}^* \left(-\hat{\theta}_x + \frac{\partial \hat{w}}{\partial y} \right) \left(-\delta\theta_x + \frac{\partial \delta w}{\partial y} \right) \right] dy + \int_0^L \left[GS_{yx}^* \left(-\hat{\theta}_z + \frac{\partial \hat{u}}{\partial y} \right) \delta\theta_z + \frac{\partial \delta u}{\partial y} \right] dy \tag{2.6.10}$$

Where,

$EI_x = EI_z = EI$ are homogenized flexural inertias. They are obtained as,

$$EI = \sum_{p=1}^{N} E_y^p I^p \tag{2.6.11}$$

Where,

$$EI = \sum_{p=1}^{N} E_y^p I^p$$

$$E_y^p = \frac{1}{\left(c^4 / E_l^t \right) + \left(s^4 / E_t^p \right) + c^2 s^2 \left(1/G_l^t - 2\upsilon_{tl}^p / E_t^p \right)} \tag{2.6.12}$$

$$I^p = \frac{R_p^4 - R_{p-1}^4}{4} \tag{2.6.13}$$

Where,

I^p is the cross section inertia R_p and R_{p-1} are external and internal radius of layer p.

$GS_{yx} = GS_{yz} = GS$ are shear rigidities such that

$$GS = k \sum_{p=1}^{N} G_{12}^p S^p \tag{2.6.14}$$

The advantage of this theory is that it can be applied to classic beam elements.

In order to validate our results we have studied the shaft initially studied by Zinberg and Symmonds [ZS70] then by Gubran and Gupta [GG05] and recently by Sino *et al.* [SCB08].All calculations are performed in Matlab.

2.6.3. Properties of Composite Rotor Shaft

Length of the shaft L = 2.47 m

Mean Radius Rm = 0.0635 m

Wall Thickness T = 1.321×10^{-3} m

Material Density ρ = 1967 Kg/m^3

E11 = 210 GPa , E22 = 24.1 GPa , G12 = 6.9 GPa , ν = 0.36

Stacking Sequence = [90, 45, -45, (0)6, 90] 10 layers of equal thickness

Homogenized Inertia and Shear Rigidity :

Using Eqs. (2.6.11) and (2.6.14),

EI = 4.5846×10^4

GS = 1.1569×10^6

2.6.4. Finite Elements Formulation

We have divided the length of the shaft into 4 no. of elements of equal length.Each element is considered to be a beam element with 2 nodes.There are 4 degrees of freedom at each node,two displacements and two rotations.

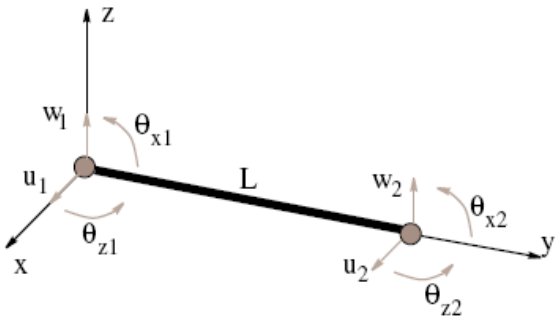

Fig. 28. Finite Element of the Beam

The finite element configuration thus becomes:

Total no. of elements = 4

Total no. of nodes = 5

DOFs per node = 4

DOF per element = 08

Total DOF of the system = 20

Order of element matrices = 8 x 8

Order of Global system matrices = 20 x 20

2.6.5. Boundary conditions:

Displacement along direction X and Z is blocked such that:

At node 1 $u_1 = 0, w_1 = 0$

At node 5 $u_2 = 0, w_2 = 0$

Order of Global system matrices after applying boundary conditions= 16 x 16

2.6.6. Calculation of Element Matrices

Shear Correction Factor for the composite shaft of circular cross-section = k_s = 0.4983

Quantity for Shear Effect= $a = \dfrac{12EI}{k_s GSL^2}$

$$I = \frac{\left(R_0 + T\right)^4 - R_0^4}{4}$$

$$S = \left(R_0 + T\right)^4 - R_0^4$$

2.6.6.1. Element Mass Matrix [S07]

$$M=\frac{\rho L}{840(1+a)^2}\begin{bmatrix} M_1 & 0 & 0 & M_7 & M_{11} & 0 & 0 & M_{29} \\ & M_1 & -M_7 & 0 & 0 & M_{11} & -M_{29} & 0 \\ & & M_6 & 0 & 0 & M_{29} & M_{24} & 0 \\ & & & M_6 & -M_{29} & 0 & 0 & M_{24} \\ & & & & M_1 & 0 & 0 & -M_7 \\ & & Sym & & & M_1 & M_7 & 0 \\ & & & & & & M_6 & 0 \\ & & & & & & & M_6 \end{bmatrix} \quad (2.6.15)$$

Where,

$$M_1 = S\left(312+588a+280a^2\right)+I\left[\frac{1008}{L^2}\right]$$

$$M_7 = -SL\left(44+77a+35a^2\right)-I\left[\frac{84-420a}{L}\right]$$

$$M_6 = SL^2\left(8+14a+7a^2\right)+I\left(112+140a+280a^2\right)$$

$$M_{11} = S\left(108+252a+140a^2\right)-I\left[\frac{1008}{L^2}\right]$$

$$M_{24} = -SL^2\left(6+14a+7a^2\right)-I\left(28+140a-140a^2\right)$$

$$M_{29} = SL\left(26+63a+35a^2\right)-I\left[\frac{84-420a}{L}\right]$$

2.6.6.2. Element Stiffness Matrix [S07]

$$K=\frac{EI}{L^3(1+a)}\begin{bmatrix} 12 & 0 & 0 & -6L & -12 & 0 & 0 & -6L \\ & 12 & 6L & 0 & 0 & -12 & 6L & 0 \\ & & (4+a)L^2 & 0 & 0 & -6L & (2-a)L^2 & 0 \\ & & & (4+a)L^2 & 6L & 0 & 0 & (2-a)L^2 \\ & & & & 12 & 0 & 0 & 6L \\ & & Sym & & & 12 & -6L & 0 \\ & & & & & & (4+a)L^2 & 0 \\ & & & & & & & (4+a)L^2 \end{bmatrix} \quad (2.6.16)$$

2.6.6.3. Element Gyroscopic Matrix [S07]

$$G = \frac{\rho I}{30L(1+a)} \begin{bmatrix} 0 & G_2 & G_4 & 0 & 0 & -G_2 & G_4 & 0 \\ & 0 & 0 & G_4 & G_2 & 0 & 0 & G_4 \\ & & 0 & G_9 & G_4 & 0 & 0 & G_{31} \\ & & & 0 & 0 & G_4 & -G_{31} & 0 \\ & & & & 0 & G_2 & -G_4 & 0 \\ & Anti- & Sym & & & 0 & 0 & -G_4 \\ & & & & & & 0 & G_9 \\ & & & & & & & 0 \end{bmatrix} \quad (2.6.17)$$

Where,

G2 = -72

G4 = -L(6-30a)

G9 = $-L^2(8+10a+20a^2)$

G31 = $L^2(2+10a-10a^2)$

The equation of motion for free vibration of un-damped gyroscopic system is given as,

$$[M]\{\ddot{X}\} + [G(\Omega)]\{\dot{X}\} + [K]\{X\} = 0 \quad (2.6.18)$$

Where,

[M] is a symmetric mass matrix.

[G (Ω)] is antisymmetric gyroscopic matrix.It depends on the speed of rotation Ω.

[K] is the elastic stiffness matrix, normally symmetric.

2.6.7. Modal Analysis (Finding natural frequencies and mode shapes)

The modes are characterized by eigenvalues and eigenvectors of the system. The eigenvalues are related to natural frequencies and eigenvectors to the mode shapes of the system.

First we have studied the system with no disk and without gyroscopic effect. The governing differential equation of motion is described by the 2nd order matrix equation:

$$[M]\{\ddot{X}\} + [K]\{X\} = 0 \quad (2.6.19)$$

The form of the solution assumed is,

$$\{X(t)\} = \{\phi_i\}e^{i\omega t} \quad (2.6.20)$$

Where,

$\{\phi_i\}$ is the mode shape and ω_i rad/sec is the corresponding natural frequency of vibration.

Subtituting Eq. (2.6.20) int Eq. (2.6.19),

$$(-\omega_i^2\ [M] + [K])\ \{\phi\} e^{i\omega t} = 0 \tag{2.6.21}$$

The above equation has a nontrivial solution if $(-\omega^2\ [M] + [K])$ is singular i.e. its determinant is zero. In other words there exist n number of ω which satisfy,

$$\left|(-\omega_i^2\ [M] + [K])\right| = \left|(\lambda_i\ [M] + [K])\right| = 0 \tag{2.6.22}$$

Where $\lambda_i = \omega_i^2$ are the eigen values of the system.

Frequencies in Hz are given by $F_i = \dfrac{\omega_i}{2\pi}$

The calculations were performed using both Matlab and RotorINSA[1]. The results obtained were compared with the published work of different authors. The results obtained in the present work are in close agreement with the results obtained by Sino and Baranger [SCB08].

2.6.8. Matlab Results

Without considering shear effect i.e. a = 0

F1 = 96 Hz , F3 = 322.2 Hz , 1st Critical Speed = 5760 rpm

Considering shear effect

F1 = 90.5 Hz , F2 = 383 Hz , 1st Critical Speed = 5430 rpm

[1] ROTORINSA® 3.4.2- Laboratoire de Mécanique des Contacts et des Structures (LaMCoS) INSA Lyon Batiment Jean d'Alembert 18-20, Rue des sciences 69621 VILLEURBANNE CEDEX France. http://rotorinsa.insa-lyon.fr

2.6.9. RotorINSA Results

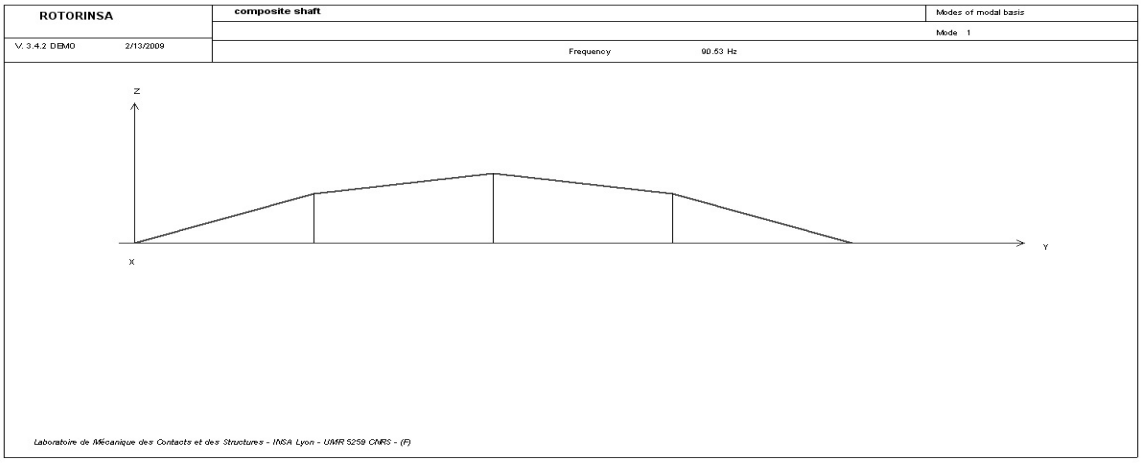

Fig. 29. 1st Mode (F1=90.5 Hz)

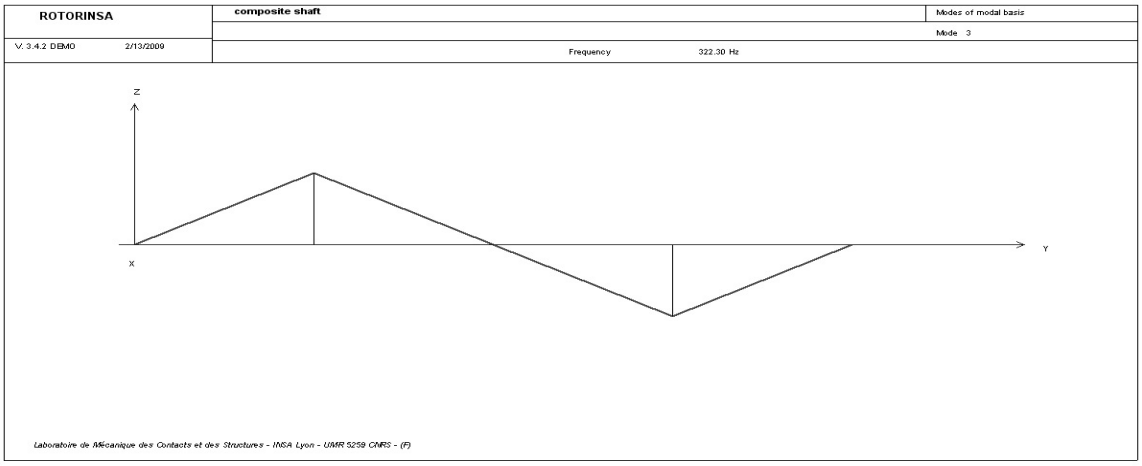

Fig. 30. 3rd Mode (F1= 322.3 Hz)

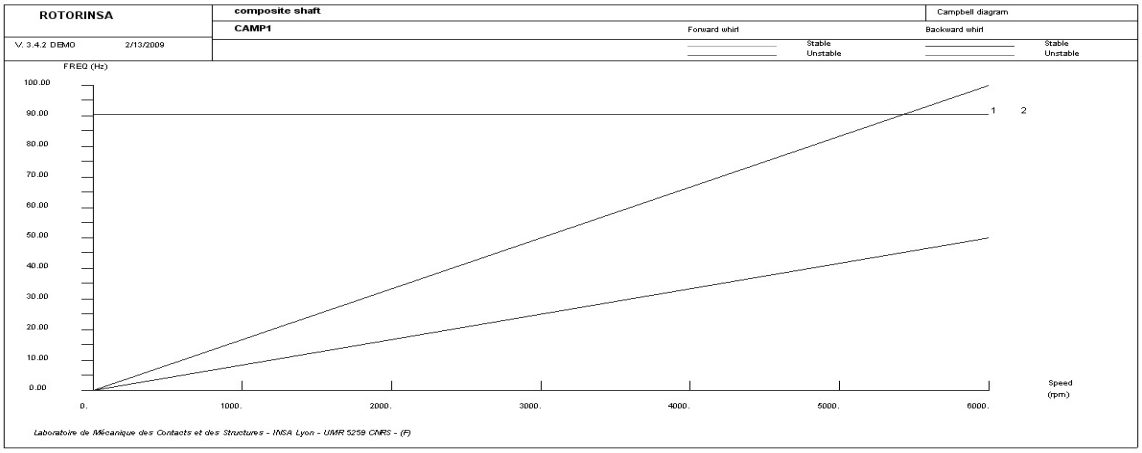

Fig. 31. Campbell Diagram

Table. 4. A comparison of critical speeds obtained by different authors

Investigator	**Critical Speed (rpm)**	**Method**
Zimberg and Symmonds (Theoretical) [ZS70]	5780	Equivalent modulus beam theory
Zimberg and Symmonds (Experimental) [ZS70]	5500	Forced vibration response for the shaft supported on rolling element bearing conditions
Singh and Gupta [SG96a]	5620	Layerwise beam theory including shear effect
Chen and Pung [CP98]	5714	Timoshenko beam theory and FEM
Gubran and Gupta [GG05]	5555 5552	Layerwise beam theory without including poisson effect Modified equivalent modulus beam theory without including poisons effect
Sino and Baranger [SCB08]	5767 5435	Simplified homogenized beam theory without including shear effect Simplified homogenized beam theory including shear effect
The results obtained in the present work.	5760 5430	Simplified homogenized beam theory without including shear effect Simplified homogenized beam theory including shear effect

2.6.10. Free Vibration Analysis of a Composite Rotor with one Disk considering gyroscopic effect

Now we consider a rotor with a composite shaft as above and a steel disk. We have also taken into account the gyroscopic effect.

2.6.10.1. Properties of the steel disk

Internal Radius R1 = Rm+T/2 m

Outer Radius R2 = 0.15 m

Thickness h = 0.05 m

Density ρ_d = 7800 Kg/m^3

Young's Modulus E = 200 GPa

Poisson's coefficient ν = 0.30

Location of the disk on the shaft l_1 = L/4

Where,

Rm is the mean radius of the composite shaft.

2.6.10.2. Element Matrices for the Disk

$$MD=\begin{bmatrix} M_d & 0 & 0 & 0 \\ 0 & M_d & 0 & 0 \\ 0 & 0 & I_{dx} & 0 \\ 0 & 0 & 0 & I_{dx} \end{bmatrix} \tag{2.6.23}$$

$$GD=\begin{bmatrix} 0 & 0 & 0 & 0 \\ 0 & 0 & 0 & 0 \\ 0 & 0 & 0 & -I_{dy} \\ 0 & 0 & I_{dy} & 0 \end{bmatrix} \tag{2.6.24}$$

Where,

MD is the element mass matrix for the disk

GD is the element gyroscopic matrix for the disk

M_d = Mass of the disk = $=\pi\left(R_2^2 - R_1^2\right)h\rho$

I_{dx} = Mass moment of Inertia in principal x direction = $\dfrac{M_d\left(3R_1^2 + 3R_2^2 + h^2\right)}{12}$

I_{dy} = Mass moment of Inertia in principal y direction = $\dfrac{M_d\left(R_1^2 + R_2^2\right)}{2}$

2.6.10.3. Modal Analysis

The mass and gyroscopic elements of the disk are added in node 2 of the global mass and gyroscopic matrices of the composite shaft. The matrix equation of motion for free vibration of un-damped gyroscopic system is given as Eq. (2.6.18) which is a 2nd order differential equation.Since we are also considering gyroscopic effect , therefore we have to treat the system of equations with three matrices.Matlab does not provide a solver for an eigenvalues problem with more than 2 matrices. We will therefore re-write Eq. (2.6.18) in first order form.

Let Y be defined as,

$$Y = \begin{Bmatrix} X \\ \dot{X} \end{Bmatrix} \tag{2.6.25}$$

Therefore,

$$\dot{Y} = \begin{Bmatrix} \dot{X} \\ \ddot{X} \end{Bmatrix} \tag{2.6.26}$$

Equation (2.6.18) can be written as,

$$[M]\{\ddot{X}\} = -[G(\Omega)]\{\dot{X}\} - [K]\{X\} \tag{2.6.27}$$

$$[K]\{\dot{X}\} = [K]\{\dot{X}\} \tag{2.6.28}$$

The above two equations can be re-written as a single set of equations as:

$$\begin{bmatrix} [M] & [0] \\ [0] & [K] \end{bmatrix} \begin{Bmatrix} \ddot{X} \\ \dot{X} \end{Bmatrix} = \begin{bmatrix} -[G] & -[K] \\ [K] & [0] \end{bmatrix} \begin{Bmatrix} \dot{X} \\ X \end{Bmatrix} \tag{2.6.29}$$

Using Y and $\dot{Y}$, the above equations it can be written as,

$$[A]\dot{Y} = [B]Y \tag{2.6.30}$$

Where,

$$[A] = \begin{bmatrix} [M] & [0] \\ [0] & [K] \end{bmatrix} \tag{2.6.31}$$

$$[B] = \begin{bmatrix} -[G] & -[K] \\ [K] & [0] \end{bmatrix} \tag{2.6.32}$$

Now we write the solution of the Eq. (2.6.18) as,

$$X = \mathrm{R}e^{\lambda t} \tag{2.6.33}$$

Therefore,

$$Y = \begin{Bmatrix} \lambda R \\ R \end{Bmatrix} e^{\lambda t} = \bar{Y} e^{\lambda t}$$
$$\dot{Y} = \lambda \bar{Y} e^{\lambda t} \tag{2.6.34}$$

Where,

$$\bar{Y} = \begin{Bmatrix} \lambda R \\ R \end{Bmatrix} \tag{2.6.35}$$

Equation (2.6.30) becomes,

$$\lambda [A] \bar{Y} = [B] \bar{Y} \tag{2.6.36}$$

The above equation is a standard 2-matrix eigenvalue problem that matlab can solve.

2.6.10.4. Matlab Procedure

The global matrices $[M]$, $[K]$ and $[G]$ are formed for the composite shaft. The dimensions of the matrices being 20 x 20.

Mass and Gyroscopic matrices for the disk are added at node 2 of matrices $[M]$ and $[G]$.

Boundary conditions are applied and the order of the new matrices is 16 x 16.

These matrices are now used to form the matrices $[A]$ and $[B]$ given above.

Eigenvalue problem given by Eq. (2.6.36) is solved as $[V_1, D] = eig(B, A)$.

Where,

$[V_1] = [\bar{Y}^{(1)}, \bar{Y}^{(2)}, ... \bar{Y}^{(2N)}]$

The diagonal values of [D] are eigenvalues for the original problem.

The eigenvalues are of the form $\pm j\omega_i$.

Where, ω_i is the frequency of free vibration. The last N positions of the jth column of $[V_1]$ are the j^{th} eigenvector $\bar{Y}^{(j)}$.

2.6.10.5. Results

Without considering shear effect i.e. a = 0

F1 = 16.8 Hz , F2 = 184 Hz , 1^{st} Critical Speed = 1008 rpm

Considering shear effect

F1 = 15.3 Hz , F2 = 153.7 Hz , 1^{st} Critical Speed = 918 rpm

2.6.10.6. RotorINSA Results:

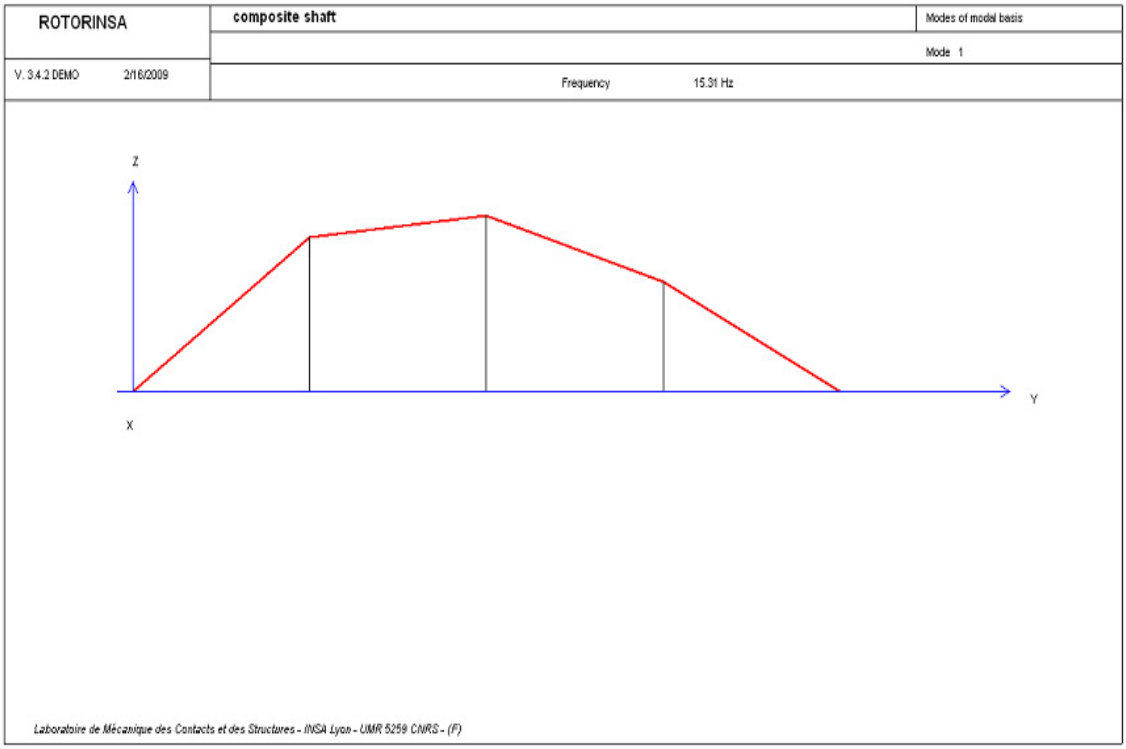

Fig. 32. 1st Mode (F1=15.3 Hz)

Fig. 33. 3rd Mode (F1=153.7 Hz)

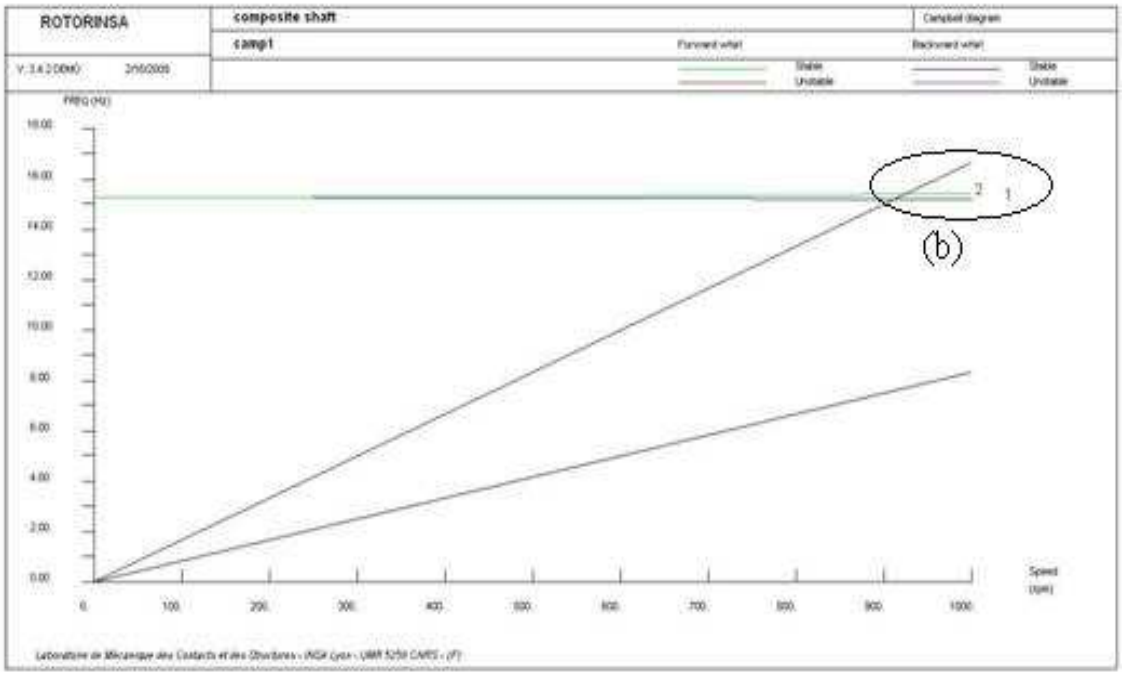

(a)

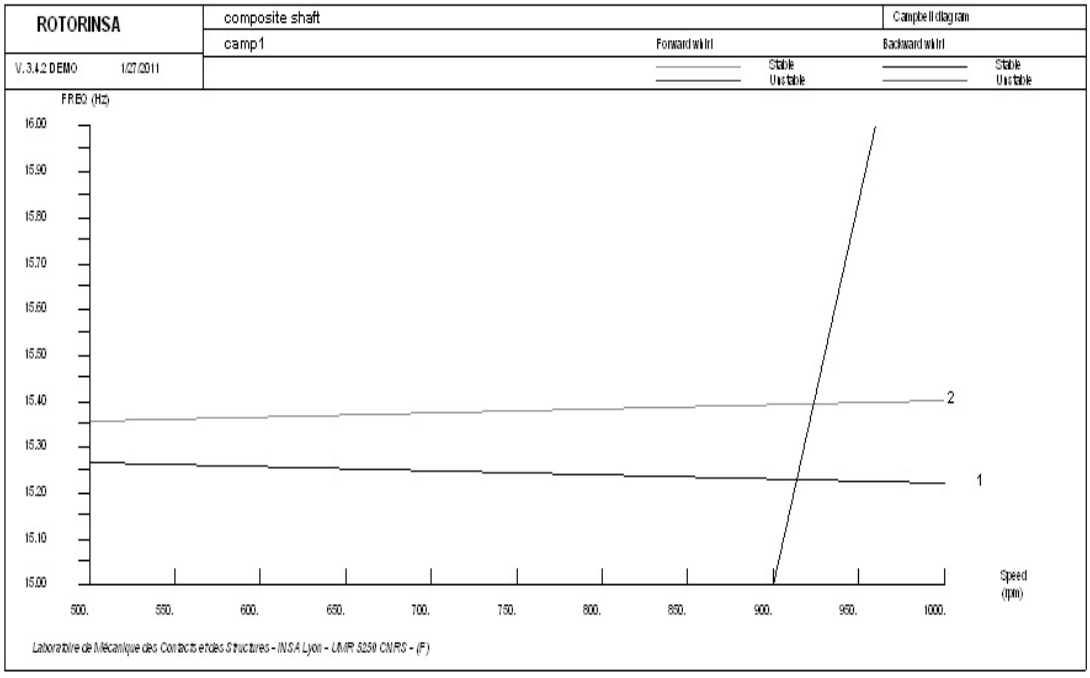

(b)

Fig. 34. Campbell Diagram for the Analysis of Gyroscopic System
(a) General View (b) Zoomed in View

2.7. Conclusions

This chapter presented the detailed mathematical modelling for analyzing the dynamic behavior of rotors. Various models containing nonlinear differential equations of motion were developed for different rotor configurations. These models consisted of 2^{nd} and 4^{th} order nonlinear differential equations of motion. Different models and hence different equations of motions were developed taking into account the various significant effects like higher order large deformations, geometric nonlinearity, shear effects, gyroscopic and rotary inertia effects are visualized and discussed. The models are developed using both the Euler Bernoulli and Timoshenko beam theories. Rayleigh-Ritz method and Hamilton's principle were used in order to obtain the equations of motion. When shear deformations are taken into account the developed equations of motion consist of 4^{th} order derivatives with respect to time as in Eqs. (2.5.34) and (2.5.35). A case study for the dynamic analysis of the composite rotors was conducted and the results obtained were compared to the works already available in the literature. The results obtained in this study were in close agreement with those previously reported in the literature.

[This page intentionally left blank]

Chapter 3: Nonlinear Analysis for Higher Order Large Deformations in Bending and a Dynamic Axial Force

In this chapter, a detailed analysis of the equations of motion developed in section 2.4.2 and 2.4.3 of chapter 2 is performed. The mathematical models developed in these two sections are combined to form the equations of motion to be analyzed in this chapter.

3.1. Equations of Motion

The new deformation energy of the rotor to study the effect of higher order large deformations and a dynamic axial force is formed by combining Eqs. (2.4.16) and (2.4.44). This gives the following equation for the deformation energy of the rotor.

$$U_R = \frac{k_1}{2}\left(U^2+W^2\right)+\frac{k_2}{8}\left(U^4+W^4+2U^2W^2\right)+\frac{k_3}{4}\left(U^4+W^4+2U^2W^2\right) + \frac{N_0}{2}k_{N_0}(U^2+W^2) \tag{3.1.1}$$

No static force will be applied therefore, substituting $N_0 = 0$ in the above equation,

$$U_R = \frac{k_1}{2}\left(U^2+W^2\right)+\frac{k_2}{8}\left(U^4+W^4+2U^2W^2\right)+\frac{k_3}{4}\left(U^4+W^4+2U^2W^2\right) \tag{3.1.2}$$

The kinetic energy of the rotor is given as in Eq. (2.3.4).

Hamilton's principle is applied as $\int_{t_1}^{t_2}\delta\left(T_R-U_R\right)dt = \int_{t_1}^{t_2}\delta T_R\,dt - \int_{t_1}^{t_2}\delta U_R\,dt = 0$

Where the first term is obtained from Eqs. (2.4.20), (2.4.21) and (2.4.22) i.e.

$$\int_{t_1}^{t_2}\delta T_R dt = -\int_{t_1}^{t_2}\Omega b_2\dot{U}\delta W dt - \int_{t_1}^{t_2}\frac{\partial}{\partial t}\left(b_1\dot{U}-\Omega b_2 W+ m_u\Omega d_1 f(l_1)\cos\Omega t\right)\delta U dt - \int_{t_1}^{t_2}\frac{\partial}{\partial t}\left(b_1\dot{W}-m_u\Omega d_1 f(l_1)\sin\Omega t\right)\delta W dt \tag{3.1.3}$$

The 2nd term is expanded as $\int_{t_1}^{t_2}\delta U_R dt = \int_{t_1}^{t_2}\left(\frac{\partial U_R}{\partial U}\delta U + \frac{\partial U_R}{\partial W}\delta W\right)dt$

Using Eq. (3.1.2), the two terms in the above equation can be written as,

$$\int_{t_1}^{t_2}\frac{\partial U_R}{\partial U}\delta U dt = \int_{t_1}^{t_2}\left(k_1 U+\left(\frac{1}{2}k_2+k_3\right)\left(U^3+UW^2\right)\right)\delta U dt \tag{3.1.4}$$

$$\int_{t_1}^{t_2}\frac{\partial U_R}{\partial W}\delta W dt = \int_{t_1}^{t_2}\left(k_1 W+\left(\frac{1}{2}k_2+k_3\right)\left(W^3+U^2W\right)\right)\delta W dt \tag{3.1.5}$$

The equations of motion can be written by collecting the terms of type $\delta U dt$ *and* $\delta W dt$ in Eqs. (3.1.3), (3.1.4) and (3.1.5).

The terms of the type $\delta U dt$ give,

$$-\int_{t_1}^{t_2} \left[\frac{\partial}{\partial t}\left(b_1 \dot{U} - \Omega b_2 W + m_u \Omega d_1 f(l_1)\cos\Omega t \right) - k_1 U - \left(\frac{1}{2}k_2 + k_3 \right)\left(U^3 + UW^2 \right) \right] \delta U dt = 0 \tag{3.1.6}$$

Similarly, the terms of the type $\delta W dt$ give,

$$-\int_{t_1}^{t_2} \left[\frac{\partial}{\partial t}\left(b_1 \dot{W} - m_u \Omega d_1 f(l_1)\sin\Omega t \right) - \Omega b_2 \dot{U} - k_1 W - \left(\frac{1}{2}k_2 + k_3 \right)\left(W^3 + U^2 W \right) \right] \delta W dt = 0 \tag{3.1.7}$$

Eqs. (3.1.6) and (3.1.7) can be written in a simplified form as,

$$b_1 \ddot{U} - \Omega b_2 \dot{W} + k_1 U + \left(\frac{1}{2}k_2 + k_3 \right)\left(U^3 + UW^2 \right) = m_u \Omega^2 d_1 f(l_1)\sin\Omega t \tag{3.1.8}$$

$$b_1 \ddot{W} + \Omega b_2 \dot{U} + k_1 W + \left(\frac{1}{2}k_2 + k_3 \right)\left(W^3 + U^2 W \right) = m_u \Omega^2 d_1 f(l_1)\cos\Omega t \tag{3.1.9}$$

Finally, the two equations of motion are,

$$\ddot{U} - \Omega\alpha_1 \dot{W} + \alpha_2 U + \left(\frac{1}{2}\beta_1 + \beta_2 \right)\left(U^3 + UW^2 \right) + c\dot{U} = m_1 \Omega^2 d_1 f(l_1)\sin\Omega t \tag{3.1.10}$$

$$\ddot{W} + \Omega\alpha_1 \dot{U} + \alpha_2 W + \left(\frac{1}{2}\beta_1 + \beta_2 \right)\left(W^3 + WU^2 \right) + c\dot{W} = m_1 \Omega^2 d_1 f(l_1)\cos\Omega t \tag{3.1.11}$$

Where,

$$\alpha_1 = b_2/b_1\ ,\ \alpha_2 = k_1/b_1\ ,\ \beta_1 = k_2/b_1\ ,\ \beta_2 = k_3/b_1\ ,\ m_1 = m_u/b_1 \tag{3.1.12}$$

3.2. Linear Analysis (Classical Approach)

The rotor was studied as a free undamped linear system to determine the natural frequencies of vibration and the Campbell diagram given in Fig. 35 (a) was plotted to determine the critical speeds. The two critical speeds ω_1 *and* ω_2 were found to be 2520 rpm (42 Hz) and 3089 rpm (51.5 Hz). The response due to mass unbalance is given in Fig. 35 (b) which shows that there is a peak in the amplitude corresponding to the 2nd critical speed.

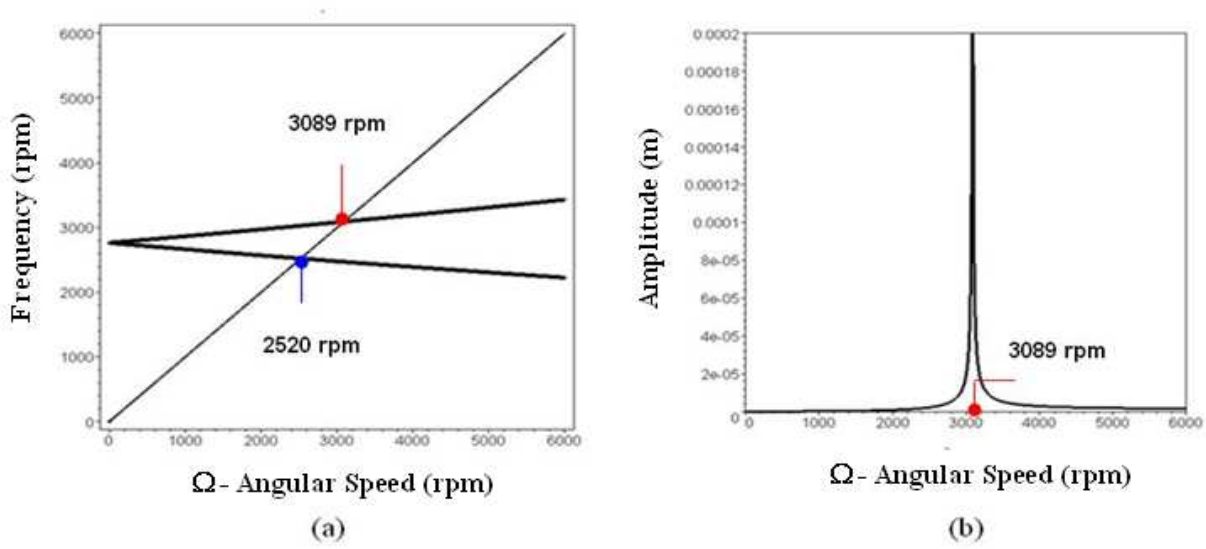

Fig. 35. (a) Campbell Diagram, (b) Mass Unbalance Response

3.3. Nonlinear Analysis (General Introduction)

The theoretical analysis of the nonlinear forced system is performed using MMS which has been proven very effective in the analysis of such systems [SMB10, HK09, MMPD08 and YKII07]. The method can be applied by two different approaches. The first one is called direct method in which the partial differential equations of motion as developed in section 2.4.1 are attacked directly along with the boundary conditions. See for example the reference [SZ03] where the authors have used this approach for the nonlinear dynamic analysis of a rotor shaft system with viscoelastically supported bearings. The other approach is called discretized method. In this method the equations of motion are first discretized using, for example, Rayleigh Ritz Method as in section 2.4.2 of chapter 2. The general method of application of these two approaches is given as below.

3.3.1. Direct Method

In this method the partial differential equations and boundary conditions are attacked directly. The method is briefly recalled in the following example. Consider the following partial differential equation.

$$\frac{\partial^2 w}{\partial x^2} = \frac{\partial^2 w}{\partial t^2} + 2\mu \frac{\partial w}{\partial t} \tag{3.3.1}$$

And the associated boundary conditions are,

$$w = 0 \; at \; x = 0$$

$$\frac{\partial^2 w}{\partial t^2} + \alpha_1 \frac{\partial w}{\partial t} + \alpha_0 w + \alpha_2 w^2 + \alpha_3 w^3 = -F \cos \Omega t \; at \; x = 1 \tag{3.3.2}$$

Where,

$$\alpha_0 = k + 3\alpha_3 b^2 \; , \; \alpha_2 = 3\alpha_3 b \tag{3.3.3}$$

We treat this for the case of primary resonance by using the method of multiple scales.

In the case of primary resonance the excitation frequency Ω is near one of the linear natural frequencies of the system. To determine an approximation to the solution of Eqs. (3.3.1) through (3.3.3), a small dimensionless measure ε of the amplitude of w is introduced as a bookkeeping device. Using the method of multiple scales an approximation solution is sought in the following form,

$$w(x,t;\varepsilon) = \varepsilon w_1(x,T_0,T_1,T_2) + \varepsilon^2 w_2(x,T_0,T_1,T_2) + \varepsilon^3 w_3(x,T_0,T_1,T_2) \tag{3.3.4}$$

Where $T_0 = t$ is a fast time scale characterizing changes occurring at the frequencies Ω and ω. Also $T_1 = \varepsilon t$ and $T_2 = \varepsilon^2 t$ are slow time scales characterizing the modulation of the amplitude and phase due to damping, nonlinearity and possible resonances and the ω_n are O(1) as $\varepsilon \to 0$. The damping μ and excitation amplitude F are ordered such a way that they balance the nonlinearity. Thus following scaling is used.

$$\mu = \varepsilon\mu \ , \ F = \varepsilon^3 F \tag{3.3.5}$$

The first and second time derivatives can be expressed as,

$$\frac{\partial}{\partial t} = D_0 + \varepsilon D_1 + \varepsilon^2 D_2 + ... \tag{3.3.6}$$

$$\frac{\partial^2}{\partial t^2} = D_0^2 + 2\varepsilon D_0 D_1 + \varepsilon^2 (D_1^2 + 2D_0 D_2) + ... \tag{3.3.7}$$

Where, $D_n = \dfrac{\partial}{\partial T_n}$. Substituting Eqs. (3.3.4) through (3.3.7) into Eqs. (3.3.1) through (3.3.3) and equating coefficients of like powers of ε, following two systems are obtained,

Order ε :

$$\frac{\partial^2 w_1}{\partial x^2} = D_0^2 w_1 \tag{3.3.8}$$

$$w_1 = 0 \ at \ x = 0 \tag{3.3.9}$$

$$D_0^2 w_1 + \alpha_1 \frac{\partial w_1}{\partial x} + \alpha_1 w_1 = 0 \ at \ x = 1 \tag{3.3.10}$$

Order ε^2 :

$$\frac{\partial^2 w_2}{\partial x^2} = D_0^2 w_2 + 2D_0 D_1 w_1 \tag{3.3.11}$$

$$w_2 = 0 \ at \ x = 0 \tag{3.3.12}$$

$$D_0^2 w_2 + \alpha_1 \frac{\partial w_2}{\partial x} + \alpha_0 w_2 = -2D_0 D_1 w_1 - \alpha_2 w_1^2 \ at \ x = 1 \tag{3.3.13}$$

Order ε^3 :

$$\frac{\partial^2 w_3}{\partial x^2} = D_0^2 w_3 + 2D_0 D_1 w_2 + (2D_0 D_2 + D_1^2) w_1 + 2\mu D_0 w_1 \tag{3.3.14}$$

$$w_3 = 0 \; at \; x = 0 \tag{3.3.15}$$

$$D_0^2 w_3 + \alpha_1 \frac{\partial w_3}{\partial x} + \alpha_0 w_3 = -2D_0 D_1 w_2 - (2D_0 D_2 + D_1^2) w_1 - 2\alpha_2 w_1 w_2 - \alpha_3 w_1^3 - F \cos \Omega T_0 \; at \; x = 1 \tag{3.3.16}$$

The general solution of Eqs. (3.3.8) through (3.3.10) can be expressed as,

$$w_1(x, T_0, T_1, T_2) = \sum_{m=1}^{\infty} \left[A_m(T_1, T_2) e^{i\omega_m T_0} + cc \right] \frac{\sin \omega_m x}{\sin \omega_m} \tag{3.3.17}$$

Where the natural frequencies ω_m are solutions of

$$\alpha_1 \omega_m + (\alpha_0 - \omega_m^2) \tan \omega_m = 0 \tag{3.3.18}$$

The complex valued functions A_m are arbitrary at this moment and *cc* denotes the complex conjugate of the preceding terms. The solution given by Eq. (3.3.17) is a linear combination of all the modes, considering the case in which Ω is near natural frequency ω_n of the nth mode when this mode is not involved in an internal resonance with any other mode. Hence, the solution of (3.3.8) to (3.3.10) consist of only the mode corresponding to ω_n, given as

$$w_1 = A(T_1, T_2) \frac{\sin \omega x}{\sin \omega} e^{i\omega T_0} + cc \tag{3.3.19}$$

Substituting Eq. (3.3.19) into Eqs. (3.3.11) through (3.3.13) gives,

$$\frac{\partial^2 w_2}{\partial x^2} = D_0^2 w_2 + 2i\omega D_1 A \frac{\sin \omega x}{\sin \omega} e^{i\omega T_0} + cc \tag{3.3.20}$$

$$\omega_2 = 0 \; at \; x = 0 \tag{3.3.21}$$

$$D_0^2 w_2 + \alpha_1 \frac{\partial w_2}{\partial x} + \alpha_0 w_2 = -2i\omega D_1 A e^{i\omega T_0} - \alpha_2 \left[A^2 e^{2i\omega T_0} + A\bar{A} \right] + cc \; at \; x = 1 \tag{3.3.22}$$

The solvability conditions [N93] demand that

$$D_1 A = 0 \tag{3.3.23}$$

Substituting Eq. (3.3.23) into (3.3.20) through (3.3.22) and solving for w_2 gives

$$w_2 = c_1 A\bar{A} x + c_2 A^2 \frac{\sin 2\omega x}{\sin 2\omega} e^{2i\omega T_0} + cc \tag{3.3.24}$$

Where,

$$c_1 = \frac{\alpha_2}{\alpha_1 + \alpha_0}$$
$$c_2 = -\frac{\alpha_2}{\alpha_0 + 4\omega^2 + 2\omega\alpha_1 \cot 2\omega} \tag{3.3.25}$$

Because A is a function of T_2, the nearness of Ω to ω by introducing the detuning parameter defined by $\Omega = \omega + \varepsilon^2\sigma$. Then substituting Eqs. (3.3.19), (3.3.23) and (3.3.24) into Eqs. (3.3.14) to (3.3.16) yields,

$$\frac{\partial^3 w_3}{\partial x^2} = D_0^2 w_3 + 2i\omega(A' + \mu A)\frac{\sin\omega x}{\sin\omega} e^{i\omega T_0} + cc \tag{3.3.26}$$

$$w_3 = 0 \ at \ x = 0 \tag{3.3.27}$$

$$D_0^2 w_3 + \alpha_1 \frac{\partial w_3}{\partial x} + \alpha_0 w_3 = -\left[2\alpha_2(2c_1 + c_2) + 3\alpha_3 A^2\bar{A}\right]e^{i\omega T_0} - 2i\omega A' e^{i\omega T_0}$$
$$-\frac{1}{2}Fe^{i(\omega T_0 + \sigma T_2)} + NST + cc \ at \ x = 1 \tag{3.3.28}$$

Where *NST* stands for Non Significant Terms that do not produce secular terms and the prime indicates the derivative with respect to T_2. Because the homogeneous parts of Eqs. (3.3.26) to (3.3.28) are the same as (3.3.8) to (3.3.10) and because the latter has a non-trivial solution, the non homogeneous equations (3.3.26) to (3.3.28) have a solution only if certain solvability conditions are satisfied. To determine the solvability conditions the solution is first written in the form,

$$w_3 = \varphi(x, T_2)e^{i\omega T_0} + cc + W_3(x, T_0, T_2) \tag{3.3.29}$$

Where W_3 is governed by Eqs. (3.3.26) to (3.3.28) with the terms proportional to $\exp(i\omega T_0)$ being deleted. Therefore, W_3 exists, is unique and free of secular terms. Substituting Eq. (3.3.29) into Eqs. (3.3.26), (3.3.27) and (3.3.28) , and equating coefficients of $\exp(i\omega T_0)$ of both sides of each equation gives,

$$\frac{d^2\varphi}{dx^2} + \omega^2\varphi = 2i\omega(A' + \mu A)\frac{\sin\omega x}{\sin\omega} \tag{3.3.30}$$

$$\varphi = 0 \ at \ x = 0 \tag{3.3.31}$$

$$\frac{d\varphi}{dx} + \alpha\varphi = \frac{1}{\alpha_1}\left[-\frac{1}{2}Fe^{i\sigma T_2} - 2i\omega A' - 2\alpha_2 BA^2\bar{A}\right] at \ x = 1 \tag{3.3.32}$$

Where,

$$\alpha = \frac{\alpha_0 - \omega^2}{\alpha_1}$$
$$B = 2c_1 + c_2 + \frac{3\alpha_3}{2\alpha_2} \tag{3.3.33}$$

Therefore, determining the solvability condition of Eqs. (3.3.8) to (3.3.10) has been transformed into determining the solvability condition of Eqs. (3.3.30) to(3.3.32). To determine this solvability condition the Eq. (3.3.30) is multiplied by $\frac{\sin \omega x}{\sin \omega}$, the solution of the adjoint homogeneous problem, the result is integrated by parts from $x = 0$ to $x = 1$, and the boundary conditions given by Eqs. (3.3.31) and (3.3.32) are applied to give,

$$2i\omega(A' + \mu A) = -\frac{\Gamma}{\alpha_1}\left[2i\omega A' + 2\alpha_2 BA^2\bar{A} + \frac{1}{2}Fe^{i\sigma T_2}\right] \tag{3.3.34}$$

Where,

$$\Gamma = \left[\int_0^1 \frac{\sin^2 \omega x}{\sin^2 \omega} dx\right]^{-1} = \frac{4\omega \sin^2 \omega}{2\omega - \sin 2\omega} \tag{3.3.35}$$

Substituting the polar form, $A = \frac{1}{2}ae^{i(\sigma T_2 - \gamma)}$ into (3.3.34) and separating the real and imaginary parts, the following equations are obtained,

$$a' = -\mu a - \frac{f}{2\omega}\sin\gamma \tag{3.3.36}$$

$$a\gamma' = \sigma a - \alpha_e a^3 - \frac{f}{2\omega}\cos\gamma \tag{3.3.37}$$

Where, a and γ are real functions of T_2.

Also,

$$\mu = \frac{\alpha_1 \mu}{(\alpha_1 + \Gamma)} \tag{3.3.38}$$

$$\alpha_e = \frac{\Gamma\alpha_2 B}{4\omega(\alpha_1 + \Gamma)} = \frac{3\alpha}{8\omega} - \frac{\alpha_2 \delta}{4\omega}\left[\frac{2}{(\alpha_1 + \alpha_0)} + \frac{1}{(\alpha_0 - 4\omega^2 + 2\omega\alpha_1 \cot 2\omega)}\right] \tag{3.3.39}$$

$$(\delta, \alpha, f) = \frac{\Gamma}{(\alpha_1 + \Gamma)}(\alpha_2, \alpha_3, F) = \frac{4\omega \sin^2 \omega}{\alpha_1(2\omega - \sin 2\omega) + 4\omega \sin^2 \omega}(\alpha_2, \alpha_3, F) \tag{3.3.40}$$

Substituting Eqs. (3.3.19) and (3.3.24) into Eq. (3.3.4) , recalling that $\Omega = \omega + \varepsilon^2\sigma$ and using Eq. (3.3.25) and polar form, the following approximation of the solution is obtained.

$$w = \varepsilon a \cos(\Omega t - \gamma)\frac{\sin \omega x}{\sin \omega} - \frac{1}{2}\varepsilon^2 \alpha_2 a^2\left[\frac{x}{(\alpha_1 + \alpha_0)} + \frac{\sin 2\omega x \cos(2\Omega t - 2\gamma)}{(\alpha_0 - 4\omega^2)\sin 2\omega + 2\omega\alpha_1 \cos 2\omega}\right] \tag{3.3.41}$$

3.3.2. Discretized Method

A method of obtaining the approximate solutions of continuous systems is to discretize the problem. In the case of the example given in the preceding section, an approximate solution is assumed in the form,

$$w(x,t) = \sum_{n=1}^{N} W_n(t)\phi_n(x) \tag{3.3.42}$$

Then in order to obtain the coupled differential equations governing $W_n(t)$, Galerkin or Rayleigh Ritz method is used. The equations thus obtained are called the discretized equations of motion. Then a perturbation or numerical method can be used to obtain the solutions of these discretized equations. Normally, the functions $\phi_n(x)$ are chosen to be the mode shapes of the undamped linear problem. If N=1, the result is called a single mode approximation.

In the present work we have chosen to apply discretized method because the application of the direct method involves complicated mathematical expressions which can lead to some errors in the final results. The application of the discretized method is simple relative to the direct method. We have used this method also due to the reason that we have tools and experience to efficiently apply this method for the analysis. The detailed application of this method is given in the next section.

3.4. Application of Discretized Method for Nonlinear Rotordynamics

In this section the equations of motion developed in section 3.1 are treated. In order to apply MMS, displacements *U* and *W* are expanded as below,

$$U(T_0,T_1) = u_0(T_0,T_1) + \varepsilon u_1(T_0,T_1) = u_0 + \varepsilon u_1 \tag{3.4.1}$$

$$W(T_0,T_1) = w_0(T_0,T_1) + \varepsilon w_1(T_0,T_1) = w_0 + \varepsilon w_1 \tag{3.4.2}$$

Where $T_n = \varepsilon^n t$ are slow time scales, T_1 being slower than T_0, and ε is a small dimensionless parameter so that $\varepsilon << 1$. T_0 is a fast time scale characterizing motions occurring at the spin rates Ω and the natural frequencies ω_n of the rotor system. Furthermore, T_1 is a slow-time scale characterizing the modulation of the amplitude and phase due to nonlinearity, damping and resonance. The nonlinear, damping and forcing terms in Eqs. (3.1.10) and (3.1.11) are scaled so that they appear in the same order of ε. Therefore the following scaling is used

$$\alpha_1 = \alpha_1, \alpha_2 = \alpha_2, \beta_1 = \varepsilon\beta_1, \beta_2 = \varepsilon\beta_2, m_1 = \varepsilon m_1, c = \varepsilon c \tag{3.4.3}$$

The assumptions in Eq. (3.4.3) takes into account the interaction of damping terms with the nonlinear forces at the same level of approximation, which is a necessary condition for a nontrivial solution of the governing equations of motion. Thus, the effect of the nonlinearity of the system can be balanced with the effect of the system damping at the same level of approximation.

Eqs. (3.1.10) and (3.1.11) can now be written as

$$\ddot{U} - \Omega\alpha_1\dot{W} + \alpha_2 U + \varepsilon\left(\frac{1}{2}\beta_1 + \beta_2\right)\left(U^3 + UW^2\right) + \varepsilon c\dot{U} = \varepsilon m_1\Omega^2 d_1 f(l_1)\sin\Omega t \tag{3.4.4}$$

$$\ddot{W} + \Omega\alpha_1\dot{U} + \alpha_2 W + \varepsilon\left(\frac{1}{2}\beta_1 + \beta_2\right)\left(W^3 + WU^2\right) + \varepsilon c\dot{W} = \varepsilon m_1\Omega^2 d_1 f(l_1)\cos\Omega t \tag{3.4.5}$$

Using the chain rule for the partial derivatives with respect to both time scales T_0 and T_1, the different time derivatives in the above equation can now be written as:

$$\dot{U}(t) = \frac{\partial}{\partial T_0}U(T_0,T_1) + \varepsilon\frac{\partial}{\partial T_1}U(T_0,T_1) \tag{3.4.6}$$

$$\dot{W}(t) = \frac{\partial}{\partial T_0}W(T_0,T_1) + \varepsilon\frac{\partial}{\partial T_1}W(T_0,T_1) \tag{3.4.7}$$

$$\ddot{U}(t) = \frac{\partial^2}{\partial T_0^{\,2}}U(T_0,T_1) + 2\varepsilon\frac{\partial^2}{\partial T_0\partial T_1}U(T_0,T_1) \tag{3.4.8}$$

$$\ddot{W}(t) = \frac{\partial^2}{\partial T_0^{\,2}}W(T_0,T_1) + 2\varepsilon\frac{\partial^2}{\partial T_0\partial T_1}W(T_0,T_1) \tag{3.4.9}$$

By substituting Eqs. (3.4.6) to (3.4.9) in Eqs. (3.4.4) and (3.4.5), using Eqs. (3.4.1) and (3.4.2) and then equating the coefficients of the like powers of ε on both sides of the resulting equations, we obtain following two systems of equations

System of order 0 equations (ε^0) :

$$\frac{\partial^2}{\partial T_0^{\,2}}u_0 + \alpha_2 u_0 - \Omega\alpha_1\frac{\partial}{\partial T_0}w_0 = 0 \tag{3.4.10}$$

$$\frac{\partial^2}{\partial T_0^{\,2}}w_0 + \alpha_2 w_0 - \Omega\alpha_1\frac{\partial}{\partial T_0}u_0 = 0 \tag{3.4.11}$$

System of order 1 equations (ε^1) :

$$\begin{aligned}&\frac{\partial^2}{\partial T_0^{\,2}}u_1 + \alpha_2 u_1 - \Omega\alpha_1\frac{\partial}{\partial T_0}w_1 = \Omega\alpha_1\frac{\partial}{\partial T_0}w_0 - 2\frac{\partial^2}{\partial T_0\partial T_1}u_0\\ &-\frac{\beta_1 u_0^{\,3}}{2} - \frac{\beta_1 u_0 w_0^{\,2}}{2} - \beta_2 u_0^{\,3} - \beta_2 u_0 w_0^{\,2} - c\frac{\partial}{\partial T_0}u_0 + m_1\Omega^2 d_1 f(l_1)\sin\Omega t\end{aligned} \tag{3.4.12}$$

$$\begin{aligned}&\frac{\partial^2}{\partial T_0^{\,2}}w_1 + \alpha_2 w_1 + \Omega\alpha_1\frac{\partial}{\partial T_0}u_1 = -\Omega\alpha_1\frac{\partial}{\partial T_0}u_0 - 2\frac{\partial^2}{\partial T_0\partial T_1}w_0\\ &-\frac{\beta_1 w_0^{\,3}}{2} - \frac{\beta_1 w_0 u_0^{\,2}}{2} - \beta_2 w_0^{\,3} - \beta_2 w_0 u_0^{\,2} - c\frac{\partial}{\partial T_0}w_0 + m_1\Omega^2 d_1 f(l_1)\cos\Omega t\end{aligned} \tag{3.4.13}$$

The solution of Eqs. (3.4.10) and (3.4.11) is given as

$$u_0 = A_1(T_1)\exp(i\omega_1 T_0) + A_2(T_1)\exp(i\omega_2 T_0) + [cc] \tag{3.4.14}$$

$$w_0 = iA_1(T_1)\exp(i\omega_1 T_0) - iA_2(T_1)\exp(i\omega_2 T_0) + [cc] \tag{3.4.15}$$

Where, ω_1, ω_2 are the natural frequencies of the system and [cc] denotes the complex conjugate.

3.4.1. Possible resonances and solvability conditions

Substitution of Eqs. (3.4.14) and (3.4.15) into Eqs. (3.4.12) and (3.4.13) gives us the following two equations

$$\begin{aligned}
&\frac{\partial^2 u_1}{\partial T_0^{\,2}} + \alpha_2 u_1 - \Omega\alpha_1 \frac{\partial}{\partial T_0} w_1 = (-2i\omega_1 \frac{\partial A_1}{\partial T_1} + i\alpha_1\Omega \frac{\partial A_1}{\partial T_1} - ic\omega_1 A_1 \\
&-2\beta_1 A_1^{\,2}\overline{A_1} - 4\beta_2 A_1^{\,2}\overline{A_1} - 4\beta_1 A_1 A_2 \overline{A_2} - 8\beta_2 A_1 A_2 \overline{A_2})\exp(i\omega_1 T_0) \\
&-(2i\omega_2 \frac{\partial A_2}{\partial T_1} + i\alpha_1\Omega \frac{\partial A_2}{\partial T_1} + icA_2\omega_2 + 2\beta_1 A_2^{\,2}\overline{A_2} + 4\beta_2 A_2^{\,2}\overline{A_2} \\
&+4\beta_1 A_1 \overline{A_1} A_2 + 8\beta_2 A_1 \overline{A_1} A_2)\exp(i\omega_2 T_0) - \frac{1}{2} i m_1 \Omega^2 d_1 f(l_1)\exp(i\Omega T_0) \\
&-(2\beta_1 A_1 A_2^{\,2} + 4\beta_2 A_1 A_2^{\,2})\exp(i(\omega_1 + 2\omega_2)T_0) \\
&-(2\beta_1 A_1^{\,2} A_2 + 4\beta_2 A_1^{\,2} A_2)\exp(i(2\omega_1 + \omega_2)T_0) + [cc]
\end{aligned} \tag{3.4.16}$$

$$\begin{aligned}
&\frac{\partial^2 w_1}{\partial T_0^{\,2}} + \alpha_2 w_1 + \Omega\alpha_1 \frac{\partial}{\partial T_0} u_1 = (-2\omega_1 \frac{\partial A_1}{\partial T_1} - \alpha_1\Omega \frac{\partial A_1}{\partial T_1} + c\omega_1 A_1 \\
&-2i\beta_1 A_1^{\,2}\overline{A_1} - 4i\beta_2 A_1^{\,2}\overline{A_1} - 4i\beta_1 A_1 A_2 \overline{A_2} - 8i\beta_2 A_1 A_2 \overline{A_2})\exp(i\omega_1 T_0) \\
&-(2\omega_2 \frac{\partial A_2}{\partial T_1} + \alpha_1\Omega \frac{\partial A_2}{\partial T_1} + c\omega_2 A_2 - 2i\beta_1 A_2^{\,2}\overline{A_2} - 4i\beta_2 A_2^{\,2}\overline{A_2} \\
&-8i\beta_2 A_1 \overline{A_1} A_2 - 4i\beta_1 A_1 \overline{A_1} A_2)\exp(i\omega_2 T_0) + \frac{1}{2} m_1 \Omega^2 d_1 f(l_1)\exp(i\Omega T_0) \\
&+(2i\beta_1 A_1 A_2^{\,2} + 4i\beta_2 A_1 A_2^{\,2})\exp(i(\omega_1 + 2\omega_2)T_0) \\
&-(2i\beta_1 A_1^{\,2} A_2 + 4i\beta_2 A_1^{\,2} A_2)\exp(i(2\omega_1 + \omega_2)T_0) + [cc]
\end{aligned} \tag{3.4.17}$$

We assume a particular solution in the form:

$$u_1 = P_1(T_1)\exp(i\omega_1 T_0) + Q_1(T_1)\exp(i\omega_2 T_0) \tag{3.4.18}$$

$$w_1 = P_2(T_1)\exp(i\omega_1 T_0) + Q_2(T_1)\exp(i\omega_2 T_0) \tag{3.4.19}$$

After substituting the particular solution given above in Eqs. (3.4.16) and (3.4.17), it can be observed from the resulting equations that there are two possible primary resonance conditions, $\Omega \approx \omega_1$ and $\Omega \approx \omega_2$.

3.4.2. Case of $\Omega \approx \omega_2$

For this case we have used $\Omega = \omega_2 + \varepsilon\sigma_1$, where, σ_1 is a detuning parameter for controlling the nearness of Ω to ω_2.

Also, the solution of Eqs. (3.4.16) and (3.4.17) exist only if certain solvability conditions are satisfied. The first step in determining these solvability conditions is to substitute $\Omega = \omega_2 + \varepsilon\sigma_1$ and the particular solution, given in Eqs. (3.4.16) and (3.4.17), in these equations. We then equate the coefficients of $\exp(i\omega_1 T_0)$ and $\exp(i\omega_2 T_0)$ on both sides of the resulting equations. The coefficients of $\exp(i\omega_1 T_0)$ for the Left Hand Side (L.H.S) of the resulting equations give,

$$\begin{aligned} R_{11} &= -P_1\omega_1^2 + \alpha_2 P_1 - \omega_1^2\alpha_1 P_2 I \\ R_{12} &= -P_2\omega_1^2 + \alpha_2 P_2 + \omega_1^2\alpha_1 P_1 I \end{aligned} \tag{3.4.20}$$

The coefficients of $\exp(i\omega_2 T_0)$ for the L.H.S. of the resulting equations give,

$$\begin{aligned} S_{11} &= -Q_1\omega_2^2 + \alpha_2 Q_1 - \omega_1\omega_2\alpha_1 Q_2 I \\ S_{12} &= -Q_2\omega_2^2 + \alpha_2 Q_2 + \omega_1\omega_2\alpha_1 Q_1 I \end{aligned} \tag{3.4.21}$$

The coefficients of $\exp(i\omega_1 T_0)$ for the Right Hand Side (R.H.S) of the resulting equations give,

$$\begin{aligned} R_{21} &= -4\beta_1 A_1 A_2 \overline{A_2} - 4\beta_2 A_1^2 \overline{A_1} - 2\beta_1 A_1^2 \overline{A_1} + \left(-2I\omega_1 + \alpha_1 I\omega_1\right)\frac{\partial A_1}{\partial T_1} \\ &-8\beta_2 A_1 A_2 \overline{A_2} - cI\omega_1 A_1 - \frac{1}{2} I\,\mathrm{m}_1\,\omega_1^2 d_1 f(l_1) e^{\sigma_1 T_1 I} \end{aligned} \tag{3.4.22}$$

$$\begin{aligned} R_{22} &= -4I\beta_1 A_1 A_2 \overline{A_2} - 4I\beta_2 A_1^2 \overline{A_1} - 2\beta_1 A_1^2 \overline{A_1} + \left(2\omega_1 - \alpha_1\omega_1\right)\frac{\partial A_1}{\partial T_1} \\ &-8\beta_2 A_1 A_2 \overline{A_2} + c\omega_1 A_1 + \frac{1}{2}\mathrm{m}_1\,\omega_1^2 d_1 f(l_1) e^{\sigma_1 T_1 I} \end{aligned} \tag{3.4.23}$$

The coefficients of $\exp(i\omega_2 T_0)$ for the R.H.S. of the resulting equations give,

$$\begin{aligned} S_{21} &= -4\beta_1 A_1 A_2 \overline{A_1} - 4\beta_2 A_2^2 \overline{A_2} - 2\beta_1 A_2^2 \overline{A_2} + \left(-2I\omega_2 - \alpha_1 I\omega_1\right)\frac{\partial A_2}{\partial T_1} \\ &-8\beta_2 A_1 A_2 \overline{A_1} - cI\omega_2 A_2 \end{aligned} \tag{3.4.24}$$

$$\begin{aligned} S_{22} &= 4I\beta_1 A_1 A_2 \overline{A_1} - 4\beta_2 A_2^2 \overline{A_2} + 2I\beta_1 A_2^2 \overline{A_2} + \left(-2\omega_2 - \alpha_1\omega_1\right)\frac{\partial A_2}{\partial T_1} \\ &+8I\beta_2 A_1 A_2 \overline{A_1} - c\omega_2 A_2 \end{aligned} \tag{3.4.25}$$

From Eqs. (3.4.20) through (3.4.25), the solvability conditions [NM95] are determined using the following relation,

$$\left(coefficient\,of\ R_{11}\ for\ P_1\right)\times\left(R_{22}\right) - \left(coefficient\,of\ R_{12}\ for\ P_1\right)\times\left(R_{21}\right) = 0 \tag{3.4.26}$$

$$\left(coefficient\,of\ S_{11}\ for\ Q_1\right)\times\left(S_{22}\right) - \left(coefficient\,of\ S_{12}\ for\ Q_1\right)\times\left(S_{21}\right) = 0 \tag{3.4.27}$$

Finally, two solvability conditions in a simplified form are given below,

$$\frac{\partial A_1}{\partial T_1} = -c_2 A_1^{\,2}\overline{A_1} - c_3 A_1 A_2 \overline{A_2} - c_5 A_1 \tag{3.4.28}$$

$$\frac{\partial A_2}{\partial T_1} = -d_2 A_2^{\,2}\overline{A_2} - d_3 A_1 \overline{A_1} A_2 - d_4 \exp(i\sigma_1 T_1) - d_5 A_2 \tag{3.4.29}$$

Where $c_2, c_3, c_5, d_3, d_4, d_5$ are constants, given in Appendix C.

Substituting the solutions of A_1 and A_2 in the polar form i.e., $A_n = (1/2)(a_n \exp(i\theta_n)$ where $n = 1..2$, in Eqs. (3.4.28) and (3.4.29), and separating the real and imaginary parts we obtain the following system of equations.

$$\begin{aligned}
&\frac{1}{2}\frac{\partial a_1}{\partial T_1} + \frac{1}{8}c_2 a_1^{\,3} + \frac{1}{8}c_3 a_1 a_2^{\,2} + \frac{1}{2}c_5 a_1 = 0 \\
&\frac{1}{2}a_1 \frac{\partial \theta_1}{\partial T_1} = 0 \\
&\frac{1}{2}\frac{\partial a_2}{\partial T_1} + \frac{1}{8}d_2 a_2^{\,3} + \frac{1}{8}d_3 a_1^{\,2} a_2 + d_4 \cos(-\theta_2 + \sigma_1 T_1) + \frac{1}{2}d_5 a_2 = 0 \\
&-\frac{1}{2}a_2\sigma_1 + \frac{1}{2}a_2 \frac{\partial \Gamma}{\partial T_1} - d_4 \sin(-\theta_2 + \sigma_1 T_1) = 0
\end{aligned} \tag{3.4.30}$$

The above system of 4 equations can be transformed to an autonomous system of 5 equations using $\Gamma = -\theta_2 + \sigma_1 T_1$. These equations are called modulation equations and are given below.

$$\frac{1}{2}\frac{\partial a_1}{\partial T_1} + \frac{1}{8}c_2 a_1^{\,3} + \frac{1}{8}c_3 a_1 a_2^{\,2} + \frac{1}{2}c_5 a_1 = 0 \tag{3.4.31}$$

$$\frac{1}{2}a_1 \frac{\partial \theta_1}{\partial T_1} = 0 \tag{3.4.32}$$

$$\frac{1}{2}\frac{\partial a_2}{\partial T_1} + \frac{1}{8}d_2 a_2^{\,3} + \frac{1}{8}d_3 a_1^{\,2} a_2 + d_4 \cos(\Gamma) + \frac{1}{2}d_5 a_2 = 0 \tag{3.4.33}$$

$$-\frac{1}{2}a_2\sigma_1 + \frac{1}{2}a_2 \frac{\partial \Gamma}{\partial T_1} - d_4 \sin(\Gamma) = 0 \tag{3.4.34}$$

$$\Gamma = -\theta_2 + \sigma_1 T_1 \tag{3.4.35}$$

Eqs.(3.4.31) and (3.4.32) show that $a_1 = 0$ is a solution. Equilibrium is also achieved in $\partial a_1 / \partial T_1 = 0$, $\partial \Gamma / \partial T_1 = 0$. Eliminating the transformed phase shift Γ from the modulation equations, the autonomous system above now reduces to two equations that can be resolved to give the following 6^{th} degree polynomial equation for plotting the resonant curves.

$$d_2^{\,2} a_E^{\,6} + 8 d_2 d_5 a_E^{\,4} + 16(d_5^{\,2} + \sigma_1^{\,2}) a_E^{\,2} - 64 d_4^{\,2} = 0 \tag{3.4.36}$$

Where, $d_2 \ldots d_5$ are coefficients of the detuning parameter and are defined in the Appendix C.

3.4.3. Case of $\Omega \approx \omega_1$

For this resonant case $\Omega = \omega_1 + \varepsilon\sigma_1$ is substituted in Eqs. (3.4.16) and (3.4.17). The solvability conditions are determined following the same procedure as in the preceding section. But this time the coefficients of $\exp(i\omega_1 T_0)$ for the L.H.S. of the resulting equations give,

$$\begin{aligned} R_{11} &= -P_1\omega_1^2 + \alpha_2 P_1 - \omega_1\omega_2\alpha_1 P_2 I \\ R_{12} &= -P_2\omega_1^2 + \alpha_2 P_2 + \omega_1\omega_2\alpha_1 P_1 I \end{aligned} \tag{3.4.37}$$

The coefficients of $\exp(i\omega_2 T_0)$ for the L.H.S. of the resulting equations give,

$$\begin{aligned} S_{11} &= -Q_1\omega_2^2 + \alpha_2 Q_1 - \omega_2^2\alpha_1 Q_2 I \\ S_{12} &= -Q_2\omega_2^2 + \alpha_2 Q_2 + \omega_2^2\alpha_1 Q_1 I \end{aligned} \tag{3.4.38}$$

The coefficients of $\exp(i\omega_1 T_0)$ for the R.H.S. of the resulting equations give,

$$R_{21} = -4\beta_1 A_1 A_2 \overline{A_2} - 4\beta_2 A_1^{\,2}\overline{A_1} - 2\beta_1 A_1^{\,2}\overline{A_1} + \left(-2I\omega_1 + \alpha_1 I\omega_2\right)\frac{\partial A_1}{\partial T_1} - 8\beta_2 A_1 A_2 \overline{A_2} - cI\omega_1 A_1 \tag{3.4.39}$$

$$R_{22} = -4I\beta_1 A_1 A_2 \overline{A_2} - 4I\beta_2 A_1^{\,2}\overline{A_1} - 2\beta_1 A_1^{\,2}\overline{A_1} + \left(2\omega_1 - \alpha_1\omega_1\right)\frac{\partial A_1}{\partial T_1} - 8\beta_2 A_1 A_2 \overline{A_2} + c\omega_1 A_1 \tag{3.4.40}$$

The coefficients of $\exp(i\omega_2 T_0)$ for the R.H.S. of the resulting equations give,

$$S_{21} = -4\beta_1 A_1 A_2 \overline{A_1} - 4\beta_2 A_2^{\,2}\overline{A_2} - 2\beta_1 A_2^{\,2}\overline{A_2} + \left(-2I\omega_2 - \alpha_1 I\omega_2\right)\frac{\partial A_2}{\partial T_1} - 8\beta_2 A_1 A_2 \overline{A_1} - cI\omega_2 A_2 - \frac{1}{2} I\,\mathrm{m}_1\omega_2^2 d_1 f(l_1) e^{\sigma_1 T_1 I} \tag{3.4.41}$$

$$S_{22} = 4I\beta_1 A_1 A_2 \overline{A_1} + 4I\beta_2 A_2^{\,2}\overline{A_2} + 2I\beta_1 A_2^{\,2}\overline{A_2} + \left(-2\omega_2 - \alpha_1\omega_2\right)\frac{\partial A_2}{\partial T_1} + 8I\beta_2 A_1 A_2 \overline{A_1} - c\omega_2 A_2 - \frac{1}{2} I\,\mathrm{m}_1\omega_2^2 d_1 f(l_1) e^{\sigma_1 T_1 I} \tag{3.4.42}$$

Applying Eqs. (3.4.26) and (3.4.27) , give the following two solvability conditions for this case,

$$\frac{\partial A_1}{\partial T_1} = -c_2 A_1^{\,2}\overline{A_1} - c_3 A_1 A_2 \overline{A_2} - c_4 \exp(i\sigma_1 T_1) - c_5 A_1 \tag{3.4.43}$$

$$\frac{\partial A_2}{\partial T_1} = -d_2 A_2{}^2 \overline{A_2} - d_3 A_1 \overline{A_1} A_2 - d_5 A_2 \tag{3.4.44}$$

Where $c_2, c_3, c_4, c_5, d_2, d_3, d_5$ are constants, given in Appendix D.

Substituting the solutions of A_1 and A_2 in the polar form i.e., $A_n = (1/2)(a_n \exp(i\theta_n)$ where $n = 1..2$, in Eqs. (3.4.43) and (3.4.44), and separating the real and imaginary parts we obtain the following system of equations.

$$\begin{aligned}
&\frac{1}{2}\frac{\partial a_1}{\partial T_1} + \frac{1}{8}c_2 a_1{}^3 + \frac{1}{8}c_3 a_1 a_2{}^2 + c_4 \cos(-\theta_1 + \sigma_1 T_1) + \frac{1}{2}c_5 a_1 = 0 \\
&\frac{1}{2}a_1 \frac{\partial \theta_1}{\partial T_1} + c_4 \sin(-\theta_1 + \sigma_1 T_1) = 0 \\
&\frac{1}{2}\frac{\partial a_2}{\partial T_1} + \frac{1}{8}d_2 a_2{}^3 + \frac{1}{8}d_3 a_1{}^2 a_2 + \frac{1}{2}d_5 a_2 = 0 \\
&-\frac{1}{2}a_2 \frac{\partial \theta_2}{\partial T_1} = 0
\end{aligned} \tag{3.4.45}$$

The modulation equations are now obtained using $\Gamma = -\theta_1 + \sigma_1 T_1$

$$\frac{1}{2}\frac{\partial a_1}{\partial T_1} + \frac{1}{8}c_2 a_1{}^3 + \frac{1}{8}c_3 a_1 a_2{}^2 + c_4 \cos\Gamma + \frac{1}{2}c_5 a_1 = 0 \tag{3.4.46}$$

$$\frac{1}{2}a_1 \frac{\partial \theta_1}{\partial T_1} + c_4 \sin\Gamma = 0 \tag{3.4.47}$$

$$\frac{1}{2}\frac{\partial a_2}{\partial T_1} + \frac{1}{8}d_2 a_2{}^3 + \frac{1}{8}d_3 a_1{}^2 a_2 + \frac{1}{2}d_5 a_2 = 0 \tag{3.4.48}$$

$$\Gamma = -\theta_1 + \sigma_1 T_1 \tag{3.4.49}$$

Eq. (3.4.48) shows that $a_2 = 0$ is a solution. Equilibrium is also achieved in $\partial a_2 / \partial T_1 = 0$, $\partial\Gamma / \partial T_1 = 0$. Eliminating the transformed phase shift Γ from the modulation equations, the autonomous system above now reduces to two equations that can be resolved to give the following 6th degree polynomial equation for plotting the resonant curves.

$$c_2{}^2 a_E{}^6 + 8c_2 c_5 a_E{}^4 + 16(c_5{}^2 + \sigma_1{}^2) a_E{}^2 - 64 c_4{}^2 = 0 \tag{3.4.50}$$

Where, $c_2 \ldots c_5$ are coefficients of the detuning parameter and are defined in the Appendix D. The polynomials given by Eqs. (3.4.36) and (3.4.50) are functions of amplitude at equilibrium a_E and detuning parameter σ_1. Solution of these polynomials gives six solutions that are symbolically complicated expressions and are not reproduced here. Therefore these polynomials are treated numerically in the next section.

3.5. Numerical Application (Resonant Curves)

The investigations were conducted using three different methods, i.e. the method of multiple scales, a continuation procedure and a step by step integration method in Matlab Simulink. All the numerical data are given in Appendix B.

3.5.1. Method of Multiple Scales

The numerical solutions for the two resonant conditions $\Omega \approx \omega_1$ and $\Omega \approx \omega_2$ are presented showing the plots of resonant curves of hard spring type Fig. 36.

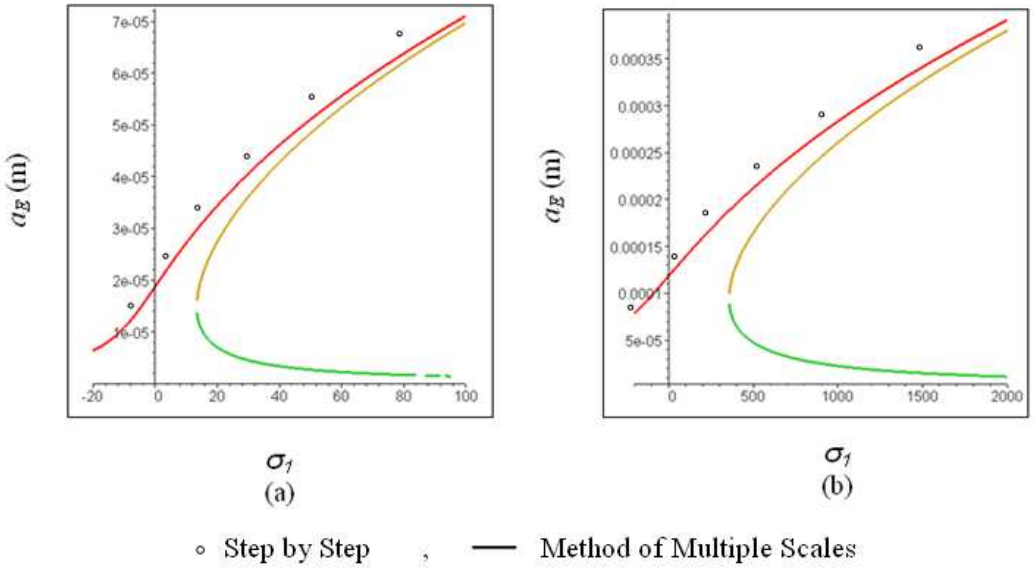

Fig. 36. Resonance curves (a) $\Omega \approx \omega_1$ (b) $\Omega \approx \omega_2$

The effect of nonlinearity has caused these curves to bend rightwards from the position of the linear response given in Fig. 35. It is interesting to note the plotting ranges of these curves to generate the same shapes. For the case $\Omega = \omega_2$ these curves are significantly expanded and the range of amplitude is higher.

3.5.2. Continuation Procedure (Matcont[2])

The bifurcation diagrams and state planes are presented in Fig. 37 and Fig. 38. For a given value of the detuning parameter there are three solutions in the positive plane. Out of these solutions, two are stable and one is unstable. The continuation procedure is capable of tracing two stable solutions which can be seen corresponding to points A and B on the curves in Fig. 37 (a) and Fig. 38 (a). The curve of the unstable solution lies somewhere between these two curves. The results of this procedure match with those obtained by MMS but the latter is more preferable as it can plot the unstable solutions as well.

[2] A. Dhooge, W. Govaerts, Yu.A. Kuznetsov, W. Mestrom, A. M. Riet, B. Sautois, MATCONT: A continuation toolbox in Matlab, http://www.matcont.ugent.be/

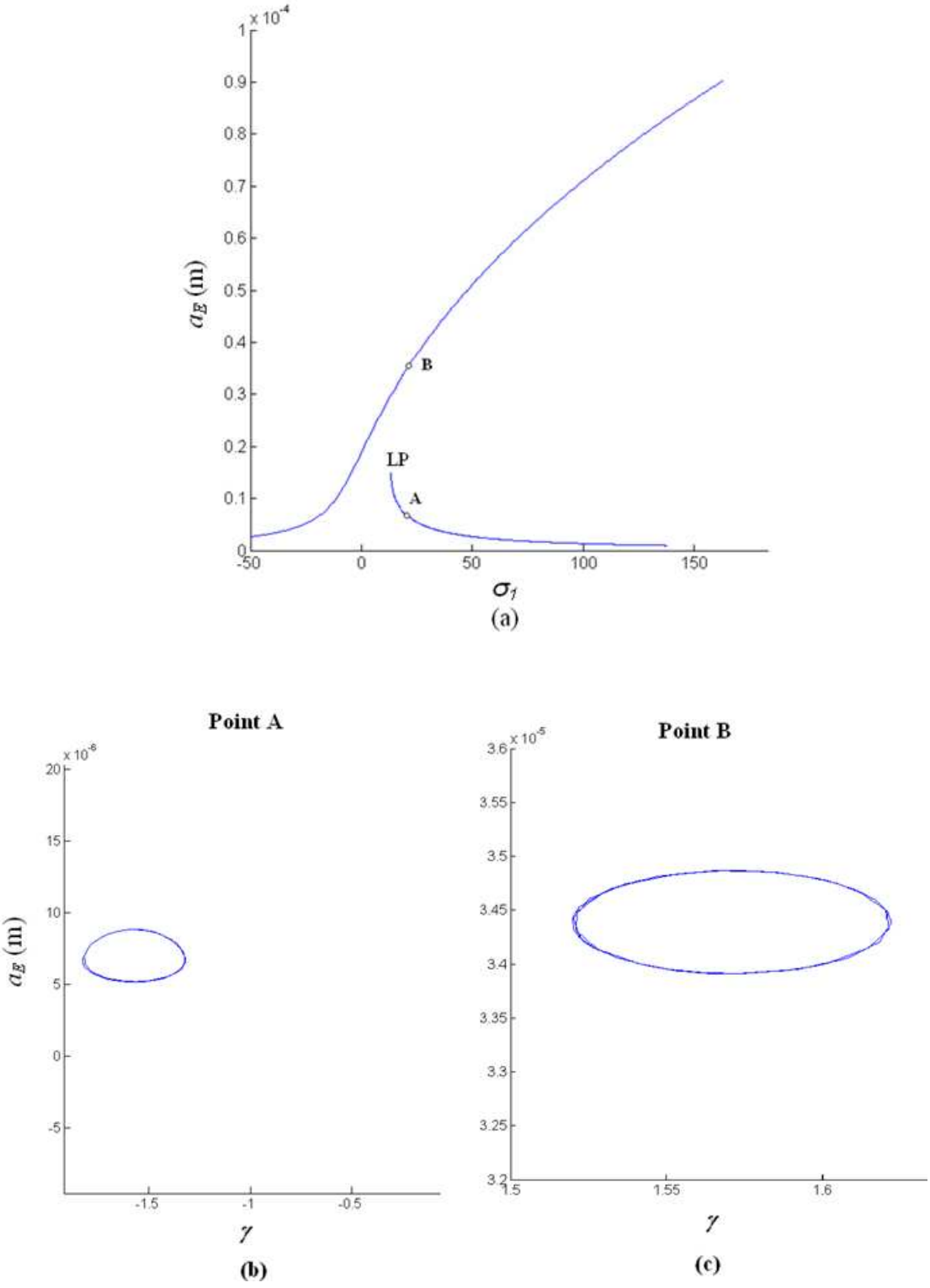

Fig. 37. Results obtained by continuation procedure using Matcont at $\sigma_1 = 20$ for $\Omega \approx \omega_1$
(a) Resonance Curves (b) State Plane at point A (c) State Plane at point B

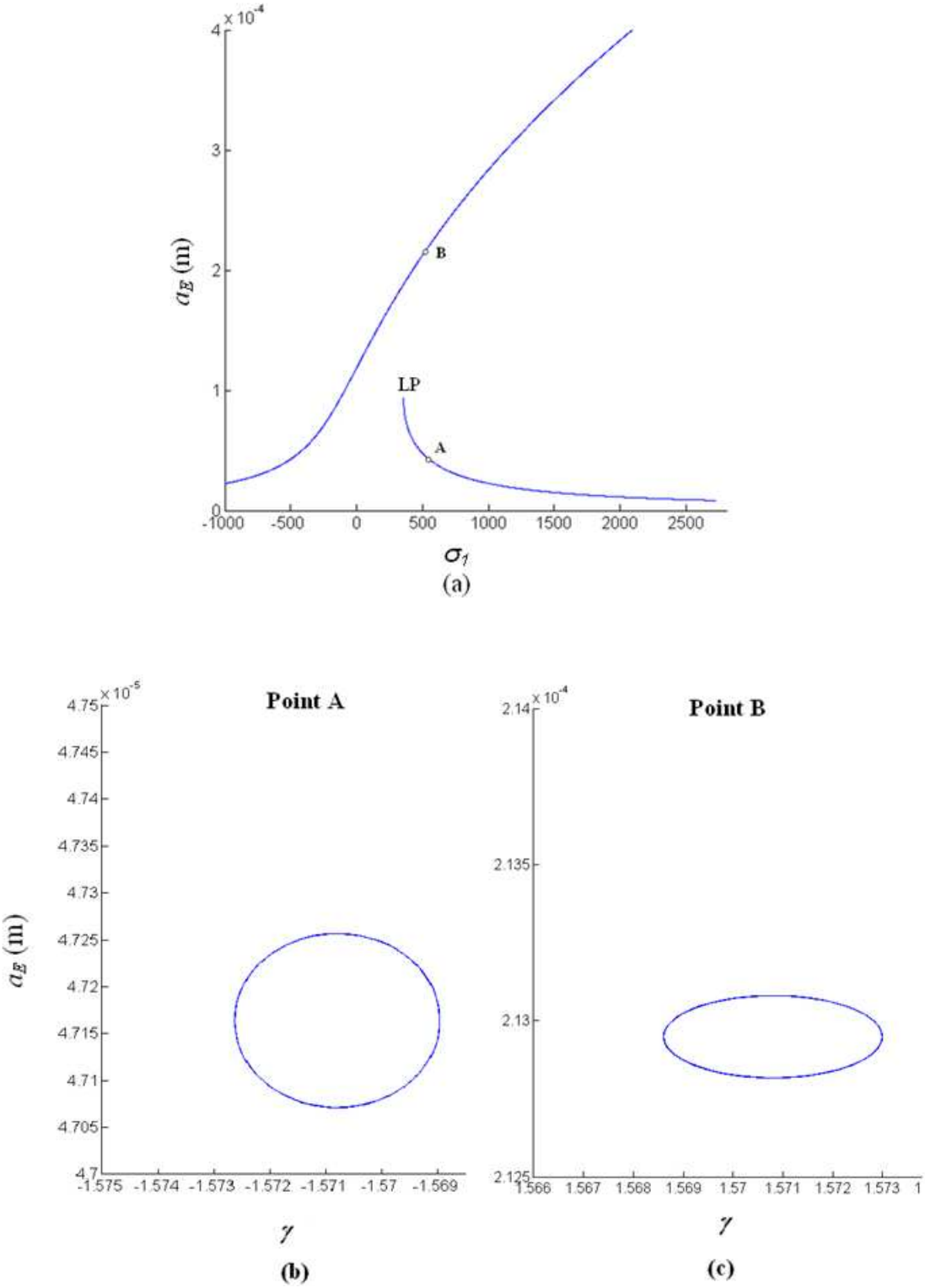

Fig. 38. Results obtained by continuation procedure using Matcont at $\sigma_1 = 504$ for $\Omega \approx \omega_2$
(a) Resonance Curves (b) State Plane at point A (c) State Plane at point B

The state planes are plotted for two different points A and B on the resonant curves given in Fig. 37 (a) and Fig. 38 (a). It can be observed that the amplitude at point A is much lower as compared to that of point B. Also the orbits corresponding to point B tend to be more oval as compared to those corresponding to point A. Therefore it can be concluded that the effect of nonlinearity due to higher order deformations is more visible at the curve at point B.

3.5.3. Direct Integration by Step by Step Method (Matlab)

A step by step analysis was conducted using the Simulink toolbox of Matlab. The equations of motion given by Eqs. (3.1.10) and (3.1.11) are treated directly. The results are compared with those obtained by MMS and are presented as dots in Fig. 36. The phase diagrams, poincaré sections and time histories of the amplitude are given in Fig. 39 and Fig. 40. The discrepancy between MMS results and step by step results in Fig. 36 are mainly due to the difficulty to obtain the maximum and minimum in the amplitude response curves. The amplitude modulation is also visible in these figures. The simulation was carried out and the phase diagrams were plotted for the last 0.2 seconds. This corresponds to 4 periods where the amplitude modulation is low. Hence as a result the 4 points on the poincaré sections lie close together.

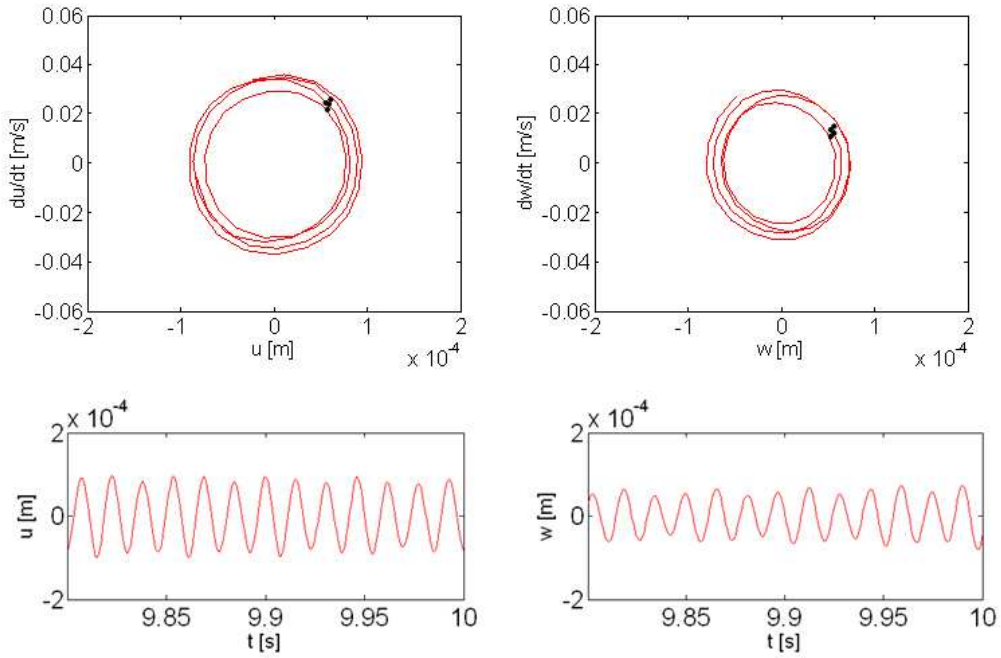

Fig. 39. Phase diagrams, poincaré sections and time amplitude responses for $\Omega \approx \omega_1$

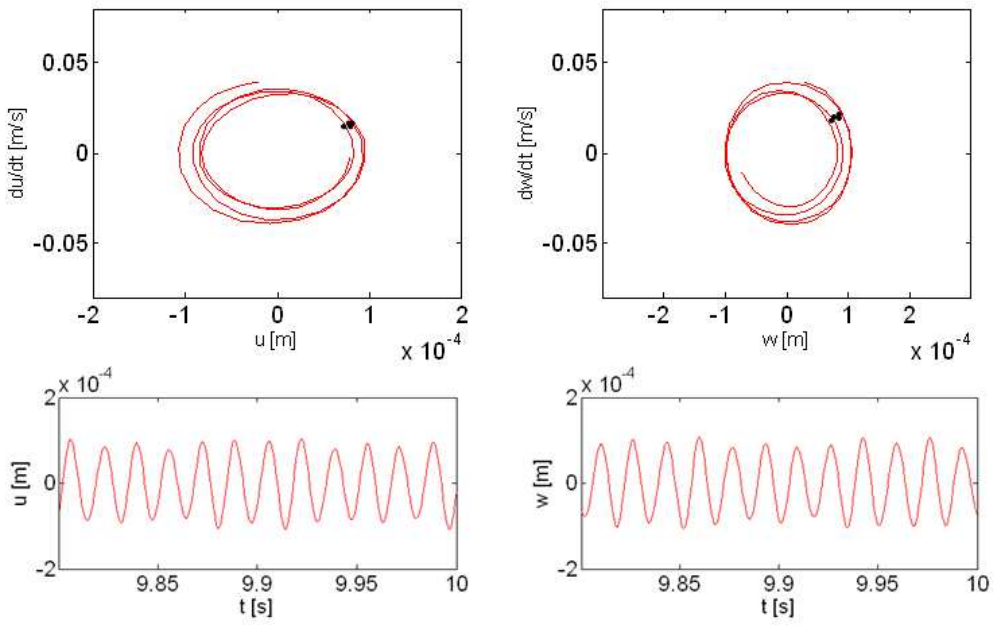

Fig. 40. Phase diagrams, poincaré sections and time amplitude responses for $\Omega \approx \omega_2$

3.6. Effect of various parameters

In regard to the limitations presented by the continuation procedure (the inefficiency in predicting unstable branch) and step by step method (difficulty in choosing the initial conditions and hence not attaining the stability in time amplitude response), in the following the method of multiple scales is used. The coefficients d_2, d_4 and d_5 are functions of various quantities $\alpha_1, \alpha_2, \beta_1, \beta_2$ and m_1 (Appendices C and D). These quantities further depend on geometric, material and mass unbalance parameters. This indicates that a change in the values of these parameters will give different numerical solutions of Eqs. (3.4.36) and (3.4.50), thus generating different resonant curves. Therefore these different parameters can be adjusted to change the behavior of the rotor significantly.

3.6.1. Effect of $\beta_2 = 0$

According to Eq. (3.1.12) quantity β_2 depends on k_3 which represents the effect of an axial dynamic force, see Eqs. (2.4.44) and (2.4.45). This implies that if we want to study the dynamics of the system without considering the effect of an axial force we can substitute $\beta_2 = 0$ in various constants given in Appendices C and D. This affects the overall response of the system. The generated resonant curves are presented in Fig. 41. A comparison of these curves with those of Fig. 36 shows that the amplitude has increased. Also a decrease in the horizontal plotting range of these curves indicates that the spring hardening effect becomes visible even at very low values of detuning parameter σ_1.

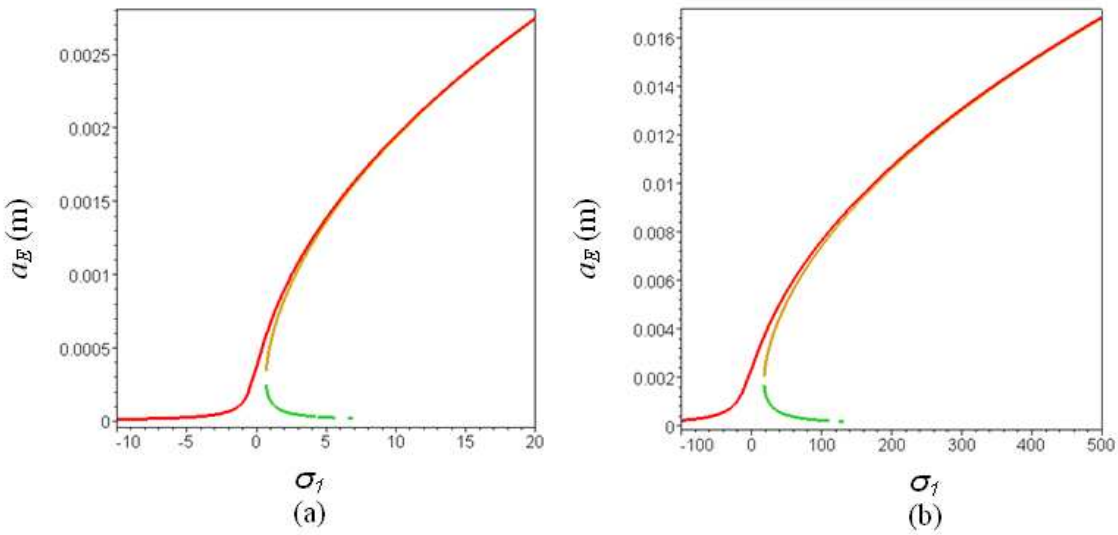

Fig. 41. Effect of $\beta_2 = 0$ on nonlinear dynamic response (a) $\Omega \approx \omega_1$ (b) $\Omega \approx \omega_2$

3.6.2. Effect of varying the mass unbalance m_u

The quantity d_4 in the polynomial given by Eq. (3.4.36) depends on the mass unbalance m_u through the quantities given in appendices C and D. Therefore the response of the system can be varied by changing the value of the mass unbalance. Fig. 42 represents the effect of varying the mass unbalance from 1 x 10^{-5} kg to 100 x 10^{-5} kg. Different resonant curves plotted on the same scale show that as the mass unbalance is increased, the horizontal component of these curves expands more to cover a greater range of detuning parameter σ_1.

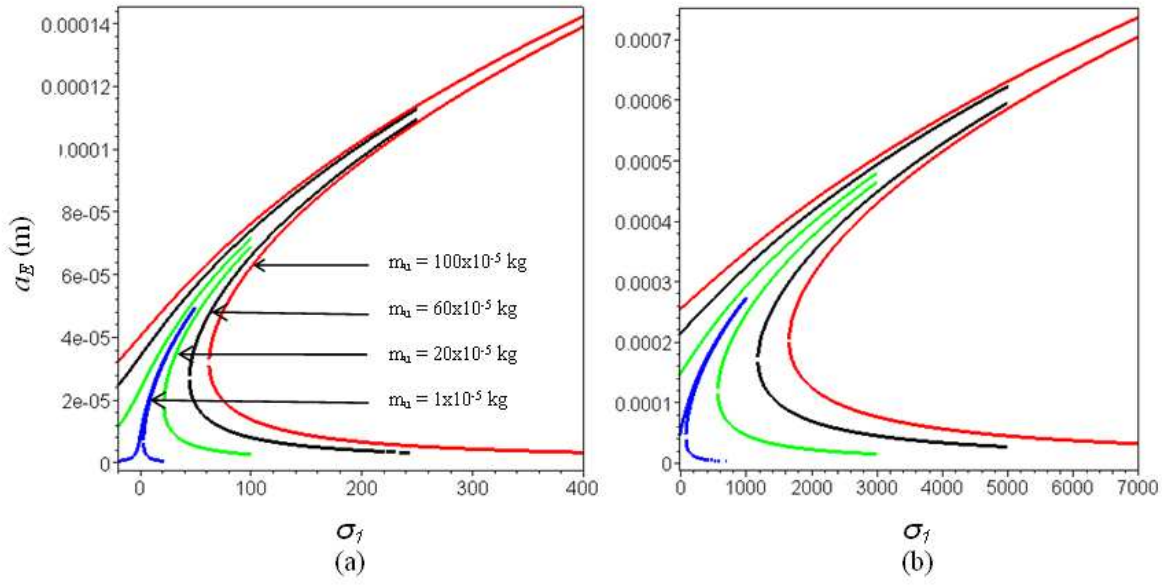

Fig. 42. Effect of variation in mass unbalance m_u on nonlinear dynamic response
(a) $\Omega \approx \omega_1$ (b) $\Omega \approx \omega_2$

3.6.3. Effect of varying shaft cross-sectional radius R_1

The quantities α_1, β_1, α_2, β_2 and m_1 in Appendices C and D are related to parameters b_1, b_2, k_1, k_2, k_3 using Eq. (3.1.12). All these parameters depend on the cross-sectional radius of the shaft. Therefore a change in the shaft radius will change the numerical values of all the parameters and quantities mentioned above. Fig. 43 shows the system response for three different values of shaft cross-sectional radius. It can be observed that the resonant curves bend more strongly towards right as the shaft narrows.

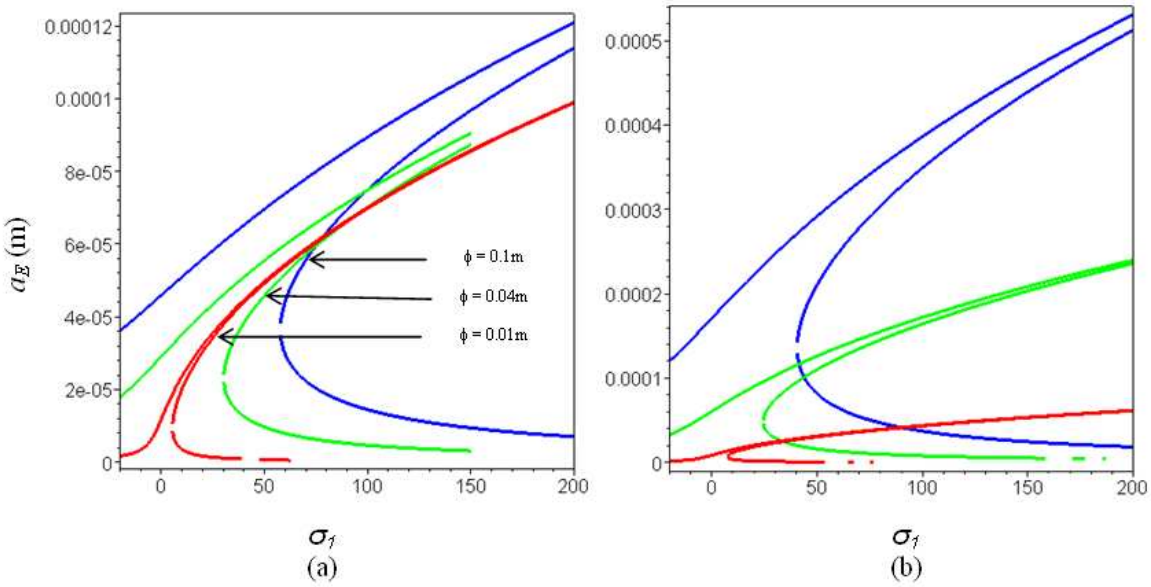

Fig. 43. Effect of variation in shaft diameter on nonlinear dynamic response
(a) $\Omega \approx \omega_1$ (b) $\Omega \approx \omega_2$

3.7. Conclusions

This chapter analyzed some of the mathematical models developed in chapter 2. The nonlinear behavior of rotor dynamics due to large deformations and a dynamic axial force was analysed for the first mode. A mathematical model with the combined effects of higher order large bending deformations and a dynamic axial force was formulated from the work presented in chapter 2. This model was solved using the multiple scales method. The numerical investigations were conducted using three methods, i.e. the method of multiple scales, a continuation procedure (Matcont) and a step by step analysis in Matlab Simulink. It is concluded that the method of multiple scales is more efficient than the other two methods as all the stable and unstable solutions can be seen in the resonant curves.

The results showed that nonlinearities along with other phenomena like gyroscopic, rotary inertia and mass unbalance effects significantly influence the dynamics of the rotor system. The linear analysis showed that resonance existed only at the second critical speed, but in the nonlinear analysis another resonance appeared at the first critical speed. Furthermore, nonlinearities caused the resonance curves to be of hard spring type. In the absence of dynamic axial force and at lower values of mass unbalance, the spring hardening effect was visible even at lower values of detuning parameter σ_1. Using the method of analysis presented here facilitated studying the changes caused by modifying different rotor system parameters, by changing the numerical values of the latter.

[This page intentionally left blank]

Chapter 4: Nonlinear Analysis Taking into Account Shear Effects

In this chapter the mathematical model developed in section 2.5.2 is analyzed. This model considers nonlinearity due to large deformations in bending and shear effects. It is composed of 4th order coupled nonlinear differential equations of motion. The equations of motion given by Eqs. (2.5.34) and (2.5.35) are referred. Both linear and nonlinear analyses are presented in the following sections.

4.1. Linear Analysis

The natural frequencies of vibration and hence the critical speeds of the rotor are determined by studying the rotor system in free undamped motion. The linear equations of motion are given as,

$$\begin{aligned} &\ddot{U} - \Omega\alpha_{21}\ddot{W} + \alpha_{31}U - \Omega\alpha_{41}\dot{W} + \alpha_{51}U = 0 \\ &\ddot{W} + \Omega\alpha_{21}\ddot{U} + \alpha_{31}W + \Omega\alpha_{41}\dot{U} + \alpha_{51}W = 0 \end{aligned} \tag{4.1.1}$$

The solutions of Eq. (4.1.1) are sought in the form,

$$U = U_1 \exp(\omega t)\ ,\ W = W_1 \exp(\omega t) \tag{4.1.2}$$

Substituting Eq. (4.1.2) in Eq. (4.1.1) gives the following set of homogeneous equations.

$$\begin{bmatrix} \omega^4 + \alpha_{31}\omega^2 + \alpha_{51} & -\Omega\alpha_{21}\omega^3 - \Omega\alpha_{41}\omega \\ \Omega\alpha_{21}\omega^3 + \Omega\alpha_{41}\omega & \omega^4 + \alpha_{31}\omega^2 + \alpha_{51} \end{bmatrix} \begin{Bmatrix} U_1 \\ W_1 \end{Bmatrix} = 0 \tag{4.1.3}$$

The expansion of the determinant of the matrix in Eq. (4.1.3) gives the following characteristic equation.

$$\begin{aligned} &\omega^8 + (2\alpha_{31} + \alpha_{21}^2\Omega^2)\omega^6 + (2\alpha_{51} + \alpha_{31}^2 + 2\alpha_{21}\alpha_{41}\Omega^2)\omega^4 \\ &+ (2\alpha_{31}\alpha_{51} + \alpha_{41}^2\Omega^2)\omega^2 + \alpha_{51}^2 = 0 \end{aligned} \tag{4.1.4}$$

The roots of Eq. (4.1.4) can be represented as $\pm i\omega_n$, where ω_n for *n = 1..4*, are the angular frequencies. The symbolic expressions of these frequencies are complicated and are therefore treated numerically. The numerical data are given in Appendix B.

The effect of shear deformations is studied for various slenderness ratios (r) where r = R1/2L. The results are obtained for a rotating shaft as well as for a shaft-disk rotor system. Also both solid and tube sections of the shaft are investigated. The results are presented in tabular form in Tables (1) and (2). The graphical representation of the results is given in Fig. 44 to Fig. 47. It can be observed that with the inclusion of shear effects, the critical speeds of the rotor decrease. The difference between critical rotor speeds with and without shear effects is increased as the slenderness ratio is increased.

This implies that the shear effects become greater for higher values of the slenderness ratio (r). Also, it is interesting to note that the difference in the 2nd critical speeds is greater than that noted with the 1st critical speeds. Comparison of Fig. 44 and Fig. 45 indicates that the shear effects are more visible in the case of a rotating shaft than that of a shaft-disk rotor system. Moreover it can be observed from Fig. 46 and Fig. 47 that the shear effects are greater with a tubular shaft than with a solid shaft.

Table. 5. Shear effects on 1st two critical speeds of a rotating shaft for various slenderness ratios (r)

Cross - Section	**Geometry (meters)**	L = 2 R_1= 0.32	L =1.5 R_1= 0.18	L =1 R_1= 0.08	L =1 R_1= 0.06	L = 0.5 R_1= 0.02
	slenderness ratio (r)	0.08	0.06	0.04	0.03	0.02
Solid	**Critical speeds without shear (rpm)**	17503 19722	18147 19438	18652 19242	14130 14381	18977 19127
	Critical speeds with shear (rpm)	16452 17961	17425 18450	18276 18804	13961 14197	18872 19018
	percentage decrease	6 % 8.93 %	4 % 5 %	2 % 2.3 %	1.2 % 1.3 %	0.5 % 0.5 %
Tube ($e = 10^{-3}$ m)	**Critical speeds without shear (rpm)**	22963.6 28831.2	24454.2 27926.7	25654.7 27256.5	19572.5 20256.6	26030.5 26421.3
	Critical speeds with shear (rpm)	19709.9 21709.5	21911.3 23662	24142.9 25284	18854.8 19415.2	25584 25941.5
	Percentage decrease	14.17 % 24.70 %	10.40 % 15.27 %	5.89 % 7.24 %	3.67 % 4.15 %	1.72 % 1.82 %

Table. 6. Shear effects on the 1st two critical speeds of a shaft-disk rotor system for various slenderness ratios (r)

Cross-section	**Geometry (meters)**	L = 2 R_1= 0.32 R_2 = 0.75 h = 0.15	L =1.5 R_1=0.18 R_2 = 0.50 h = 0.10	L =1 R_1=0.08 R_2 = 0.3 h = 0.06	L =1 R_1=0.06 R_2 = 0.3 h = 0.06	L =0.5 R_1=0.02 R_2 = .15 h = 0.03
	Slenderness ratio (r)	0.08	0.06	0.04	0.03	0.02
Solid	**Critical speeds without shear (rpm)**	13838 16286	13542 15247	12064 13275	7456 8284	7158 8068
	Critical speeds with shear (rpm)	13332 15227	13255 14743	11970 13124	7433.5 8247	7153 8059
	percentage decrease	3.65 % 6.50 %	2.34 % 3.31 %	0.78 % 1.14 %	0.30 % 0.45 %	0.07 % 0.11 %
Tube ($e = 10^{-3}$ m)	**Critical speeds without shear (rpm)**	2505.6 3200.5	2997.4 3618.3	3471.7 4017.9	2223.4 2563.6	3300.6 3791.3
	Critical speeds with shear (rpm)	2500.8 3184.6	2992.5 3605.8	3468.1 4010.4	2222.4 2561.3	3299.8 3789.7
	Percentage decrease	0.19 % 0.50 %	0.16 % 0.35 %	0.10 % 0.19 %	0.04 % 0.09 %	0.02 % 0.04 %

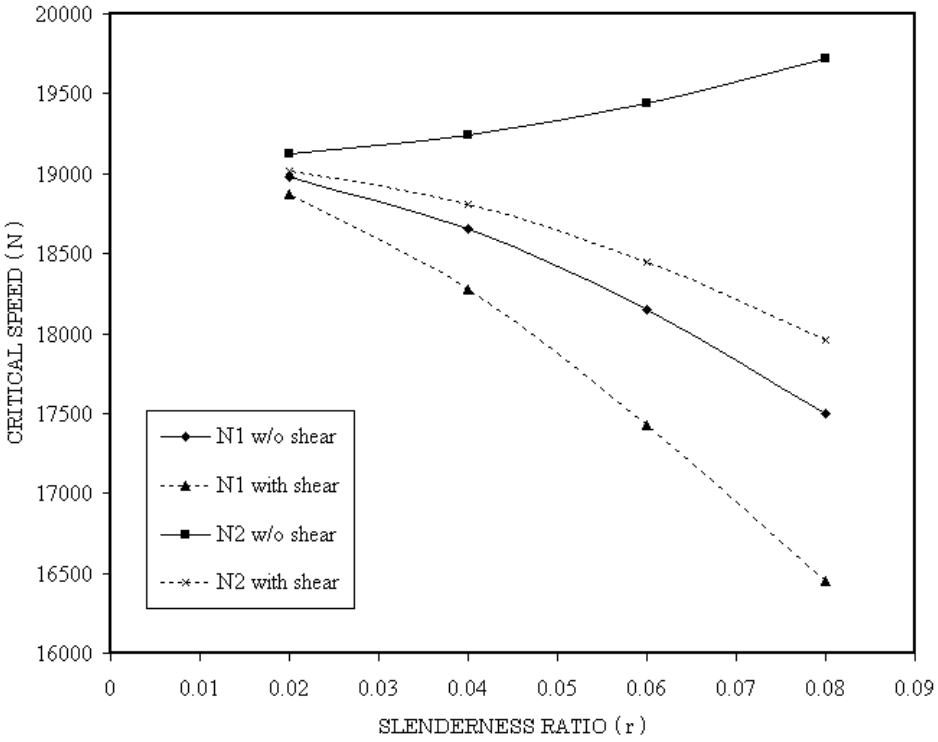

Fig. 44. Effect of shear and slenderness ratio (r) on the critical speeds of a solid shaft

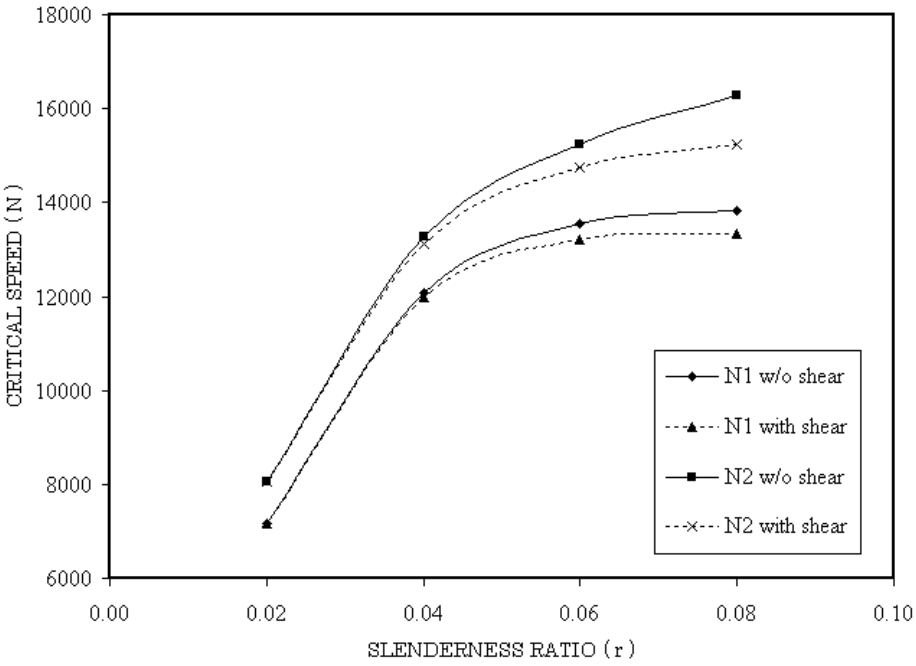

Fig. 45. Effect of shear and slenderness ratio (r) on the critical speeds of a shaft-disk rotor system

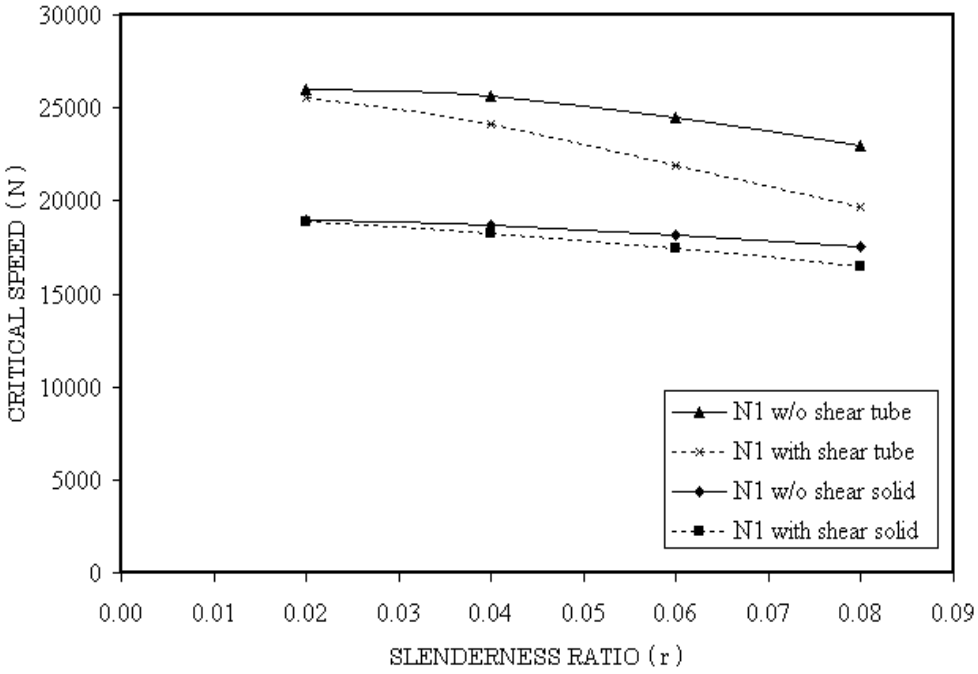

Fig. 46. Comparison of 1st critical speeds of a solid and a tube shaft for various slenderness ratios

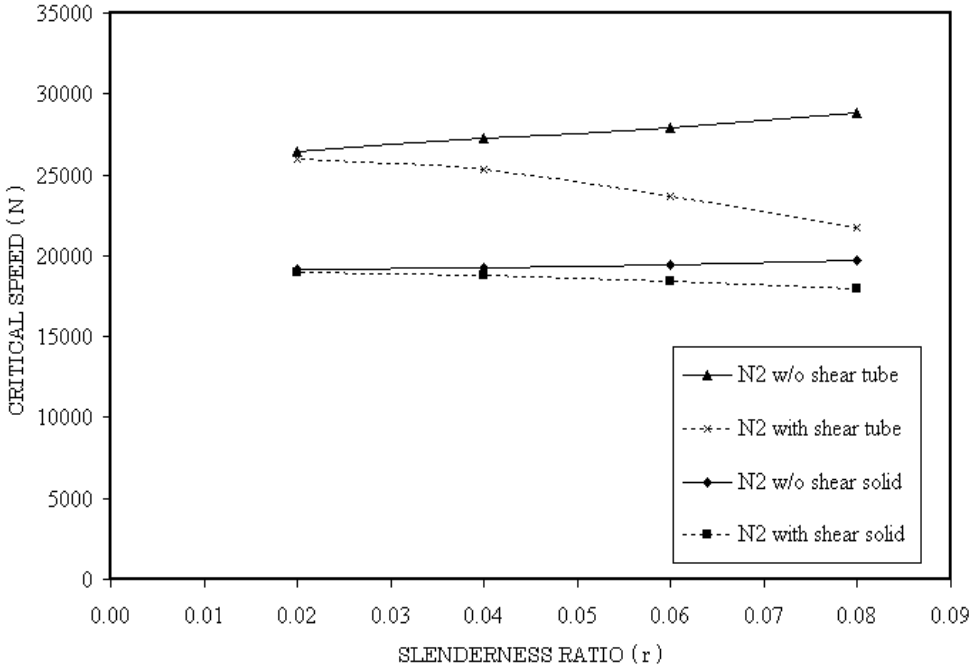

Fig. 47. Comparison of 2nd critical speeds of a solid and a tube shaft for various slenderness ratios

4.2. Nonlinear Analysis

The complete set of equations of motion including nonlinear terms given by Eqs. (2.5.34) and (2.5.35) are analyzed using MMS. In this section MMS is applied for 4th order derivatives with respect to time. Displacements U and W are expanded as the power series of ε to the first order,

$$\begin{aligned} U(T_0,T_1) &= u_0(T_0,T_1)+\varepsilon u_1(T_0,T_1) = u_0+\varepsilon u_1 \\ W(T_0,T_1) &= w_0(T_0,T_1)+\varepsilon w_1(T_0,T_1) = w_0+\varepsilon w_1 \end{aligned} \tag{4.2.1}$$

Where $T_n = \varepsilon^n t$ are slow time scales, T_1 being slower than T_0, and ε is a small dimensionless parameter; $\varepsilon << 1$. The nonlinear, damping and forcing terms in Eqs. (2.5.34) and (2.5.35) are scaled so that the damping and forcing terms appear in the same perturbation equations as the nonlinear terms. This is done so that the effect of damping is balanced with the effect of nonlinearity. Therefore the following scaling is used.

$$\alpha_1=\alpha_1,\alpha_2=\alpha_2,\beta_{11}=\varepsilon\beta_{11},\beta_{21}=\varepsilon\beta_{21},\beta_{31}=\varepsilon\beta_{31},\beta_{41}=\varepsilon\beta_{41},m_1=\varepsilon m_1,c=\varepsilon c \tag{4.2.2}$$

The resulting equations are given as,

$$\begin{aligned} &\ddot{U}-\Omega\alpha_{21}\ddot{W}+\alpha_{31}\ddot{U}-\Omega\alpha_{41}\dot{W}+\alpha_{51}U+\varepsilon c\dot{W}=(-3/2)\varepsilon\beta_{11}(W^2\ddot{U}+2UW\ddot{W}+ \\ &3U^2\ddot{U})-(3/2)\varepsilon\beta_{21}(U\ddot{W}^2+2W\ddot{U}\ddot{W}+3U\ddot{U}^2)-(3/4)\varepsilon\beta_{31}(U^3+UW^2)- \\ &(3/16)\varepsilon\beta_{41}(\ddot{U}^3+\ddot{U}\ddot{W}^2)+\varepsilon m_1\Omega^2\sin\Omega t \end{aligned} \tag{4.2.3}$$

$$\begin{aligned} &\ddot{W}+\Omega\alpha_{21}\ddot{U}+\alpha_{31}\ddot{W}+\Omega\alpha_{41}\dot{U}+\alpha_{51}W+\varepsilon c\dot{U}=(-3/2)\varepsilon\beta_{11}(U^2\ddot{W}+2WU\ddot{U}+ \\ &3W^2\ddot{W})-(3/2)\varepsilon\beta_{21}(W\ddot{U}^2+2U\ddot{U}\ddot{W}+3W\ddot{W}^2)-(3/4)\varepsilon\beta_{31}(W^3+WU^2)- \\ &(3/16)\varepsilon\beta_{41}(\ddot{W}^3+\ddot{W}\ddot{U}^2)+\varepsilon m_1\Omega^2\cos\Omega t \end{aligned} \tag{4.2.4}$$

Using Eq. (4.2.1) all the time derivatives appearing in Eqs. (4.2.3) and (4.2.4) are found. After substituting these derivatives in these equations and equating like powers of ε on both sides of the resulting equations, we obtain the two following systems of equations.

4.2.1. System of order 0 equations (ε^0)

$$\begin{aligned} &\frac{\partial^4}{\partial T_0^4}u_0-\Omega\alpha_{21}\frac{\partial^3}{\partial T_0^3}w_0+\alpha_{31}\frac{\partial^2}{\partial T_0^2}u_0-\Omega\alpha_{41}\frac{\partial}{\partial T_0}w_0+\alpha_{51}u_0=0 \\ &\frac{\partial^4}{\partial T_0^4}w_0+\Omega\alpha_{21}\frac{\partial^3}{\partial T_0^3}u_0+\alpha_{31}\frac{\partial^2}{\partial T_0^2}w_0+\Omega\alpha_{41}\frac{\partial}{\partial T_0}u_0+\alpha_{51}w_0=0 \end{aligned} \tag{4.2.5}$$

4.2.2. System of order 1 equations (ε^1)

$$\frac{\partial^4}{\partial T_0^4}u_1 - \Omega\alpha_{21}\frac{\partial^3}{\partial T_0^3}w_1 + \alpha_{31}\frac{\partial^2}{\partial T_0^2}u_1 - \Omega\alpha_{41}\frac{\partial}{\partial T_0}w_1 + \alpha_{51}u_1 =$$
$$-(9/2)\beta_{21}u_0\left(\frac{\partial^2}{\partial T_0^2}u_0\right)^2 - 3\beta_{21}w_0\frac{\partial^2}{\partial T_0^2}u_0\frac{\partial^2}{\partial T_0^2}w_0 - c\frac{\partial}{\partial T_0}u_0$$
$$-3\beta_{11}u_0w_0\frac{\partial^2}{\partial T_0^2}w_0 - 4\frac{\partial^4}{\partial T_0^3\partial T_1}u_0 - (3/16)\beta_{41}\left(\frac{\partial^2}{\partial T_0^2}u_0\right)^3$$
$$-(3/4)\beta_{31}u_0^3 - (3/2)\beta_{11}w_0^2\frac{\partial^2}{\partial T_0^2}u_0 - (9/2)\beta_{11}u_0^2\left(\frac{\partial^2}{\partial T_0^2}u_0\right)$$
$$-(3/2)\beta_{21}u_0\left(\frac{\partial^2}{\partial T_0^2}w_0\right)^2 - (3/16)\beta_{41}\frac{\partial^2}{\partial T_0^2}u_0\left(\frac{\partial^2}{\partial T_0^2}w_0\right)^2$$
$$+m_1\Omega^2\sin(\Omega T_0) - (3/4)\beta_{31}u_0w_0^2 - 2\frac{\partial^3}{\partial T_0^2\partial T_1}u_0$$
$$+3\Omega\alpha_{21}\frac{\partial^4}{\partial T_0^3\partial T_1}w_0 + \Omega\alpha_{41}\frac{\partial}{\partial T_1}w_0 \qquad (4.2.6)$$

$$\frac{\partial^4}{\partial T_0^4}w_1 + \Omega\alpha_{21}\frac{\partial^3}{\partial T_0^3}u_1 + \alpha_{31}\frac{\partial^2}{\partial T_0^2}w_1 + \Omega\alpha_{41}\frac{\partial}{\partial T_0}u_1 + \alpha_{51}w_1 =$$
$$-(9/2)\beta_{21}w_0\left(\frac{\partial^2}{\partial T_0^2}w_0\right)^2 - 3\beta_{21}u_0\frac{\partial^2}{\partial T_0^2}w_0\frac{\partial^2}{\partial T_0^2}u_0 - c\frac{\partial}{\partial T_0}w_0$$
$$-3\beta_{11}w_0u_0\frac{\partial^2}{\partial T_0^2}u_0 - 4\frac{\partial^4}{\partial T_0^3\partial T_1}w_0 - (3/16)\beta_{41}\left(\frac{\partial^2}{\partial T_0^2}w_0\right)^3$$
$$-(3/4)\beta_{31}w_0^3 - (3/2)\beta_{11}u_0^2\frac{\partial^2}{\partial T_0^2}w_0 - (9/2)\beta_{11}w_0^2\left(\frac{\partial^2}{\partial T_0^2}w_0\right)$$
$$-(3/2)\beta_{21}w_0\left(\frac{\partial^2}{\partial T_0^2}u_0\right)^2 - (3/16)\beta_{41}\frac{\partial^2}{\partial T_0^2}w_0\left(\frac{\partial^2}{\partial T_0^2}u_0\right)^2$$
$$+m_1\Omega^2\cos(\Omega T_0) - (3/4)\beta_{31}w_0u_0^2 - 2\frac{\partial^3}{\partial T_0^2\partial T_1}w_0$$
$$-3\Omega\alpha_{21}\frac{\partial^4}{\partial T_0^3\partial T_1}u_0 - \Omega\alpha_{41}\frac{\partial}{\partial T_1}u_0 \qquad (4.2.7)$$

The general solution of Eq. (4.2.5) can be written as,

$$\begin{aligned} u_0 &= A_1(T_1)\exp(i\omega_1 T_0) + A_2(T_1)\exp(i\omega_2 T_0) + A_3(T_1)\exp(i\omega_3 T_0) \\ &\quad + A_4(T_1)\exp(i\omega_4 T_0) + [cc] \\ w_0 &= iA_1(T_1)\exp(i\omega_1 T_0) - iA_2(T_1)\exp(i\omega_2 T_0) + iA_3(T_1)\exp(i\omega_3 T_0) \\ &\quad - iA_4(T_1)\exp(i\omega_4 T_0) + [cc] \end{aligned} \tag{4.2.8}$$

Where [cc] denotes the complex conjugate of the preceding terms.

Also a particular solution is assumed for u_1 and w_1 in the following form,

$$\begin{aligned} u_1 &= P_1(T_1)\exp(i\omega_1 T_0) + P_2(T_1)\exp(i\omega_2 T_0) + P_3(T_1)\exp(i\omega_3 T_0) \\ &\quad + P_4(T_1)\exp(i\omega_4 T_0) \\ w_1 &= Q_1(T_1)\exp(i\omega_1 T_0) + Q_2(T_1)\exp(i\omega_2 T_0) + Q_3(T_1)\exp(i\omega_3 T_0) \\ &\quad + Q_4(T_1)\exp(i\omega_4 T_0) \end{aligned} \tag{4.2.9}$$

After substituting Eqs. (4.2.8) and (4.2.9) into Eqs. (4.2.6) and (4.2.7), it can be observed from the resulting equations that there are various possible resonance cases. The two cases of primary resonance of interest are $\Omega = \omega_1$ and $\Omega = \omega_2$. These two cases can be treated separately but in a similar manner.

4.2.3. Case of $\Omega \approx \omega_1$

In the resulting equations mentioned above, Ω is substituted as $\Omega = \omega_1 + \varepsilon\sigma_1$ where σ_1 is a detuning parameter for controlling the nearness of Ω to ω_1 and ε is a small dimensionless book-keeping parameter. We then equate the coefficients of $\exp(i\omega_n T_0)$ where $n = 1..4$, on both sides of the resulting equations.

4.2.4. Solvability Conditions

In order to obtain the solutions of these equations there are certain solvability conditions that must be satisfied. These conditions are determined according to the procedure given in Chapter 3 and are given below.

$$\begin{aligned} \frac{dA_1}{dT_1} &= c_1 A_1^2 \overline{A_1} + c_2 A_1 A_2 \overline{A_2} - c_3 A_1 A_3 \overline{A_3} - c_4 A_1 A_4 \overline{A_4} - c_5 A_1 - c_6 \exp(i\sigma_1 T_1) \\ \frac{dA_2}{dT_1} &= d_1 A_2^2 \overline{A_2} + d_2 A_2 A_1 \overline{A_1} + d_3 A_2 A_3 \overline{A_3} + d_4 A_2 A_4 \overline{A_4} - d_5 A_2 \\ \frac{dA_3}{dT_1} &= f_1 A_3^2 \overline{A_3} + f_2 A_3 A_1 \overline{A_1} + f_3 A_3 A_2 \overline{A_2} + f_4 A_3 A_4 \overline{A_4} + f_5 A_3 \\ \frac{dA_4}{dT_1} &= g_1 A_4^2 \overline{A_4} + g_2 A_4 A_1 \overline{A_1} + g_3 A_4 A_2 \overline{A_2} + g_4 A_4 A_3 \overline{A_3} + g_5 A_4 \end{aligned} \tag{4.2.10}$$

Where $c_1..c_6$, $d_1..d_5$, $f_1..f_5$ and $g_1..g_5$ are functions of geometric and material properties of the rotor and $\omega_1..\omega_4$. Their mathematical expressions are given in Appendix E.

The solutions of A_n are substituted in Eq. (4.2.10) in the polar form given by $A_n = (1/2)(a_n \exp(i\theta_n))$, where, $n = 1..4$. The resulting equations are separated into real and imaginary parts to obtain the following autonomous system of first-order partial differential equations.

$$\frac{da_1}{dT_1} - \frac{1}{4}(c_1 a_1^2 + c_2 a_2^2 - c_3 a_3^2 - c_4 a_4^2 - 4c_5)a_1 + 2c_6 \cos\Gamma = 0 \tag{4.2.11}$$

$$\left(\sigma_1 - \frac{d\Gamma}{dT_1}\right)a_1 + 2c_6 \sin\Gamma = 0 \tag{4.2.12}$$

$$\frac{da_2}{dT_1} - \frac{1}{4}(d_1 a_2^2 + d_2 a_1^2 + d_3 a_3^2 + d_4 a_4^2 - 4d_5)a_2 = 0 \tag{4.2.13}$$

$$a_2 \frac{d\theta_2}{dT_1} = 0 \tag{4.2.14}$$

$$\frac{da_3}{dT_1} - \frac{1}{4}(f_1 a_3^2 + f_2 a_1^2 + f_3 a_2^2 + f_4 a_4^2 + 4f_5)a_3 = 0 \tag{4.2.15}$$

$$a_3 \frac{d\theta_3}{dT_1} = 0 \tag{4.2.16}$$

$$\frac{da_4}{dT_1} - \frac{1}{4}(g_1 a_4^2 + g_2 a_1^2 - g_3 a_2^2 + g_4 a_3^2 + 4g_5)a_4 = 0 \tag{4.2.17}$$

$$a_4 \frac{d\theta_4}{dT_1} = 0 \tag{4.2.18}$$

$$\frac{d\Gamma}{dT_1} = \sigma_1 - \frac{d\theta_1}{dT_1} \tag{4.2.19}$$

In Eqs. (4.2.11), (4.2.12) and (4.2.19), $\Gamma = \sigma_1 T_1 - \theta_1$

At equilibrium, amplitude and phase do not change with respect to time, i.e.:

$$\frac{da_1}{dT_1} = \frac{da_2}{dT_1} = \frac{da_3}{dT_1} = \frac{da_4}{dT_1} = \frac{d\Gamma}{dT_1} = \frac{d\theta_2}{dT_1} = \frac{d\theta_3}{dT_1} = \frac{d\theta_4}{dT_1} = 0 \tag{4.2.20}$$

The autonomous system given by Eqs. (4.2.11) to (4.2.19) is now reduced to:

$$(c_1 a_1^2 + c_2 a_2^2 - c_3 a_3^2 - c_4 a_4^2 - 4c_5)a_1 + 2c_6 \cos\Gamma = 0 \tag{4.2.21}$$

$$\sigma_1 a_1 + 2c_6 \sin\Gamma = 0 \tag{4.2.22}$$

$$(d_1 a_2^2 + d_2 a_1^2 + d_3 a_3^2 + d_4 a_4^2 - 4d_5)a_2 = 0 \tag{4.2.23}$$

$$(f_1 a_3^2 + f_2 a_1^2 + f_3 a_2^2 + f_4 a_4^2 + 4f_5)a_3 = 0 \tag{4.2.24}$$

$$(g_1 a_4^2 + g_2 a_1^2 - g_3 a_2^2 + g_4 a_3^2 + 4g_5)a_4 = 0 \tag{4.2.25}$$

It can be observed from the system of Eqs. (4.2.21) to (4.2.25) that $a_2 = a_3 = a_4 = 0$ is a trivial solution. Therefore this system can be resolved to give the following 6th degree polynomial equation

$$c_1^2 a_E^6 - 8c_1 c_5 a_E^4 + 16(c_5^2 + \sigma_1^2) a_E^2 - 64 c_6^4 = 0 \tag{4.2.26}$$

The above polynomial is a function of amplitude at equilibrium a_E and the detuning parameter σ_1. Solving Eq. (4.2.26) gives six solutions that, using symbols, are complicated expressions and are not reproduced here. Therefore this polynomial is treated numerically in the next section.

4.2.5. Case of $\Omega \approx \omega_2$

This case can be treated in the same way as the previous one. The results can be obtained directly by changing ω_2 with ω_1 in equations resulting from Eqs. (4.2.6) and (4.2.7) and considering a new detuning parameter defined as $\Omega = \omega_2 + \varepsilon\sigma_1$.

The solvability conditions for this case are given as below,

$$\begin{aligned}
\frac{dA_1}{dT_1} &= c_1 A_1^2 \overline{A_1} + c_2 A_1 A_2 \overline{A_2} - c_3 A_1 A_3 \overline{A_3} - c_4 A_1 A_4 \overline{A_4} - c_5 A_1 \\
\frac{dA_2}{dT_1} &= d_1 A_2^2 \overline{A_2} + d_2 A_2 A_1 \overline{A_1} + d_3 A_2 A_3 \overline{A_3} + d_4 A_2 A_4 \overline{A_4} - d_5 A_2 - d_6 \exp(i\sigma_1 T_1) \\
\frac{dA_3}{dT_1} &= f_1 A_3^2 \overline{A_3} + f_2 A_3 A_1 \overline{A_1} + f_3 A_3 A_2 \overline{A_2} + f_4 A_3 A_4 \overline{A_4} + f_5 A_3 \\
\frac{dA_4}{dT_1} &= g_1 A_4^2 \overline{A_4} + g_2 A_4 A_1 \overline{A_1} + g_3 A_4 A_2 \overline{A_2} + g_4 A_4 A_3 \overline{A_3} + g_5 A_4
\end{aligned} \tag{4.2.27}$$

Where $c_1..c_5$, $d_1..d_6$, $f_1..f_5$ and $g_1..g_5$ are functions of geometric and material properties of the rotor and $\omega_1..\omega_4$. Their mathematical expressions are given in Appendix F.

The solutions of A_n are substituted in Eq. (4.2.27) in the polar form given by $A_n = (1/2)(a_n \exp(i\theta_n))$, where, $n = 1..4$. The resulting equations are separated into real and imaginary parts to obtain the following autonomous system of first-order partial differential equations.

$$\frac{da_1}{dT_1} - \frac{1}{4}(c_1 a_1^2 + c_2 a_2^2 - c_3 a_3^2 - c_4 a_4^2 - 4c_5) a_1 = 0 \tag{4.2.28}$$

$$\left(\sigma_1 - \frac{d\Gamma}{dT_1}\right) a_1 = 0 \tag{4.2.29}$$

$$\frac{da_2}{dT_1} - \frac{1}{4}(d_1 a_2^2 + d_2 a_1^2 + d_3 a_3^2 + d_4 a_4^2 - 4d_5) a_2 + d_6 \cos\Gamma = 0 \tag{4.2.30}$$

$$a_2 \frac{d\theta_2}{dT_1} + 2d_6 \sin\Gamma = 0 \tag{4.2.31}$$

$$\frac{da_3}{dT_1} - \frac{1}{4}(f_1 a_3^2 + f_2 a_1^2 + f_3 a_2^2 + f_4 a_4^2 + 4f_5) a_3 = 0 \tag{4.2.32}$$

$$a_3 \frac{d\theta_3}{dT_1} = 0 \tag{4.2.33}$$

$$\frac{da_4}{dT_1} - \frac{1}{4}(g_1 a_4^2 + g_2 a_1^2 - g_3 a_2^2 + g_4 a_3^2 + 4g_5) a_4 = 0 \tag{4.2.34}$$

$$a_4 \frac{d\theta_4}{dT_1} = 0 \tag{4.2.35}$$

$$\frac{d\Gamma}{dT_1} = \sigma_1 - \frac{d\theta_2}{dT_1} \tag{4.2.36}$$

In Eqs. (4.2.29), (4.2.30) , (4.2.31) and (4.2.36) $\Gamma = \sigma_1 T_1 - \theta_2$.

At equilibrium, the amplitude and phase do not change with respect to time, i.e.:

$$\frac{da_1}{dT_1} = \frac{da_2}{dT_1} = \frac{da_3}{dT_1} = \frac{da_4}{dT_1} = \frac{d\Gamma}{dT_1} = \frac{d\theta_2}{dT_1} = \frac{d\theta_3}{dT_1} = \frac{d\theta_4}{dT_1} = 0 \tag{4.2.37}$$

Autonomous system given by Eqs. (4.2.28) to (4.2.36) is now reduced to:

$$(c_1 a_1^2 + c_2 a_2^2 - c_3 a_3^2 - c_4 a_4^2 - 4c_5) a_1 = 0 \tag{4.2.38}$$

$$\sigma_1 a_1 = 0 \tag{4.2.39}$$

$$(d_1 a_2^2 + d_2 a_1^2 + d_3 a_3^2 + d_4 a_4^2 - 4d_5) a_2 + 4d_6 \cos\Gamma = 0 \tag{4.2.40}$$

$$(f_1 a_3^2 + f_2 a_1^2 + f_3 a_2^2 + f_4 a_4^2 + 4f_5) a_3 = 0 \tag{4.2.41}$$

$$(g_1 a_4^2 + g_2 a_1^2 - g_3 a_2^2 + g_4 a_3^2 + 4g_5) a_4 = 0 \tag{4.2.42}$$

It can be observed from the system of Eqs. (4.2.38) to (4.2.42) that $a_1 = a_3 = a_4 = 0$ is a trivial solution. Therefore this system can be resolved to give the following 6th degree polynomial equation

$$d_1^2 a_E^6 - 8d_1 d_5 a_E^4 + 16(d_5^2 + \sigma_1^2) a_E^2 - 64 d_6^4 = 0 \tag{4.2.43}$$

Like the polynomial of Eq. (4.2.26), the above polynomial is also a function of amplitude at equilibrium a_E and the detuning parameter σ_1. Solving Eq. (4.2.43) gives six solutions that, using symbols, are complicated expressions and are not reproduced here. Therefore this polynomial is also treated numerically in the next section.

4.3. Numerical Application and Discussion of Results

The nonlinear response of the rotor system under study was examined using three different approaches, i.e. the method of multiple scales, a continuation procedure and a step-by-step integration method in which equations of motion are treated directly. All the numerical data are given in Appendix B.

4.3.1. Resonant curves

Method of Multiple Scales

For studying the nonlinear dynamic response, a shaft-disk rotor system has been considered whose numerical data are given in Appendix B. In Fig. 48 the numerical solutions for the two resonant conditions $\Omega \approx \omega_1$ and $\Omega \approx \omega_2$ are presented showing resonant curves. The effect of nonlinearity has caused these curves to bend rightwards from the position of the linear response. Therefore, these curves are of the hard spring type.

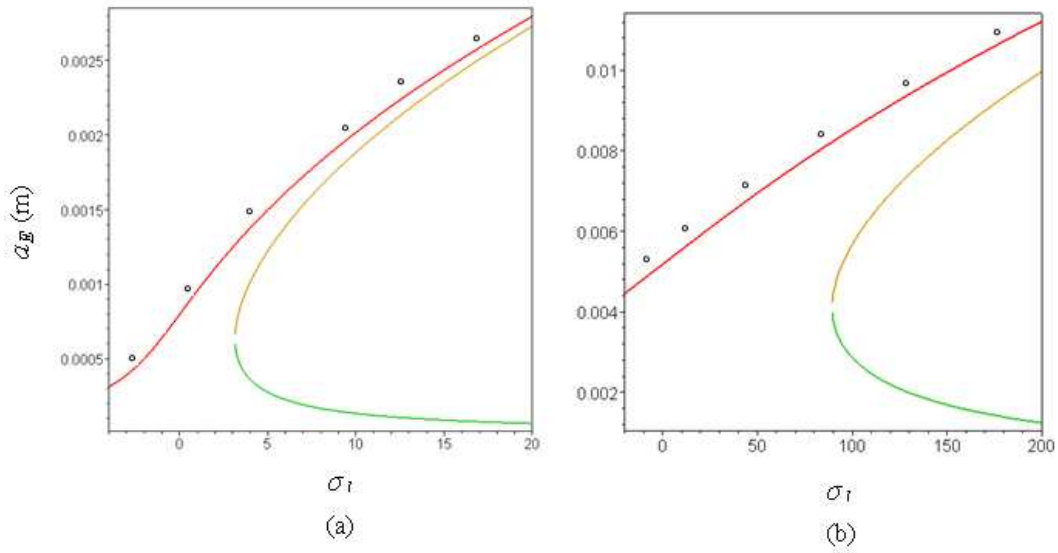

Fig. 48. Resonance curves for nonlinear dynamic response of a shaft-disk rotor system (a) $\Omega \approx \omega_1$ (b) $\Omega \approx \omega_2$

Continuation Procedure (Matcont)

A continuation procedure in Matlab called Matcont was applied. This method is capable of treating the first order differential equations given by Eqs. (4.2.11) to (4.2.19). The bifurcation diagrams and state planes are presented in Fig. 49 and Fig. 50. For a given value of the detuning parameter there are three solutions in the positive plane. Out of these solutions, two are stable and one is unstable. The continuation procedure is capable of tracing two stable solutions which can be seen corresponding to points A and B in the curves in Fig. 49 (a) and Fig. 50 (a), where LP is the limit point of the bifurcation. The curve of the unstable solution lies somewhere between these two curves. The results of this procedure match with those obtained by MMS but the latter is preferable as it can plot the unstable solutions as well.

The state planes are plotted for two different points, A and B, on the resonant curves given in Fig. 49 (a) and Fig. 50 (a). It can be observed that the amplitude at point A is much lower than that of point B. As compared to point A, the orbit corresponding to point B is more oval, i.e. the effect of nonlinearity is more visible at this point.

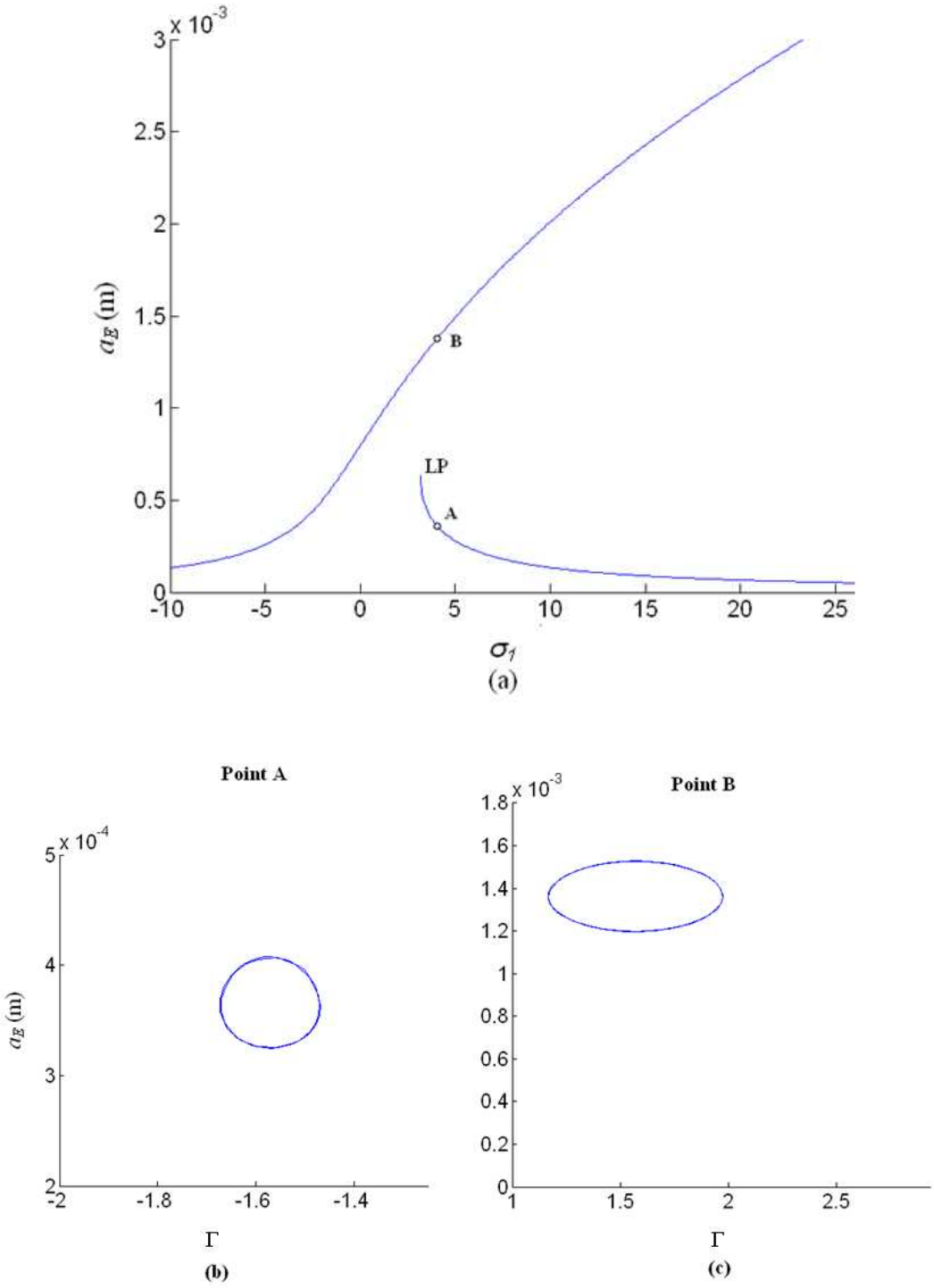

Fig. 49. Results obtained by continuation procedure using Matcont at $\sigma_1 = 4$ for $\Omega \approx \omega_1$
(a) Resonance Curves (b) State Plane at point A (c) State Plane at point B

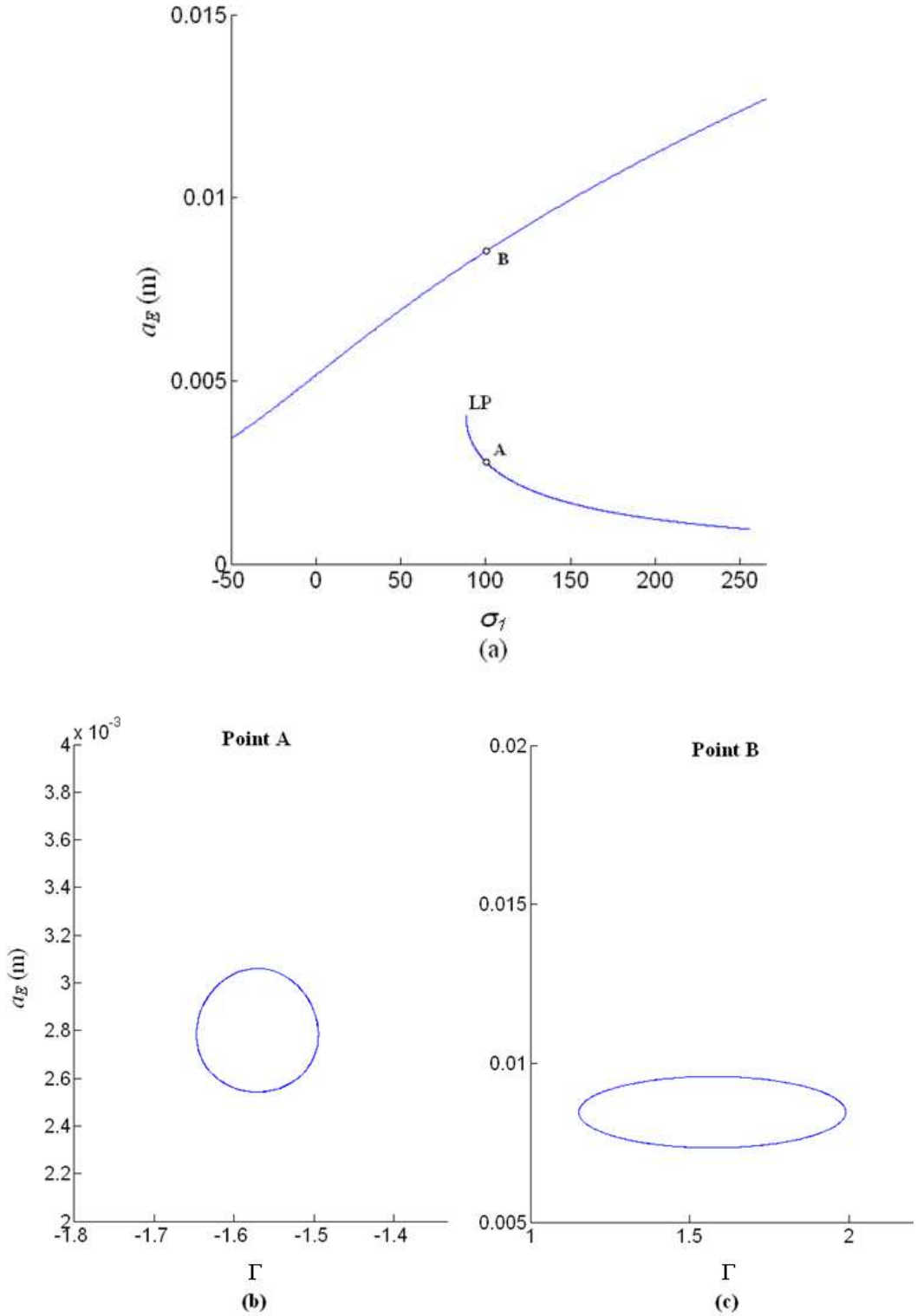

Fig. 50. Results obtained by continuation procedure using Matcont at $\sigma_1 = 100$ for $\Omega \approx \omega_2$
(a) Resonance Curves (b) State Plane at point A (c) State Plane at point B

Direct Integration using the Step-by-Step Method (Matlab)

In order to further validate the nonlinear findings achieved by previous two methods, a step-by-step analysis was conducted using the Simulink toolbox of Matlab. In this method, the equations of motion given by Eqs. (2.4.34) and (2.3.45) were solved directly. The results were compared with those obtained by MMS and are presented as dots in Fig. 48.

4.3.2. Effect of Slenderness Ratio

The slenderness ratio is varied from 0.02 to 0.08 and the effect of this variation is presented in Fig. 51. It can be observed that as the slenderness ratio is decreased, the response curves bend strongly towards the right and expand more horizontally. This indicates that for higher values of slenderness ratio the nonlinear spring hardening effect appears even at smaller values of detuning parameter σ_1 which is directly proportional to the speed of rotation of the rotor system. This trend is similar for both resonance cases except the fact that the response amplitude and horizontal range of the detuning parameter is much higher when $\Omega = \omega_2$.

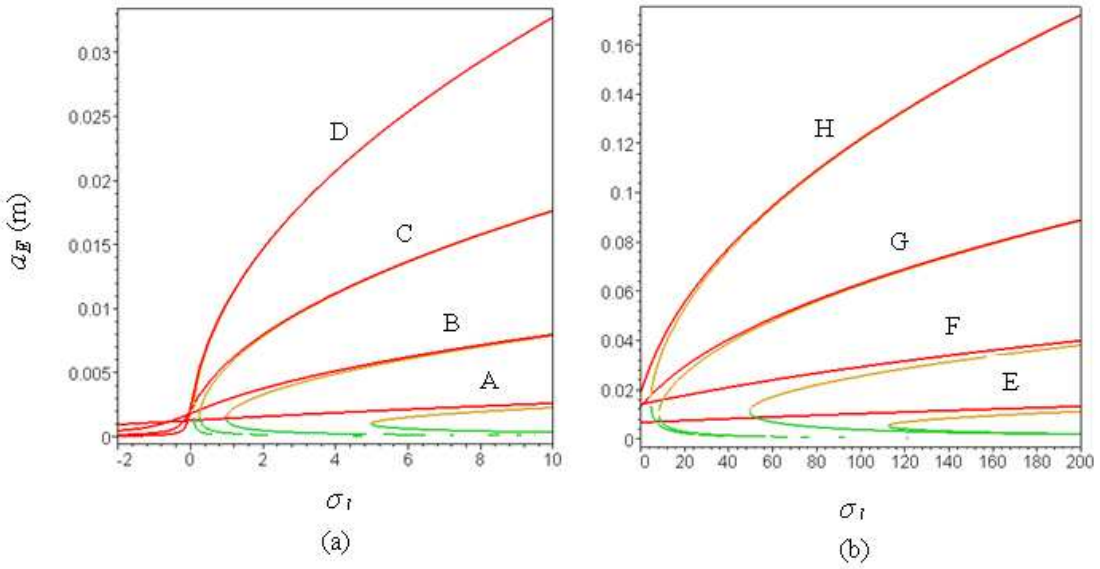

Plot	A , E	B , F	C , G	D , H
r	0.02	0.04	0.06	0.08

Fig. 51. Effect of slenderness ratio (r) on the nonlinear dynamic response of a shaft-disk rotor system (a) $\Omega \approx \omega_1$ (b) $\Omega \approx \omega_2$

4.3.3. Effect of Varying the Unbalance Mass

Fig. 52 represents the effect of varying the mass unbalance from 1x 10^{-5} kg to 100 x 10^{-5} kg. Different resonant curves plotted on the same scale show that as the mass unbalance is increased, the horizontal component of these curves expands more to cover a greater range of the detuning parameter σ_1. Also the amplitude of the response is higher for higher values of unbalance mass.

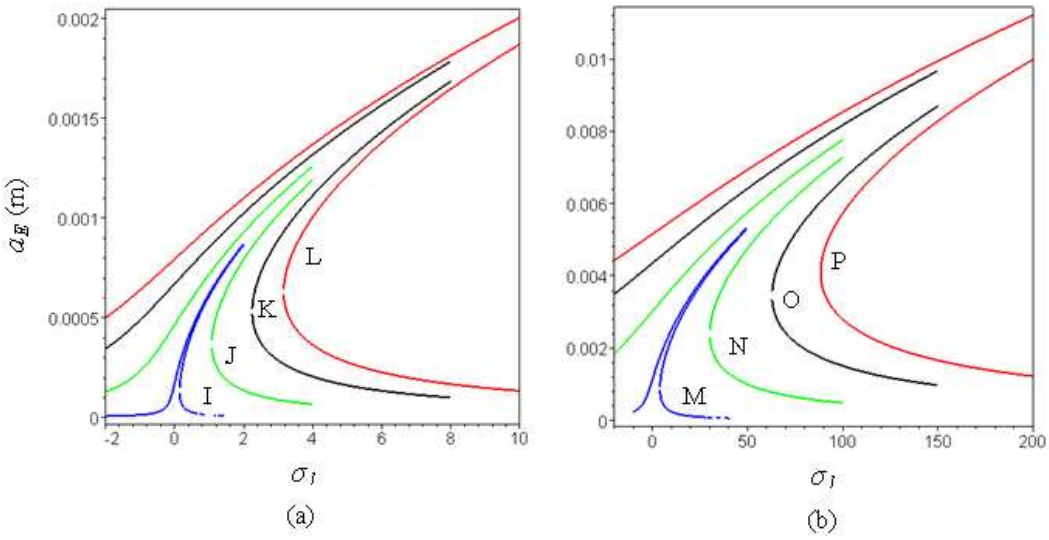

Plot	I , M	J , N	K , O	L , P
m_u (kg)	1 x 10^{-5}	20 x 10^{-5}	60 x 10^{-5}	100 x 10^{-5}

Fig. 52. Effect of mass unbalance (m_u) on nonlinear dynamic response of a shaft-disk rotor system: (a) $\Omega \approx \omega_1$ (b) $\Omega \approx \omega_2$

4.3.4. Effect of Shear Deformations

Fig. 53 and Fig. 54, present the response curves for three different slenderness ratios at $\Omega \approx \omega_1$ and $\Omega \approx \omega_2$ respectively. The results were obtained for the nonlinear response of the rotor system with and without considering the shear effects. It is concluded that the shear effects on the nonlinear response are not very significant for lower values of the slenderness ratio. But, for their higher values the response curves without shear effects tend to bend more strongly towards the right. This can be clearly observed by comparing curves P3 and Q3 in Fig. 53 and curves R3 and S3 in Fig. 54. There is not a notable difference in the response amplitude with and without shear effects with the 1st resonance. But a difference of amplitude can be observed for the 2nd resonance.

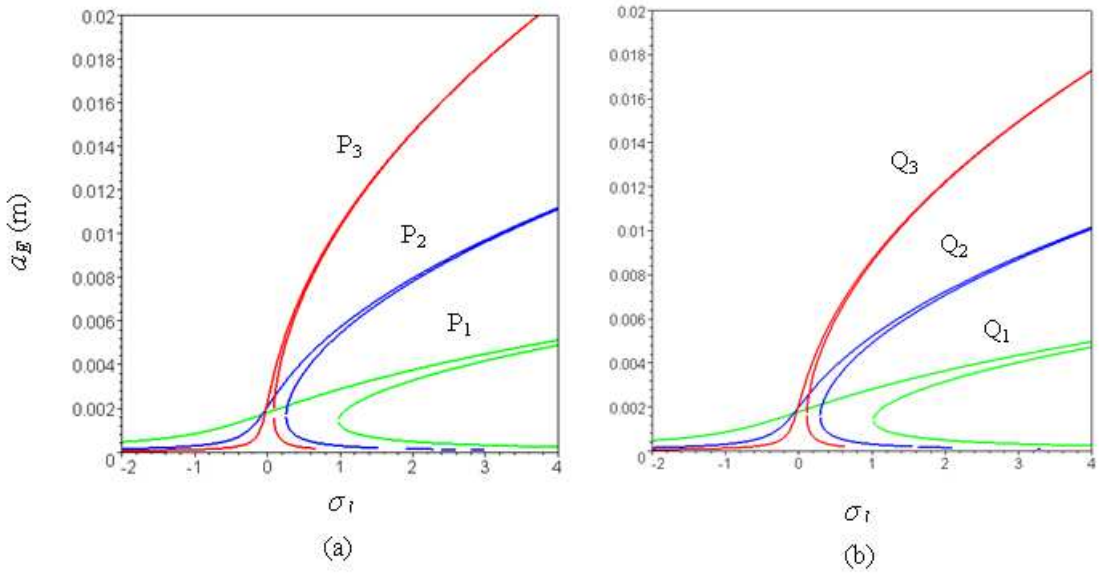

Plot	P_1 , Q_1	P_2 , Q_2	P_3 , Q_3
r	0.04	0.06	0.08

Fig. 53. Effect of shear deformations on the nonlinear dynamic response of a shaft-disk rotor system at $\Omega \approx \omega_1$: (a) with shear (b) without shear

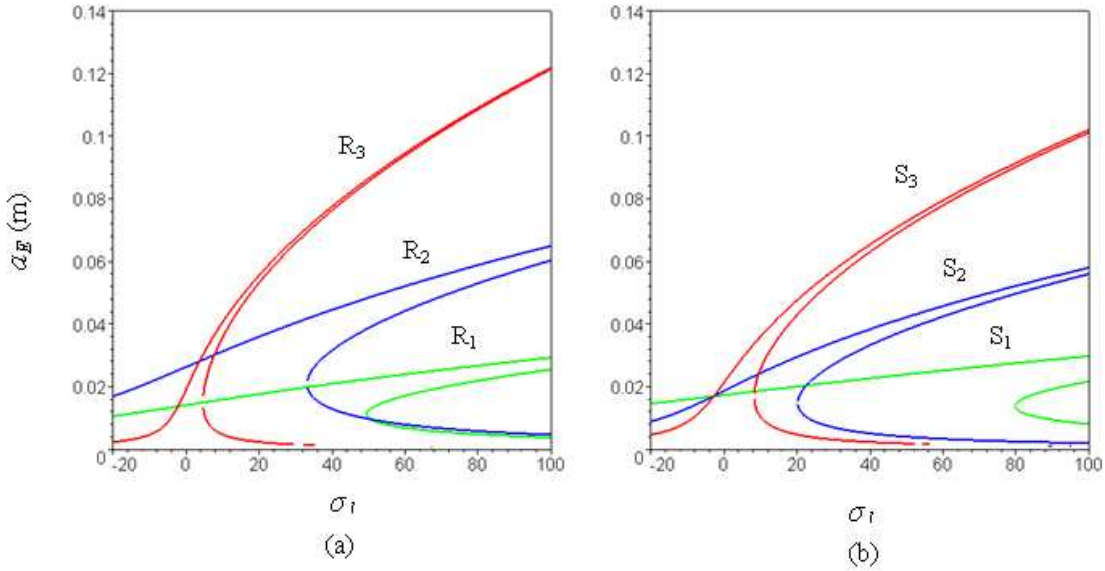

Plot	R_1 , S_1	R_2 , S_2	R_3 , S_3
r	0.04	0.06	0.08

Fig. 54. Effect of shear deformations on the nonlinear dynamic response of a shaft-disk rotor system at $\Omega \approx \omega_2$: (a) with shear (b) without shear

4.4. Conclusions

This chapter focused on the combined effect of nonlinearities and shear effects on the linear and nonlinear dynamic behavior of the rotors. The mathematical model which was treated in this chapter consisted of 4^{th} order nonlinear differential equations of motion. The method of multiple scales was applied to the 4^{th} order of derivatives with respect to time. The effects of shear were discussed in detail both on the linear as well as nonlinear response of the rotor system under study.

The results of the linear analysis for a rotating shaft and a shaft-disk rotor system, both for solid and tube section, showed that with the inclusion of shear deformations the critical speeds of the rotor tend to decrease. This difference becomes more visible for higher values of the slenderness ratio r. As compared to a shaft-disk rotor system the shear effects have more notable influence in the case of a solid and tube sections of the shaft.

In the nonlinear analysis, the resonant response curves are plotted. These curves are of hard spring type. The response amplitude and horizontal plotting range of the detuning parameter is higher in case of the resonance condition corresponding to 2^{nd} critical speed of the rotor. The overall dynamic behavior of the rotors can be greatly varied with the variations in the slenderness ratio and the unbalance mass. The effects of shear deformations are more significant for higher values of the slenderness ratio. As an overall concluding remark, the higher order and shear deformations have a significant effect on the dynamic behavior of the rotor systems. Therefore, for an accurate analysis ensuring improved safety and efficiency of the rotor systems, these deformations cannot be ignored.

Chapter 5: Overall Conclusions and Future Perspectives

This chapter discusses the overall conclusions of the thesis. Also, based on the work performed for this thesis, there are future perspectives, which are also mentioned in detail. A description of the work already carried out is given which can be extended in future. The main perspectives include the study of nonlinear dynamic behavior of the rotors under some base movements. i.e. the supports of the rotor are not fixed but can be subjected to different movements like simple translation, a constant acceleration, sinusoidal translatory motion, simple rotation and sinusoidal rotation.

5.1. Conclusions

This thesis presents a detailed development of various mathematical models and their analysis for studying the nonlinear dynamic behavior of rotors. First a state of the art for the dynamic analysis of the rotors has been discussed and a brief introduction of various important aspects of rotordynamics is given. From the state of the art it is concluded that the study of the dynamic behavior of rotors has been a subject of practical importance for many years. A lot of work has been carried out in predicting the dynamics of metallic as well as composite rotors. But this is still an ongoing research especially when nonlinear effects are included to be investigated which being the main objective of the present thesis works.

Then a detailed mathematical modelling is presented for analyzing the dynamic behavior of rotors. Various models containing nonlinear differential equations of motion have been developed for different rotor configurations. These models consist of 2^{nd} and 4^{th} order nonlinear differential equations of motion. Different models and hence different equations of motions have been developed taking into account the various significant effects like higher order large deformations, geometric nonlinearity, shear effects, gyroscopic and rotary inertia effects. The models are developed using both the Euler Bernoulli and Timoshenko beam theories. Rayleigh-Ritz method and Hamilton's principle have been used in order to obtain the equations of motion. When shear deformations are taken into account the developed equations of motion consist of 4^{th} order derivatives with respect to time. A case study for the dynamic analysis of the composite rotors has been conducted and the results obtained are compared to the works already available in the literature. The results obtained for the dynamic analysis of composite rotors in this study are in close agreement with those previously reported in the literature.

Some of the equations of motion developed in the modeling section have been investigated to study the nonlinear dynamic behavior of the rotors. Firstly, the nonlinear behavior of rotor dynamics due to large deformations and a dynamic axial force was analysed for the first mode using MMS. The numerical investigations have been conducted using three methods, i.e. the method of multiple scales, a continuation procedure (Matcont) and a step by step analysis in Matlab Simulink. It is concluded that the method of multiple scales is more efficient than the other two methods as all the stable and unstable solutions can be seen in the resonant curves. The results show that nonlinearities along with other phenomena like gyroscopic, rotary inertia and mass unbalance effects significantly influence the dynamics of the rotor system. The linear analysis showed that resonance existed only at the second critical speed, but in the nonlinear analysis another resonance appeared at the first critical speed. Furthermore, nonlinearities caused the resonance curves to be of hard spring type. In

the absence of dynamic axial force and at lower values of mass unbalance, the spring hardening effect was visible even at lower values of detuning parameter σ_1. Using the method of analysis presented here facilitated studying the changes caused by modifying different rotor system parameters, by changing the numerical values of the latter.

The combined effect of nonlinearities and shear effects on the linear and nonlinear dynamic behavior of the rotors has been also studied. The mathematical model which was treated in for this case consisted of 4^{th} order nonlinear differential equations of motion. The method of multiple scales was applied to the 4^{th} order of derivatives with respect to time. The effects of shear were discussed in detail both on the linear as well as nonlinear response of the rotor system under study. The results of the linear analysis for a rotating shaft and a shaft-disk rotor system, both for solid and tube section, showed that with the inclusion of shear deformations the critical speeds of the rotor tend to decrease. This difference becomes more visible for higher values of the slenderness ratio r. As compared to a shaft-disk rotor system the shear effects have more notable influence in the case of a solid and tube sections of the shaft.

In the nonlinear analysis, the resonant response curves were plotted. These curves are of hard spring type. The response amplitude and horizontal plotting range of the detuning parameter is higher in case of the resonance condition corresponding to 2^{nd} critical speed of the rotor. The overall dynamic behavior of the rotors can be greatly varied with the variations in the slenderness ratio and the unbalance mass. The effects of shear deformations are more significant for higher values of the slenderness ratio. As an overall concluding remark, the higher order and shear deformations have a significant effect on the dynamic behavior of the rotor systems. Therefore, for an accurate analysis ensuring improved safety and efficiency of the rotor systems, these deformations cannot be ignored.

5.2. Future Perspectives

This chapter discusses the future scopes of this thesis work. This includes:

The investigations of nonlinear effects discussed in the present work on the dynamic behavior of Onboard Rotors, i.e. the rotors subjected to some base movements.

Another important future perspective is the experimental validation of the analytical and numerical results obtained in the present PhD work. The development of the experimental setup is in progress.

Rotors Subjected to Base Movements

The dynamics of a rotor under some movements of the supports both in translation and in rotation can introduce new interesting phenomenon to be investigated. The displacement of the supports can be divided into two major categories: the seismic excitations and onboard excitations. The example of the latter is a case where the rotor is mounted in a vehicle which is in motion. Rotor vibrations caused by large time-varying base motion are of considerable importance as there are a good number of rotors, e.g., the ship and aircraft turbine rotors, which are often subject to excitations, as the rotor base, i.e. the vehicle, undergoes large time varying linear and angular displacements as a result of different manoeuvres. Due to such motions of the base, the equations of vibratory motion of a flexible rotor–shaft relative to the base (which forms a non-inertial reference frame) contains terms due to Coriolis effect as well as inertial excitations (generally asynchronous to rotor spin) generated by different system parameters. Such equations of motion are linear but can be time-varying in nature, invoking the possibility of parametric instability under certain frequency–amplitude combinations of the base motion.

The study of dynamic behavior of rotors has been a topic of ongoing research in recent years. Duchemin *et al*. [DBF06] investigated the dynamic behavior of flexible rotor systems subjected to base excitation (support movements) both theoretically and experimentally. Their study was focused on the behavior in bending near the critical speeds of rotation. A mathematical model was developed to calculate the kinetic energy and the strain energy. The equations of motion were derived using Lagrange equations and the Rayleigh-Ritz method was used to study the basic phenomena on simple systems. Also, the method of multiple scales was applied to study stability when the system mounting was subjected to a sinusoidal rotation. An experimental setup was used to validate the presented results.

Driot *et al*. [DLB06] studied the dynamic behavior of a flexible rotor system subjected to support excitation (imposed displacements of its base). The effect of an excitation on lateral displacements was investigated from theoretical and experimental points of view. The study focused on behavior in bending. A mathematical model with two gyroscopic and parametrical coupled equations was derived using the Rayleigh-Ritz method. The theoretical study was based on both the multiple scales method and the normal form approach. An experimental setup was then developed to observe the dynamic behavior permitting the measurement of lateral displacements when the system's support was subjected to a sinusoidal rotation.

In another study Driot *et al*. [DLB07] investigated the dynamical behavior of an asymmetrical rotor subjected to a base translational motion. The amplitude of the parametric excitation was modeled as a random parameter in order to investigate the robustness of the dynamics. The forced steady state

response was considered. The original Taguchi's method was used to provide statistical moments of the forced response.

Das *et al*. in a very recent study [DDR10] investigated active vibration control of an unbalanced rotor–shaft system on moving bases with electromagnetic control force provided by an actuator consisting of four electromagnetic exciters, placed on the stator in a suitable plane around the rotor–shaft. The equations of motion of the rotor–shaft continuum were first written with respect to the non-inertial reference frame (the moving base in this case) including the effect of rotor internal damping. A conventional model for the electromagnetic exciter was used. Numerical simulations performed on the flexible rotor–shaft modelled using beam finite elements showed that the control action was successful in avoiding the parametric instability, postponing the instability due to internal material damping and reducing the rotor response relative to the rigid base significantly, with sufficiently low demand of control current in comparison with the bias current in the actuator coils.

In all the works reported above the bending of the shaft was assumed linear and the terms due to higher order large bending deformations were not taken into account. If these terms are also considered, the resulting equations of motion, when investigated, can give rise to new interesting phenomenon in the dynamic analysis of such rotors. This study is included in the future perspectives of this thesis. Based on the works of the present thesis and the work performed by Duchemin *et al*. [DBF06], some advancements are already made particularly in developing a mathematical model which includes the combined effect of nonlinear large deformations and the base movements on the dynamic analysis of rotors.

The kinetic energies of the disk, the shaft and the mass unbalance are same as developed by Duchemin *et al*. [DBF06]. These energy equations are reproduced for reference. The inclusion of the nonlinearities due to higher order large bending deformations affects the deformation energy of the shaft. The derivation of this new deformation energy and based on this, the development of a new mathematical model is presented in the following paragraphs.

The geometry of the rotor is shown in Fig. 55 [DBF06].

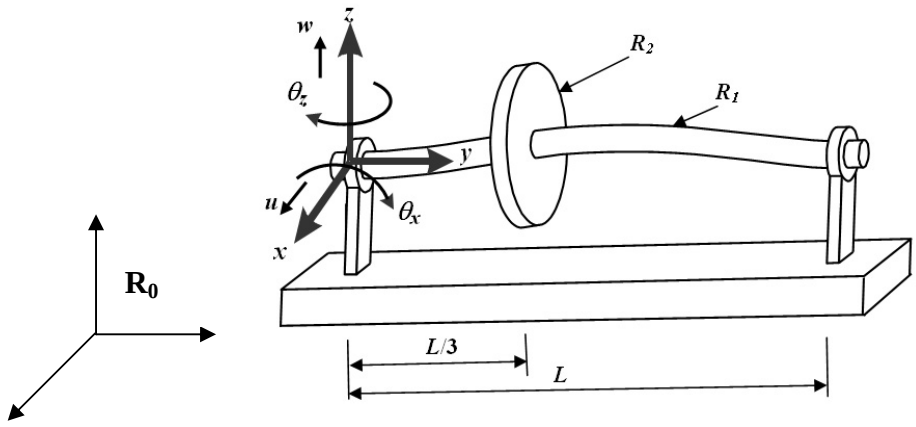

Fig. 55. Geometry of the Rotor

The kinetic energies of the disk, shaft and mass unbalance are given in Appendix G.

Strain Energy of the Shaft

The strain energy of the shaft is not affected by the movements of the supports of the rotor. But it is affected by the nonlinearity due to higher order large deformations in bending. The derivation of the following strain energy of the shaft is similar to as given in section 2.4.2 of chapter 2.

$$U = \int_0^L \frac{EI}{2}\left[\left(\frac{\partial \theta}{\partial y}\right)^2 + \left(\frac{\partial \psi}{\partial y}\right)^2\right] dy + \int_0^L \frac{EA}{2}\left[\frac{1}{4}\theta^4 + \frac{1}{4}\psi^4 + \frac{1}{2}\theta^2\psi^2\right] dy \tag{5.1.1}$$

The above equations can be compared to Eq.(2.4.12), where θ_x and θ_z are replaced with θ and ψ respectively.

Application of Rayleigh-Ritz Method

The method of Rayleigh-Ritz allows to express the displacements $u\,(y,t)$ and w (y,t) along the directions x and z to be expressed as follows,

$$\begin{aligned} u(y,t) &= f(y)\; q_1(t) = f(y)q_1 \\ w(y,t) &= f(y)\; q_2(t) = f(y)q_2 \end{aligned} \tag{5.1.2}$$

Where, f(y) is the modal deformation and q_1, q_2 are generalized independent coordinates.The angles θ and ψ are approximated as,

$$\begin{aligned} \theta &= \frac{\partial w}{\partial y} = \frac{d\,f(y)}{d\,y} q_2 = g(y)q_2 \\ \Psi &= -\frac{\partial u}{\partial y} = -\frac{d\,f(y)}{d\,y} q_1 = -g(y)q_1 \end{aligned} \tag{5.1.3}$$

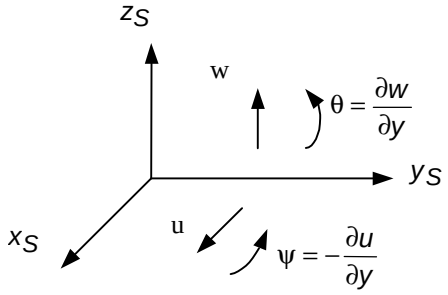

Fig. 56. Degrees of Freedom of a Beam

The 2nd derivatives of u and w are:

$$\begin{aligned} \frac{\partial^2 u}{\partial^2 y} &= \frac{d^2 f(y)}{dy^2} q_1 = h(y)q_1 \\ \frac{\partial^2 w}{\partial^2 y} &= \frac{d^2 f(y)}{dy^2} q_2 = h(y)q_2 \end{aligned} \tag{5.1.4}$$

The function f (y) is chosen as the displacement function for a pinned-pinned beam in bending.

$$f(y) = \sin\left(\frac{n\pi\, y}{\mathrm{L}}\right) \tag{5.1.5}$$

Where, n is the no. of the mode studied.

Using the Rayleigh-Ritz method, the kinetic energy of the rotor which is the sum of the kinetic energies of the disk, shaft and the mass unbalance can be given as,

$$\begin{aligned}
T &= T_D + T_a + T_u \\
&= \frac{M_T}{2}\left(\dot{X} + \beta_S Z - \gamma_S Y\right)^2 + \left(\dot{Y} + \gamma_S X - \alpha_S Z\right)^2 + \left(\dot{Z} + \alpha_S Y - \beta_S X\right)^2 \\
&+ M_3\left(-\gamma_S\left(\dot{X} + \beta_S Z - \gamma_S Y\right) + \alpha_S\left(\dot{Z} + \alpha_S Y - \beta_S X\right)\right) + \frac{M_4}{2}\left(\alpha_S{}^2 + \gamma_S{}^2\right) \\
&+ M_1\left(\left(\dot{X} + \beta_S Z - \gamma_S Y\right)\left(\dot{q}_1 + \beta_S q_2\right) + \left(\dot{Y} + \gamma_S X - \alpha_S Z\right)\left(\gamma_S q_1 - \alpha_S q_2\right) + \left(\dot{Z} + \alpha_S Y - \beta_S X\right)\left(\dot{q}_2 - \beta_S q_1\right)\right) \\
&+ \frac{M_2}{2}\left(\left(\dot{q}_1 + \beta_S q_2\right)^2 + \left(\gamma_S q_1 - \alpha_S q_2\right)^2 + \left(\dot{q}_2 - \beta_S q_1\right)^2\right) + M_5\left(-\gamma_S\left(\dot{q}_1 + \beta_S q_2\right) + \gamma_S\left(\dot{q}_2 - \beta_S q_1\right)\right) \\
&+ \frac{I_{mT}}{2}\left(\alpha_S{}^2 + \gamma_S{}^2\right) + I_{m1}\left(-\beta_S\left(\alpha_S q_1 + \gamma_S q_2\right) - \gamma_S \dot{q}_1 + \alpha_S \dot{q}_2\right) \\
&+ \frac{I_{m2}}{2}\left(\beta_S{}^2\left(q_1^2 + q_2^2\right) - \alpha_S{}^2 q_1^2 - \gamma_S{}^2 q_2^2 + \dot{q}_1^2 + \dot{q}_2^2 + 2\beta_S\left(\dot{q}_1 q_2 - q_1 \dot{q}_2\right) - 2\alpha_S \gamma_S q_1 q_2\right) \\
&+ \frac{I_{yT}}{2}\left(\beta_S + \Omega\right)^2 + I_{y1}\left(\beta_S + \Omega\right)\left(\gamma_S q_2 + \alpha_S q_1\right) + \frac{I_{y2}}{2}\left(\left(\gamma_S q_2 + \alpha_S q_1\right)^2 - 2\left(\beta_S + \Omega\right)\left(\dot{q}_1 q_2 + \frac{\beta_S}{2}\left(q_1^2 + q_2^2\right)\right)\right) \\
&+ \frac{I_{aT}}{2}\left(\left(\alpha_S^2 - \gamma_S^2\right)\cos 2\Omega t - 2\alpha_S \gamma_S \sin 2\Omega t\right) \\
&+ I_{a1}\left(\beta_S\left(\gamma_S q_2 - \alpha_S q_1\right) + \gamma_S \dot{q}_1 + \alpha_S \dot{q}_2\right)\cos 2\Omega t + \left(\beta_S\left(\gamma_S q_1 + \alpha_S q_2\right) + \alpha_S \dot{q}_1 - \gamma_S \dot{q}_2\right)\sin 2\Omega t \\
&+ \frac{I_{a2}}{2}\left(\beta_S{}^2\left(q_1^2 - q_2^2\right) - \alpha_S{}^2 q_1^2 + \gamma_S{}^2 q_2^2 - \dot{q}_1^2 + \dot{q}_2^2 - 2\beta_S\left(q_1 \dot{q}_2 + \dot{q}_1 q_2\right) + 2\alpha_S \gamma_S q_1 q_2\right)\cos 2\Omega t \\
&+ 2\left(\left(\alpha_S^2 - \beta_S^2\right) q_1 q_2 + \frac{\alpha_S \gamma_S}{2}\left(q_1^2 + q_2^2\right) + \beta_S\left(\dot{q}_2 q_2 - q_1 \dot{q}_1\right) + \dot{q}_1 \dot{q}_2\right)\sin 2\Omega t \\
&+ \frac{1}{2} m_u d^2\left(\Omega + \beta_S\right)^2 + \left(\gamma_S \sin\Omega t - \alpha_S \cos\Omega t\right)^2 \\
&+ m_u d\left(\dot{X} + f(l_1)\dot{q}_1 + \beta_S\left(Z + f(l_1) q_2\right) - \gamma_S\left(Y + l_1\right)\right)\left(\Omega + \beta_S\right)\cos\Omega t \\
&+ \left(\dot{Y} + \gamma_S\left(X + f(l_1) q_1\right) - \alpha_S\left(Z + f(l_1) q_2\right)\right)\left(\gamma_S \sin\Omega t - \alpha_S \cos\Omega t\right) \\
&- \left(\dot{Z} + f(l_1)\dot{q}_2 + \alpha_S\left(Y + l_1\right) - \beta_S\left(X + f(l_1) q_1\right)\right)\left(\Omega + \beta_S\right)\sin\Omega t
\end{aligned} \tag{5.1.6}$$

Applying Rayleigh-Ritz method to Eq. (5.1.1), the deformation energy of the rotor for a symmetric shaft can be given as,

$$U = \frac{k_1}{2}\left(q_1^2 + q_2^2\right) + \frac{k_2}{8}\left(q_1^4 + q_2^4 + 2q_1^2 q_2^2\right) \tag{5.1.7}$$

Where,

$$k_1 = EI\int_0^L h^2(y)dy \quad ; \quad k_2 = EA\int_0^L g^4(y)dy \tag{5.1.8}$$

Application of Lagrange Equations

After application of Lagrange equations to Eqs. (5.1.6) and (5.1.7), the following system of two equations of motion is obtained,

$$\begin{aligned} &[M]\begin{Bmatrix}\ddot{q}_1\\ \ddot{q}_2\end{Bmatrix} + \left([C] + [C^*]\right)\begin{Bmatrix}\dot{q}_1\\ \dot{q}_2\end{Bmatrix} + \left([K_1] + [K^*]\right)\begin{Bmatrix}q_1\\ q_2\end{Bmatrix} + \frac{1}{2}[K_2]\begin{Bmatrix}q_1^3\\ q_2^3\end{Bmatrix} + \\ &\frac{1}{2}[K_2]\begin{bmatrix}q_1 q_2^2\\ q_2 q_1^2\end{bmatrix} = \{F\} + \{F^*\} \end{aligned} \tag{5.1.9}$$

Where, the matrices [M], [C], et $[K_1]$ are the classical matrices obtained in the case of a linear rotor with fixed supports.

$$[M] = \begin{bmatrix} M_2 + I_{m2} & 0 \\ 0 & M_2 + I_{m2} \end{bmatrix} \tag{5.1.10}$$

$$[C] = \begin{bmatrix} 0 & \Omega I_{y2} \\ -\Omega I_{y2} & 0 \end{bmatrix} \tag{5.1.11}$$

$$[K_1] = \begin{bmatrix} k_1 & 0 \\ 0 & k_1 \end{bmatrix} \tag{5.1.12}$$

The vector {F} is the contribution of the mass unbalance for a rotor with fixed supports.

$$\{F\} = \begin{Bmatrix} m_u d\, f(l_1)\Omega^2 \sin\Omega t \\ m_u d\, f(l_1)\Omega^2 \cos\Omega t \end{Bmatrix} \tag{5.1.13}$$

The vector $\{F^*\}$ represents the supplementary terms due to the movement of the supports of the rotor.

$$\{F^*\} = \begin{Bmatrix} f_1 \\ f_2 \end{Bmatrix} \tag{5.1.14}$$

Where,

$$
\begin{aligned}
f_1 = m_u\, d\, f(l_1)\, \{ & -(\ddot{\beta}_S + \alpha_S\, \ddot{\gamma}_S)\cos\Omega t + (\beta_S^{\,2} + 2\Omega\dot{\beta}_S + \gamma_S^{\,2})\sin\Omega t \} \\
& + (M_5 + I_{m1})\,(\ddot{\alpha}_S - \alpha_S\,\beta_S) + I_{y1}\,\alpha_S\,(\Omega + \dot{\beta}_S) \\
& + M_1\,\{ \gamma_S\,(2\dot{Y} + \gamma_S\, X - \alpha_S\, Z) - \beta_S\,(2\dot{Z} + \alpha_S\, Y - \beta_S\, X) - \ddot{X} - \dot{\beta}_S\, Z + \dot{\alpha}_S\, Y \}
\end{aligned} \tag{5.1.15}
$$

$$
\begin{aligned}
f_2 = m_u\, d\, f(l_1)\, \{ & -(\ddot{\beta}_S - \alpha_S\, \ddot{\gamma}_S)\sin\Omega t + (\beta_S^{\,2} + 2\Omega\dot{\beta}_S + \alpha_S^{\,2})\cos\Omega t \} \\
& - (M_5 + I_{m1})\,(\ddot{\alpha}_S + \gamma_S\,\beta_S) + I_{y1}\,\gamma_S\,(\Omega + \dot{\beta}_S) \\
& + M_1\,\{ -\alpha_S\,(2\dot{Y} + \gamma_S\, X - \alpha_S\, Z) + \beta_S\,(2\dot{X} + \beta_S\, Z - \gamma_S\, Y) - \ddot{Z} + \dot{\beta}_S\, X - \dot{\alpha}_S\, Y \}
\end{aligned} \tag{5.1.16}
$$

The matrices $[C^*]$ and $[K^*]$ are due the movement of the assembly of the rotor.

$$
[C^*] = \begin{bmatrix} 0 & \beta_S\,(2M_2 + 2I_{m2} - I_{y2}) \\ -\beta_S\,(2M_2 + 2I_{m2} - I_{y2}) & 0 \end{bmatrix} \tag{5.1.17}
$$

$$
[K^*] = \begin{bmatrix} k_{11} & k_{12} \\ k_{21} & k_{22} \end{bmatrix} \tag{5.1.18}
$$

Where,

$$
k_{11} = \alpha_S^{\,2}(I_{m2} - I_{y2}) - \beta_S^{\,2}(M_2 + I_{m2} - I_{y2}) - \gamma_S^{\,2}\, M_2 + \dot{\beta}_S\,\Omega\, I_{y2} \tag{5.1.19}
$$

$$
k_{22} = \gamma_S^{\,2}(I_{m2} - I_{y2}) - \beta_S^{\,2}(M_2 + I_{m2} - I_{y2}) - \alpha_S^{\,2} M_2 + \dot{\beta}_S\,\Omega\, I_{y2} \tag{5.1.20}
$$

$$
k_{12} = (\alpha_S\,\gamma_S + \ddot{\beta}_S)\,(M_2 + I_{m2} - I_{y2}) \tag{5.1.21}
$$

$$
k_{21} = (\alpha_S\,\gamma_S - \ddot{\beta}_S)\,(M_2 + I_{m2}) - I_{y2}\,\alpha_S\,\gamma_S \tag{5.1.22}
$$

The matrix $[K_2]$ is due to the consideration of higher order large deformations in bending.

$$
[K_2] = \begin{bmatrix} k_2 & 0 \\ 0 & k_2 \end{bmatrix} \tag{5.1.23}
$$

Where, k_2 is given by Eq. (5.1.8).

Eq. (5.1.9) is a new equation of motion which includes the combined effect of the movement of the base of the rotor and the nonlinearity due to higher order large bending deformations. This equation can be treated using the method of multiple scales as in chapter 3 and 4 of the present thesis. Different types of movements of the base of the rotor can be investigated, for example, simple translation, a constant acceleration, sinusoidal translatory motion, simple rotation and sinusoidal rotation.

Publications by the Author

International peer-reviewed journals

R. Shad, G. Michon, and A. Berlioz, May 2011, "Modeling and Analysis of Nonlinear Rotordynamics due to Higher Order Deformations in Bending", Journal of Applied Mathematical Modeling, In Press, **35** (5), pp. 2145-2159. doi:10.1016/j.apm.2010.11.043.

R. Shad, G. Michon, and A. Berlioz, 2011, "Effects of Shear and Large Bending Deformations on the Nonlinear Dynamic Behavior of Rotors", ASME Journal of Vibrations and Acoustics (under review).

R. Shad, G. Michon, and A. Berlioz, 2011, "A Study of the Dynamic Behavior of Geometrically Nonlinear Shaft-disk Rotor Systems Using Analytical and Numerical Approaches", Mécanique & Industries, (under review).

International conferences with proceedings

R. Shad, G. Michon, and A. Berlioz, 2010, "Nonlinear Dynamics of Rotors due to Large Deformations and Shear Effects", in Proceedings of the International Conference on Aerospace and Mechanical Engineering (ICMAE), Kuala Lumpur, Malaysia, pp. 100-104. ISBN: 978-1-4244-8770-7.

R. Shad, G. Michon, and A. Berlioz, 2010, "Analytical and numerical investigations of nonlinear dynamics of rotors taking into account higher order large deformations and a dynamic axial force," XVIIth Symposium on Vibrations, Shocks and Noise, Lyon, France.

[This page intentionally left blank]

References

[A09] Almasi, A., 2009, "Nonlinear Large Deformation Analysis of Rotor, World Academy of Science," Engineering and Technology, **55**, pp. 330-333.

[AA01] Adams, L.M., and Adams, J.R., 2001, *Rotating Machinery Vibrations from Analysis to Troubleshooting*, Dekker, New York.

[B94] Bielefield, M., 1994, "Fabrication of Braided RTM Driveshaft Tubes for the RAH-60 Comanche," Proceedings of the 50th Annual Forum of American Helicopter Society, Washington DC, USA, **2**, pp. 1001-1015.

[B93] Bert, C. W., 1993, "The Effect of Bending-Twisting Coupling on the Critical Speed of a Driveshaft," Proceedings 6th Japan-US Conference on Composite Materials, Orlando, FL, Techonomic, Lancaster, PA, pp. 29-36.

[CLR02] Chatelet, E., Lornage, D., and Richardet, G.J., 2002, "A Three Dimensional Modelling Of The Dynamic Behaviour Of Composite Rotors," International Journal of Rotating Machinery, **8** (3), pp. 185-192.

[CP98] Chen, L.W., and Peng, W.K., 1998, "Dynamic stability of rotating composite shafts under periodic axial compressive loads," Journal of Sound and Vib, **2** (212), pp. 215-230.

[CC93] Chang, C.O., and Cheng, J.W., 1993, "Nonlinear Dynamics and Instability of a rotating shaft disk system," Journal of Sound and Vibration, **160** (3), pp. 433-454.

[C66] Cowper, G. R., 1966, "The shear coefficient in Timoshenko beam theory," J. Appl. Mech. **33** (2), pp. 335-340.

[DDR10] Das, A.S., Dutt, J.K., and Ray, K., 2010, "Active vibration control of unbalanced flexible rotor–shaft systems parametrically excited due to base motion," Applied Mathematical Modelling, **34** (9), pp. 2353-2369.

[DBL09] Driot, N., Berlioz, A., and Lamarque, C. H., 2009, "Stability and Stationary Response of a Skew Jeffcott Rotor with Geometric Uncertainty," ASME Journal of Computational and Nonlinear Dynamics, Trans of ASME, **4**(2).

[DLB07] Driot, N., Lamarque, C. H., and Berlioz, A., June 2007, "Dynamics of a rotor subjected to a base translational motion and an uncertain parametric excitation," 12th IFToMM World Congress, Besançon (France).

[DBF06] Duchemin, M., Berlioz, A. and Ferraris, G., 2006, "Dynamic Behavior and Stability of a Rotor under Base Excitations," Journal of Vibration and Acoustics, **128**(5), pp. 576-585.

[DLB06] Driot, N., Lamarque, C.H., and Berlioz, A., 2006, "Theoretical and Experimental Analysis of a Base Excited Rotor," ASME Journal of Computational and Nonlinear Dynamics, Trans of ASME, **1**(4), pp. 257-263.

[DRP05] Das, S. K., Ray, P. C., and Pohit, G., 2005, "Large Amplitude Free Vibration Analysis of a Rotating Beam with Non-linear Spring and Mass System," Journal of Vibration and Control, **11**(12), pp. 1511–1533.

[DBF04] Duchemin, M., Berlioz, A., and Ferraris, G., 2004, "Etude du Comportement Dynamique des Dotors Embarqués: Modélisation – Expérimentation, Essais Industriels," ASTE, **30**, pp. 27-33.

[E08] Ehrich, F., 2008, "Observations of Nonlinear Phenomena in Rotordynamics," Journal of System Design and Dynamics, **2**(3), pp. 641-651.

[E02] El-Bassiouny, A.F., 2002 "Parametrically excited non-linear systems: a comparison of two models," Applied Mathematics and Computation, **132**, pp. 385-410.

[EG00] Mahdy, E.L., and Gadelrab, T.H., 2000, "Free vibration of unidirectional fiber reinforcement composite rotor," Journal of Sound and Vib, **1**(230), pp. 195-202.

[E99] Ehrich, F.F., 1999, *Handbook of Rotor Dynamics*, Krieger, Malabar.

[EE69] Eshleman, R.L., and Eubanks, R.A., 1969, "On the critical speeds of a continuous rotor," J. Engng Ind. ASME **91**, pp. 1180–1188.

[E08] Ehrich, F.F., 2008, "Observations of nonlinear phenomena in rotordynamics, journal of system design and dynamics," **2** (3), pp. 641-651.

[GR92] Geradin, M., and Rixen, D., 1992, *Theorie Des Vibrations-Application A La Dynamique Des Structures*, Masson, Paris, pp. 196-199.

[G05] G. Genta, 2005, *Dynamics of Rotating Systems*, Springer, New York.

[GG05] Gubran, HBH., Gupta, K., 2005, "The effect of stacking sequence and coupling mechanisms on natural frequencies of composite shafts," Journal of Sound and Vib., **282**, pp. 231-248.

[HM87] Haquang, N., and Mook, D.T., 1987, "Non-linear structural vibration under combined parametric and external excitation," Journal of Sound and Vibration, **118** (2), pp. 291–306.

[HKD90] Hetherington, E L., Kraus, R. E., and Darlow, M. S., 1990, "Demonstration of a Super Critical Composite Helicopter Power Transmission Shaft," Journal of American Helicopter Society, pp. 23-28.

[HK09] Hosseini, S., and Khadem, S., 2009, "Free Vibration Analysis of a Rotating Shaft with Nonlinearities in Curvature and Inertia," Mechanism and Machine Theory, **44**, pp. 272-288.

[H01] Hutchinson j. R., 2001, "Shear Coefficients for Timoshenko Beam Theory," Journal of Applied Mechanics , **68**(1), pp. 87-92.

[IKM98] Iwatsubo, T., Kawamura, S., and Moon, B.Y., 1998, "Non-linear Vibration Analysis of Rotor System Using Substructure Synthesis Method (Analysis with Consideration of Non-linearity of Rotor)," JSME International Journal Series **C 41**(4), pp. 727-733.

[INIL96] Ishida, Y., Nagasaka, I., Inoue, T., and Lee, S., 1996, "Forced Oscillations of a Vertical Continuous Rotor with Geometric Nonlinearity," Nonlinear Dynamics, **11**, pp. 107-120.

[JL03] Ji, J.C., and Leung, A.Y.T., 2003, "Nonlinear Oscillations of a Rotor Magnetic Bearing System under Superharmonic Resonance Conditions," Internations Journal of Non-linear Mechanics, **38**, pp. 829-835.

[JZ98] Ji ,Z., Zu, J.W., 1998, "Method Of Multiple Scales For Vibration Analysis Of Rotor–Shaft Systems With Non-Linear Bearing Pedestal Model," Journal of Sound and Vibration, pp. 293-305.

[J83] Jensen, J. J., 1983, "On the shear coefficient in Timoshenko's beam theory," Journal of Sound and Vibration **87(**4), pp. 621-635.

[KWC02] Karpenco, E.V., Wiercigroch, M., and Cartmell, M.P., 2002, "Regular and Chaotic Dynamics of a Discontinuously Non-linear Rotor System," Chaos Solutions & Fractals **13**, pp. 1231-1242.

[L02] Luczko, J., 2002, "A Geometrically Nonlinear Model of Rotating Shafts with Internal Resonance and Self Excited Vibrations," Journal of Sound and Vibrations, **255**(3), pp. 433-456.

[LJ01] L.M. Adams, and J.R. Adama, 2001, *Rotating Machinery Vibrations from Analysis to Troubleshooting*, Dekker, New York.

[LF98] Lalanne, M., and Ferraris, G., 1998, *Rotordynamics Prediction in Engineering, John Wiley & Sons*, pp. 1-34.

[LD86] Lim, J. W., and Darlow, M. S., 1986, "Optimal Sizing of Composite Power Transmission Shafting," Journal of American Helicopter Society, **31**(1), pp. 75-83.

[LC83I] Levinson, M., and Cook, D.W., 1983, "Thick rectangular plates - I: The generalized Navier solution," International Journal of Mechanics Science, **25(**3).

[LC83II] Levinson, M., and Cook, D.W., 1983, "Thick rectangular plates - II: The generalized Levy solution," International Journal of Mechanics Science, **25(**3).

[MMPD08] Michon, G., Manin, L., Parker, R.G., and Dufour, R., 2008, "Duffing Oscillator With Parametric Excitation: Analytical and Experimental Investigation on a Belt-Pulley System," ASME Journal of Computational and Nonlinear Dynamics, **3**, p. 031001-1.

[MK03] Moon, B.Y., and Kang, B.S., 2003, "Vibration Analysis of Harmonically Excited Non-linear System Using Method of Multiple Scales," Journal of Sound and Vibration, **263**(1), pp. 1-20.

[MKY99] Moon, B.Y., Kim, J.-W., and Yang, B.-S., 1999, "Non-linear vibration analysis of mechanical structure system using substructure synthesis method," KSME International Journal, **13** (9), pp. 620–629.

[M78] Mook, D.T., 1978, "The influence of an internal resonance conditions," Journal of Sound and Vibration **102** (4), pp. 473–492, 1978.

[NM95] Nayfeh, A.H., and Mook, D.T., 1995, *Nonlinear Oscillations*, Wiley-VCH, Weinheim, pp. 379-500.

[N93] Nayfeh, A.H., 1993, *Introduction to Perturbation Techniques*, Wiley Interscience, New York, pp. 100-300.

[R07] Sino, R., 2007, "Comportement Dynamique et Stabilite Des Rotors: Application Aux Rotor Composites, " Thèse de doctorat, INSA LYON.

[R05] Rangwala, R. S., 2005, *Turbo-Machinery Dynamics Design and Operation*, McGraw-Hill.

[RBX95] Rao, C., Bhat,R.B., and Xistris, G.D., 1995, "Experimental Verification of Simultaneous Forward and Backward Whirling at Different Points of a Jeffcott Rotor Supported on Identical Journal Bearings," Journal of Sound and Vibration, pp. 379-388.

[SMB10] R. Shad, G. Michon, and A. Berlioz, May 2011, "Modeling and Analysis of Nonlinear Rotordynamics due to Higher Order Deformations in Bending", Journal of Applied Mathematical Modeling, In Press, **35**(5), pp. 2145-2159. doi:10.1016/j.apm.2010.11.043.

[SCB08] Sino R, Chatelet E, Baranger TN, and Jaquet-Richardet G., 2008, "Dynamic analysis of a rotating composite shaft," Composites Science and Technology **68**, pp. 337-345.

[SPW05] Swanson, E.E., Powel, C.D., Weissman, S., A Practical Review of Rotating Machinery Critical Speeds and Modes, Sound and Vibration, pp. 10-17, May 2005.

[SZ03] Shabaneh, N., and Zu, J., 2003, "Nonlinear Dynamic Analysis of a Rotor Shaft System With Viscoelastically Supported Bearings," Transactions of the ASME, **125**, pp. 290-298.

[SGG97] Singh, S.P., Gubran, H.B.H., and Gupta, K., 1997, "Developments in Dynamics of Composite Material Shafts," International Journal of Rotating Machinery, **3**(3), pp 189-198.

[SG96a] Singh, S. P., and Gupta, K., 1996a, "Rotordynamic Experiments on Composite Shafts," ASTM Journal of Composite Technology and Research, **18**(4).

[SG96] Singh, S.P., and Gupta, K., 1996, "Dynamic Analysis of Composite Rotors," International Journal of Rotating Machinery, **2**(3), pp. 179-186.

[SG95] Singh, S. E., and Gupta, K., 1995, "Composite Shaft Rotordynamic Analysis using a Layerwise theory," Journal of Sound and Vibration.

[S92] Singh, S. E., 1992, "Some Studies on Dynamics of Composite Shafts," Ph.D thesis, Mech. Engg. Deptt., IIT, Delhi.

[T65] Tondl, A., 1965, *Some Problems of Rotordynamics*, Czechoslovak Academy of Sciences, Prague, in coedition with Chapman & Hall, London.

[VST05] Villa, C.V.S., Sinou, J.J., and Thouverez, F., 2005, "The invariant manifold approach applied to Nonlinear dynamics of a rotor-bearing system," European Journal of Mechanics and Solids **24**, pp. 676-689.

[WI09] Wauer, J., Ishida, Y., 2009, "Special Issue on Recent Advances in Nonlinear Rotordynamics," Nonlinear Dynamics, **57** (4), p. 479.

[WB00] W.Kwon Y, and Bang H, 2000, *The Finite Element Method Using Matlab, 2nd edition*. CRC Mechanical Engineering Series.

[XQZZ09] Xia, Z., Qiao, G., Zheng, T., and Zhang, W., 2009, "Nonlinear Modelling and Dynamic Analysis of the Rotor-Bearing System," Nonlinear Dynamics, **57**, pp. 559-577.

[YKII07] Yabuno, H., Kunitho, Y., Inoue, T., and Ishida, Y., 2007, "Nonlinear Analysis of Rotor Dynamics by Using Method of Multiple Scales," IUTAM Symposium on Dynamics and Control of Nonlinear Systems with Uncertainty **2**(3), pp. 167-176.

[YI01] Yamamoto, T., and Ishida, Y., 2001, *Linear and Nonlinear Rotordynamics: A Modern Treatment with Applications*, Wiley-Interscience, New York, pp. 45-125.

[ZGTW09] Xia, Z., Qiao, G., Zheng, T., and Zhang, W., 2009, "Nonlinear modelling and dynamic analysis of the rotor-bearing system," Nonlinear Dynamics **57**, pp. 559-577.

[ZG85] Zorzi, E. S., and Giordano, J. C., 1985, "Composite Shaft Rotordynamic Evaluation," ASME Design Engineering Conference on Mechanical Vibrations and Noise, ASME, paper no. 85-DET-114.

[ZS70] Zinberg, H., and Symmonds, M. F., 1970, "The Development of an Advanced Composite Tail Rotor Driveshaft," Presented at 26th Annual National Forum of American Helicopter Society, Washington, DC.

List of Figures

List of Tables

Appendix A: Strain Energy of the shaft

The shaft is modeled as a beam of circular cross section in bending (Fig.A). The displacements in the *x, y* and *z* directions of the beam are given below.

$$u_x = u \ , \ u_y = -z\theta_x + x\theta_z \ , \ u_z = w \tag{A.1}$$

The longitudinal strain (deformation) in the *y* direction can be shown to be

$$\varepsilon_{yy} = \underbrace{-z\frac{\partial \theta_x}{\partial y} + x\frac{\partial \theta_z}{\partial y}}_{\varepsilon_l} + \underbrace{\frac{1}{2}\theta_x^{\,2} + \frac{1}{2}\theta_z^{\,2}}_{\varepsilon_{nl}\,(\text{higher order deformations})} \tag{A.2}$$

The strain energy can be given as:

$$U_{s1} = \frac{1}{2}\int_0^L \iint_A \left(\sigma_{yy}\varepsilon_{yy}\right) dA dy \tag{A.3}$$

By using the relation $\sigma_{yy} = E\varepsilon_{yy}$, the strain energy can be written as:

$$U_{s1} = \frac{E}{2}\int_0^L \iint_A \varepsilon_{yy}^{\,2}\, dA dy \tag{A.4}$$

By using Eq. A.2,

$$U_{s1} = \frac{E}{2}\int_0^L \iint_A \left[-z\frac{\partial \theta_x}{\partial y} + x\frac{\partial \theta_z}{\partial y} + \frac{1}{2}\theta_x^{\,2} + \frac{1}{2}\theta_z^{\,2}\right]^2 dA dy \tag{A.5}$$

$$U_{s1} = \frac{E}{2}\int_0^L \iint_A \left[z^2\left(\frac{\partial \theta_x}{\partial y}\right)^2 + x^2\left(\frac{\partial \theta_z}{\partial y}\right)^2 - 2xz\left(\frac{\partial \theta_x}{\partial y}\right)\left(\frac{\partial \theta_z}{\partial y}\right) + \frac{1}{4}\theta_x^{\,4} + \frac{1}{4}\theta_z^{\,4} + \frac{1}{2}\theta_x^{\,2}\theta_z^{\,2} - 2\left[z\frac{\partial \theta_x}{\partial y} + x\frac{\partial \theta_z}{\partial y}\right]\left[\frac{1}{2}\theta_x^{\,2} + \frac{1}{2}\theta_z^{\,2}\right]\right] dA dy \tag{A.6}$$

The 3rd and 7th term in the above equation can be neglected due to the symmetry of the cross-section. Also, $I_x = \int_A z^2 dA$, $I_z = \int_A x^2 dA$, $I = I_x = I_z$ (due to symmetry) and $\int_S ds = A$ is the area of the cross section.

Therefore, Eq. (A.6) becomes,

$$U_{s1} = \frac{EI}{2}\int_0^L \left[\left(\frac{\partial \theta_x}{\partial y}\right)^2 + \left(\frac{\partial \theta_z}{\partial y}\right)^2\right] dy + \frac{EA}{2}\int_0^L \left[\frac{1}{4}\theta_x^{\,4} + \frac{1}{4}\theta_z^{\,4} + \frac{1}{2}\theta_x^{\,2}\theta_z^{\,2}\right] dy \tag{A.7}$$

Appendix B: Numerical Data

$\rho = 7800\,\mathrm{kg\,m^{-3}}$, $E = 2\times10^{11}\,\mathrm{N\,m^{-2}}$, $c = 0.001$, $L = 0.4\,\mathrm{m}$, $R_1 = 0.01\,\mathrm{m}$

$R_2 = 0.15\,\mathrm{m}$, $h = 0.03\,\mathrm{m}$, $m_u = 1\times10^{-4}\,\mathrm{kg}$, $d_1 = R_2 = 0.15\,\mathrm{m}$

$M_d = \pi(R_2^{\,2} - R_1^{\,2})h\rho = 16.47\,\mathrm{kg}$

$I_{dx} = M_d(3R_1^{\,2} + 3R_2^{\,2} + h^2)/12 = 9.427\times10^{-2}\,\mathrm{kg\,m^2}$

$I_{dy} = M_d(R_1^{\,2} + R_2^{\,2})/2 = 1.861\times10^{-1}\,\mathrm{kg\,m^2}$

$A = \pi R_1^{\,2} = 3.142\times10^{-4}\,\mathrm{m^2}$

$I = \pi R_1^{\,4}/4 = 7.854\times10^{-9}\,\mathrm{m^4}$

For the geometry and material properties of the rotor system given above, the numerical values of different constants are given as,

$\alpha_1 = 2.0084\,\mathrm{x}10^{-1}, \alpha_2 = 83.623\mathrm{x}10^{3}, \beta_1 = 2.5087\mathrm{x}10^{9}, \beta_2 = 9.5457\mathrm{x}10^{12}$

$\omega_1 = 258, \omega_2 = 323, f(l_1) = 8.660\mathrm{x}10^{-1}, d_1 = 0.15, c = 0.001$

Appendix C: Coefficients of Solvability Conditions for Chapter 3 for the case of $\Omega = \omega_2$

$c_2 = C_2 / C_1$, $c_3 = C_3 / C_1$, $c_5 = C_5 / C_1$

$d_2 = D_2 / D_1, d_3 = D_3 / D_1, d_4 = D_4 / D_1, d_5 = D_5 / D_1$

where

$$C_1 = -2\omega_1^3 - \alpha_1\omega_1^2\omega_2 + \alpha_1^2\omega_1\omega_2^2 + 2\alpha_2\omega_1 - \alpha_1\alpha_2\omega_2$$

$$C_2 = 2i(\beta_1 + 2\beta_2)(\omega_1^2 + \alpha_1\omega_1\omega_2 - \alpha_2)$$

$$C_3 = 4i(\beta_1 + 2\beta_2)(\omega_1^2 + \alpha_1\omega_1\omega_2 - \alpha_2) = 2C_2$$

$$C_5 = -c(\omega_1^3 + \alpha_1\omega_1^2\omega_2 - \alpha_2\omega_1)$$

$$D_1 = (-\alpha_1 - \alpha_1^2 + 2)\omega_2^3 - \alpha_2(\alpha_1 + 2)\omega_2$$

$$D_2 = 2i(\beta_1 + 2\beta_2)[(\alpha_1 - 1)\omega_2^2 + \alpha_2]$$

$$D_3 = 4i(\beta_1 + 2\beta_2)[(\alpha_1 - 1)\omega_2^2 + \alpha_2] = 2D_2$$

$$D_4 = \frac{1}{2}m_1 d_1 f(l_1)[(\alpha_1 - 1)\omega_2^4 + \alpha_2\omega_2^2]$$

$$D_5 = c[(1 - \alpha_1)\omega_2^3 - \alpha_2\omega_2]$$

<u>Appendix D</u>: Coefficients of Solvability Conditions for Chapter 3 for the case of $\Omega = \omega_1$

$c_2 = C_2 / C_1$, $c_3 = C_3 / C_1$, $c_4 = C_4 / C_1$, $c_5 = C_5 / C_1$

$d_2 = D_2 / D_1, d_3 = D_3 / D_1$, $d_5 = D_5 / D_1$

$$C_1 = -2\omega_1^3 - \alpha_1\omega_1^3 + \alpha_1^2\omega_1^3 + 2\alpha_2\omega_1 - \alpha_1\alpha_2\omega_1$$

$$C_2 = 2i(\beta_1 + 2\beta_2)(\omega_1^2 + \alpha_1\omega_1^2 - \alpha_2)$$

$$C_3 = 4i(\beta_1 + 2\beta_2)(\omega_1^2 + \alpha_1\omega_1^2 - \alpha_2) = 2C_2$$

$$C_4 = \frac{1}{2} m_1 d_1 f(l_1)[(\alpha_1 - 1)\omega_1^4 + \alpha_2\omega_1^2]$$

$$C_5 = -c(\omega_1^3 + \alpha_1\omega_1^3 - \alpha_2\omega_1)$$

$$D_1 = -2\,\alpha 2\,\omega_2 + 2\,\omega_2^3 - \alpha 2\,\omega_1\,\alpha 1 - \omega_2^2\,\omega_1\,\alpha 1 - \omega_1^2\,\alpha 1^2\,\omega_2$$

$$D_2 = 2\,\omega_1\,\alpha 1\,\omega_2\,\beta 1 + 4\,\omega_1\,\alpha 1\,\omega_2\,\beta 2 - 4\,\omega_2^2\,\beta 2 + 4\,\alpha 2\,\beta 2 + 2\,\alpha 2\,\beta 1 - 2\,\omega_2^2\,\beta 1$$

$$D_3 = 8\,\alpha 2\,\beta 2 - 8\,\omega_2^2\,\beta 2 + 8\,\omega_1\,\alpha 1\,\omega_2\,\beta 2 + 4\,\omega_1\,\alpha 1\,\omega_2\,\beta 1 + 4\,\alpha 2\,\beta 1 - 4\,\omega_2^2\,\beta 1$$

$$D_5 = \omega_2^3\,c1 - \alpha 2\,c1\,\omega_2 - \omega_1\,\alpha 1\,\omega_2^2\,c1$$

<u>Appendix E</u>: Coefficients of Solvability conditions for Chapter 4 for the case of $\Omega = \omega_1$

$$c_1 = \frac{C_2}{C_1}\ ,\ c_2 = \frac{C_3}{C_1}\ ,\ c_3 = \frac{C_4}{C_1}\ ,\ c_4 = \frac{C_5}{C_1}\ ,\ c_5 = \frac{C_6}{C_1}\ ,\ c_6 = \frac{C_7}{C_1}$$

$$d_1 = \frac{D_2}{D_1}\ ,\ d_2 = \frac{D_3}{D_1}\ ,\ d_3 = \frac{D_4}{D_1}\ ,\ d_4 = \frac{D_5}{D_1}\ ,\ d_5 = \frac{D_6}{D_1}$$

$$f_1 = \frac{F_2}{F_1}\ ,\ f_2 = \frac{F_3}{F_1}\ ,\ f_3 = \frac{F_4}{F_1}\ ,\ f_4 = \frac{F_5}{F_1}\ ,\ f_5 = \frac{F_6}{F_1}$$

$$g_1 = \frac{G_2}{G_1}\ ,\ g_2 = \frac{G_3}{G_1}\ ,\ g_3 = \frac{G_4}{G_1}\ ,\ g_4 = \frac{G_5}{G_1}\ ,\ g_5 = \frac{G_6}{G_1}$$

Where,

$$\begin{aligned}
C_1 = {} & -4\,\alpha_{51}\,\omega_1^{\,3} + 3\,\omega_1^{\,7}\,\alpha_{21}^{\,2} + 6\,\omega_1^{\,5}\,\alpha_{31} - 2\,\alpha_{31}^{\,2}\,\omega_1^{\,3} + \omega_1^{\,3}\,\alpha_{41}^{\,2} \\
& - \alpha_{31}\,\omega_1^{\,3}\,\alpha_{41} - \omega_1^{\,7}\,\alpha_{21} - \alpha_{31}\,\omega_1^{\,5}\,\alpha_{21} - \alpha_{51}\,\omega_1\,\alpha_{41} + 2\,\alpha_{51}\,\alpha_{31}\,\omega_1 \\
& + 3\,\omega_1^{\,5}\,\alpha_{41} - 4\,\omega_1^{\,5}\,\alpha_{41}\,\alpha_{21} + 3\,\alpha_{51}\,\omega_1^{\,3}\,\alpha_{21} - 4\,\omega_1^{\,7}
\end{aligned}$$

$$\begin{aligned}
C_2 = {} & 3\,I\,\omega_1^{\,2}\,\alpha_{41}\,\beta_{31} - \frac{3}{4}I\,\alpha_{31}\,\omega_1^{\,8}\,\beta_{41} + \frac{3}{4}I\,\omega_1^{\,10}\,\alpha_{21}\,\beta_{41} - 18\,I\,\omega_1^{\,8}\,\alpha_{21}\,\beta_{21} \\
& - 3\,I\,\omega_1^{\,4}\,\beta_{31} - 18\,I\,\alpha_{31}\,\omega_1^{\,4}\,\beta_{11} + \frac{3}{4}I\,\omega_1^{\,10}\,\beta_{41} + 18\,I\,\omega_1^{\,6}\,\alpha_{21}\,\beta_{11} \\
& - 18\,I\,\omega_1^{\,8}\,\beta_{21} - 3\,I\,\alpha_{51}\,\beta_{31} - 3\,I\,\omega_1^{\,4}\,\alpha_{21}\,\beta_{31} - \frac{3}{4}I\,\omega_1^{\,8}\,\alpha_{41}\,\beta_{41} \\
& + 18\,I\,\omega_1^{\,6}\,\alpha_{41}\,\beta_{21} + 18\,I\,\alpha_{51}\,\beta_{11}\,\omega_1^{\,2} + 18\,I\,\alpha_{31}\,\omega_1^{\,6}\,\beta_{21} + 18\,I\,\omega_1^{\,6}\,\beta_{11} \\
& - 18\,I\,\alpha_{51}\,\beta_{21}\,\omega_1^{\,4} - 18\,I\,\omega_1^{\,4}\,\alpha_{41}\,\beta_{11} + 3\,I\,\alpha_{31}\,\omega_1^{\,2}\,\beta_{31} + \frac{3}{4}I\,\alpha_{51}\,\beta_{41}\,\omega_1^{\,6}
\end{aligned}$$

$$\begin{aligned}
C_3 = {} & 24\,I\,\omega_1^{\,4}\,\alpha_{21}\,\beta_{11}\,\omega_2^{\,2} + 12\,I\,\alpha_{31}\,\omega_1^{\,2}\,\beta_{21}\,\omega_2^{\,4} - 24\,I\,\omega_1^{\,6}\,\alpha_{21}\,\beta_{21}\,\omega_2^{\,2} \\
& - 24\,I\,\omega_1^{\,2}\,\alpha_{41}\,\beta_{11}\,\omega_2^{\,2} + 12\,I\,\omega_1^{\,2}\,\alpha_{41}\,\beta_{21}\,\omega_2^{\,4} + 24\,I\,\omega_1^{\,4}\,\alpha_{41}\,\beta_{21}\,\omega_2^{\,2} \\
& - 12\,I\,\omega_1^{\,4}\,\alpha_{21}\,\beta_{21}\,\omega_2^{\,4} + \frac{3}{2}I\,\alpha_{51}\,\beta_{41}\,\omega_2^{\,4}\,\omega_1^{\,2} - 24\,I\,\alpha_{51}\,\beta_{21}\,\omega_1^{\,2}\,\omega_2^{\,2} \\
& + 12\,I\,\omega_1^{\,6}\,\beta_{11} + 24\,I\,\alpha_{31}\,\omega_1^{\,4}\,\beta_{21}\,\omega_2^{\,2} - 24\,I\,\alpha_{31}\,\omega_1^{\,2}\,\beta_{11}\,\omega_2^{\,2} \\
& - \frac{3}{2}I\,\alpha_{31}\,\omega_1^{\,4}\,\beta_{41}\,\omega_2^{\,4} - \frac{3}{2}I\,\omega_1^{\,4}\,\alpha_{41}\,\beta_{41}\,\omega_2^{\,4} - 6\,I\,\omega_1^{\,4}\,\beta_{31} \\
& + \frac{3}{2}I\,\omega_1^{\,6}\,\alpha_{21}\,\beta_{41}\,\omega_2^{\,4} + 24\,I\,\alpha_{51}\,\beta_{11}\,\omega_2^{\,2} - 12\,I\,\alpha_{51}\,\beta_{21}\,\omega_2^{\,4} - 6\,I\,\alpha_{51}\,\beta_{31} \\
& + 12\,I\,\alpha_{51}\,\beta_{11}\,\omega_1^{\,2} + 6\,I\,\alpha_{31}\,\omega_1^{\,2}\,\beta_{31} - 12\,I\,\alpha_{31}\,\omega_1^{\,4}\,\beta_{11}
\end{aligned}$$

$$
\begin{aligned}
&- 24\, I\, \omega_1^{\,6}\, \beta_{21}\, \omega_2^{\,2} + 24\, I\, \omega_1^{\,4}\, \beta_{11}\, \omega_2^{\,2} + \frac{3}{2} I\, \omega_1^{\,6}\, \beta_{41}\, \omega_2^{\,4} \\
&+ 12\, I\, \omega_1^{\,6}\, \alpha_{21}\, \beta_{11} - 12\, I\, \omega_1^{\,4}\, \beta_{21}\, \omega_2^{\,4} - 6\, I\, \omega_1^{\,4}\, \alpha_{21}\, \beta_{31} \\
&- 12\, I\, \omega_1^{\,4}\, \alpha_{41}\, \beta_{11} + 6\, I\, \omega_1^{\,2}\, \alpha_{41}\, \beta_{31}
\end{aligned}
$$

$$
\begin{aligned}
C_4 = &-24\, I\, \alpha_{31}\, \omega_1^{\,2}\, \beta_{11}\, \omega_3^{\,2} - \frac{3}{2} I\, \alpha_{31}\, \omega_1^{\,4}\, \beta_{41}\, \omega_3^{\,4} - 24\, I\, \alpha_{51}\, \beta_{21}\, \omega_1^{\,2}\, \omega_3^{\,2} \\
&- 24\, I\, \omega_1^{\,6}\, \beta_{21}\, \omega_3^{\,2} + 24\, I\, \alpha_{51}\, \beta_{11}\, \omega_3^{\,2} - 12\, I\, \alpha_{51}\, \beta_{21}\, \omega_3^{\,4} + 12\, I\, \omega_1^{\,6}\, \beta_{11} \\
&+ 24\, I\, \omega_1^{\,4}\, \beta_{11}\, \omega_3^{\,2} - 6\, I\, \omega_1^{\,4}\, \beta_{31} + 12\, I\, \omega_1^{\,2}\, \alpha_{41}\, \beta_{21}\, \omega_3^{\,4} \\
&+ \frac{3}{2} I\, \alpha_{51}\, \beta_{41}\, \omega_1^{\,2}\, \omega_3^{\,4} + 24\, I\, \alpha_{31}\, \omega_1^{\,4}\, \beta_{21}\, \omega_3^{\,2} + \frac{3}{2} I\, \omega_1^{\,6}\, \beta_{41}\, \omega_3^{\,4} \\
&- \frac{3}{2} I\, \omega_1^{\,4}\, \alpha_{41}\, \beta_{41}\, \omega_3^{\,4} + 24\, I\, \omega_1^{\,4}\, \alpha_{21}\, \beta_{11}\, \omega_3^{\,2} + 24\, I\, \omega_1^{\,4}\, \alpha_{41}\, \beta_{21}\, \omega_3^{\,2} \\
&- 12\, I\, \omega_1^{\,4}\, \alpha_{21}\, \beta_{21}\, \omega_3^{\,4} - 24\, I\, \omega_1^{\,6}\, \alpha_{21}\, \beta_{21}\, \omega_3^{\,2} + \frac{3}{2} I\, \omega_1^{\,6}\, \alpha_{21}\, \beta_{41}\, \omega_3^{\,4} \\
&+ 12\, I\, \alpha_{31}\, \omega_1^{\,2}\, \beta_{21}\, \omega_3^{\,4} - 24\, I\, \omega_1^{\,2}\, \alpha_{41}\, \beta_{11}\, \omega_3^{\,2} - 12\, I\, \omega_1^{\,4}\, \beta_{21}\, \omega_3^{\,4} \\
&- 6\, I\, \alpha_{51}\, \beta_{31} + 12\, I\, \alpha_{51}\, \beta_{11}\, \omega_1^{\,2} + 6\, I\, \alpha_{31}\, \omega_1^{\,2}\, \beta_{31} - 12\, I\, \alpha_{31}\, \omega_1^{\,4}\, \beta_{11} \\
&+ 12\, I\, \omega_1^{\,6}\, \alpha_{21}\, \beta_{11} - 6\, I\, \omega_1^{\,4}\, \alpha_{21}\, \beta_{31} - 12\, I\, \omega_1^{\,4}\, \alpha_{41}\, \beta_{11} + 6\, I\, \omega_1^{\,2}\, \alpha_{41}\, \beta_{31}
\end{aligned}
$$

$$
\begin{aligned}
C_5 = &-12\, I\, \alpha_{51}\, \beta_{21}\, \omega_4^{\,4} + 24\, I\, \alpha_{51}\, \beta_{11}\, \omega_4^{\,2} - 24\, I\, \omega_1^{\,6}\, \beta_{21}\, \omega_4^{\,2} \\
&+ 24\, I\, \omega_1^{\,4}\, \beta_{11}\, \omega_4^{\,2} - 12\, I\, \omega_1^{\,4}\, \beta_{21}\, \omega_4^{\,4} + 12\, I\, \omega_1^{\,6}\, \beta_{11} + \frac{3}{2} I\, \omega_1^{\,6}\, \beta_{41}\, \omega_4^{\,4} \\
&- 6\, I\, \omega_1^{\,4}\, \beta_{31} - 24\, I\, \alpha_{31}\, \omega_1^{\,2}\, \beta_{11}\, \omega_4^{\,2} - 24\, I\, \omega_1^{\,2}\, \alpha_{41}\, \beta_{11}\, \omega_4^{\,2} \\
&+ 24\, I\, \alpha_{31}\, \omega_1^{\,4}\, \beta_{21}\, \omega_4^{\,2} - 24\, I\, \alpha_{51}\, \beta_{21}\, \omega_1^{\,2}\, \omega_4^{\,2} - \frac{3}{2} I\, \alpha_{31}\, \omega_1^{\,4}\, \beta_{41}\, \omega_4^{\,4} \\
&+ \frac{3}{2} I\, \alpha_{51}\, \beta_{41}\, \omega_1^{\,2}\, \omega_4^{\,4} - 12\, I\, \omega_1^{\,4}\, \alpha_{21}\, \beta_{21}\, \omega_4^{\,4} - \frac{3}{2} I\, \omega_1^{\,4}\, \alpha_{41}\, \beta_{41}\, \omega_4^{\,4} \\
&+ \frac{3}{2} I\, \omega_1^{\,6}\, \alpha_{21}\, \beta_{41}\, \omega_4^{\,4} + 12\, I\, \omega_1^{\,2}\, \alpha_{41}\, \beta_{21}\, \omega_4^{\,4} + 12\, I\, \alpha_{31}\, \omega_1^{\,2}\, \beta_{21}\, \omega_4^{\,4} \\
&+ 24\, I\, \omega_1^{\,4}\, \alpha_{21}\, \beta_{11}\, \omega_4^{\,2} + 24\, I\, \omega_1^{\,4}\, \alpha_{41}\, \beta_{21}\, \omega_4^{\,2} - 24\, I\, \omega_1^{\,6}\, \alpha_{21}\, \beta_{21}\, \omega_4^{\,2} \\
&- 6\, I\, \alpha_{51}\, \beta_{31} + 12\, I\, \alpha_{51}\, \beta_{11}\, \omega_1^{\,2} + 6\, I\, \alpha_{31}\, \omega_1^{\,2}\, \beta_{31} - 12\, I\, \alpha_{31}\, \omega_1^{\,4}\, \beta_{11} \\
&+ 12\, I\, \omega_1^{\,6}\, \alpha_{21}\, \beta_{11} - 6\, I\, \omega_1^{\,4}\, \alpha_{21}\, \beta_{31} - 12\, I\, \omega_1^{\,4}\, \alpha_{41}\, \beta_{11} + 6\, I\, \omega_1^{\,2}\, \alpha_{41}\, \beta_{31}
\end{aligned}
$$

$$C_6 = -\alpha_{31}\, \omega_1^{\,3}\, c + \omega_1^{\,5}\, c + \alpha_{51}\, c\, \omega_1 - \omega_1^{\,3}\, \alpha_{41}\, c + \omega_1^{\,5}\, \alpha_{21}\, c$$

$$C_7 = \frac{1}{2} \alpha_{51}\, m_1\, \omega_1^{\,2} - \frac{1}{2} \alpha_{31}\, \omega_1^{\,4}\, m_1 + \frac{1}{2} \omega_1^{\,6}\, \alpha_{21}\, m_1 + \frac{1}{2} \omega_1^{\,6}\, m_1 - \frac{1}{2} \omega_1^{\,4}\, \alpha_{41}\, m_1$$

$$
\begin{aligned}
\mathrm{D}_1 = &\, 4\, \alpha_{51}\, \omega_2^{\,3} - \omega_1^{\,2}\, \alpha_{41}^{\,2}\, \omega_2 - \alpha_{51}\, \omega_1\, \alpha_{41} + 3\, \omega_2^{\,4}\, \omega_1\, \alpha_{41} + 4\, \omega_2^{\,7} \\
&+ 2\, \alpha_{31}^{\,2}\, \omega_2^{\,3} - 6\, \omega_2^{\,5}\, \alpha_{31} + 4\, \omega_1^{\,2}\, \alpha_{21}\, \omega_2^{\,3}\, \alpha_{41} + 3\, \alpha_{51}\, \omega_1\, \alpha_{21}\, \omega_2^{\,2} \\
&- \omega_2^{\,6}\, \omega_1\, \alpha_{21} - 3\, \omega_1^{\,2}\, \alpha_{21}^{\,2}\, \omega_2^{\,5} - 2\, \alpha_{51}\, \alpha_{31}\, \omega_2 - \alpha_{31}\, \omega_2^{\,4}\, \omega_1\, \alpha_{21}
\end{aligned}
$$

$$
\begin{aligned}
D_2 = &-18\, I\, \omega_2^{\,6}\, \beta_{11} - 18\, I\, \omega_1\, \alpha_{21}\, \omega_2^{\,7}\, \beta_{21} - 3\, I\, \alpha_{31}\, \omega_2^{\,2}\, \beta_{31} \\
&+ 18\, I\, \omega_1\, \alpha_{21}\, \omega_2^{\,5}\, \beta_{11} + \frac{3}{4} I\, \alpha_{31}\, \omega_2^{\,8}\, \beta_{41} - \frac{3}{4} I\, \omega_2^{\,10}\, \beta_{41} \\
&+ 3\, I\, \omega_1\, \alpha_{41}\, \omega_2\, \beta_{31} - 18\, I\, \alpha_{31}\, \omega_2^{\,6}\, \beta_{21} - 18\, I\, \alpha_{51}\, \beta_{11}\, \omega_2^{\,2} + 3\, I\, \alpha_{51}\, \beta_{31} \\
&- \frac{3}{4} I\, \omega_1\, \alpha_{41}\, \omega_2^{\,7}\, \beta_{41} - 3\, I\, \omega_1\, \alpha_{21}\, \omega_2^{\,3}\, \beta_{31} + 18\, I\, \omega_2^{\,8}\, \beta_{21} \\
&+ \frac{3}{4} I\, \omega_1\, \alpha_{21}\, \omega_2^{\,9}\, \beta_{41} + 3\, I\, \omega_2^{\,4}\, \beta_{31} + 18\, I\, \alpha_{31}\, \omega_2^{\,4}\, \beta_{11} \\
&+ 18\, I\, \omega_1\, \alpha_{41}\, \omega_2^{\,5}\, \beta_{21} - 18\, I\, \omega_1\, \alpha_{41}\, \omega_2^{\,3}\, \beta_{11} - \frac{3}{4} I\, \alpha_{51}\, \beta_{41}\, \omega_2^{\,6} \\
&+ 18\, I\, \alpha_{51}\, \beta_{21}\, \omega_2^{\,4}
\end{aligned}
$$

$$
\begin{aligned}
D_3 = &-6\, I\, \alpha_{31}\, \omega_2^{\,2}\, \beta_{31} - \frac{3}{2} I\, \omega_2^{\,6}\, \beta_{41}\, \omega_1^{\,4} + 24\, I\, \omega_2^{\,6}\, \beta_{21}\, \omega_1^{\,2} + 12\, I\, \omega_2^{\,4}\, \beta_{21}\, \omega_1^{\,4} \\
&- 12\, I\, \alpha_{51}\, \beta_{11}\, \omega_2^{\,2} + 6\, I\, \alpha_{51}\, \beta_{31} - 12\, I\, \omega_2^{\,6}\, \beta_{11} + 6\, I\, \omega_2^{\,4}\, \beta_{31} \\
&+ 24\, I\, \alpha_{51}\, \beta_{21}\, \omega_1^{\,2}\, \omega_2^{\,2} - \frac{3}{2} I\, \alpha_{51}\, \beta_{41}\, \omega_1^{\,4}\, \omega_2^{\,2} + 12\, I\, \omega_1\, \alpha_{21}\, \omega_2^{\,5}\, \beta_{11} \\
&- 24\, I\, \omega_2^{\,4}\, \beta_{11}\, \omega_1^{\,2} + 12\, I\, \alpha_{31}\, \omega_2^{\,4}\, \beta_{11} + 12\, I\, \alpha_{51}\, \beta_{21}\, \omega_1^{\,4} \\
&- 24\, I\, \alpha_{51}\, \beta_{11}\, \omega_1^{\,2} + 12\, I\, \omega_1^{\,5}\, \alpha_{41}\, \omega_2\, \beta_{21} - 12\, I\, \omega_1\, \alpha_{41}\, \omega_2^{\,3}\, \beta_{11} \\
&+ \frac{3}{2} I\, \omega_1^{\,5}\, \alpha_{21}\, \omega_2^{\,5}\, \beta_{41} - 12\, I\, \omega_1^{\,5}\, \alpha_{21}\, \omega_2^{\,3}\, \beta_{21} + 6\, I\, \omega_1\, \alpha_{41}\, \omega_2\, \beta_{31} \\
&- 6\, I\, \omega_1\, \alpha_{21}\, \omega_2^{\,3}\, \beta_{31} - 24\, I\, \omega_1^{\,3}\, \alpha_{21}\, \omega_2^{\,5}\, \beta_{21} - 24\, I\, \omega_1^{\,3}\, \alpha_{41}\, \omega_2\, \beta_{11} \\
&+ 24\, I\, \omega_1^{\,3}\, \alpha_{21}\, \omega_2^{\,3}\, \beta_{11} + \frac{3}{2} I\, \alpha_{31}\, \omega_2^{\,4}\, \beta_{41}\, \omega_1^{\,4} - 12\, I\, \alpha_{31}\, \omega_2^{\,2}\, \beta_{21}\, \omega_1^{\,4} \\
&- \frac{3}{2} I\, \omega_1^{\,5}\, \alpha_{41}\, \omega_2^{\,3}\, \beta_{41} + 24\, I\, \alpha_{31}\, \omega_2^{\,2}\, \beta_{11}\, \omega_1^{\,2} + 24\, I\, \omega_1^{\,3}\, \alpha_{41}\, \omega_2^{\,3}\, \beta_{21} \\
&- 24\, I\, \alpha_{31}\, \omega_2^{\,4}\, \beta_{21}\, \omega_1^{\,2}
\end{aligned}
$$

$$
\begin{aligned}
D_4 = &\frac{3}{2} I\, \alpha_{31}\, \omega_2^{\,4}\, \beta_{41}\, \omega_3^{\,4} + 24\, I\, \alpha_{51}\, \beta_{21}\, \omega_2^{\,2}\, \omega_3^{\,2} + 24\, I\, \alpha_{31}\, \omega_2^{\,2}\, \beta_{11}\, \omega_3^{\,2} \\
&- 12\, I\, \alpha_{31}\, \omega_2^{\,2}\, \beta_{21}\, \omega_3^{\,4} - 24\, I\, \alpha_{31}\, \omega_2^{\,4}\, \beta_{21}\, \omega_3^{\,2} - 6\, I\, \alpha_{31}\, \omega_2^{\,2}\, \beta_{31} \\
&+ 24\, I\, \omega_1\, \alpha_{21}\, \omega_2^{\,3}\, \beta_{11}\, \omega_3^{\,2} - 12\, I\, \alpha_{51}\, \beta_{11}\, \omega_2^{\,2} - 12\, I\, \omega_1\, \alpha_{21}\, \omega_2^{\,3}\, \beta_{21}\, \omega_3^{\,4} \\
&+ 6\, I\, \alpha_{51}\, \beta_{31} - 12\, I\, \omega_2^{\,6}\, \beta_{11} + 6\, I\, \omega_2^{\,4}\, \beta_{31} - 24\, I\, \omega_1\, \alpha_{21}\, \omega_2^{\,5}\, \beta_{21}\, \omega_3^{\,2} \\
&+ 12\, I\, \omega_1\, \alpha_{21}\, \omega_2^{\,5}\, \beta_{11} + 12\, I\, \alpha_{31}\, \omega_2^{\,4}\, \beta_{11} - 12\, I\, \omega_1\, \alpha_{41}\, \omega_2^{\,3}\, \beta_{11} \\
&- 24\, I\, \omega_1\, \alpha_{41}\, \omega_2\, \beta_{11}\, \omega_3^{\,2} + 6\, I\, \omega_1\, \alpha_{41}\, \omega_2\, \beta_{31} - 6\, I\, \omega_1\, \alpha_{21}\, \omega_2^{\,3}\, \beta_{31}
\end{aligned}
$$

$$+ 24\, I\, \omega_1\, \alpha_{41}\, {\omega_2}^3\, \beta_{21}\, {\omega_3}^2 - \frac{3}{2} I\, \omega_1\, \alpha_{41}\, {\omega_2}^3\, \beta_{41}\, {\omega_3}^4$$
$$+ 12\, I\, \omega_1\, \alpha_{41}\, \omega_2\, \beta_{21}\, {\omega_3}^4 + \frac{3}{2} I\, \omega_1\, \alpha_{21}\, {\omega_2}^5\, \beta_{41}\, {\omega_3}^4 - \frac{3}{2} I\, {\omega_2}^6\, \beta_{41}\, {\omega_3}^4$$
$$- 24\, I\, {\omega_2}^4\, \beta_{11}\, {\omega_3}^2 - 24\, I\, \alpha_{51}\, \beta_{11}\, {\omega_3}^2 + 12\, I\, {\omega_2}^4\, \beta_{21}\, {\omega_3}^4$$
$$+ 24\, I\, {\omega_2}^6\, \beta_{21}\, {\omega_3}^2 - \frac{3}{2} I\, \alpha_{51}\, \beta_{41}\, {\omega_2}^2\, {\omega_3}^4 + 12\, I\, \alpha_{51}\, \beta_{21}\, {\omega_3}^4$$

$$D_5 = 24\, I\, \alpha_{51}\, \beta_{21}\, {\omega_2}^2\, {\omega_4}^2 - \frac{3}{2} I\, \alpha_{51}\, \beta_{41}\, {\omega_2}^2\, {\omega_4}^4 - 24\, I\, \alpha_{31}\, {\omega_2}^4\, \beta_{21}\, {\omega_4}^2$$
$$+ 24\, I\, \alpha_{31}\, {\omega_2}^2\, \beta_{11}\, {\omega_4}^2 + \frac{3}{2} I\, \alpha_{31}\, {\omega_2}^4\, \beta_{41}\, {\omega_4}^4 - 6\, I\, \alpha_{31}\, {\omega_2}^2\, \beta_{31}$$
$$- 12\, I\, \alpha_{51}\, \beta_{11}\, {\omega_2}^2 + 6\, I\, \alpha_{51}\, \beta_{31} - 12\, I\, {\omega_2}^6\, \beta_{11} + 6\, I\, {\omega_2}^4\, \beta_{31}$$
$$+ 12\, I\, {\omega_2}^4\, \beta_{21}\, {\omega_4}^4 + 24\, I\, {\omega_2}^6\, \beta_{21}\, {\omega_4}^2 + 12\, I\, \alpha_{51}\, \beta_{21}\, {\omega_4}^4$$
$$- \frac{3}{2} I\, {\omega_2}^6\, \beta_{41}\, {\omega_4}^4 - 24\, I\, {\omega_2}^4\, \beta_{11}\, {\omega_4}^2 - 12\, I\, \alpha_{31}\, {\omega_2}^2\, \beta_{21}\, {\omega_4}^4$$
$$- 24\, I\, \alpha_{51}\, \beta_{11}\, {\omega_4}^2 + 12\, I\, \omega_1\, \alpha_{21}\, {\omega_2}^5\, \beta_{11} + 12\, I\, \alpha_{31}\, {\omega_2}^4\, \beta_{11}$$
$$- 12\, I\, \omega_1\, \alpha_{41}\, {\omega_2}^3\, \beta_{11} + 6\, I\, \omega_1\, \alpha_{41}\, \omega_2\, \beta_{31} - 6\, I\, \omega_1\, \alpha_{21}\, {\omega_2}^3\, \beta_{31}$$
$$- 12\, I\, \omega_1\, \alpha_{21}\, {\omega_2}^3\, \beta_{21}\, {\omega_4}^4 - 24\, I\, \omega_1\, \alpha_{21}\, {\omega_2}^5\, \beta_{21}\, {\omega_4}^2$$
$$+ \frac{3}{2} I\, \omega_1\, \alpha_{21}\, {\omega_2}^5\, \beta_{41}\, {\omega_4}^4 - 24\, I\, \omega_1\, \alpha_{41}\, \omega_2\, \beta_{11}\, {\omega_4}^2$$
$$+ 24\, I\, \omega_1\, \alpha_{21}\, {\omega_2}^3\, \beta_{11}\, {\omega_4}^2 + 24\, I\, \omega_1\, \alpha_{41}\, {\omega_2}^3\, \beta_{21}\, {\omega_4}^2$$
$$- \frac{3}{2} I\, \omega_1\, \alpha_{41}\, {\omega_2}^3\, \beta_{41}\, {\omega_4}^4 + 12\, I\, \omega_1\, \alpha_{41}\, \omega_2\, \beta_{21}\, {\omega_4}^4$$

$$D_6 = -\alpha_{51}\, c\, \omega_2 + \alpha_{31}\, {\omega_2}^3\, c - {\omega_2}^5\, c + \omega_1\, \alpha_{21}\, {\omega_2}^4\, c - \omega_1\, \alpha_{41}\, {\omega_2}^2\, c$$

$$F_1 = -\alpha_{51}\, \omega_1\, \alpha_{41} + 3\, {\omega_1}^2\, {\alpha_{21}}^2\, {\omega_3}^5 + 2\, \alpha_{51}\, \alpha_{31}\, \omega_3 + 3\, {\omega_3}^4\, \omega_1\, \alpha_{41}$$
$$- \omega_1\, \alpha_{41}\, {\omega_3}^2\, \alpha_{31} - \omega_1\, \alpha_{21}\, {\omega_3}^6 - 4\, \alpha_{51}\, {\omega_3}^3 - 2\, {\alpha_{31}}^2\, {\omega_3}^3$$
$$- \omega_1\, \alpha_{21}\, {\omega_3}^4\, \alpha_{31} - 4\, {\omega_3}^7 + {\omega_1}^2\, {\alpha_{41}}^2\, \omega_3 + 3\, \alpha_{51}\, \omega_1\, \alpha_{21}\, {\omega_3}^2$$
$$- 4\, {\omega_1}^2\, \alpha_{21}\, {\omega_3}^3\, \alpha_{41} + 6\, {\omega_3}^5\, \alpha_{31}$$

$$F_2 = 18\, I\, \alpha_{31}\, {\omega_3}^6\, \beta_{21} + 3\, I\, \alpha_{31}\, {\omega_3}^2\, \beta_{31} + 3\, I\, \omega_1\, \alpha_{41}\, \omega_3\, \beta_{31} + \frac{3}{4} I\, \alpha_{51}\, \beta_{41}\, {\omega_3}^6$$
$$- \frac{3}{4} I\, \omega_1\, \alpha_{41}\, {\omega_3}^7\, \beta_{41} - 18\, I\, {\omega_3}^8\, \beta_{21} + 18\, I\, \omega_1\, \alpha_{41}\, {\omega_3}^5\, \beta_{21} + \frac{3}{4} I\, {\omega_3}^{10}\, \beta_{41}$$
$$- 18\, I\, \alpha_{31}\, {\omega_3}^4\, \beta_{11} - 18\, I\, \omega_1\, \alpha_{41}\, {\omega_3}^3\, \beta_{11} - 3\, I\, \alpha_{51}\, \beta_{31} + 18\, I\, {\omega_3}^6\, \beta_{11}$$
$$- 18\, I\, \omega_1\, \alpha_{21}\, {\omega_3}^7\, \beta_{21} + 18\, I\, \omega_1\, \alpha_{21}\, {\omega_3}^5\, \beta_{11} - \frac{3}{4} I\, \alpha_{31}\, {\omega_3}^8\, \beta_{41}$$
$$- 3\, I\, \omega_1\, \alpha_{21}\, {\omega_3}^3\, \beta_{31} - 3\, I\, {\omega_3}^4\, \beta_{31} - 18\, I\, \alpha_{51}\, \beta_{21}\, {\omega_3}^4$$
$$+ \frac{3}{4} I\, \omega_1\, \alpha_{21}\, {\omega_3}^9\, \beta_{41} + 18\, I\, \alpha_{51}\, \beta_{11}\, {\omega_3}^2$$

$$
\begin{aligned}
F_3 = & -6\,I\,\omega_3^{\,4}\,\beta_{31} - 24\,I\,\alpha_{31}\,\omega_1^{\,2}\,\beta_{11}\,\omega_3^{\,2} - 24\,I\,\omega_1^{\,3}\,\alpha_{21}\,\omega_3^{\,5}\,\beta_{21} \\
& + 12\,I\,\alpha_{31}\,\omega_3^{\,2}\,\beta_{21}\,\omega_1^{\,4} - \frac{3}{2}I\,\alpha_{31}\,\omega_1^{\,4}\,\beta_{41}\,\omega_3^{\,4} - 24\,I\,\alpha_{51}\,\beta_{21}\,\omega_1^{\,2}\,\omega_3^{\,2} \\
& + \frac{3}{2}I\,\omega_1^{\,5}\,\alpha_{21}\,\omega_3^{\,5}\,\beta_{41} + 12\,I\,\omega_1\,\alpha_{21}\,\omega_3^{\,5}\,\beta_{11} - 6\,I\,\omega_1\,\alpha_{21}\,\omega_3^{\,3}\,\beta_{31} \\
& - 12\,I\,\omega_1^{\,5}\,\alpha_{21}\,\omega_3^{\,3}\,\beta_{21} + 24\,I\,\omega_1^{\,3}\,\alpha_{21}\,\omega_3^{\,3}\,\beta_{11} + \frac{3}{2}I\,\alpha_{51}\,\beta_{41}\,\omega_1^{\,4}\,\omega_3^{\,2} \\
& + 24\,I\,\alpha_{31}\,\omega_3^{\,4}\,\beta_{21}\,\omega_1^{\,2} + 6\,I\,\omega_1\,\alpha_{41}\,\omega_3\,\beta_{31} - \frac{3}{2}I\,\omega_1^{\,5}\,\alpha_{41}\,\omega_3^{\,3}\,\beta_{41} \\
& + 24\,I\,\omega_1^{\,3}\,\alpha_{41}\,\omega_3^{\,3}\,\beta_{21} - 12\,I\,\omega_1\,\alpha_{41}\,\omega_3^{\,3}\,\beta_{11} + 12\,I\,\omega_1^{\,5}\,\alpha_{41}\,\omega_3\,\beta_{21} \\
& - 24\,I\,\omega_1^{\,3}\,\alpha_{41}\,\omega_3\,\beta_{11} - 12\,I\,\omega_1^{\,4}\,\beta_{21}\,\omega_3^{\,4} + \frac{3}{2}I\,\omega_3^{\,6}\,\beta_{41}\,\omega_1^{\,4} \\
& + 24\,I\,\alpha_{51}\,\beta_{11}\,\omega_1^{\,2} + 24\,I\,\omega_3^{\,4}\,\beta_{11}\,\omega_1^{\,2} + 12\,I\,\alpha_{51}\,\beta_{11}\,\omega_3^{\,2} \\
& - 12\,I\,\alpha_{51}\,\beta_{21}\,\omega_1^{\,4} + 6\,I\,\alpha_{31}\,\omega_3^{\,2}\,\beta_{31} - 12\,I\,\alpha_{31}\,\omega_3^{\,4}\,\beta_{11} \\
& - 24\,I\,\omega_3^{\,6}\,\beta_{21}\,\omega_1^{\,2} - 6\,I\,\alpha_{51}\,\beta_{31} + 12\,I\,\omega_3^{\,6}\,\beta_{11}
\end{aligned}
$$

$$
\begin{aligned}
F_4 = & \; 12\,I\,\omega_1\,\alpha_{41}\,\omega_3\,\beta_{21}\,\omega_2^{\,4} - 6\,I\,\omega_3^{\,4}\,\beta_{31} + 12\,I\,\omega_1\,\alpha_{21}\,\omega_3^{\,5}\,\beta_{11} \\
& - 6\,I\,\omega_1\,\alpha_{21}\,\omega_3^{\,3}\,\beta_{31} + 6\,I\,\omega_1\,\alpha_{41}\,\omega_3\,\beta_{31} - 12\,I\,\omega_1\,\alpha_{41}\,\omega_3^{\,3}\,\beta_{11} \\
& - 12\,I\,\omega_3^{\,4}\,\beta_{21}\,\omega_2^{\,4} + \frac{3}{2}I\,\omega_3^{\,6}\,\beta_{41}\,\omega_2^{\,4} + 24\,I\,\omega_3^{\,4}\,\beta_{11}\,\omega_2^{\,2} \\
& - 24\,I\,\omega_3^{\,6}\,\beta_{21}\,\omega_2^{\,2} - 24\,I\,\alpha_{51}\,\beta_{21}\,\omega_2^{\,2}\,\omega_3^{\,2} + \frac{3}{2}I\,\alpha_{51}\,\beta_{41}\,\omega_2^{\,4}\,\omega_3^{\,2} \\
& - 24\,I\,\alpha_{31}\,\omega_3^{\,2}\,\beta_{11}\,\omega_2^{\,2} + 12\,I\,\alpha_{31}\,\omega_3^{\,2}\,\beta_{21}\,\omega_2^{\,4} - \frac{3}{2}I\,\alpha_{31}\,\omega_3^{\,4}\,\beta_{41}\,\omega_2^{\,4} \\
& + 24\,I\,\alpha_{31}\,\omega_3^{\,4}\,\beta_{21}\,\omega_2^{\,2} + 12\,I\,\alpha_{51}\,\beta_{11}\,\omega_3^{\,2} + 6\,I\,\alpha_{31}\,\omega_3^{\,2}\,\beta_{31} \\
& - 12\,I\,\alpha_{31}\,\omega_3^{\,4}\,\beta_{11} + 24\,I\,\alpha_{51}\,\beta_{11}\,\omega_2^{\,2} - 12\,I\,\alpha_{51}\,\beta_{21}\,\omega_2^{\,4} - 6\,I\,\alpha_{51}\,\beta_{31} \\
& + 12\,I\,\omega_3^{\,6}\,\beta_{11} - 12\,I\,\omega_1\,\alpha_{21}\,\omega_3^{\,3}\,\beta_{21}\,\omega_2^{\,4} + \frac{3}{2}I\,\omega_1\,\alpha_{21}\,\omega_3^{\,5}\,\beta_{41}\,\omega_2^{\,4} \\
& + 24\,I\,\omega_1\,\alpha_{21}\,\omega_3^{\,3}\,\beta_{11}\,\omega_2^{\,2} - 24\,I\,\omega_1\,\alpha_{41}\,\omega_3\,\beta_{11}\,\omega_2^{\,2} \\
& - 24\,I\,\omega_1\,\alpha_{21}\,\omega_3^{\,5}\,\beta_{21}\,\omega_2^{\,2} + 24\,I\,\omega_1\,\alpha_{41}\,\omega_3^{\,3}\,\beta_{21}\,\omega_2^{\,2} \\
& - \frac{3}{2}I\,\omega_1\,\alpha_{41}\,\omega_3^{\,3}\,\beta_{41}\,\omega_2^{\,4}
\end{aligned}
$$

$$
\begin{aligned}
F_5 = & -12\,I\,\omega_1\,\alpha_{21}\,\omega_3^{\,3}\,\beta_{21}\,\omega_4^{\,4} - 24\,I\,\omega_1\,\alpha_{21}\,\omega_3^{\,5}\,\beta_{21}\,\omega_4^{\,2} \\
& + \frac{3}{2}I\,\omega_1\,\alpha_{21}\,\omega_3^{\,5}\,\beta_{41}\,\omega_4^{\,4} + 24\,I\,\omega_1\,\alpha_{21}\,\omega_3^{\,3}\,\beta_{11}\,\omega_4^{\,2} \\
& - \frac{3}{2}I\,\omega_1\,\alpha_{41}\,\omega_3^{\,3}\,\beta_{41}\,\omega_4^{\,4} + 24\,I\,\omega_1\,\alpha_{41}\,\omega_3^{\,3}\,\beta_{21}\,\omega_4^{\,2} - 6\,I\,\omega_3^{\,4}\,\beta_{31} \\
& - 24\,I\,\omega_1\,\alpha_{41}\,\omega_3\,\beta_{11}\,\omega_4^{\,2} + 12\,I\,\omega_1\,\alpha_{41}\,\omega_3\,\beta_{21}\,\omega_4^{\,4} + 12\,I\,\omega_1\,\alpha_{21}\,\omega_3^{\,5}\,\beta_{11} \\
& - 6\,I\,\omega_1\,\alpha_{21}\,\omega_3^{\,3}\,\beta_{31} + 6\,I\,\omega_1\,\alpha_{41}\,\omega_3\,\beta_{31} - 12\,I\,\omega_1\,\alpha_{41}\,\omega_3^{\,3}\,\beta_{11}
\end{aligned}
$$

$$
\begin{aligned}
&- 12\, I\, \alpha_{51}\, \beta_{21}\, \omega_4^{\,4} + 24\, I\, \alpha_{51}\, \beta_{11}\, \omega_4^{\,2} + 24\, I\, \omega_3^{\,4}\, \beta_{11}\, \omega_4^{\,2} \\
&+ \frac{3}{2} I\, \omega_3^{\,6}\, \beta_{41}\, \omega_4^{\,4} - 12\, I\, \omega_3^{\,4}\, \beta_{21}\, \omega_4^{\,4} - 24\, I\, \omega_3^{\,6}\, \beta_{21}\, \omega_4^{\,2} \\
&- \frac{3}{2} I\, \alpha_{31}\, \omega_3^{\,4}\, \beta_{41}\, \omega_4^{\,4} - 24\, I\, \alpha_{51}\, \beta_{21}\, \omega_3^{\,2}\, \omega_4^{\,2} + \frac{3}{2} I\, \alpha_{51}\, \beta_{41}\, \omega_3^{\,2}\, \omega_4^{\,4} \\
&+ 12\, I\, \alpha_{31}\, \omega_3^{\,2}\, \beta_{21}\, \omega_4^{\,4} - 24\, I\, \alpha_{31}\, \omega_3^{\,2}\, \beta_{11}\, \omega_4^{\,2} + 12\, I\, \alpha_{51}\, \beta_{11}\, \omega_3^{\,2} \\
&+ 24\, I\, \alpha_{31}\, \omega_3^{\,4}\, \beta_{21}\, \omega_4^{\,2} + 6\, I\, \alpha_{31}\, \omega_3^{\,2}\, \beta_{31} - 12\, I\, \alpha_{31}\, \omega_3^{\,4}\, \beta_{11} - 6\, I\, \alpha_{51}\, \beta_{31} \\
&+ 12\, I\, \omega_3^{\,6}\, \beta_{11}
\end{aligned}
$$

$$
F_6 = -\omega_1\, \alpha_{41}\, \omega_3^{\,2}\, c + \omega_1\, \alpha_{21}\, \omega_3^{\,4}\, c + \alpha_{51}\, c\, \omega_3 - \alpha_{31}\, \omega_3^{\,3}\, c + \omega_3^{\,5}\, c
$$

$$
\begin{aligned}
G_1 = &-\omega_4^{\,6}\, \omega_1\, \alpha_{21} + 2\, \alpha_{31}^{\,2}\, \omega_4^{\,3} - \omega_1^{\,2}\, \alpha_{41}^{\,2}\, \omega_4 + 4\, \omega_1^{\,2}\, \alpha_{41}\, \omega_4^{\,3}\, \alpha_{21} \\
&- \omega_1\, \alpha_{41}\, \omega_4^{\,2}\, \alpha_{31} - \alpha_{51}\, \omega_1\, \alpha_{41} + 4\, \alpha_{51}\, \omega_4^{\,3} - 6\, \omega_4^{\,5}\, \alpha_{31} \\
&+ 3\, \alpha_{51}\, \omega_1\, \alpha_{21}\, \omega_4^{\,2} - \alpha_{31}\, \omega_4^{\,4}\, \omega_1\, \alpha_{21} - 3\, \omega_1^{\,2}\, \alpha_{21}^{\,2}\, \omega_4^{\,5} + 3\, \omega_4^{\,4}\, \omega_1\, \alpha_{41} \\
&+ 4\, \omega_4^{\,7} - 2\, \alpha_{51}\, \alpha_{31}\, \omega_4
\end{aligned}
$$

$$
\begin{aligned}
G_2 = &-3\, I\, \omega_1\, \alpha_{21}\, \omega_4^{\,3}\, \beta_{31} + 18\, I\, \omega_1\, \alpha_{41}\, \omega_4^{\,5}\, \beta_{21} - 18\, I\, \omega_1\, \alpha_{41}\, \omega_4^{\,3}\, \beta_{11} \\
&+ 18\, I\, \alpha_{51}\, \beta_{21}\, \omega_4^{\,4} + 3\, I\, \omega_4^{\,4}\, \beta_{31} - 18\, I\, \alpha_{31}\, \omega_4^{\,6}\, \beta_{21} + \frac{3}{4} I\, \alpha_{31}\, \omega_4^{\,8}\, \beta_{41} \\
&+ 3\, I\, \omega_1\, \alpha_{41}\, \omega_4\, \beta_{31} - 18\, I\, \omega_1\, \alpha_{21}\, \omega_4^{\,7}\, \beta_{21} + 3\, I\, \alpha_{51}\, \beta_{31} \\
&+ \frac{3}{4} I\, \omega_1\, \alpha_{21}\, \omega_4^{\,9}\, \beta_{41} + 18\, I\, \alpha_{31}\, \omega_4^{\,4}\, \beta_{11} - \frac{3}{4} I\, \omega_4^{\,10}\, \beta_{41} \\
&+ 18\, I\, \omega_1\, \alpha_{21}\, \omega_4^{\,5}\, \beta_{11} + 18\, I\, \omega_4^{\,8}\, \beta_{21} - 18\, I\, \omega_4^{\,6}\, \beta_{11} - \frac{3}{4} I\, \alpha_{51}\, \beta_{41}\, \omega_4^{\,6} \\
&- 18\, I\, \alpha_{51}\, \beta_{11}\, \omega_4^{\,2} - \frac{3}{4} I\, \omega_1\, \alpha_{41}\, \omega_4^{\,7}\, \beta_{41} - 3\, I\, \alpha_{31}\, \omega_4^{\,2}\, \beta_{31}
\end{aligned}
$$

$$
\begin{aligned}
G_3 = &\, 6\, I\, \omega_4^{\,4}\, \beta_{31} + 6\, I\, \alpha_{51}\, \beta_{31} + 12\, I\, \alpha_{31}\, \omega_4^{\,4}\, \beta_{11} - 12\, I\, \alpha_{51}\, \beta_{11}\, \omega_4^{\,2} \\
&- 6\, I\, \alpha_{31}\, \omega_4^{\,2}\, \beta_{31} + 12\, I\, \omega_4^{\,4}\, \beta_{21}\, \omega_1^{\,4} - \frac{3}{2} I\, \omega_4^{\,6}\, \beta_{41}\, \omega_1^{\,4} - 24\, I\, \omega_4^{\,4}\, \beta_{11}\, \omega_1^{\,2} \\
&+ 24\, I\, \omega_4^{\,6}\, \beta_{21}\, \omega_1^{\,2} + 12\, I\, \alpha_{51}\, \beta_{21}\, \omega_1^{\,4} - 24\, I\, \alpha_{51}\, \beta_{11}\, \omega_1^{\,2} \\
&- 12\, I\, \alpha_{31}\, \omega_4^{\,2}\, \beta_{21}\, \omega_1^{\,4} + \frac{3}{2} I\, \alpha_{31}\, \omega_4^{\,4}\, \beta_{41}\, \omega_1^{\,4} - 24\, I\, \omega_1^{\,3}\, \alpha_{21}\, \omega_4^{\,5}\, \beta_{21} \\
&- 24\, I\, \omega_1^{\,3}\, \alpha_{41}\, \omega_4\, \beta_{11} + 24\, I\, \omega_1^{\,3}\, \alpha_{21}\, \omega_4^{\,3}\, \beta_{11} + 6\, I\, \omega_1\, \alpha_{41}\, \omega_4\, \beta_{31}
\end{aligned}
$$

$$+\frac{3}{2} I \omega_1^{\,5} \alpha_{21} \omega_4^{\,5} \beta_{41} - 12\, I \omega_1^{\,5} \alpha_{21} \omega_4^{\,3} \beta_{21} - \frac{3}{2} I \omega_1^{\,5} \alpha_{41} \omega_4^{\,3} \beta_{41}$$
$$+ 12\, I \omega_1^{\,5} \alpha_{41} \omega_4 \beta_{21} - 6\, I \omega_1 \alpha_{21} \omega_4^{\,3} \beta_{31} + 24\, I \alpha_{51} \beta_{21} \omega_1^{\,2} \omega_4^{\,2}$$
$$+ 12\, I \omega_1 \alpha_{21} \omega_4^{\,5} \beta_{11} + 24\, I \omega_1^{\,3} \alpha_{41} \omega_4^{\,3} \beta_{21} - \frac{3}{2} I \alpha_{51} \beta_{41} \omega_1^{\,4} \omega_4^{\,2}$$
$$+ 24\, I \alpha_{31} \omega_4^{\,2} \beta_{11} \omega_1^{\,2} - 12\, I \omega_1 \alpha_{41} \omega_4^{\,3} \beta_{11} - 24\, I \alpha_{31} \omega_4^{\,4} \beta_{21} \omega_1^{\,2}$$
$$- 12\, I \omega_4^{\,6} \beta_{11}$$

$$G_4 = 6\, I \omega_4^{\,4} \beta_{31} + 24\, I \alpha_{51} \beta_{21} \omega_2^{\,2} \omega_4^{\,2} + 24\, I \alpha_{31} \omega_2^{\,2} \beta_{11} \omega_4^{\,2}$$
$$+\frac{3}{2} I \alpha_{31} \omega_2^{\,4} \beta_{41} \omega_4^{\,4} + 6\, I \alpha_{51} \beta_{31} + 12\, I \omega_2^{\,4} \beta_{21} \omega_4^{\,4}$$
$$+ 12\, I \omega_1 \alpha_{41} \omega_4 \beta_{21} \omega_2^{\,4} - 24\, I \omega_1 \alpha_{21} \omega_4^{\,5} \beta_{21} \omega_2^{\,2}$$
$$+ 24\, I \omega_1 \alpha_{21} \omega_4^{\,3} \beta_{11} \omega_2^{\,2} - \frac{3}{2} I \omega_1 \alpha_{41} \omega_4^{\,3} \beta_{41} \omega_2^{\,4}$$
$$+ 24\, I \omega_1 \alpha_{41} \omega_4^{\,3} \beta_{21} \omega_2^{\,2} - 12\, I \omega_1 \alpha_{21} \omega_4^{\,3} \beta_{21} \omega_2^{\,4}$$
$$+\frac{3}{2} I \omega_1 \alpha_{21} \omega_4^{\,5} \beta_{41} \omega_2^{\,4} - 24\, I \omega_1 \alpha_{41} \omega_4 \beta_{11} \omega_2^{\,2} + 12\, I \alpha_{31} \omega_4^{\,4} \beta_{11}$$
$$- 12\, I \alpha_{51} \beta_{11} \omega_4^{\,2} - 6\, I \alpha_{31} \omega_4^{\,2} \beta_{31} + 6\, I \omega_1 \alpha_{41} \omega_4 \beta_{31}$$
$$- 6\, I \omega_1 \alpha_{21} \omega_4^{\,3} \beta_{31} + 12\, I \omega_1 \alpha_{21} \omega_4^{\,5} \beta_{11} - 12\, I \omega_1 \alpha_{41} \omega_4^{\,3} \beta_{11}$$
$$- 24\, I \alpha_{31} \omega_4^{\,4} \beta_{21} \omega_2^{\,2} - \frac{3}{2} I \alpha_{51} \beta_{41} \omega_2^{\,4} \omega_4^{\,2} - 12\, I \alpha_{31} \omega_4^{\,2} \beta_{21} \omega_2^{\,4}$$
$$- 12\, I \omega_4^{\,6} \beta_{11} - 24\, I \alpha_{51} \beta_{11} \omega_2^{\,2} - 24\, I \omega_4^{\,4} \beta_{11} \omega_2^{\,2} + 24\, I \omega_4^{\,6} \beta_{21} \omega_2^{\,2}$$
$$+ 12\, I \alpha_{51} \beta_{21} \omega_2^{\,4} - \frac{3}{2} I \omega_4^{\,6} \beta_{41} \omega_2^{\,4}$$

$$G_5 = 6\, I \omega_4^{\,4} \beta_{31} + 6\, I \alpha_{51} \beta_{31} - 24\, I \omega_1 \alpha_{21} \omega_4^{\,5} \beta_{21} \omega_3^{\,2}$$
$$+ 24\, I \alpha_{31} \omega_4^{\,2} \beta_{11} \omega_3^{\,2} + 24\, I \alpha_{51} \beta_{21} \omega_3^{\,2} \omega_4^{\,2} - 12\, I \alpha_{31} \omega_4^{\,2} \beta_{21} \omega_3^{\,4}$$
$$- 24\, I \alpha_{31} \omega_4^{\,4} \beta_{21} \omega_3^{\,2} + \frac{3}{2} I \alpha_{31} \omega_4^{\,4} \beta_{41} \omega_3^{\,4} - \frac{3}{2} I \alpha_{51} \beta_{41} \omega_3^{\,4} \omega_4^{\,2}$$
$$+ 12\, I \alpha_{31} \omega_4^{\,4} \beta_{11} - 12\, I \alpha_{51} \beta_{11} \omega_4^{\,2} - 6\, I \alpha_{31} \omega_4^{\,2} \beta_{31}$$
$$- 24\, I \omega_1 \alpha_{41} \omega_4 \beta_{11} \omega_3^{\,2} - \frac{3}{2} I \omega_1 \alpha_{41} \omega_4^{\,3} \beta_{41} \omega_3^{\,4}$$
$$- 12\, I \omega_1 \alpha_{21} \omega_4^{\,3} \beta_{21} \omega_3^{\,4} + 24\, I \omega_1 \alpha_{21} \omega_4^{\,3} \beta_{11} \omega_3^{\,2}$$

$$+\frac{3}{2} I\,\omega_1\,\alpha_{21}\,\omega_4^{\,5}\,\beta_{41}\,\omega_3^{\,4} + 12\,I\,\omega_1\,\alpha_{41}\,\omega_4\,\beta_{21}\,\omega_3^{\,4}$$

$$+ 24\,I\,\omega_1\,\alpha_{41}\,\omega_4^{\,3}\,\beta_{21}\,\omega_3^{\,2} + 6\,I\,\omega_1\,\alpha_{41}\,\omega_4\,\beta_{31} - 6\,I\,\omega_1\,\alpha_{21}\,\omega_4^{\,3}\,\beta_{31}$$

$$+ 12\,I\,\omega_1\,\alpha_{21}\,\omega_4^{\,5}\,\beta_{11} - 12\,I\,\omega_1\,\alpha_{41}\,\omega_4^{\,3}\,\beta_{11} - 12\,I\,\omega_4^{\,6}\,\beta_{11}$$

$$- 24\,I\,\alpha_{51}\,\beta_{11}\,\omega_3^{\,2} + 12\,I\,\alpha_{51}\,\beta_{21}\,\omega_3^{\,4} - \frac{3}{2} I\,\omega_4^{\,6}\,\beta_{41}\,\omega_3^{\,4}$$

$$+ 12\,I\,\omega_4^{\,4}\,\beta_{21}\,\omega_3^{\,4} - 24\,I\,\omega_4^{\,4}\,\beta_{11}\,\omega_3^{\,2} + 24\,I\,\omega_4^{\,6}\,\beta_{21}\,\omega_3^{\,2}$$

$$G_6 = -\omega_4^{\,5}\,c - \omega_1\,\alpha_{41}\,\omega_4^{\,2}\,c + \omega_1\,\alpha_{21}\,\omega_4^{\,4}\,c - \alpha_{51}\,c\,\omega_4 + \alpha_{31}\,\omega_4^{\,3}\,c$$

<u>Appendix F</u>: Coefficients of Solvability conditions for Chapter 4 for the case of $\Omega = \omega_2$

$$c_1 = \frac{C_2}{C_1}\ ,\ c_2 = \frac{C_3}{C_1}\ ,\ c_3 = \frac{C_4}{C_1}\ ,\ c_4 = \frac{C_5}{C_1}\ ,\ c_5 = \frac{C_6}{C_1}$$

$$d_1 = \frac{D_2}{D_1}\ ,\ d_2 = \frac{D_3}{D_1}\ ,\ d_3 = \frac{D_4}{D_1}\ ,\ d_4 = \frac{D_5}{D_1}\ ,\ d_5 = \frac{D_6}{D_1}\ ,\ d_6 = \frac{D_7}{D_1}$$

$$f_1 = \frac{F_2}{F_1}\ ,\ f_2 = \frac{F_3}{F_1}\ ,\ f_3 = \frac{F_4}{F_1}\ ,\ f_4 = \frac{F_5}{F_1}\ ,\ f_5 = \frac{F_6}{F_1}$$

$$g_1 = \frac{G_2}{G_1}\ ,\ g_2 = \frac{G_3}{G_1}\ ,\ g_3 = \frac{G_4}{G_1}\ ,\ g_4 = \frac{G_5}{G_1}\ ,\ g_5 = \frac{G_6}{G_1}$$

$$\begin{aligned}
C_1 = {} & -\alpha_{31}\,\omega_1^{\,2}\,\omega_2\,\alpha_{41} + 3\,\omega_2^{\,2}\,\alpha_{21}^{\,2}\,\omega_1^{\,5} + \omega_2^{\,2}\,\alpha_{41}^{\,2}\,\omega_1 - \omega_2\,\alpha_{21}\,\omega_1^{\,6} \\
& - \alpha_{51}\,\omega_2\,\alpha_{41} - \alpha_{31}\,\omega_1^{\,4}\,\omega_2\,\alpha_{21} - 4\,\omega_1^{\,7} + 3\,\omega_1^{\,4}\,\omega_2\,\alpha_{41} + 2\,\alpha_{51}\,\alpha_{31}\,\omega_1 \\
& - 4\,\omega_2^{\,2}\,\alpha_{41}\,\omega_1^{\,3}\,\alpha_{21} + 3\,\alpha_{51}\,\omega_2\,\alpha_{21}\,\omega_1^{\,2} + 6\,\omega_1^{\,5}\,\alpha_{31} - 4\,\alpha_{51}\,\omega_1^{\,3}
\end{aligned}$$

$$\begin{aligned}
C_2 = {} & -18\,\alpha_{31}\,\omega_1^{\,4}\,\beta_{11} - 18\,\alpha_{51}\,\beta_{21}\,\omega_1^{\,4} - \frac{3}{4}\,\omega_2\,\alpha_{41}\,\omega_1^{\,7}\,\beta_{41} \\
& - 18\,\omega_2\,\alpha_{41}\,\omega_1^{\,3}\,\beta_{11} - 3\,\omega_2\,\alpha_{21}\,\omega_1^{\,3}\,\beta_{31} + 18\,\omega_2\,\alpha_{41}\,\omega_1^{\,5}\,\beta_{21} \\
& + 3\,\alpha_{31}\,\omega_1^{\,2}\,\beta_{31} + \frac{3}{4}\,\omega_1^{\,10}\,\beta_{41} - 3\,\alpha_{51}\,\beta_{31} + 3\,\omega_2\,\alpha_{41}\,\omega_1\,\beta_{31} \\
& - 18\,\omega_2\,\alpha_{21}\,\omega_1^{\,7}\,\beta_{21} + 18\,\omega_1^{\,6}\,\beta_{11} - 18\,\omega_1^{\,8}\,\beta_{21} + 18\,\alpha_{51}\,\beta_{11}\,\omega_1^{\,2} \\
& - \frac{3}{4}\,\alpha_{31}\,\omega_1^{\,8}\,\beta_{41} - 3\,\omega_1^{\,4}\,\beta_{31} + 18\,\alpha_{31}\,\omega_1^{\,6}\,\beta_{21} + \frac{3}{4}\,\omega_2\,\alpha_{21}\,\omega_1^{\,9}\,\beta_{41} \\
& + \frac{3}{4}\,\alpha_{51}\,\beta_{41}\,\omega_1^{\,6} + 18\,\omega_2\,\alpha_{21}\,\omega_1^{\,5}\,\beta_{11}
\end{aligned}$$

$$\begin{aligned}
C_3 = {} & -24\,\omega_1^{\,6}\,\beta_{21}\,\omega_2^{\,2} - 24\,\omega_2^{\,3}\,\alpha_{41}\,\omega_1\,\beta_{11} - 12\,\alpha_{31}\,\omega_1^{\,4}\,\beta_{11} - 12\,\omega_1^{\,4}\,\beta_{21}\,\omega_2^{\,4} \\
& + \frac{3}{2}\,\omega_1^{\,6}\,\beta_{41}\,\omega_2^{\,4} - 12\,\alpha_{51}\,\beta_{21}\,\omega_2^{\,4} + 24\,\omega_1^{\,4}\,\beta_{11}\,\omega_2^{\,2} + 24\,\alpha_{51}\,\beta_{11}\,\omega_2^{\,2} \\
& + \frac{3}{2}\,\alpha_{51}\,\beta_{41}\,\omega_1^{\,2}\,\omega_2^{\,4} + 12\,\omega_1^{\,6}\,\beta_{11} - 6\,\alpha_{51}\,\beta_{31} + \frac{3}{2}\,\omega_2^{\,5}\,\alpha_{21}\,\omega_1^{\,5}\,\beta_{41} \\
& + 12\,\omega_2^{\,5}\,\alpha_{41}\,\omega_1\,\beta_{21} + 24\,\omega_2^{\,3}\,\alpha_{41}\,\omega_1^{\,3}\,\beta_{21} + 6\,\alpha_{31}\,\omega_1^{\,2}\,\beta_{31}
\end{aligned}$$

$$
\begin{aligned}
&- 24\,\alpha_{51}\,\beta_{21}\,\omega_1^{\,2}\,\omega_2^{\,2} - 12\,\omega_2^{\,5}\,\alpha_{21}\,\omega_1^{\,3}\,\beta_{21} - \frac{3}{2}\,\omega_2^{\,5}\,\alpha_{41}\,\omega_1^{\,3}\,\beta_{41} \\
&+ 24\,\omega_2^{\,3}\,\alpha_{21}\,\omega_1^{\,3}\,\beta_{11} - \frac{3}{2}\,\alpha_{31}\,\omega_1^{\,4}\,\beta_{41}\,\omega_2^{\,4} - 24\,\alpha_{31}\,\omega_1^{\,2}\,\beta_{11}\,\omega_2^{\,2} \\
&+ 12\,\alpha_{31}\,\omega_1^{\,2}\,\beta_{21}\,\omega_2^{\,4} - 24\,\omega_2^{\,3}\,\alpha_{21}\,\omega_1^{\,5}\,\beta_{21} + 24\,\alpha_{31}\,\omega_1^{\,4}\,\beta_{21}\,\omega_2^{\,2} \\
&+ 12\,\alpha_{51}\,\beta_{11}\,\omega_1^{\,2} + 12\,\omega_2\,\alpha_{21}\,\omega_1^{\,5}\,\beta_{11} + 6\,\omega_2\,\alpha_{41}\,\omega_1\,\beta_{31} \\
&- 6\,\omega_2\,\alpha_{21}\,\omega_1^{\,3}\,\beta_{31} - 12\,\omega_2\,\alpha_{41}\,\omega_1^{\,3}\,\beta_{11} - 6\,\omega_1^{\,4}\,\beta_{31}
\end{aligned}
$$

$$
\begin{aligned}
C_4 = {} & 24\,\alpha_{51}\,\beta_{11}\,\omega_3^{\,2} - 12\,\omega_1^{\,4}\,\beta_{21}\,\omega_3^{\,4} - \frac{3}{2}\,\alpha_{31}\,\omega_1^{\,4}\,\beta_{41}\,\omega_3^{\,4} - 12\,\alpha_{31}\,\omega_1^{\,4}\,\beta_{11} \\
&+ 24\,\omega_1^{\,4}\,\beta_{11}\,\omega_3^{\,2} - 24\,\alpha_{31}\,\omega_1^{\,2}\,\beta_{11}\,\omega_3^{\,2} + \frac{3}{2}\,\omega_1^{\,6}\,\beta_{41}\,\omega_3^{\,4} - 24\,\omega_1^{\,6}\,\beta_{21}\,\omega_3^{\,2} \\
&+ \frac{3}{2}\,\alpha_{51}\,\beta_{41}\,\omega_1^{\,2}\,\omega_3^{\,4} - 12\,\alpha_{51}\,\beta_{21}\,\omega_3^{\,4} - 24\,\omega_2\,\alpha_{21}\,\omega_1^{\,5}\,\beta_{21}\,\omega_3^{\,2} \\
&+ 12\,\omega_2\,\alpha_{41}\,\omega_1\,\beta_{21}\,\omega_3^{\,4} + 24\,\alpha_{31}\,\omega_1^{\,4}\,\beta_{21}\,\omega_3^{\,2} - 24\,\alpha_{51}\,\beta_{21}\,\omega_1^{\,2}\,\omega_3^{\,2} \\
&+ 12\,\omega_1^{\,6}\,\beta_{11} + 12\,\alpha_{31}\,\omega_1^{\,2}\,\beta_{21}\,\omega_3^{\,4} - 6\,\alpha_{51}\,\beta_{31} - 12\,\omega_2\,\alpha_{21}\,\omega_1^{\,3}\,\beta_{21}\,\omega_3^{\,4} \\
&+ 24\,\omega_2\,\alpha_{41}\,\omega_1^{\,3}\,\beta_{21}\,\omega_3^{\,2} - 24\,\omega_2\,\alpha_{41}\,\omega_1\,\beta_{11}\,\omega_3^{\,2} + \frac{3}{2}\,\omega_2\,\alpha_{21}\,\omega_1^{\,5}\,\beta_{41}\,\omega_3^{\,4} \\
&+ 24\,\omega_2\,\alpha_{21}\,\omega_1^{\,3}\,\beta_{11}\,\omega_3^{\,2} - \frac{3}{2}\,\omega_2\,\alpha_{41}\,\omega_1^{\,3}\,\beta_{41}\,\omega_3^{\,4} + 6\,\alpha_{31}\,\omega_1^{\,2}\,\beta_{31} \\
&+ 12\,\alpha_{51}\,\beta_{11}\,\omega_1^{\,2} + 12\,\omega_2\,\alpha_{21}\,\omega_1^{\,5}\,\beta_{11} + 6\,\omega_2\,\alpha_{41}\,\omega_1\,\beta_{31} \\
&- 6\,\omega_2\,\alpha_{21}\,\omega_1^{\,3}\,\beta_{31} - 12\,\omega_2\,\alpha_{41}\,\omega_1^{\,3}\,\beta_{11} - 6\,\omega_1^{\,4}\,\beta_{31}
\end{aligned}
$$

$$
\begin{aligned}
C_5 = {} & -12\,\alpha_{51}\,\beta_{21}\,\omega_4^{\,4} + 24\,\alpha_{31}\,\omega_1^{\,4}\,\beta_{21}\,\omega_4^{\,2} - 12\,\alpha_{31}\,\omega_1^{\,4}\,\beta_{11} \\
&+ 24\,\omega_1^{\,4}\,\beta_{11}\,\omega_4^{\,2} - 24\,\alpha_{31}\,\omega_1^{\,2}\,\beta_{11}\,\omega_4^{\,2} + \frac{3}{2}\,\omega_1^{\,6}\,\beta_{41}\,\omega_4^{\,4} + 24\,\alpha_{51}\,\beta_{11}\,\omega_4^{\,2} \\
&+ 12\,\omega_1^{\,6}\,\beta_{11} - 24\,\omega_1^{\,6}\,\beta_{21}\,\omega_4^{\,2} - 12\,\omega_1^{\,4}\,\beta_{21}\,\omega_4^{\,4} - 6\,\alpha_{51}\,\beta_{31} \\
&- \frac{3}{2}\,\alpha_{31}\,\omega_1^{\,4}\,\beta_{41}\,\omega_4^{\,4} + 6\,\alpha_{31}\,\omega_1^{\,2}\,\beta_{31} - 12\,\omega_2\,\alpha_{21}\,\omega_1^{\,3}\,\beta_{21}\,\omega_4^{\,4} \\
&+ 24\,\omega_2\,\alpha_{21}\,\omega_1^{\,3}\,\beta_{11}\,\omega_4^{\,2} + 12\,\omega_2\,\alpha_{41}\,\omega_1\,\beta_{21}\,\omega_4^{\,4} \\
&+ 24\,\omega_2\,\alpha_{41}\,\omega_1^{\,3}\,\beta_{21}\,\omega_4^{\,2} - 24\,\omega_2\,\alpha_{41}\,\omega_1\,\beta_{11}\,\omega_4^{\,2} - \frac{3}{2}\,\omega_2\,\alpha_{41}\,\omega_1^{\,3}\,\beta_{41}\,\omega_4^{\,4} \\
&- 24\,\omega_2\,\alpha_{21}\,\omega_1^{\,5}\,\beta_{21}\,\omega_4^{\,2} + \frac{3}{2}\,\omega_2\,\alpha_{21}\,\omega_1^{\,5}\,\beta_{41}\,\omega_4^{\,4} + 12\,\alpha_{51}\,\beta_{11}\,\omega_1^{\,2} \\
&+ 12\,\omega_2\,\alpha_{21}\,\omega_1^{\,5}\,\beta_{11} + 6\,\omega_2\,\alpha_{41}\,\omega_1\,\beta_{31} - 6\,\omega_2\,\alpha_{21}\,\omega_1^{\,3}\,\beta_{31} \\
&- 12\,\omega_2\,\alpha_{41}\,\omega_1^{\,3}\,\beta_{11} + 12\,\alpha_{31}\,\omega_1^{\,2}\,\beta_{21}\,\omega_4^{\,4} - 24\,\alpha_{51}\,\beta_{21}\,\omega_1^{\,2}\,\omega_4^{\,2} \\
&- 6\,\omega_1^{\,4}\,\beta_{31} + \frac{3}{2}\,\alpha_{51}\,\beta_{41}\,\omega_1^{\,2}\,\omega_4^{\,4}
\end{aligned}
$$

$$
C_6 = -\alpha_{31}\,\omega_1^{\,3}\,c + \alpha_{51}\,c\,\omega_1 + \omega_1^{\,5}\,c - \omega_2\,\alpha_{41}\,\omega_1^{\,2}\,c + \omega_2\,\alpha_{21}\,\omega_1^{\,4}\,c
$$

$$
\begin{aligned}
D_1 = {} & -\omega_2^{\,3}\,\alpha_{41}^{\,2} - 6\,\omega_2^{\,5}\,\alpha_{31} - \alpha_{31}\,\omega_2^{\,3}\,\alpha_{41} + 3\,\omega_2^{\,5}\,\alpha_{41} + 2\,\alpha_{31}^{\,2}\,\omega_2^{\,3} \\
& - 3\,\omega_2^{\,7}\,\alpha_{21}^{\,2} + 4\,\omega_2^{\,7} - 2\,\alpha_{51}\,\alpha_{31}\,\omega_2 - \omega_2^{\,7}\,\alpha_{21} + 4\,\alpha_{51}\,\omega_2^{\,3} \\
& + 3\,\alpha_{51}\,\omega_2^{\,3}\,\alpha_{21} + 4\,\omega_2^{\,5}\,\alpha_{41}\,\alpha_{21} - \alpha_{51}\,\omega_2\,\alpha_{41} - \alpha_{31}\,\omega_2^{\,5}\,\alpha_{21}
\end{aligned}
$$

$$
\begin{aligned}
D_2 = {} & 3\,\omega_2^{\,2}\,\alpha_{41}\,\beta_{31} + 18\,\omega_2^{\,8}\,\beta_{21} + 18\,\omega_2^{\,6}\,\alpha_{21}\,\beta_{11} + 18\,\alpha_{51}\,\beta_{21}\,\omega_2^{\,4} \\
& - 18\,\omega_2^{\,8}\,\alpha_{21}\,\beta_{21} - \frac{3}{4}\,\omega_2^{\,8}\,\alpha_{41}\,\beta_{41} - \frac{3}{4}\,\omega_2^{\,10}\,\beta_{41} + 18\,\alpha_{31}\,\omega_2^{\,4}\,\beta_{11} \\
& - \frac{3}{4}\,\alpha_{51}\,\beta_{41}\,\omega_2^{\,6} - 3\,\alpha_{31}\,\omega_2^{\,2}\,\beta_{31} + 18\,\omega_2^{\,6}\,\alpha_{41}\,\beta_{21} + 3\,\alpha_{51}\,\beta_{31} + 3\,\omega_2^{\,4}\,\beta_{31} \\
& + \frac{3}{4}\,\alpha_{31}\,\omega_2^{\,8}\,\beta_{41} - 3\,\omega_2^{\,4}\,\alpha_{21}\,\beta_{31} - 18\,\omega_2^{\,4}\,\alpha_{41}\,\beta_{11} - 18\,\alpha_{31}\,\omega_2^{\,6}\,\beta_{21} \\
& + \frac{3}{4}\,\omega_2^{\,10}\,\alpha_{21}\,\beta_{41} - 18\,\alpha_{51}\,\beta_{11}\,\omega_2^{\,2} - 18\,\omega_2^{\,6}\,\beta_{11}
\end{aligned}
$$

$$
\begin{aligned}
D_3 = {} & 12\,\alpha_{31}\,\omega_2^{\,4}\,\beta_{11} + 12\,\alpha_{51}\,\beta_{21}\,\omega_1^{\,4} + 12\,\omega_2^{\,6}\,\alpha_{21}\,\beta_{11} + 12\,\omega_1^{\,4}\,\beta_{21}\,\omega_2^{\,4} \\
& - 6\,\omega_2^{\,4}\,\alpha_{21}\,\beta_{31} + 12\,\omega_2^{\,2}\,\alpha_{41}\,\beta_{21}\,\omega_1^{\,4} - 24\,\omega_2^{\,2}\,\alpha_{41}\,\beta_{11}\,\omega_1^{\,2} \\
& + 24\,\omega_2^{\,4}\,\alpha_{41}\,\beta_{21}\,\omega_1^{\,2} - 12\,\omega_2^{\,4}\,\alpha_{21}\,\beta_{21}\,\omega_1^{\,4} - 24\,\omega_2^{\,6}\,\alpha_{21}\,\beta_{21}\,\omega_1^{\,2} \\
& + \frac{3}{2}\,\omega_2^{\,6}\,\alpha_{21}\,\beta_{41}\,\omega_1^{\,4} - \frac{3}{2}\,\omega_2^{\,4}\,\alpha_{41}\,\beta_{41}\,\omega_1^{\,4} - \frac{3}{2}\,\alpha_{51}\,\beta_{41}\,\omega_1^{\,4}\,\omega_2^{\,2} \\
& + 24\,\omega_2^{\,4}\,\alpha_{21}\,\beta_{11}\,\omega_1^{\,2} - 12\,\alpha_{51}\,\beta_{11}\,\omega_2^{\,2} + 24\,\omega_2^{\,6}\,\beta_{21}\,\omega_1^{\,2} + 6\,\alpha_{51}\,\beta_{31} \\
& + 6\,\omega_2^{\,2}\,\alpha_{41}\,\beta_{31} + 6\,\omega_2^{\,4}\,\beta_{31} - 6\,\alpha_{31}\,\omega_2^{\,2}\,\beta_{31} - 12\,\omega_2^{\,4}\,\alpha_{41}\,\beta_{11} \\
& - \frac{3}{2}\,\omega_2^{\,6}\,\beta_{41}\,\omega_1^{\,4} - 24\,\omega_2^{\,4}\,\beta_{11}\,\omega_1^{\,2} + 24\,\alpha_{51}\,\beta_{21}\,\omega_1^{\,2}\,\omega_2^{\,2} \\
& + \frac{3}{2}\,\alpha_{31}\,\omega_1^{\,4}\,\beta_{41}\,\omega_2^{\,4} + 24\,\alpha_{31}\,\omega_1^{\,2}\,\beta_{11}\,\omega_2^{\,2} - 12\,\omega_2^{\,6}\,\beta_{11} \\
& - 24\,\alpha_{31}\,\omega_1^{\,2}\,\beta_{21}\,\omega_2^{\,4} - 12\,\alpha_{31}\,\omega_1^{\,4}\,\beta_{21}\,\omega_2^{\,2} - 24\,\alpha_{51}\,\beta_{11}\,\omega_1^{\,2}
\end{aligned}
$$

$$
\begin{aligned}
D_4 = {} & 12\,\alpha_{31}\,\omega_2^{\,4}\,\beta_{11} - 24\,\alpha_{51}\,\beta_{11}\,\omega_3^{\,2} + 12\,\omega_2^{\,6}\,\alpha_{21}\,\beta_{11} - 6\,\omega_2^{\,4}\,\alpha_{21}\,\beta_{31} \\
& - 12\,\alpha_{31}\,\omega_2^{\,2}\,\beta_{21}\,\omega_3^{\,4} + 24\,\omega_2^{\,4}\,\alpha_{21}\,\beta_{11}\,\omega_3^{\,2} - 24\,\omega_2^{\,2}\,\alpha_{41}\,\beta_{11}\,\omega_3^{\,2} \\
& + 24\,\alpha_{31}\,\omega_2^{\,2}\,\beta_{11}\,\omega_3^{\,2} - 24\,\omega_2^{\,4}\,\beta_{11}\,\omega_3^{\,2} + 24\,\omega_2^{\,4}\,\alpha_{41}\,\beta_{21}\,\omega_3^{\,2} \\
& - 24\,\omega_2^{\,6}\,\alpha_{21}\,\beta_{21}\,\omega_3^{\,2} + \frac{3}{2}\,\omega_2^{\,6}\,\alpha_{21}\,\beta_{41}\,\omega_3^{\,4} - 12\,\omega_2^{\,4}\,\alpha_{21}\,\beta_{21}\,\omega_3^{\,4} \\
& + 12\,\omega_2^{\,4}\,\beta_{21}\,\omega_3^{\,4} + \frac{3}{2}\,\alpha_{31}\,\omega_2^{\,4}\,\beta_{41}\,\omega_3^{\,4} + 24\,\omega_2^{\,6}\,\beta_{21}\,\omega_3^{\,2} \\
& - 24\,\alpha_{31}\,\omega_2^{\,4}\,\beta_{21}\,\omega_3^{\,2} - \frac{3}{2}\,\alpha_{51}\,\beta_{41}\,\omega_2^{\,2}\,\omega_3^{\,4} - \frac{3}{2}\,\omega_2^{\,6}\,\beta_{41}\,\omega_3^{\,4} \\
& + 12\,\alpha_{51}\,\beta_{21}\,\omega_3^{\,4} + 24\,\alpha_{51}\,\beta_{21}\,\omega_2^{\,2}\,\omega_3^{\,2} - \frac{3}{2}\,\omega_2^{\,4}\,\alpha_{41}\,\beta_{41}\,\omega_3^{\,4} \\
& + 12\,\omega_2^{\,2}\,\alpha_{41}\,\beta_{21}\,\omega_3^{\,4} - 12\,\alpha_{51}\,\beta_{11}\,\omega_2^{\,2} + 6\,\alpha_{51}\,\beta_{31} + 6\,\omega_2^{\,2}\,\alpha_{41}\,\beta_{31} \\
& + 6\,\omega_2^{\,4}\,\beta_{31} - 6\,\alpha_{31}\,\omega_2^{\,2}\,\beta_{31} - 12\,\omega_2^{\,4}\,\alpha_{41}\,\beta_{11} - 12\,\omega_2^{\,6}\,\beta_{11}
\end{aligned}
$$

$$
\begin{aligned}
D_5 = {} & 12\,\alpha_{31}\,\omega_2^{\,4}\,\beta_{11} + 12\,\alpha_{51}\,\beta_{21}\,\omega_4^{\,4} + 12\,\omega_2^{\,6}\,\alpha_{21}\,\beta_{11} - 6\,\omega_2^{\,4}\,\alpha_{21}\,\beta_{31} \\
& - 24\,\omega_2^{\,4}\,\beta_{11}\,\omega_4^{\,2} - 24\,\alpha_{51}\,\beta_{11}\,\omega_4^{\,2} + 12\,\omega_2^{\,4}\,\beta_{21}\,\omega_4^{\,4} \\
& + 24\,\omega_2^{\,4}\,\alpha_{21}\,\beta_{11}\,\omega_4^{\,2} + 24\,\omega_2^{\,6}\,\beta_{21}\,\omega_4^{\,2} - 12\,\alpha_{51}\,\beta_{11}\,\omega_2^{\,2} \\
& - 24\,\omega_2^{\,6}\,\alpha_{21}\,\beta_{21}\,\omega_4^{\,2} - 12\,\alpha_{31}\,\omega_2^{\,2}\,\beta_{21}\,\omega_4^{\,4} - 12\,\omega_2^{\,4}\,\alpha_{21}\,\beta_{21}\,\omega_4^{\,4} \\
& + 12\,\omega_2^{\,2}\,\alpha_{41}\,\beta_{21}\,\omega_4^{\,4} + 24\,\omega_2^{\,4}\,\alpha_{41}\,\beta_{21}\,\omega_4^{\,2} - \frac{3}{2}\,\alpha_{51}\,\beta_{41}\,\omega_4^{\,4}\,\omega_2^{\,2} \\
& - \frac{3}{2}\,\omega_2^{\,6}\,\beta_{41}\,\omega_4^{\,4} - 24\,\alpha_{31}\,\omega_2^{\,4}\,\beta_{21}\,\omega_4^{\,2} + \frac{3}{2}\,\alpha_{31}\,\omega_2^{\,4}\,\beta_{41}\,\omega_4^{\,4} \\
& + 24\,\alpha_{31}\,\omega_2^{\,2}\,\beta_{11}\,\omega_4^{\,2} - \frac{3}{2}\,\omega_2^{\,4}\,\alpha_{41}\,\beta_{41}\,\omega_4^{\,4} + 24\,\alpha_{51}\,\beta_{21}\,\omega_2^{\,2}\,\omega_4^{\,2} \\
& - 24\,\omega_2^{\,2}\,\alpha_{41}\,\beta_{11}\,\omega_4^{\,2} + \frac{3}{2}\,\omega_2^{\,6}\,\alpha_{21}\,\beta_{41}\,\omega_4^{\,4} + 6\,\alpha_{51}\,\beta_{31} + 6\,\omega_2^{\,2}\,\alpha_{41}\,\beta_{31} \\
& + 6\,\omega_2^{\,4}\,\beta_{31} - 6\,\alpha_{31}\,\omega_2^{\,2}\,\beta_{31} - 12\,\omega_2^{\,4}\,\alpha_{41}\,\beta_{11} - 12\,\omega_2^{\,6}\,\beta_{11}
\end{aligned}
$$

$$D_6 = \omega_2^{\,5}\,\alpha_{21}\,c + \alpha_{31}\,\omega_2^{\,3}\,c - \omega_2^{\,3}\,\alpha_{41}\,c - \alpha_{51}\,c\,\omega_2 - \omega_2^{\,5}\,c$$

$$D_7 = \frac{1}{2}\,\omega_2^{\,6}\,m_1 + \frac{1}{2}\,\alpha_{51}\,m_1\,\omega_2^{\,2} + \frac{1}{2}\,\omega_2^{\,6}\,\alpha_{21}\,m_1 - \frac{1}{2}\,\omega_2^{\,4}\,\alpha_{41}\,m_1 - \frac{1}{2}\,\alpha_{31}\,\omega_2^{\,4}\,m_1$$

$$
\begin{aligned}
F_1 = {} & -\alpha_{51}\,\omega_2\,\alpha_{41} + 3\,\omega_2^{\,2}\,\alpha_{21}^{\,2}\,\omega_3^{\,5} - \omega_3^{\,6}\,\omega_2\,\alpha_{21} - \omega_2\,\alpha_{41}\,\omega_3^{\,2}\,\alpha_{31} \\
& - \omega_2\,\alpha_{21}\,\omega_3^{\,4}\,\alpha_{31} + 2\,\alpha_{51}\,\alpha_{31}\,\omega_3 - 4\,\omega_3^{\,7} - 4\,\alpha_{51}\,\omega_3^{\,3} - 2\,\alpha_{31}^{\,2}\,\omega_3^{\,3} \\
& + 6\,\omega_3^{\,5}\,\alpha_{31} + \omega_2^{\,2}\,\alpha_{41}^{\,2}\,\omega_3 - 4\,\omega_2^{\,2}\,\alpha_{41}\,\omega_3^{\,3}\,\alpha_{21} + 3\,\alpha_{51}\,\omega_2\,\alpha_{21}\,\omega_3^{\,2}
\end{aligned}
$$

$$
\begin{aligned}
F_2 = {} & 18\,\alpha_{51}\,\beta_{11}\,\omega_3^{\,2} + 3\,\alpha_{31}\,\omega_3^{\,2}\,\beta_{31} - 18\,\alpha_{31}\,\omega_3^{\,4}\,\beta_{11} - 3\,\alpha_{51}\,\beta_{31} \\
& - \frac{3}{4}\,\omega_2\,\alpha_{41}\,\omega_3^{\,7}\,\beta_{41} - 3\,\omega_3^{\,4}\,\beta_{31} + 3\,\omega_2\,\alpha_{41}\,\omega_3\,\beta_{31} - \frac{3}{4}\,\alpha_{31}\,\omega_3^{\,8}\,\beta_{41} \\
& + 18\,\omega_2\,\alpha_{21}\,\omega_3^{\,5}\,\beta_{11} + \frac{3}{4}\,\alpha_{51}\,\beta_{41}\,\omega_3^{\,6} + 18\,\omega_3^{\,6}\,\beta_{11} + \frac{3}{4}\,\omega_2\,\alpha_{21}\,\omega_3^{\,9}\,\beta_{41} \\
& - 18\,\omega_2\,\alpha_{21}\,\omega_3^{\,7}\,\beta_{21} + \frac{3}{4}\,\omega_3^{\,10}\,\beta_{41} - 18\,\omega_3^{\,8}\,\beta_{21} - 18\,\omega_2\,\alpha_{41}\,\omega_3^{\,3}\,\beta_{11} \\
& + 18\,\omega_2\,\alpha_{41}\,\omega_3^{\,5}\,\beta_{21} - 18\,\alpha_{51}\,\beta_{21}\,\omega_3^{\,4} + 18\,\alpha_{31}\,\omega_3^{\,6}\,\beta_{21} \\
& - 3\,\omega_2\,\alpha_{21}\,\omega_3^{\,3}\,\beta_{31}
\end{aligned}
$$

$$
\begin{aligned}
F_3 = {} & 12\,\alpha_{51}\,\beta_{11}\,\omega_3^{\,2} - 12\,\alpha_{51}\,\beta_{21}\,\omega_1^{\,4} - 24\,\omega_3^{\,6}\,\beta_{21}\,\omega_1^{\,2} + 24\,\omega_3^{\,4}\,\beta_{11}\,\omega_1^{\,2} \\
& - 12\,\omega_1^{\,4}\,\beta_{21}\,\omega_3^{\,4} - \frac{3}{2}\,\alpha_{31}\,\omega_1^{\,4}\,\beta_{41}\,\omega_3^{\,4} - 24\,\alpha_{31}\,\omega_1^{\,2}\,\beta_{11}\,\omega_3^{\,2} \\
& + 12\,\alpha_{31}\,\omega_1^{\,4}\,\beta_{21}\,\omega_3^{\,2} - 24\,\alpha_{51}\,\beta_{21}\,\omega_1^{\,2}\,\omega_3^{\,2} + 24\,\alpha_{31}\,\omega_1^{\,2}\,\beta_{21}\,\omega_3^{\,4} \\
& - 6\,\alpha_{51}\,\beta_{31} - 12\,\omega_2\,\alpha_{41}\,\omega_3^{\,3}\,\beta_{11} - 6\,\omega_2\,\alpha_{21}\,\omega_3^{\,3}\,\beta_{31} + 6\,\omega_2\,\alpha_{41}\,\omega_3\,\beta_{31} \\
& + 12\,\omega_2\,\alpha_{21}\,\omega_3^{\,5}\,\beta_{11} + 12\,\omega_3^{\,6}\,\beta_{11} + \frac{3}{2}\,\alpha_{51}\,\beta_{41}\,\omega_1^{\,4}\,\omega_3^{\,2} - 12\,\alpha_{31}\,\omega_3^{\,4}\,\beta_{11} \\
& + 6\,\alpha_{31}\,\omega_3^{\,2}\,\beta_{31} + 12\,\omega_2\,\alpha_{41}\,\omega_3\,\beta_{21}\,\omega_1^{\,4} + 24\,\omega_2\,\alpha_{41}\,\omega_3^{\,3}\,\beta_{21}\,\omega_1^{\,2}
\end{aligned}
$$

$$
\begin{aligned}
&- 24\,\omega_2\,\alpha_{21}\,\omega_3^{\,5}\,\beta_{21}\,\omega_1^{\,2} + \frac{3}{2}\,\omega_2\,\alpha_{21}\,\omega_3^{\,5}\,\beta_{41}\,\omega_1^{\,4} - \frac{3}{2}\,\omega_2\,\alpha_{41}\,\omega_3^{\,3}\,\beta_{41}\,\omega_1^{\,4} \\
&- 24\,\omega_2\,\alpha_{41}\,\omega_3\,\beta_{11}\,\omega_1^{\,2} - 12\,\omega_2\,\alpha_{21}\,\omega_3^{\,3}\,\beta_{21}\,\omega_1^{\,4} \\
&+ 24\,\omega_2\,\alpha_{21}\,\omega_3^{\,3}\,\beta_{11}\,\omega_1^{\,2} - 6\,\omega_3^{\,4}\,\beta_{31} + 24\,\alpha_{51}\,\beta_{11}\,\omega_1^{\,2} + \frac{3}{2}\,\omega_3^{\,6}\,\beta_{41}\,\omega_1^{\,4}
\end{aligned}
$$

$$
\begin{aligned}
F_4 = {} & 12\,\alpha_{51}\,\beta_{11}\,\omega_3^{\,2} - 12\,\alpha_{51}\,\beta_{21}\,\omega_2^{\,4} + 24\,\alpha_{31}\,\omega_2^{\,2}\,\beta_{21}\,\omega_3^{\,4} \\
&- 24\,\alpha_{31}\,\omega_2^{\,2}\,\beta_{11}\,\omega_3^{\,2} - 12\,\omega_2^{\,4}\,\beta_{21}\,\omega_3^{\,4} - \frac{3}{2}\,\alpha_{31}\,\omega_2^{\,4}\,\beta_{41}\,\omega_3^{\,4} \\
&+ 12\,\alpha_{31}\,\omega_2^{\,4}\,\beta_{21}\,\omega_3^{\,2} - 24\,\alpha_{51}\,\beta_{21}\,\omega_2^{\,2}\,\omega_3^{\,2} + 24\,\alpha_{51}\,\beta_{11}\,\omega_2^{\,2} \\
&+ \frac{3}{2}\,\omega_3^{\,6}\,\beta_{41}\,\omega_2^{\,4} - 6\,\alpha_{51}\,\beta_{31} - 24\,\omega_3^{\,6}\,\beta_{21}\,\omega_2^{\,2} + 24\,\omega_3^{\,4}\,\beta_{11}\,\omega_2^{\,2} \\
&- 12\,\omega_2\,\alpha_{41}\,\omega_3^{\,3}\,\beta_{11} - 6\,\omega_2\,\alpha_{21}\,\omega_3^{\,3}\,\beta_{31} + 6\,\omega_2\,\alpha_{41}\,\omega_3\,\beta_{31} \\
&+ 12\,\omega_2\,\alpha_{21}\,\omega_3^{\,5}\,\beta_{11} + 12\,\omega_3^{\,6}\,\beta_{11} - 12\,\alpha_{31}\,\omega_3^{\,4}\,\beta_{11} + 6\,\alpha_{31}\,\omega_3^{\,2}\,\beta_{31} \\
&- 6\,\omega_3^{\,4}\,\beta_{31} + \frac{3}{2}\,\alpha_{51}\,\beta_{41}\,\omega_2^{\,4}\,\omega_3^{\,2} - 24\,\omega_2^{\,3}\,\alpha_{21}\,\omega_3^{\,5}\,\beta_{21} \\
&+ \frac{3}{2}\,\omega_2^{\,5}\,\alpha_{21}\,\omega_3^{\,5}\,\beta_{41} - 24\,\omega_2^{\,3}\,\alpha_{41}\,\omega_3\,\beta_{11} + 12\,\omega_2^{\,5}\,\alpha_{41}\,\omega_3\,\beta_{21} \\
&+ 24\,\omega_2^{\,3}\,\alpha_{41}\,\omega_3^{\,3}\,\beta_{21} - 12\,\omega_2^{\,5}\,\alpha_{21}\,\omega_3^{\,3}\,\beta_{21} - \frac{3}{2}\,\omega_2^{\,5}\,\alpha_{41}\,\omega_3^{\,3}\,\beta_{41} \\
&+ 24\,\omega_2^{\,3}\,\alpha_{21}\,\omega_3^{\,3}\,\beta_{11}
\end{aligned}
$$

$$
\begin{aligned}
F_5 = {} & 12\,\alpha_{51}\,\beta_{11}\,\omega_3^{\,2} - 12\,\alpha_{51}\,\beta_{21}\,\omega_4^{\,4} - 12\,\omega_3^{\,4}\,\beta_{21}\,\omega_4^{\,4} + \frac{3}{2}\,\omega_3^{\,6}\,\beta_{41}\,\omega_4^{\,4} \\
&- 24\,\omega_3^{\,6}\,\beta_{21}\,\omega_4^{\,2} + 24\,\alpha_{51}\,\beta_{11}\,\omega_4^{\,2} - 6\,\alpha_{51}\,\beta_{31} + 24\,\omega_3^{\,4}\,\beta_{11}\,\omega_4^{\,2} \\
&- 12\,\omega_2\,\alpha_{41}\,\omega_3^{\,3}\,\beta_{11} - 6\,\omega_2\,\alpha_{21}\,\omega_3^{\,3}\,\beta_{31} + 6\,\omega_2\,\alpha_{41}\,\omega_3\,\beta_{31} \\
&+ 12\,\omega_2\,\alpha_{21}\,\omega_3^{\,5}\,\beta_{11} + 12\,\omega_3^{\,6}\,\beta_{11} - 12\,\alpha_{31}\,\omega_3^{\,4}\,\beta_{11} + 6\,\alpha_{31}\,\omega_3^{\,2}\,\beta_{31} \\
&- 6\,\omega_3^{\,4}\,\beta_{31} - \frac{3}{2}\,\omega_2\,\alpha_{41}\,\omega_3^{\,3}\,\beta_{41}\,\omega_4^{\,4} - \frac{3}{2}\,\alpha_{31}\,\omega_3^{\,4}\,\beta_{41}\,\omega_4^{\,4} \\
&+ \frac{3}{2}\,\omega_2\,\alpha_{21}\,\omega_3^{\,5}\,\beta_{41}\,\omega_4^{\,4} + 24\,\omega_2\,\alpha_{41}\,\omega_3^{\,3}\,\beta_{21}\,\omega_4^{\,2} + 24\,\alpha_{31}\,\omega_3^{\,4}\,\beta_{21}\,\omega_4^{\,2} \\
&+ 12\,\omega_2\,\alpha_{41}\,\omega_3\,\beta_{21}\,\omega_4^{\,4} + 24\,\omega_2\,\alpha_{21}\,\omega_3^{\,3}\,\beta_{11}\,\omega_4^{\,2} \\
&- 12\,\omega_2\,\alpha_{21}\,\omega_3^{\,3}\,\beta_{21}\,\omega_4^{\,4} - 24\,\omega_2\,\alpha_{41}\,\omega_3\,\beta_{11}\,\omega_4^{\,2} - 24\,\alpha_{51}\,\beta_{21}\,\omega_3^{\,2}\,\omega_4^{\,2} \\
&- 24\,\omega_2\,\alpha_{21}\,\omega_3^{\,5}\,\beta_{21}\,\omega_4^{\,2} - 24\,\alpha_{31}\,\omega_3^{\,2}\,\beta_{11}\,\omega_4^{\,2} + 12\,\alpha_{31}\,\omega_3^{\,2}\,\beta_{21}\,\omega_4^{\,4} \\
&+ \frac{3}{2}\,\alpha_{51}\,\beta_{41}\,\omega_4^{\,4}\,\omega_3^{\,2}
\end{aligned}
$$

$$
F_6 = -\alpha_{31}\,\omega_3^{\,3}\,c + \alpha_{51}\,c\,\omega_3 + \omega_3^{\,5}\,c - \omega_2\,\alpha_{41}\,\omega_3^{\,2}\,c + \omega_2\,\alpha_{21}\,\omega_3^{\,4}\,c
$$

$$
\begin{aligned}
G_1 = & -3\,\omega_2^{\,2}\,\alpha_{21}^{\,2}\,\omega_4^{\,5} + 4\,\omega_2^{\,2}\,\alpha_{21}\,\omega_4^{\,3}\,\alpha_{41} + 3\,\omega_2\,\alpha_{41}\,\omega_4^{\,4} + 4\,\alpha_{51}\,\omega_4^{\,3} \\
& + 3\,\alpha_{51}\,\omega_2\,\alpha_{21}\,\omega_4^{\,2} - \omega_2\,\alpha_{21}\,\omega_4^{\,4}\,\alpha_{31} - \omega_2^{\,2}\,\alpha_{41}^{\,2}\,\omega_4 - \alpha_{51}\,\omega_2\,\alpha_{41} \\
& - \omega_2\,\alpha_{21}\,\omega_4^{\,6} - 2\,\alpha_{51}\,\alpha_{31}\,\omega_4 - \omega_2\,\alpha_{41}\,\omega_4^{\,2}\,\alpha_{31} + 4\,\omega_4^{\,7} - 6\,\omega_4^{\,5}\,\alpha_{31} \\
G_2 = & \; 3\,\omega_2\,\alpha_{41}\,\omega_4\,\beta_{31} + 18\,\omega_2\,\alpha_{21}\,\omega_4^{\,5}\,\beta_{11} - \frac{3}{4}\,\omega_4^{\,10}\,\beta_{41} - \frac{3}{4}\,\omega_2\,\alpha_{41}\,\omega_4^{\,7}\,\beta_{41} \\
& - 18\,\omega_2\,\alpha_{41}\,\omega_4^{\,3}\,\beta_{11} - 18\,\alpha_{51}\,\beta_{11}\,\omega_4^{\,2} + 18\,\omega_4^{\,8}\,\beta_{21} - 18\,\omega_2\,\alpha_{21}\,\omega_4^{\,7}\,\beta_{21} \\
& + \frac{3}{4}\,\alpha_{31}\,\omega_4^{\,8}\,\beta_{41} - 3\,\omega_2\,\alpha_{21}\,\omega_4^{\,3}\,\beta_{31} + 3\,\alpha_{51}\,\beta_{31} - \frac{3}{4}\,\alpha_{51}\,\beta_{41}\,\omega_4^{\,6} \\
& + 18\,\omega_2\,\alpha_{41}\,\omega_4^{\,5}\,\beta_{21} - 3\,\alpha_{31}\,\omega_4^{\,2}\,\beta_{31} + 3\,\omega_4^{\,4}\,\beta_{31} + 18\,\alpha_{31}\,\omega_4^{\,4}\,\beta_{11} \\
& - 18\,\alpha_{31}\,\omega_4^{\,6}\,\beta_{21} - 18\,\omega_4^{\,6}\,\beta_{11} + \frac{3}{4}\,\omega_2\,\alpha_{21}\,\omega_4^{\,9}\,\beta_{41} + 18\,\alpha_{51}\,\beta_{21}\,\omega_4^{\,4} \\
G_3 = & \; 12\,\alpha_{51}\,\beta_{21}\,\omega_1^{\,4} - 12\,\alpha_{31}\,\omega_1^{\,4}\,\beta_{21}\,\omega_4^{\,2} + 24\,\alpha_{31}\,\omega_1^{\,2}\,\beta_{11}\,\omega_4^{\,2} \\
& - 24\,\omega_4^{\,4}\,\beta_{11}\,\omega_1^{\,2} - \frac{3}{2}\,\omega_4^{\,6}\,\beta_{41}\,\omega_1^{\,4} - 12\,\alpha_{51}\,\beta_{11}\,\omega_4^{\,2} + 12\,\omega_1^{\,4}\,\beta_{21}\,\omega_4^{\,4} \\
& + 6\,\alpha_{51}\,\beta_{31} + 24\,\omega_4^{\,6}\,\beta_{21}\,\omega_1^{\,2} + \frac{3}{2}\,\alpha_{31}\,\omega_1^{\,4}\,\beta_{41}\,\omega_4^{\,4} - 6\,\alpha_{31}\,\omega_4^{\,2}\,\beta_{31} \\
& - 12\,\omega_4^{\,6}\,\beta_{11} - 24\,\alpha_{51}\,\beta_{11}\,\omega_1^{\,2} + 6\,\omega_2\,\alpha_{41}\,\omega_4\,\beta_{31} + 12\,\omega_2\,\alpha_{21}\,\omega_4^{\,5}\,\beta_{11} \\
& - 6\,\omega_2\,\alpha_{21}\,\omega_4^{\,3}\,\beta_{31} - 12\,\omega_2\,\alpha_{41}\,\omega_4^{\,3}\,\beta_{11} + 12\,\alpha_{31}\,\omega_4^{\,4}\,\beta_{11} \\
& - \frac{3}{2}\,\alpha_{51}\,\beta_{41}\,\omega_1^{\,4}\,\omega_4^{\,2} - \frac{3}{2}\,\omega_2\,\alpha_{41}\,\omega_4^{\,3}\,\beta_{41}\,\omega_1^{\,4} - 24\,\omega_2\,\alpha_{21}\,\omega_4^{\,5}\,\beta_{21}\,\omega_1^{\,2} \\
& - 12\,\omega_2\,\alpha_{21}\,\omega_4^{\,3}\,\beta_{21}\,\omega_1^{\,4} - 24\,\omega_2\,\alpha_{41}\,\omega_4\,\beta_{11}\,\omega_1^{\,2} + \frac{3}{2}\,\omega_2\,\alpha_{21}\,\omega_4^{\,5}\,\beta_{41}\,\omega_1^{\,4} \\
& + 12\,\omega_2\,\alpha_{41}\,\omega_4\,\beta_{21}\,\omega_1^{\,4} + 24\,\omega_2\,\alpha_{21}\,\omega_4^{\,3}\,\beta_{11}\,\omega_1^{\,2} \\
& + 24\,\omega_2\,\alpha_{41}\,\omega_4^{\,3}\,\beta_{21}\,\omega_1^{\,2} + 6\,\omega_4^{\,4}\,\beta_{31} - 24\,\alpha_{31}\,\omega_1^{\,2}\,\beta_{21}\,\omega_4^{\,4} \\
& + 24\,\alpha_{51}\,\beta_{21}\,\omega_1^{\,2}\,\omega_4^{\,2} \\
G_4 = & -24\,\omega_4^{\,4}\,\beta_{11}\,\omega_2^{\,2} + 12\,\alpha_{51}\,\beta_{21}\,\omega_2^{\,4} - 12\,\alpha_{51}\,\beta_{11}\,\omega_4^{\,2} + 12\,\omega_2^{\,4}\,\beta_{21}\,\omega_4^{\,4} \\
& - 24\,\alpha_{51}\,\beta_{11}\,\omega_2^{\,2} - 24\,\alpha_{31}\,\omega_2^{\,2}\,\beta_{21}\,\omega_4^{\,4} - 12\,\alpha_{31}\,\omega_2^{\,4}\,\beta_{21}\,\omega_4^{\,2} \\
& + \frac{3}{2}\,\alpha_{31}\,\omega_2^{\,4}\,\beta_{41}\,\omega_4^{\,4} + 24\,\alpha_{31}\,\omega_2^{\,2}\,\beta_{11}\,\omega_4^{\,2} + 24\,\alpha_{51}\,\beta_{21}\,\omega_2^{\,2}\,\omega_4^{\,2} \\
& + 6\,\alpha_{51}\,\beta_{31} + 24\,\omega_4^{\,6}\,\beta_{21}\,\omega_2^{\,2} - 6\,\alpha_{31}\,\omega_4^{\,2}\,\beta_{31} - 12\,\omega_4^{\,6}\,\beta_{11} \\
& + 6\,\omega_2\,\alpha_{41}\,\omega_4\,\beta_{31} + 12\,\omega_2\,\alpha_{21}\,\omega_4^{\,5}\,\beta_{11} - 6\,\omega_2\,\alpha_{21}\,\omega_4^{\,3}\,\beta_{31} \\
& - 12\,\omega_2\,\alpha_{41}\,\omega_4^{\,3}\,\beta_{11} + 12\,\alpha_{31}\,\omega_4^{\,4}\,\beta_{11} + 6\,\omega_4^{\,4}\,\beta_{31} - \frac{3}{2}\,\omega_2^{\,5}\,\alpha_{41}\,\omega_4^{\,3}\,\beta_{41}
\end{aligned}
$$

$$
\begin{aligned}
&- 12\,\omega_2^{\,5}\,\alpha_{21}\,\omega_4^{\,3}\,\beta_{21} + 24\,\omega_2^{\,3}\,\alpha_{21}\,\omega_4^{\,3}\,\beta_{11} - 24\,\omega_2^{\,3}\,\alpha_{21}\,\omega_4^{\,5}\,\beta_{21} \\
&+ \frac{3}{2}\,\omega_2^{\,5}\,\alpha_{21}\,\omega_4^{\,5}\,\beta_{41} - 24\,\omega_2^{\,3}\,\alpha_{41}\,\omega_4\,\beta_{11} + 12\,\omega_2^{\,5}\,\alpha_{41}\,\omega_4\,\beta_{21} \\
&- \frac{3}{2}\,\alpha_{51}\,\beta_{41}\,\omega_2^{\,4}\,\omega_4^{\,2} + 24\,\omega_2^{\,3}\,\alpha_{41}\,\omega_4^{\,3}\,\beta_{21} - \frac{3}{2}\,\omega_4^{\,6}\,\beta_{41}\,\omega_2^{\,4}
\end{aligned}
$$

$$
\begin{aligned}
G_5 = &-24\,\alpha_{51}\,\beta_{11}\,\omega_3^{\,2} + 24\,\omega_4^{\,6}\,\beta_{21}\,\omega_3^{\,2} - 24\,\omega_4^{\,4}\,\beta_{11}\,\omega_3^{\,2} + 12\,\omega_3^{\,4}\,\beta_{21}\,\omega_4^{\,4} \\
&- 12\,\alpha_{51}\,\beta_{11}\,\omega_4^{\,2} + 12\,\alpha_{51}\,\beta_{21}\,\omega_3^{\,4} - \frac{3}{2}\,\omega_4^{\,6}\,\beta_{41}\,\omega_3^{\,4} + 6\,\alpha_{51}\,\beta_{31} \\
&- 6\,\alpha_{31}\,\omega_4^{\,2}\,\beta_{31} + \frac{3}{2}\,\alpha_{31}\,\omega_3^{\,4}\,\beta_{41}\,\omega_4^{\,4} - 12\,\alpha_{31}\,\omega_3^{\,4}\,\beta_{21}\,\omega_4^{\,2} - 12\,\omega_4^{\,6}\,\beta_{11} \\
&+ 24\,\alpha_{51}\,\beta_{21}\,\omega_3^{\,2}\,\omega_4^{\,2} + 24\,\alpha_{31}\,\omega_3^{\,2}\,\beta_{11}\,\omega_4^{\,2} - 24\,\alpha_{31}\,\omega_3^{\,2}\,\beta_{21}\,\omega_4^{\,4} \\
&+ 6\,\omega_2\,\alpha_{41}\,\omega_4\,\beta_{31} + 12\,\omega_2\,\alpha_{21}\,\omega_4^{\,5}\,\beta_{11} - 6\,\omega_2\,\alpha_{21}\,\omega_4^{\,3}\,\beta_{31} \\
&- 12\,\omega_2\,\alpha_{41}\,\omega_4^{\,3}\,\beta_{11} + 12\,\alpha_{31}\,\omega_4^{\,4}\,\beta_{11} + 6\,\omega_4^{\,4}\,\beta_{31} \\
&- \frac{3}{2}\,\omega_2\,\alpha_{41}\,\omega_4^{\,3}\,\beta_{41}\,\omega_3^{\,4} + 24\,\omega_2\,\alpha_{21}\,\omega_4^{\,3}\,\beta_{11}\,\omega_3^{\,2} \\
&+ 24\,\omega_2\,\alpha_{41}\,\omega_4^{\,3}\,\beta_{21}\,\omega_3^{\,2} + 12\,\omega_2\,\alpha_{41}\,\omega_4\,\beta_{21}\,\omega_3^{\,4} + \frac{3}{2}\,\omega_2\,\alpha_{21}\,\omega_4^{\,5}\,\beta_{41}\,\omega_3^{\,4} \\
&- 12\,\omega_2\,\alpha_{21}\,\omega_4^{\,3}\,\beta_{21}\,\omega_3^{\,4} - 24\,\omega_2\,\alpha_{21}\,\omega_4^{\,5}\,\beta_{21}\,\omega_3^{\,2} \\
&- 24\,\omega_2\,\alpha_{41}\,\omega_4\,\beta_{11}\,\omega_3^{\,2} - \frac{3}{2}\,\alpha_{51}\,\beta_{41}\,\omega_3^{\,4}\,\omega_4^{\,2}
\end{aligned}
$$

$$
G_6 = -\alpha_{51}\,c\,\omega_4 + \alpha_{31}\,\omega_4^{\,3}\,c - \omega_4^{\,5}\,c + \omega_2\,\alpha_{21}\,\omega_4^{\,4}\,c - \omega_2\,\alpha_{41}\,\omega_4^{\,2}\,c
$$

Appendix G: Kinetic Energies of the Rotor Subjected to Base Movements

Kinetic Energy of the disk [DBF06]

The disk is supposed to be rigid and is characterized by its kinetic energy given below [DBF06],

$$
\begin{aligned}
T_D = {} & \frac{M_D}{2}\Big\{2\,\Big[\dot{\alpha}_S\left(\dot{Z}+\dot{w}(y)+\dot{\alpha}_S Y - \dot{\beta}_S\left(X+u(y)\right)\right)-\dot{\gamma}_S\left(\dot{X}+\dot{u}(y)- \dot{\gamma}_S Y+\dot{\beta}_S\left(Z+w(y)\right)\right)\Big]y \\
& +\left[\dot{\alpha}_S^2+\dot{\gamma}_S^2\right]y^2+\left(\dot{X}+\dot{u}(y)+\dot{\beta}_S\left(Z+w(y)\right) - \dot{\gamma}_S Y\right)^2+\left(\dot{Y}+\dot{\gamma}_S\left(X+u(y)\right) - \dot{\alpha}_S\left(Z+w(y)\right)\right)^2 \\
& +\left(\dot{Z}+\dot{w}(y)+\dot{\alpha}_S Y - \dot{\beta}_S\left(X+u(y)\right)\right)^2\Big\} \\
& +\frac{I_{Dm}}{2}\Big\{\left(\dot{\alpha}_S^2+\dot{\gamma}_S^2\right)+\left(\dot{\theta}(y)^2+\dot{\psi}(y)^2\right)+\theta(y)^2\left(\dot{\beta}_S^2-\dot{\gamma}_S^2\right)+\psi(y)^2\left(\dot{\beta}_S^2-\dot{\alpha}_S^2\right) \\
& +2\,\Big[\dot{\alpha}_S\,\dot{\theta}(y)+\dot{\gamma}_S\,\dot{\psi}(y)+\dot{\beta}_S\left(\psi(y)\,\dot{\theta}(y)-\theta(y)\dot{\psi}(y)\right)\Big] \\
& \quad +\dot{\beta}_S\left(\dot{\alpha}_S\,\psi(y)-\dot{\gamma}_S\,\theta(y)\right)+\dot{\alpha}_S\,\dot{\gamma}_S\,\psi(y)\,\theta(y)\Big] \\
& +\frac{I_{Dy}}{2}\Big\{\left(\dot{\beta}_S+\Omega+\dot{\gamma}_S\,\theta(y)-\dot{\alpha}_S\,\psi(y)\right)^2+\left(\dot{\beta}_S+\Omega\right)\Big[2\dot{\psi}(y)\,\theta(y)-\dot{\beta}_S\left(\psi(y)^2+\theta(y)^2\right)\Big]\Big\} \\
& +\frac{I_{Da}}{2}\Big\{\Big[2\left(\dot{\beta}_S\left(\dot{\alpha}_S\,\psi(y)+\dot{\gamma}_S\,\theta(y)\right)+\dot{\alpha}_S\,\dot{\theta}(y)-\dot{\gamma}_S\,\dot{\psi}(y)\right)+\dot{\beta}_S^2\left(\psi(y)^2-\theta(y)^2\right)+\left(\dot{\alpha}_S^2-\dot{\gamma}_S^2\right)+\dot{\theta}(y)^2 \\
& -\dot{\psi}(y)^2+\dot{\gamma}_S^2\,\theta(y)^2-\dot{\alpha}_S^2\psi(y)^2+2\,\dot{\beta}_S\left(\psi(y)\,\dot{\theta}(y)+\theta(y)\dot{\psi}(y)\right)-2\,\dot{\alpha}_S\,\dot{\gamma}_S\,\psi(y)\,\theta(y)\Big]\cos 2\,\Omega\,t \\
& -\Big[2\,\dot{\alpha}_S\,\dot{\gamma}_S+2\,\dot{\beta}_S\left(\dot{\gamma}_S\,\psi(y)-\dot{\alpha}_S\,\theta(y)\right)+2\,\dot{\alpha}_S\,\dot{\psi}(y)+2\,\dot{\gamma}_S\,\dot{\theta}(y)+2\left(\dot{\alpha}_S^2-\dot{\beta}_S^2\right)\psi(y)\,\theta(y) \\
& -\dot{\alpha}_S\dot{\gamma}_S\left(\theta(y)^2+\psi(y)^2\right)+2\,\dot{\beta}_S\left(\psi(y)\,\dot{\psi}(y)-\theta(y)\,\dot{\theta}(y)\right)+2\dot{\psi}(y)\,\dot{\theta}(y)\Big]\sin 2\,\Omega\,t\Big\}
\end{aligned}
$$

This expression contains the classical terms of the dynamic of rotors:

$\frac{I_{Dy}}{2}\Omega^2$: A constant terms representing the rotational energy of the disk. It does not have an influence on the equations of motion.

$\frac{M_D}{2}\left(\dot{u}(y)^2+\dot{w}(y)^2\right)$: Kinetic energy of an element in translation in a plane.

$\frac{I_{Dm}}{2}\left(\dot{\psi}(y)^2+\dot{\theta}(y)^2\right)$: Rotational kinetic energy about the axis x and z.

$I_{Dy}\,\Omega\,\dot{\psi}(y)\,\theta(y)$: Gyroscopic (Coriolis) effect.

The other terms are due to the movement of the rotor assembly.

Kinetic Energy of the shaft [DBF06]

The kinetic energy of the shaft can be derived from the kinetic energy expression of the disk above by extending it for an element L of thin section, of the thickness dy, the constant cross section S , the density ρ and the constant inertias of the section I_x et I_z.

The kinetic energy of the shaft can be written as,

$$
\begin{aligned}
T_a = {} & \frac{1}{2}\int_0^L \rho S \Big\{ 2\Big[\dot{\alpha}_S \left(\dot{Z} + \dot{w}(y) + \dot{\alpha}_S Y - \dot{\beta}_S \left(X + u(y)\right)\right) - \dot{\gamma}_S \left(\dot{X} + \dot{u}(y) - \dot{\gamma}_S Y + \dot{\beta}_S \left(Z + w(y)\right)\right)\Big] y \\
& + \left[\dot{\alpha}_S^2 + \dot{\gamma}_S^2\right] y^2 + \left(\dot{X} + \dot{u}(y) + \dot{\beta}_S \left(Z + w(y)\right) - \dot{\gamma}_S Y\right)^2 + \left(\dot{Y} + \dot{\gamma}_S \left(X + u(y)\right) - \dot{\alpha}_S \left(Z + w(y)\right)\right)^2 \\
& + \left(\dot{Z} + \dot{w}(y) + \dot{\alpha}_S Y - \dot{\beta}_S \left(X + u(y)\right)\right)^2 \Big\} dy \\
& + \frac{1}{2}\int_0^L \rho I_m \Big\{ \left(\dot{\alpha}_S^2 + \dot{\gamma}_S^2\right) + \left(\dot{\theta}(y)^2 + \dot{\psi}(y)^2\right) + \theta(y)^2 \left(\dot{\beta}_S^2 - \dot{\gamma}_S^2\right) + \psi(y)^2 \left(\dot{\beta}_S^2 - \dot{\alpha}_S^2\right) \\
& + 2\left[\dot{\alpha}_S \dot{\theta}(y) + \dot{\gamma}_S \dot{\psi}(y) + \dot{\beta}_S \left(\psi(l_1)\, \dot{\theta}(l_1) - \theta(y) \dot{\psi}(y)\right) + \dot{\beta}_S \left(\dot{\alpha}_S \psi(y) - \dot{\gamma}_S \theta(y)\right) + \dot{\alpha}_S \dot{\gamma}_S \psi(y) \theta(y)\right] \Big\} dy \\
& + \int_0^L \rho I_m \Big\{ \left(\dot{\beta}_S + \Omega + \dot{\gamma}_S \theta(y) - \dot{\alpha}_S \psi(y)\right)^2 + \left(\dot{\beta}_S + \Omega\right) \left[-2\dot{\psi}(y)\, \theta(y) - \dot{\beta}_S \left(\psi(y)^2 + \theta(y)^2\right)\right] \Big\} dy \\
& + \frac{1}{2}\int_0^L \rho \mathrm{I_a} \Big\{ \Big[2 \left(\dot{\beta}_S \left(\dot{\alpha}_S \psi(y) + \dot{\gamma}_S \theta(y)\right) + \dot{\alpha}_S \dot{\theta}(y) - \dot{\gamma}_S \dot{\psi}(y)\right) + \dot{\beta}_S^2 \left(\psi(y)^2 - \theta(y)^2\right) + \left(\dot{\alpha}_S^2 - \dot{\gamma}_S^2\right) + \dot{\theta}(y)^2 \\
& - \dot{\psi}(y)^2 + \dot{\gamma}_S^2 \theta(y)^2 - \dot{\alpha}_S^2 \psi(y)^2 + 2\dot{\beta}_S \left(\psi(y)\, \dot{\theta}(y) + \theta(y) \dot{\psi}(y)\right) - 2\dot{\alpha}_S \dot{\gamma}_S \psi(y) \theta(y)\Big] \cos 2\,\Omega\, t \\
& - \Big[2\dot{\alpha}_S \dot{\gamma}_S + 2\dot{\beta}_S \left(\dot{\gamma}_S \psi(y) - \dot{\alpha}_S \theta(y)\right) + 2\dot{\alpha}_S \dot{\psi}(y) + 2\dot{\gamma}_S \dot{\theta}(y) + 2\left(\dot{\alpha}_S^2 - \dot{\beta}_S^2\right) \psi(y)\, \theta(y) \\
& - \dot{\alpha}_S \dot{\gamma}_S \left(\theta(y)^2 + \psi(y)^2\right) + 2\dot{\beta}_S \left(\psi(y)\, \dot{\psi}(y) - \theta(y)\, \dot{\theta}(y)\right) + 2\dot{\psi}(y)\, \dot{\theta}(y)\Big] \sin 2\,\Omega\, t \Big\} dy
\end{aligned}
$$

The above expression contains the classical terms of dynamics of rotors.

$\rho I_m L \Omega^2$: A constant terms representing the rotational energy of the shaft. It does not have an influence on the equations of motion.

$\frac{\rho S}{2}\int_0^L \left(\dot{u}(y)^2 + \dot{w}(y)^2\right) dy$: Expression of the kinetic energy of a beam in bending.

$\frac{\rho I_m}{2}\int_0^L \left(\dot{\psi}(y)^2 + \dot{\theta}(y)^2\right) dy$: Secondary effects of rotary inertia.

$2\rho I_m \Omega \int_0^L \dot{\psi}(y)\, \theta(y)\, dy$: Gyroscopic effect.

The other terms are due to the movement of the rotor assembly.

Kinetic Energy of the Mass Unbalance [DBF06]

The mass unbalance is supposed to be situated at a distance d from the geometric center C of the disk and is represented by m_u. See fig. where point A represents the geometric center of the undeformed shaft.

The kinetic energy of the mass unbalance is given as below,

$$
\begin{aligned}
T_u = {} & \frac{1}{2} m_u \, d^2 \left(\left(\Omega + \dot{\beta}_S \right)^2 + \left(\dot{\alpha}_S \sin \Omega t - \dot{\alpha}_S \cos \Omega t \right)^2 \right) \\
& + m_u \, d \left[\left(\ddot{X} + \ddot{u} + \dot{\beta}_S \left(Z + w \right) - \ddot{\alpha}_S \left(Y + y \right) \right) \left(\Omega + \dot{\beta}_S \right) \cos \Omega t \right. \\
& + \left(\ddot{Y} + \ddot{v} + \ddot{\alpha}_S \left(X + u \right) - \dot{\alpha}_S \left(Z + w \right) \right) \left(\dot{\alpha}_S \sin \Omega t - \dot{\alpha}_S \cos \Omega t \right) \\
& \left. - \left(\ddot{Z} + \ddot{w} + \dot{\alpha}_S \left(Y + y \right) - \dot{\beta}_S \left(X + u \right) \right) \left(\Omega + \dot{\beta}_S \right) \sin \Omega t \right]
\end{aligned}
$$

Résumé de Thèse

La dynamique des rotors est un domaine important dans de nombreuses applications d'ingénieries telles que les moteurs à réaction, les rotors d'hélicoptères, les turbines, les compresseurs ou encore les broches de machines-outils. L'énergie cinétique de rotation de ces éléments constitue une source interne d'énergie, qui, dans certaines circonstances, peut conduire à des vibrations de grandes amplitudes du rotor et perturber le fonctionnement de la machine, réduire sa durée de vie et conduire à sa destruction. Pour l'évaluation de la fiabilité et de la sécurité, les scénarios possibles de dysfonctionnement du système, il est nécessaire de modéliser et d'analyser le comportement dynamique des rotors prenant en compte ces grandes déformations. Par conséquent, le fonctionnement de la machine doit être assuré par la connaissance des déformations du rotor et les efforts de liaisons avec les composants de la machine.

Ainsi, l'objectif de ce travail de thèse est d'étudier analytiquement et numériquement le comportement dynamique non-linéaire des rotors, en prenant en compte des effets significatifs comme les grandes déformations en flexion, les non-linéarités géométriques et le cisaillement.

Le travail de cette thèse est divisé en trois parties principales. Dans la première partie, le principe de Hamilton est utilisé pour formuler les équations du mouvement qui prennent en compte un ensemble d'effets non-linéaires comme des déformations d'ordre supérieur en flexion et le cisaillement. De plus, si les supports du rotor ne permettent pas à l'arbre de se déplacer dans la direction axiale, il y a alors une force dynamique harmonique agissant axialement sur le rotor en fonctionnement. Ces modèles se composent d'équations différentielles non linéaires du deuxième ordre lorsque les déformations de cisaillement ne sont pas considérées. Lorsque les effets du cisaillement sont également pris en compte, les modèles mathématiques développés se composent d'équations différentielles non linéaires du quatrième ordre.

Les deux parties suivantes sont consacrées à la résolution des différents modèles non-linéaires développés dans la première partie. Des méthodes analytiques et numériques sont appliquées afin de traiter les équations non linéaires du mouvement. Afin de résoudre le modèle complet, une méthode basée sur des développement asymptotiques, la méthode des échelles multiples (MEM) est appliquée. Il s'agit d'une méthode des perturbations qui s'est avérée très efficace pour résoudre les équations non linéaires de mouvement. Les courbes de réponse sont tracées pour différentes résonances possibles et l'effet de la non-linéarité est discuté par rapport à l'analyse linéaire. La réponse forcée du système provoquée par un balourd est également présentée pour plusieurs configurations du rotor. Lorsque les déformations de cisaillement sont prises en compte, l'analyse est effectuée pour différents élancements afin de mettre en évidence cet effet sur la dynamique d'un axe en rotation d'une part et d'un système arbre-disque d'autre part.

Les paragraphes suivants présentent un bref résumé de chaque chapitre de la thèse.

Chapitre 1

Ce chapitre présente un état de l'art concernant le domaine de l'analyse du comportement dynamique des rotors. Les comportements de base sont décrits et les techniques et les outils utilisés pour traiter les problèmes spécifiques présentés. L'objectif et la contribution de la thèse sont discutés à

la lumière de l'état de l'art et des travaux de recherche disponibles à ce jour dans la littérature. Une introduction concernant les divers aspects importants liés aux rotors en composites est aussi exposée.

Chapitre 2

Ce chapitre est dédié à la modélisation mathématique pour analyser le comportement dynamique des rotors. Les théories des poutres de type Euler-Bernoulli et de type Timoshenko sont rappelées pour la modélisation de l'arbre. Le principe de Hamilton est utilisé pour formuler les équations de base du mouvement. Différents modèles sont proposés :

Prise en compte des effets secondaires de flexion et d'une force axiale statique N_0.

L'influence de ces effets se caractérise par une modification de l'énergie de déformation. Ceci conduit aux deux équations du mouvement :

$$\begin{cases} \ddot{U} - \Omega\alpha_1\dot{W} + \alpha_2 U + \left(\frac{1}{2}\beta_1 + \beta_2\right)\left(U^3 + UW^2\right) + N_0 k_{N_0} U + c\dot{U} = m_1\Omega^2 d_1 f(l_1)\sin\Omega t \\ \ddot{W} + \Omega\alpha_1\dot{U} + \alpha_2 W + \left(\frac{1}{2}\beta_1 + \beta_2\right)\left(W^3 + WU^2\right) + N_0 k_{N_0} W + c\dot{W} = m_1\Omega^2 d_1 f(l_1)\cos\Omega t \end{cases}$$

Prise en compte des effets dynamiques de variation de la force axiale.

Lorsque le rotor est contraint dans son déplacement axial (conditions d'appui), la variation de l'effort axial a une influence sur l'énergie de déformation. Les équations du mouvement sont :

$$\begin{cases} \ddot{U} - \Omega\alpha_1\dot{W} + \alpha_2 U + \left(\frac{1}{2}\beta_1 + \beta_2\right)\left(U^3 + UW^2\right) + c\dot{U} = m_1\Omega^2 d_1 f(l_1)\sin\Omega t \\ \ddot{W} + \Omega\alpha_1\dot{U} + \alpha_2 W + \left(\frac{1}{2}\beta_1 + \beta_2\right)\left(W^3 + WU^2\right) + c\dot{W} = m_1\Omega^2 d_1 f(l_1)\cos\Omega t \end{cases}$$

Prise en compte des effets provenant du cisaillement.

Le modèle de base est repris avec la prise en compte de l'influence des termes liés à la participation du cisaillement. Ces modifications ont une influence dans l'énergie de déformation. Il apparait alors des termes non linéaires dans les deux équations différentielles du mouvement qui comportement des dérivées 4ème en temps. Les équations du mouvement sont :

$$\begin{cases} \ddot{\dot{U}} - \Omega\alpha_{21}\ddot{\dot{W}} + \alpha_{31}\ddot{U} - \Omega\alpha_{41}\dot{W} + \alpha_{51}U + c\dot{W} = (-3/2)\beta_{11}(W^2\ddot{U} + 2UW\ddot{W} \\ + 3U^2\ddot{U}) - (3/2)\beta_{21}(U\dot{W}^2 + 2W\dot{U}\dot{W} + 3U\dot{U}^2) - (3/4)\beta_{31}(U^3 + UW^2) \\ - (3/16)\beta_{41}(\dot{U}^3 + \dot{U}\dot{W}^2) + m_1\Omega^2\sin\Omega t \\ \\ \ddot{\dot{W}} + \Omega\alpha_{21}\ddot{\dot{U}} + \alpha_{31}\ddot{W} + \Omega\alpha_{41}\dot{U} + \alpha_{51}W + c\dot{U} = (-3/2)\beta_{11}(U^2\ddot{W} + 2WU\ddot{U} \\ + 3W^2\ddot{W}) - (3/2)\beta_{21}(W\dot{U}^2 + 2U\dot{U}\dot{W} + 3W\dot{W}^2) - (3/4)\beta_{31}(W^3 + WU^2) \\ - (3/16)\beta_{41}(\dot{W}^3 + \dot{W}\dot{U}^2) + m_1\Omega^2\cos\Omega t \end{cases}$$

Une introduction est faite pour l'application des ces modèles dans le cas de rotors en composite. Une méthode de discrétisation par éléments-finis est utilisée pour le modèle linéaire et une approche de type Rayleigh est utilisée pour les modèles non linéaires.

Chapitre 3

Dans ce chapitre, les aspects techniques et théoriques de la prise en compte de l'influence des déformations d'ordre supérieur et des efforts axiaux (statique et dynamique) sont étudiés. Trois méthodes sont utilisées pour analyser les résultats : la méthode des échelles multiples (MEM), une méthode d'intégration directe pas à pas des équations du mouvement et une méthode de type continuation.

Pour la MEM, les inconnues ont recherchées sous la forme de développement en séries de puissance. Les systèmes d'équations linéaires obtenues sont résolus 'en cascade'. Un intérêt particulier est porté à l'étude autour des deux fréquences de résonance du rotor avec l'utilisation d'un paramètre de désaccordage σ.

Une approche par discrétisation par éléments finis est appliquée afin de trouver la réponse dynamique linéaire des équations du mouvement.

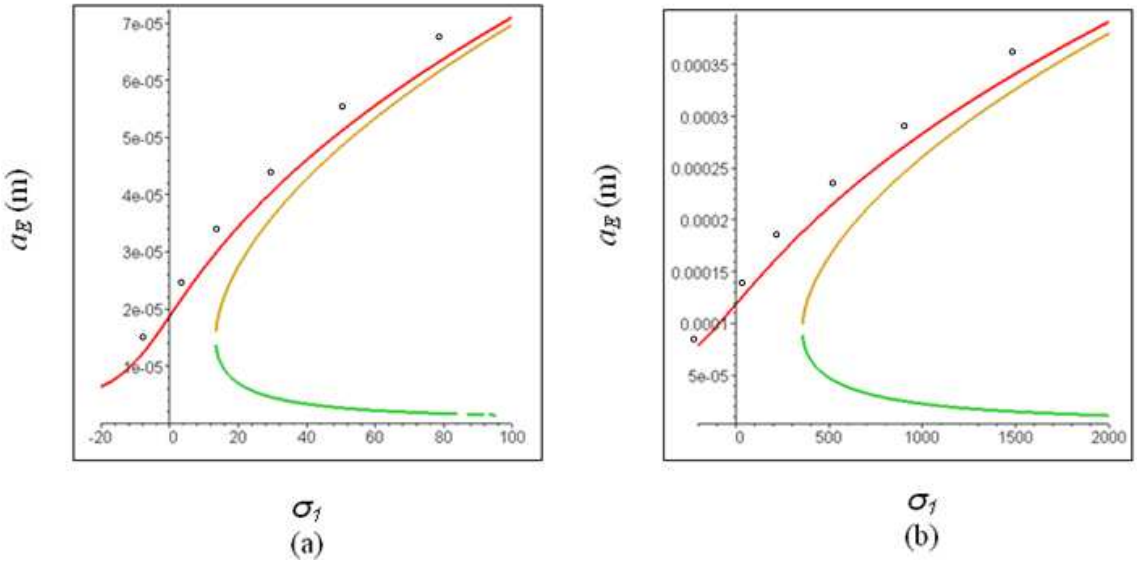

∘∘∘∘ *Méthode pas à pas* ___ *Méthode des Echelles Multiples*

Amplitudes en fonction de la fréquence (a) $\Omega = \omega_1$ *(b)* $\Omega = \omega_2$

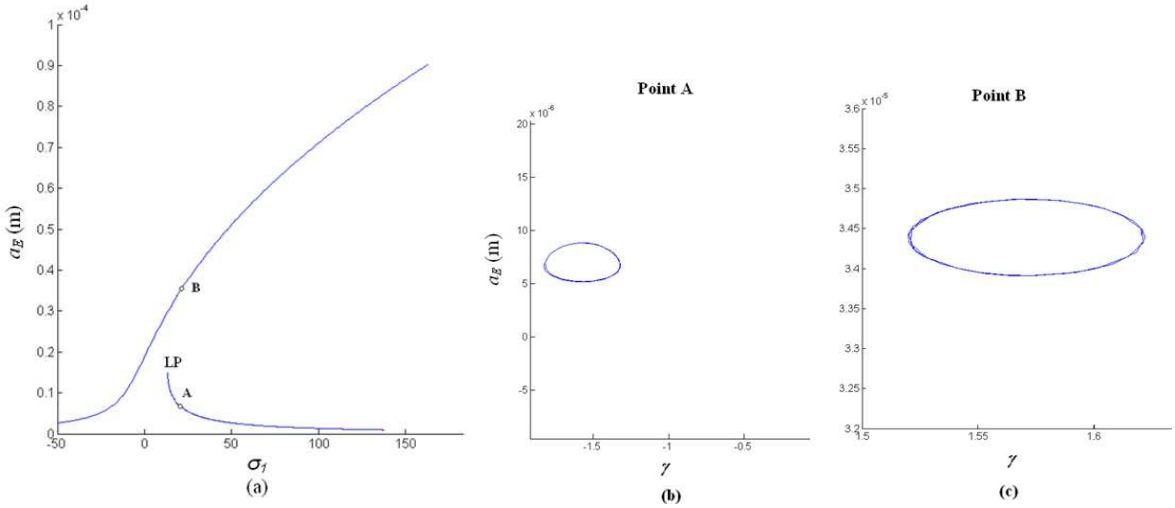

Résultats obtenus par une méthode continuation (MatCont) $\sigma_1 = 20$ *autour* $\Omega = \omega_1$
(a) Amplitudes-Fréquences (b) Plan de Phase au point A (c) Plan de Phase au point B

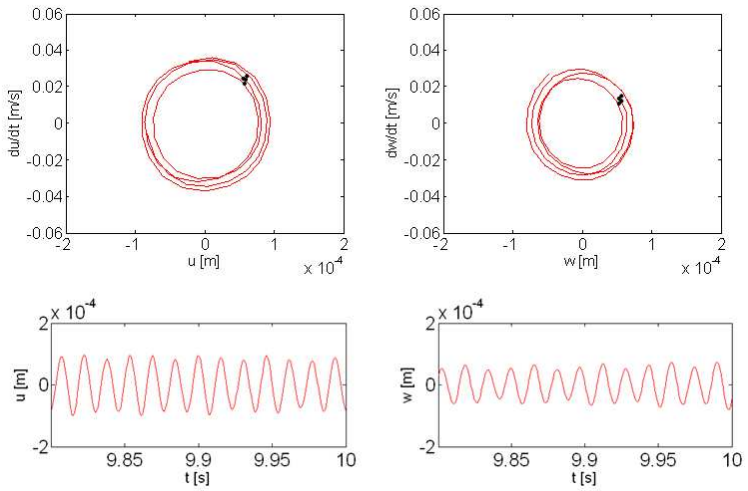

Diagrammes dans le plan de Phase et sections de Poincaré, amplitudes en fonction du temps pour $\Omega = \omega_1$

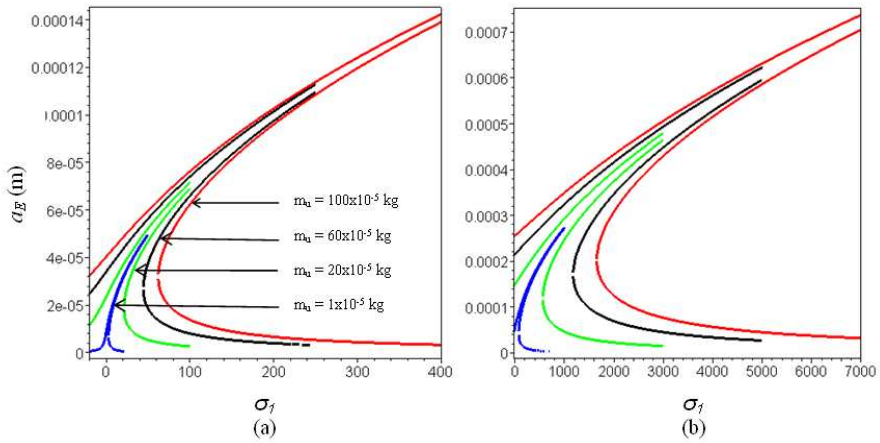

Influence de la variation du balourd m_u *sur la réponse. (a)* $\Omega = \omega_1$ *(b)* $\Omega = \omega_2$

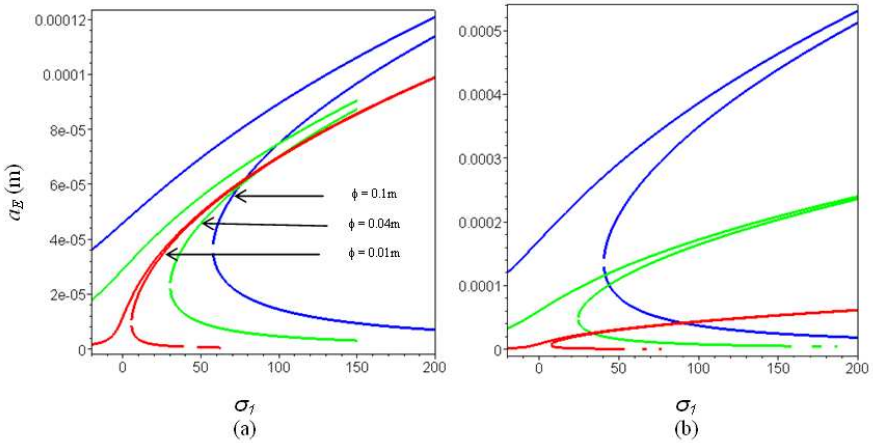

Effet de la variation du diamètre de l'arbre sur la réponse. (a) $\Omega = \omega_1$ *(b)* $\Omega = \omega_2$

Les effets des différents paramètres mécaniques (longueur, diamètre, …) sont étudiés et il apparait aussi que tous ces paramètres sont liés et ont une influence commune sur le comportement dynamique.

Chapitre 4

Ce chapitre analyse l'effet combiné des non-linéarités et de la prise en compte du cisaillement sur le comportement dynamique linéaire et non linéaire des rotors. Le modèle mathématique qui est traité dans ce chapitre se compose des équations différentielles du mouvement non linéaires contenant des dérivées d'ordre 4 par rapport au temps. La méthode des échelles multiples est appliquée directement pour ces équations.

L'influence des différents paramètres sur la réponse linéaire et non linéaire du système est analysée. Les réponses du système en régime permanent sont calculées par les trois méthodes. Les résultats sont présentés graphiquement et les effets du cisaillement sur le comportement sont discutés en détail.

Certains résultats de l'analyse linéaire et non linéaires sont présentés ci-dessous.

Table. 1. Effets du cisaillement sur les 2 premières fréquences propres pour les système arbre-disque en fonction du « slenderness ratios (r) ».

Cross-section	Geometry (meters)	L = 2 R_1= 0.32 R_2 = 0.75 h = 0.15	L =1.5 R_1=0.18 R_2 = 0.50 h = 0.10	L =1 R_1=0.08 R_2 = 0.3 h = 0.06	L =1 R_1=0.06 R_2 = 0.3 h = 0.06	L =0.5 R_1=0.02 R_2 = .15 h = 0.03
	Slenderness ratio (r)	0.08	0.06	0.04	0.03	0.02
Solid	Critical speeds without shear (rpm)	13838 16286	13542 15247	12064 13275	7456 8284	7158 8068
	Critical speeds with shear (rpm)	13332 15227	13255 14743	11970 13124	7433.5 8247	7153 8059
	percentage decrease	3.65 % 6.50 %	2.34 % 3.31 %	0.78 % 1.14 %	0.30 % 0.45 %	0.07 % 0.11 %
Tube ($e = 10^{-3}$ m)	Critical speeds without shear (rpm)	2505.6 3200.5	2997.4 3618.3	3471.7 4017.9	2223.4 2563.6	3300.6 3791.3
	Critical speeds with shear (rpm)	2500.8 3184.6	2992.5 3605.8	3468.1 4010.4	2222.4 2561.3	3299.8 3789.7
	Percentage decrease	0.19 % 0.50 %	0.16 % 0.35 %	0.10 % 0.19 %	0.04 % 0.09 %	0.02 % 0.04 %

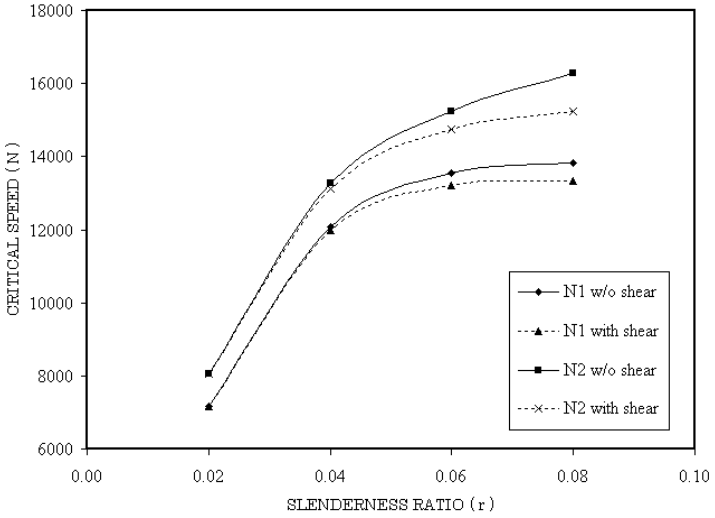

Effet du 'slenderness ratio' (r) sur la vitesse critique d'un système arbre+disque

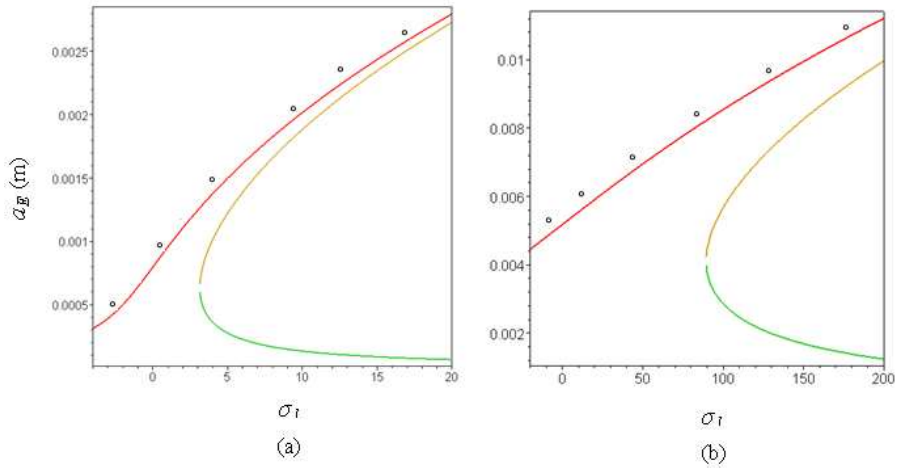

Amplitude avec prise en compte du cisaillement sur un système arbre+disque. (a) Ω = ω_1 (b) Ω = ω_2

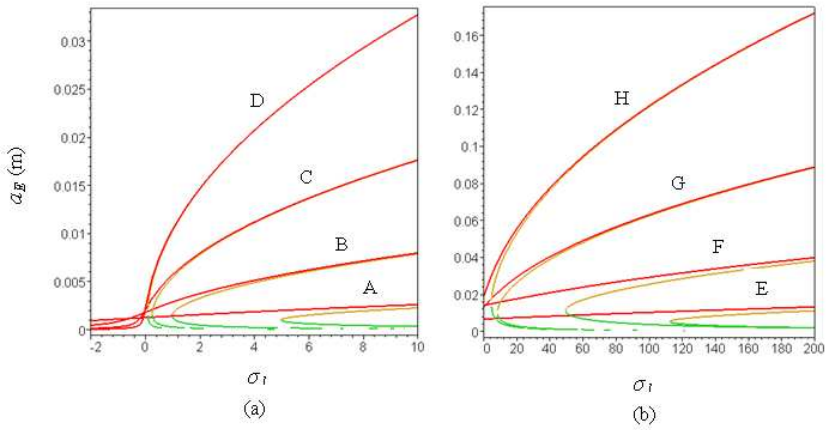

Plot	A , E	B , F	C , G	D , H
r	0.02	0.04	0.06	0.08

Effet du 'slenderness ratio' (r) sur la réponse non linéaire d'un système arbre+disque (a) Ω = ω_1 (b) Ω = ω_2

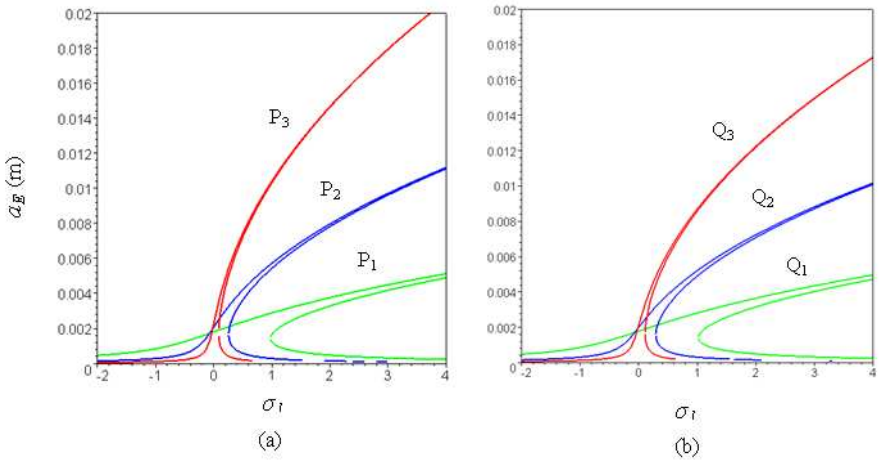

Plot	P_1 , Q_1	P_2 , Q_2	P_3 , Q_3
r	0.04	0.06	0.08

Effet du 'slenderness ratio' (r) sur la réponse non linéaire d'un système arbre+disque pour Ω = ω_1: (a) avec cisaillement (b) sans cisaillement

Chapitre 5

Les conclusions générales de la thèse sont présentées dans ce chapitre. Une description du travail déjà effectué est dressée. En outre, sur la base des travaux effectués pour cette thèse, les perspectives d'avenir, sont également mentionnées dans le détail. Les principales perspectives comprennent l'étude du comportement dynamique non linéaire des rotors avec une sollicitation par la base de base. Cette dernière n'est plus fixe et peut être soumis à différents mouvements comme une rotation simple rotation sinusoïdal ou des déplacements quelconques.

Cette thèse présente une élaboration détaillée de différents modèles mathématiques et leur analyse pour étudier le comportement dynamique non linéaire des rotors. D'abord, un état de l'art concernant l'analyse dynamique des rotors a été discuté et une brève présentation de divers aspects importants de la dynamique des rotors est présentée. De l'état de l'art il est conclu que l'étude du comportement dynamique des rotors a été un sujet d'importance pratique depuis de nombreuses années. Beaucoup de travaux ont été réalisés pour prévoir la dynamique des rotors en matériaux métalliques ou composites. Les travaux se poursuivent avec, en particulier, la prise en compte des effets non linéaires. Ceci est l'objectif principal des travaux de la présente thèse.

Ensuite, une modélisation mathématique détaillée est présentée pour analyser le comportement dynamique des rotors. Différents modèles contenant des équations différentielles non linéaires du mouvement ont été développés pour différentes configurations de rotor. Ces modèles se composent d'équations du mouvement différentielles non linéaires du second et quatrième ordre. Différents modèles ont été élaborés en tenant compte des différents effets importants comme des grandes déformations, des non-linéarités géométriques, les effets de cisaillement, des effets gyroscopiques d'inertie de rotation. Les modèles sont développés en utilisant le principe de Hamilton afin d'obtenir les équations du mouvement. Lorsque les déformations de cisaillement sont prises en compte les équations du mouvement développées sont composées des dérivés d'ordre 4 par rapport au temps. Une étude de cas pour l'analyse dynamique des rotors en composite a été réalisée et les résultats obtenus sont comparés aux travaux existants dans la littérature. Les résultats obtenus pour l'analyse dynamique des rotors en composite dans cette étude sont en accord avec ceux rapportés antérieurement dans la littérature.

Les équations de mouvement développées dans la partie modélisation ont été étudiées pour décrire le comportement dynamique non linéaire des rotors. Tout d'abord, le comportement non linéaire de la dynamique des rotors provoqué par de grandes déformations et une force axiale dynamique a été analysé. Les études numériques ont été réalisées en utilisant trois méthodes, à savoir la méthode asymptotique des échelles multiples, une procédure de continuation (Matcont) et une analyse pas à pas dans Matlab Simulink. Par comparaisons la méthode des échelles multiples est plus efficace que les deux autres méthodes, toutes les solutions stables et instables peuvent être observées dans les courbes de résonance. Les résultats montrent que les non-linéarités ainsi que d'autres phénomènes comme les effets gyroscopiques, les effets d'inertie de rotation et du balourd ont une influence significative sur la dynamique du système tournant. L'analyse linéaire montre que la résonance existe uniquement à la deuxième vitesse critique, cependant que dans l'analyse non linéaire une autre résonance apparait à la

première vitesse critique. De plus, les effets secondaires rendent le système non linéarité de type ‘hard spring’.

En l'absence de la force axiale dynamique et à des valeurs de balourd plus faibles, l'effet de durcissement de la raideur était visible même pour de faibles valeurs de terme de perturbation σ. L’utilisant de la méthode d'analyse présentée ici facilite la mise en place d’étude paramétrique. Les valeurs numériques des paramètres de système du rotor sont intégrées dans la réponse du calcul.

L'effet combiné des non-linéarités et des effets de cisaillement sur le comportement linéaire et non linéaire dynamique des rotors a été également étudié. Le modèle mathématique qui a été traité dans ce cas était composé d’équations du mouvement non linéaires d’ordre 4. La méthode des échelles multiples a été appliquée directement aux dérivées d'ordre 4 par rapport au temps.

Les effets du cisaillement ont été discutés en détail à la fois sur la réponse non linéaire du système de rotor étudie. Les résultats de l'analyse linéaire pour un arbre en rotation et un système arbre-disque, pour une section pleine et creuse, ont montré que la prise en compte des déformations de cisaillement réduit les vitesses critiques du rotor. Cette différence devient plus nette pour des valeurs plus élevées de ‘slenderness ratio’ r. Par rapport à un système arbre-disque les effets de cisaillement ont plus d'influence d’un arbre, de section pleine ou creuse. Dans l'analyse non linéaire, les courbes de réponse de résonance ont été tracées. Ces courbes sont de type ‘hard spring’. L'amplitude de la réponse et la plage sont plus étendues dans le cas de résonance correspondant à la $2^{ème}$ vitesse critique du rotor. Les comportements dynamiques globaux des rotors peuvent être très divers selon les variations de ‘r’ et de la masse du balourd. Les effets des déformations de cisaillement sont plus importants pour des valeurs plus élevées de l'élancement.

En conclusion, les grandes déformations et cisaillement ont un effet significatif sur le comportement dynamique des systèmes de rotor. Par conséquent, pour une analyse précise assurant une meilleure sécurité et une efficacité des systèmes de rotor, ces déformations ne peuvent être ignorées.

Summary of the Thesis

The objective of the present work is to investigate the nonlinear dynamic behavior of the rotor systems analytically and numerically, taking into account the significant effects, for example, higher order large deformations in bending, geometric nonlinearity and shear effects.This thesis is divided into two major parts. In the first part, Hamilton's principle is used to derive the equations of motion which take into account various effects, for example, nonlinearity due to higher order large deformations in bending and shear effects. In addition, if the supports of the rotor do not allow the shaft to move in the axial direction, then there will be a dynamical force acting axially on the rotor as it operates. The mathematical models are composed of coupled nonlinear differential equations of the 2^{nd} and the 4^{th} order.

In the second part, the resolution of various nonlinear models developed in the first part is addressed. Analytical and numerical methods are applied for treating the nonlinear equations of motion. A method based on asymptotic developments, the method of multiple scales (MMS) is used. The response curves are plotted for different possible resonance conditions and the effect of nonlinearity is discussed with respect to the linear analysis. The forced response of the system due to a mass unbalance is also presented for various configurations of the rotor. When shear deformations are taken into account, the analysis is performed for various slenderness ratios to highlight shear effects on the dynamics of the shaft-disk rotor systems.

Keywords : Rotordynamics ; Nonlinear ; Higher Order Deformations ; Dynamic Axial Force ; Shear Effects ; Method of Multiple Scales.

Résumé de Thèse

L'objectif de ce travail de thèse est d'étudier analytiquement et numériquement le comportement dynamique non-linéaire des rotors, en prenant en compte des effets significatifs comme les grandes déformations en flexion, les non-linéarités géométriques et le cisaillement. Le manuscrit est divisé en trois parties principales. Dans la première partie, le principe de Hamilton est utilisé pour formuler les équations du mouvement qui prennent en compte un ensemble d'effets non-linéaires comme des déformations d'ordre supérieur en flexion et le cisaillement. De plus, si les supports du rotor ne permettent pas à l'arbre de se déplacer dans la direction axiale, il y a alors une force dynamique harmonique agissant axialement sur le rotor en fonctionnement. Ces modèles se composent d'équations différentielles non-linéaires du deuxième et du quatrième ordre.

Les deux parties suivantes sont consacrées à la résolution des différents modèles non-linéaires développés dans la première partie. Des méthodes analytiques et numériques sont appliquées afin de traiter les équations non-linéaires du mouvement. Une méthode basée sur des développements asymptotiques, la méthode des échelles multiples (MEM) est utilisée. Les courbes de réponse sont tracées pour différentes résonances possibles et l'effet de la non-linéarité est discuté par rapport à l'analyse linéaire. La réponse forcée du système provoquée par un balourd est également présentée pour plusieurs configurations du rotor. Lorsque les déformations de cisaillement sont prises en compte, l'analyse est effectuée pour différents élancements afin de mettre en évidence cet effet sur la dynamique d'un système arbre-disque.

Mots Clés : Dynamique des Rotors ; Non-linéaire ; Grandes Déformations ; Force Dynamique Axiale ; Cisaillement ; Methode des Echelles Multiples.